

Optimization of Classification Results by Controlling of Hydrocyclone Process Parameters

Submitted to attain the academic degree of a Doktor der montanistischen
Wissenschaften at the Montanuniversitaet Leoben



Submitted by:

Dipl.-Ing. Roman van Ommen, MBA

First Reader: Univ.-Prof. Dr.mont. Helmut Flachberger

Second Reader: Univ.-Doz. Univ.-Prof. Dr.mont. Richard Nötstaller

Eidesstattliche Erklärung:

Ich erkläre an Eides statt, dass ich diese Arbeit selbstständig verfasst, andere als die angegebenen Quellen und Hilfsmittel nicht benutzt und mich auch sonst keiner unerlaubten Hilfsmittel bedient habe.

Affidavit:

I declare in lieu of oath, that I wrote this thesis and performed the associated research by myself, using only literature cited in this volume.

Podersdorf am See, im Mai 2011

Dipl.-Ing Roman van Ommen, MBA

Acknowledgements

The idea of long life learning was always fascinating to me and still is, but I had realized during my MBA years that this is not an easy task when working at the same time. As a matter of fact I wanted to keep my learning profile low after finishing my MBA at California State University. However in 2003 I resumed writing technical papers about hydrocyclones as part of my professional work. In fall 2006, at an excursion to Quarzwerke Melk in Austria, Professor Flachberger from Montanuniversitaet Leoben planted the idea of making a PHD about my favorite discipline, hydrocyclones, into my mind. To make a long story short, in March 2007 I submitted the application for my PHD thesis to the University board. Now, 4 years later, after many hours spent I am proud of the product generated and the work finished.

Therefore my initial thanks go to the Head of the Chair of Mineral Processing at the Montanuniversitaet Leoben, Professor Helmut Flachberger. First for being the spark to a flame and second for all the professional support, coaching and time spent with me. Also thanks for the patience and understanding of the time constraints faced when conducting such an exercise while having a demanding position in the industry at the same time.

I am also deeply indebted to Mr. Franz Plochberger and Mr. Jürgen Gleissenberg from CEMTEC, Cement & Mining Technology GmbH, Enns, Austria. Mr. Plochberger provided me a home in his pilot plant for making research test work for this thesis as a corporate sponsor. Mr. Gleissenberg set up the pilot plant and was a driving force during the test work. He also organized the required raw material and conducted all analytical work on the raw material as well as on the sampled products. Without CEMTEC the pilot plant test work would not have been possible.

My thanks also go to Professor Nötstaller who showed very much patience in finally receiving the economical part of this work and for the tolerance an economist must apply when dealing with a technical orientated person.

Further thanks go to ao.Univ.-Prof. Dr. Jörg Thuswaldner for supporting me whenever my mathematical knowledge needed support.

Also I wish to thank FLS Krebs and Pat Turner for sponsoring the cyclones and pumps needed to set up the milling circuit at CEMTEC as well as for many fruitful theoretical discussions about hydrocyclones.

Last but not least my thanks go to my family, especially my wife Brigitta for all the weekends spent without me working on this thesis. I joyfully look forward to make up the missed time with her and my son Eric.

Scope and slope of the dissertation (Abstract)

The cyclone is perhaps the most dramatic illustration of the old engineering axiom - the most efficient and dependable machines are those with the smallest number of working parts. With no moving parts at all, the cyclone is not only remarkably clean in design, but is also uniquely efficient in dynamic classification.

Unlike other machines used for mineral processing, the quality of a cyclone operation set up cannot be seen easily. Only a complete sampling campaign with a full set of data will show the process engineer how a cyclone performs.

The main instrument for a process engineer in a plant to influence cyclone performance is the alteration of its density regime. This is a straight forward concept for open classification, but in closed circuit grinding the set up of the complete system comprising of new feed, the grinding mill, cyclone and pump is changed when the cyclone density regime is altered.

Comminution is the most expensive process in mineral processing and as a consequence the importance of correct cyclone operation is significant because of the attached financial consequences. At the same time the overall circuit reaction of a grinding system to cyclone density variation is very poorly understood in the industry, even worse is the understanding of the possible economical impact.

This work shall contribute to better understand the overall closed circuit grinding systems reaction to varying cyclone density regimes, both from a practical and a theoretical perspective. The criteria for optimization are overflow particle size distribution (quality of product) and overall circuit power consumption and throughput.

As the main focus of mineral processing is the production of a sellable product, the financial impact and consequences need to be highlighted as well as understood by metallurgists. The economic aspect is displayed in selected examples taken from existing industrial installations. Furthermore a theoretical focus on investment calculation is made to show the great value to a plant owner on investments made to improve this capital intensive process of closed circuit grinding.

Table of Content

Acknowledgements	3
Scope and slope of the dissertation (Abstract).....	5
Table of Content	6
Table of Figures.....	11
CHAPTER 1: Definition of the assignment, structure of the work, and conceptual approach	14
CHAPTER 2: Summary.....	16
2.1. Introduction.....	16
2.2. Hypothesis.....	16
2.3. Conducted work.....	17
2.3. Technical results.....	17
2.3.1. Apex capacity and cyclone cone angle	17
2.3.2. Achievable underflow density with varying particle size distribution...18	
2.3.3. Basic reaction of the grinding circuit to cyclone underflow density variation	20
2.3.3.1. The influence of underflow density to the circulating load of a closed grinding circuit	20
2.3.3.2. The influence of circulating load to slurry viscosity in closed circuit grinding	20
2.3.3.3. The influence of underflow density to hydrocyclone D50 in closed circuit grinding	21
2.3.4. The influence of underflow density to the overflow product quality in closed circuit grinding	22
2.3.7. Recovery curve shapes and cyclone simulation	27
2.4. Economical results	31
2.5. Conclusions and evaluation of hypothesis.....	32
CHAPTER 3: Scientific background and state of knowledge	33
3.1 A brief history of hydrocyclones used in grinding circuits	33
3.2. The basic function of a hydrocyclone	36
3.3. Models for calculating hydrocyclone performance.....	39
3.3.1. Simple, fundamental theories that take little or no account of the effect of flow split, feed density and particle size distribution.....	39
The influence of hydrocyclone geometrical parameters is included in these types of models.....	39
3.3.1.1. The equilibrium orbit theory:.....	39
3.3.1.2. The residence time theory.....	39

3.3.2. Two phase flow theory taking the effects of slurry feed density and mean particle size distribution into account	39
3.3.3. Crowding theory, considering also the effect of the apex diameter to cyclone performance.....	39
3.3.4. Empirical models.....	40
3.3.5. Chemical engineering approach, which is combining the above models	41
3.3.6. Analytical mathematical models of the flow patterns inside the hydrocyclone, particle trajectories including the boundary layer flow, the short circuit flow and the internal eddies.	41
These models describe the performance at low densities only.	41
3.3.7. Numerical models using CFD	42
3.4. Evaluation of cyclone performance.....	43
3.4.1. Cut Point – D50.....	43
3.4.2. EP and Alpha value.....	43
3.4.3. Imperfection	44
3.4.4. The Recovery Curve (Tromp Curve).....	44
3.4.4.1. Introduction and Fines Bypass	44
3.4.4.2. The Recovery Curve (Tromp Curve)	45
3.4.4.3. The Corrected Recovery curve.....	46
3.4.4.4. The Reduced Recovery curve	47
3.5. Variables effecting Hydrocyclone performance	48
3.5.1. Particle Size	49
3.5.2. Inlet velocity	49
3.5.3. Solid/Liquid density	49
3.5.4. Cyclone diameter and up scaling	50
3.5.5. Slurry Viscosity	50
3.5.6. Circulating load	51
3.5.7. Cylinder Length.....	51
3.5.8. Vortex Finder Diameter	51
3.5.9. Apex Diameter	51
3.5.10. Cone angle and cone combinations	52
3.5.11. Manifold distribution system.....	54
3.6. Selected Chapters of cyclone Theory	55
3.6.1. Cyclone Capacity	55
3.6.2. Horizontal Cyclones	56
3.6.3. Air Core, discharge patterns and Roping, Apex sizing	56
3.6.4. Preferential classification	59

3.7. Cyclone design and development.....	59
3.7.1. Sharper separation.....	60
3.7.2. Finer separation	61
3.7.3. Modular design	61
3.7.4. Product development using CFD at FLS Krebs	62
3.8. Special Types of Hydrocyclones.....	73
3.8.1. Flat Bottom Cyclone.....	73
3.8.2. Water only cyclone.....	73
3.8.3. Dense media cyclones	74
3.8.4. SSC cyclones.....	74
3.8.5. Cyclowash.....	75
3.8.6. Desanders.....	75
3.8.7. Liquid – Liquid cyclones.....	75
CHAPTER 4: Hypothesis	77
CHAPTER 5: Practical work and results	78
5.1. Test and research work at FLS Krebs in Tucson AZ	78
5.1.1. Apex capacity and cyclone cone angle	78
5.1.2. Achievable underflow density with varying particle size distribution...80	
5.2. Experiences gained in consultancy selling	81
5.3. Pilot plant test work at CEMTEC, Austria	82
5.3.1. Initial circuit calculations.....	82
5.3.2. Pilot Plant Set Up/Flow Sheet.....	83
5.3.2.1. Grinding Mill	84
5.3.2.2. Hydrocyclone.....	84
5.3.2.3. Slurry Pumps.....	85
5.3.3. Raw material used	85
5.3.4. Conduct of test work	85
5.3.4.1. Practical sequence of test work.....	86
5.3.4.2. Manpower and responsibilities	86
5.3.5. Results and laboratory work.....	87
5.3.5.1. Laboratory Equipment	87
5.3.5.2. Table of Test results and data used for evaluation.....	88
5.3.5.3. Cyclone Discharge Patterns	90
5.3.5.4. Feed rate	90
5.3.5.5. Power consumption	90
CHAPTER 6: Technical Conclusions	91

6.1. Introduction	91
6.2. Conclusions and Discussion of data obtained from test work	91
6.2.1. The influence of underflow density to the circulating load of a closed grinding circuit	91
6.2.2. The influence of circulating load to slurry viscosity in closed circuit grinding	92
6.2.3. The influence of underflow density to hydrocyclone D50 in closed circuit grinding	93
6.2.4. The influence of underflow density to the overflow product quality in closed circuit grinding	94
6.2.5. Recovery curve shapes and cyclone simulation	99
6.3. New approach to cyclone recovery curve simulation	101
6.3.1. Shortcomings of existing models	101
6.3.2. Advanced model of cyclone recovery curve simulation and analysis	102
CHAPTER 7: Economical Considerations	105
7.1. Objective of the chapter	105
7.2. Conclusions and Summary of Chapter 7	105
7.3. Introduction	106
7.4. Correct operation and maintenance of hydrocyclones	106
7.5. Knowledge Management	107
7.5.1. Intellectual Capital – Unique assets	109
7.5.1.1. Human capital	109
7.5.1.2. Intellectual assets	110
7.5.1.3. Intellectual property	111
7.5.2. Value creation and measurement systems	111
7.5.3. Selected regional trends and examples of corporate culture	113
7.5.3.1. Europe	113
7.5.3.2. Africa	113
7.5.3.3. Russia	114
7.6. Cyclone sizing and change out of outdated equipment	114
7.7. Investment analysis and Capital budgeting	116
7.7.1. Methods of investment analysis and capital project evaluation	116
7.7.1.1. Payback and accounting rate of return	117
7.7.1.2. Discounted payback	117
7.7.1.3. Net Present Value (NPV)	117
7.7.1.4. Internal rate of Return (IRR)	118

7.7.1.5. Modified IRR – MIRR.....	118
7.7.1.6. Profitability index	119
7.8. Selected Examples from the industry	120
7.8.1. Goldfields Ghana, Tarkwa; operating cost gMAX versus 20 degree cone cyclones	120
7.8.2. AngloGold Ashanti, Geita Gold Mine; Change out case story.....	122
7.8.3. A sand plant in Europe – a thought experiment	124
7.8.4. Siguir Pump Project (Guinea, Africa).....	125
7.9. Optimization potential for various mineral commodities.....	127
CHAPTER 8: Literature	128
CHAPTER 9: APPENDIX – TABLES, REPORTS AND DATA.....	137

Table of Figures

Figures 17, 18, 23, 26, 29, 32, 33, 34, 35, 37, 38, 40, 41, 42, 43, 44, 45, 46, 47, 48, 49, 50, 51, 52, 53, 54, 55, 54, 55, 56, 57, 59, 60, 61, 62, 62, 63, 64, 65, 66, 67, 68, 69, 70, are the Intellectual Property from FLSmidth Krebs and the author was granted the right for use of these graphics in this publication.

Figure 1: Apex capacity chart envelope	18
Figure 2: AFS number and achievable cyclone underflow density	19
Figure 3: Apex diameter and circulating load	20
Figure 4: Apex diameter versus slurry viscosity	21
Figure 5: Apex diameter versus D50	22
Figure 6: Apex diameter versus alpha value	23
Figure 7: -20 and -10 μm particles in underflow versus apex diameter	23
Figure 8: Recoveries to underflow of -15 μm versus apex diameter	24
Figure 9: +140 μm and +180 μm particles in cyclone overflow versus apex diameter	24
Figure 10: Recovery of +140 μm and +180 μm to overflow versus apex diameter	25
Figure 11: P80 and P99 for various test runs and P80/P99 ratio	26
Figure 12: P80 and P99 versus apex diameter	26
Figure 13: Apex diameter versus P80/P99 ratio	26
Figure 14: Recovery curve for optimized underflow (Run24) and too dilute underflow (Run02).....	27
Figure 15: Picture of underflow discharge. Left run 24 and right run 02	28
Figure 16: Actual versus reduced recovery curve with traditional	30
Figure 17: The Bretney cyclone	33
Figure 18: Parts of a hydrocyclone.....	36
Figure 19: Velocities in a hydrocyclone ²	37
Figure 20: Velocities in a hydrocyclone ²	37
Figure 21: Migration of particles ²	37
Figure 22: Particle trajectories and flow patterns ³	38
Figure 23: Major area of turbulence	38
Figure 24: Recovery curve correlation values	43
Figure 25: Typical recovery curve of a hydrocyclone ⁴	45
Figure 26: Actual and corrected recovery curve ⁵	46
Figure 27: Reduced recovery curve ⁷	47
Figure 28: Forces on a particle.....	48
Figure 29: Slurry viscosity versus slurry density.....	50
Figure 30: Flow patterns ⁹	51

Figure 31: D50 versus apex diameter ¹⁰	52
Figure 32: Comparison of a 20° and a 10° cone on a 250 mm cyclones with 3,096 mm ² inlet, 100 mm vortex finder, operating at 1.4 bar and 57 % feed solids by weight.....	53
Figure 33: Various cone angle arrangements	53
Figure 34: Inline and radial feed distribution	54
Figure 35: Hydrocyclone capacity curve	55
Figure 37: Free vortex ¹¹	56
Figure 36: Typical apex discharge patterns	57
Figure 38: General apex capacity chart	58
Figure 39: Individualized apex capacity chart ¹³	58
Figure 40: Warman inlet head.....	60
Figure 41: Krebs gMAX inlet head	60
Figure 42: CFD image of tangential velocity distribution	61
Figure 43: Prototype inlet	63
Figure 44: 3D model of inlet head	63
Figure 45: Wear/paint test new inlet.....	64
Figure 46: Wear/paint test standard inlet	64
Figure 47: CFD erosion old inlet.....	65
Figure 48: CFD erosion new inlet.....	65
Figure 49: CFD erosion 250 mm cyclone new head	66
Figure 50: CFD erosion 250 mm cyclone old head	66
Figure 51: Laboratory test results - standard and gMAX head.....	66
Figure 52: 250 mm cyclone air core	67
Figure 53: 250 mm cyclone grid	67
Figure 54: Contours of static pressure	68
Figure 55: Contours of tangential velocity	68
Figure 56: Coarse particle tracking new head	68
Figure 57: Coarse and fine particle tracking old head	68
Figure 58: CFD validation of hydrocyclone inlet pressure	69
Figure 59: Actual recovery curves	70
Figure 60: Validation data of 89 mm and 64 mm vortex finder tests	71
Figure 61: gMAX mesh	71
Figure 62: gMAX pressure distribution	71
Figure 63: gMAX Tangential velocity distribution	71
Figure 64: Recover curve validation	72
Figure 65: Water only cyclone.....	73
Figure 66: Particle movement in a heavy media cyclone	74
Figure 67: SSC cyclone	Error! Bookmark not defined.

Figure 68: CycloWash.....	75
Figure 69: Desander	75
Figure 70: Liquid-liquid cyclone.....	76
Figure 71: Apex capacity test results	79
Figure 72: Apex capacity chart envelope	79
Figure 73: AFS number calculation example.....	80
Figure 74: AFS number and achievable cyclone underflow density	81
Figure 75: Pilot plant at CEMTEC	84
Figure 76: Raw material in big bag.....	85
Figure 77: Hydrocyclones in test set up	85
Figure 78: Apex diameter and circulating load	91
Figure 79: Apex diameter versus slurry viscosity	93
Figure 80: Apex diameter versus D50.....	94
Figure 81: Apex diameter versus alpha value	95
Figure 82: -20 and -10 μm particles in underflow versus apex diameter	95
Figure 83: Recoveries to underflow of -15 μm versus apex diameter	96
Figure 84: +140 μm and +180 μm particles in cyclone overflow versus apex diameter	96
Figure 85: Recovery of +140 μm and +180 μm to overflow versus apex diameter	97
Figure 86: P80 and P99 for various test runs and P80/P99 ratio	98
Figure 87: P80 and P99 versus apex diameter	98
Figure 88: Apex diameter versus P80/P99 ratio.....	98
Figure 89: Recovery curve for optimized underflow (Run 24) and too dilute underflow (Run 02).....	99
Figure 90: Picture of underflow discharge. Left run24 and right run 02.....	100
Figure 91: Actual versus reduced recovery curve with traditional and advanced model	104
Figure 92: A model of a knowledge company	108
Figure 93: Tarkwa Gold, expansion 2008. On the left side the original plant and on the right side extension plant with new mill, pumps and cyclones, picture Roman van Ommen, 2009.....	120
Figure 94: Cost comparison for Geita expansion	121
Figure 95: Geita Gold Mine, hydrocyclones, 2x16 units gMAX15, top fed by a central feed distributor, picture Roman van Ommen, 2008	122
Figure 96: NPV and IRR calculation of a sand plant	124
Figure 97: Cyclone comparison and energy savings Siguirí.....	126
Figure 98: NPV and IRR on Siguirí project.....	126

CHAPTER 1: Definition of the assignment, structure of the work, and conceptual approach

The assignment “Optimization of Classification Results by Controlling of Hydrocyclone Process Parameters” opens a wide range of possible topics and areas of research. The exact scope of this dissertation needs to be defined more precisely as a matter of fact. This work is an attempt to highlight the influence of the variation of the density regime of a cyclone to the quality of its overflow product in a closed circuit grinding system. It is important that the reaction towards product quality of an entire closed grinding circuit system (mill, cyclone, pump) is investigated and not that of a single isolated cyclone.

The structure comprises of four main sections.

The first part of this work (chapter 3) summarizes common knowledge and the “state of art” about hydrocyclone technology. This section provides a general introduction to various hydrocyclone designs, theories on cyclone modelling, a good number of practical knowledge about applications and some in depth research results that impact the basis and advanced focus on the assignment.

The second part (chapters 4, 5, 6) defines the hypothesis and highlights the research work both from a practical and a result orientated view.

The third part (chapter 7) ties in seamlessly with the second part, describing the economical aftermath.

Finally the fourth part (chapters 8, 9) lists important and relevant literature, and summarizes all relevant data, pictures, calculations and various other appendices.

The conceptual approach differs compared to the majority of today’s published research work about hydrocyclones. A myriad of publications can be found on cyclone technology and cyclone performance. Most of the publications however focus on small diameter cyclones that can easily be investigated in laboratories. This may be interesting as such, however very little practical knowledge can be gained when focussing on industry scale cyclone operation. Therefore the major focus is put on large scale installations and the creation of a theory that also has large scale relevance for operational processing plants. Also most publications deal with open cyclone classification only and this is one of the very few works that deal with a cyclones based system reaction in closed circuit grinding.

Three areas of activities were used for knowledge generation:

1. Long time world wide practical plant experience by the author.
2. Joint research activities with the Krebs R&D department.
3. Focussed pilot plant testing at CEMTEC in Enns, Austria.

In today's mineral processing industry, technology and economy are interlinked very close and the economic approach is more important than ever. Although the economic trough of 2009 is passed today and 2010 was a year of constant growth continuing now in 2011, we now have to develop technologies and knowledge for more difficult times. On the economic part a practical approach with the use of case studies describing the financial benefits of process improvement gained from cyclone operation optimization is taken, as well as a theoretical excursus to investment calculation which is the investment decision making tool for plant performance improvements. Furthermore the importance and structure of knowledge management and creation is highlighted as the best technology will not generate the desired results without qualified process engineer operating it.

CHAPTER 2: Summary

2.1. Introduction

Growing demands for product quality in the minerals industry are of more importance than ever and a growing challenge for all producers. The first step in mineral processing is usually comminution. In this process step, the correct particle size distribution for all downstream processing is produced and such the foundation for final efficiency and product quality is laid. The product of a milling circuit is finally produced with a classifier which is a hydrocyclone in most plants. In such a circuit the quality of the product can be influenced significantly by changing the cyclone density regime. With the change of the density regime not only the operation of the cyclone, but the operation and quality of the overall circuit is changed.

The majority of the literature and test work conducted on cyclones was done on open classification which does not explain the outcome on a system based view. The influence of underflow density variation to overflow product quality and overall circuit performance, although being of highest economical interest to all production sites, was never investigated in detail. This thesis and the subsequent test work is an attempt to quantify and qualify this influence both from a technical and an economical point of view.

2.2. Hypothesis

The quality of milled product in closed circuit grinding can be influenced significantly by controlling the underflow density of a hydrocyclone.

On a generalist's approach the guideline to operate hydrocyclones at their lowest possible overflow density and their highest possible underflow density in closed circuit grinding is of common knowledge. The underlying principle is minimizing of recycled ultrafines back to the mill.

To describe the recovery curve of a hydrocyclone, two separate curves have to be evaluated. There is a recovery curve for the solids and one for the liquid. The two main figures to evaluate a recovery curve are the D50 and the shape of the curve.

The water recovery curve depends on the ratio of apex and vortex finder diameter. Ultrafine particles in larger cyclones (150 mm and larger) are not separated according to the recovery curve of the solids, but follow the recovery curve of the water. In other words the ultrafines are carried along with the water.

This explains why hydrocyclones shall be operated with the highest possible underflow density. The higher the underflow density the lower is the amount of water that reports to the underflow and consequently the less the content of ultrafines in the underflow. This is important because these ultrafines represent final ground material that shall report to the overflow and not being recycled back to the mill feed. If excessive amounts of fines are recycled back to the mill the result will be over grinding and consequential losses in recovery downstream.

The overall performance of a grinding circuit can be altered by just changing the Apex diameter. In practice this effect can be seen when apex inserts wear out on large installations with the consequence of reduced mill circuit capacity.

2.3. Conducted work

The practical research work can be divided into 3 segments being pilot plant test work at CEMTEC, laboratory/pilot plant test and research work at Krebs' headquarters in Tucson, AZ, USA, and many years of consultancy work at many operations worldwide with main focus on the gold industry in East and West Africa.

2.3. Technical results

2.3.1. Apex capacity and cyclone cone angle

After the introduction of the gMAX cyclone practical field data strongly suggested that the capacity of the apex differs significantly with the variation of cyclone cone angles. The results are summarized in a new apex capacity chart envelope (Figure 1) that now allows selecting the correct apex diameter for various cone angles in hydrocyclones.

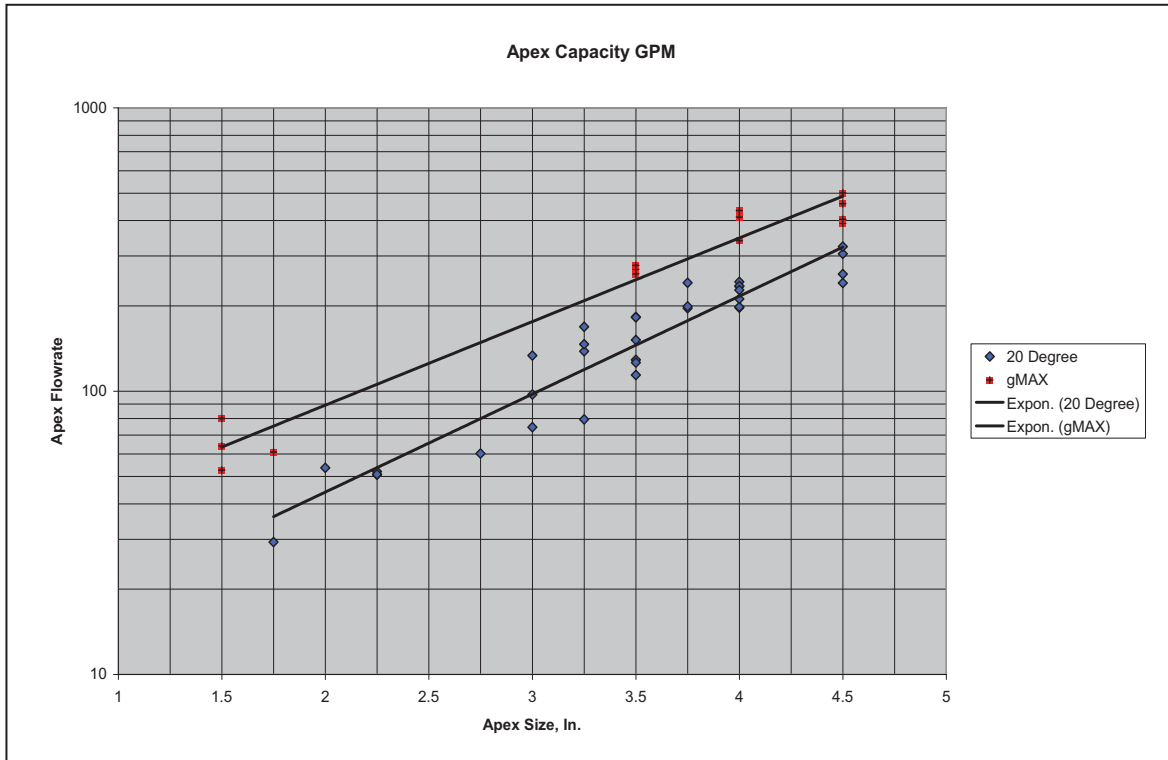


Figure 1: Apex capacity chart envelope

2.3.2. Achievable underflow density with varying particle size distribution

Field data and literature strongly suggest that the achievable underflow density in a hydrocyclone does not only depend on the apex diameter but also to a great part on the feed particle size distribution.

In a new approach the AFS (American Foundry Sand) Number was selected as a comparison criterion for particle size distributions and a strong affinity to achievable underflow density was found. This approach now allows to evaluate the achievable cyclone underflow density for a given feed particle size distribution as per Figure 2.

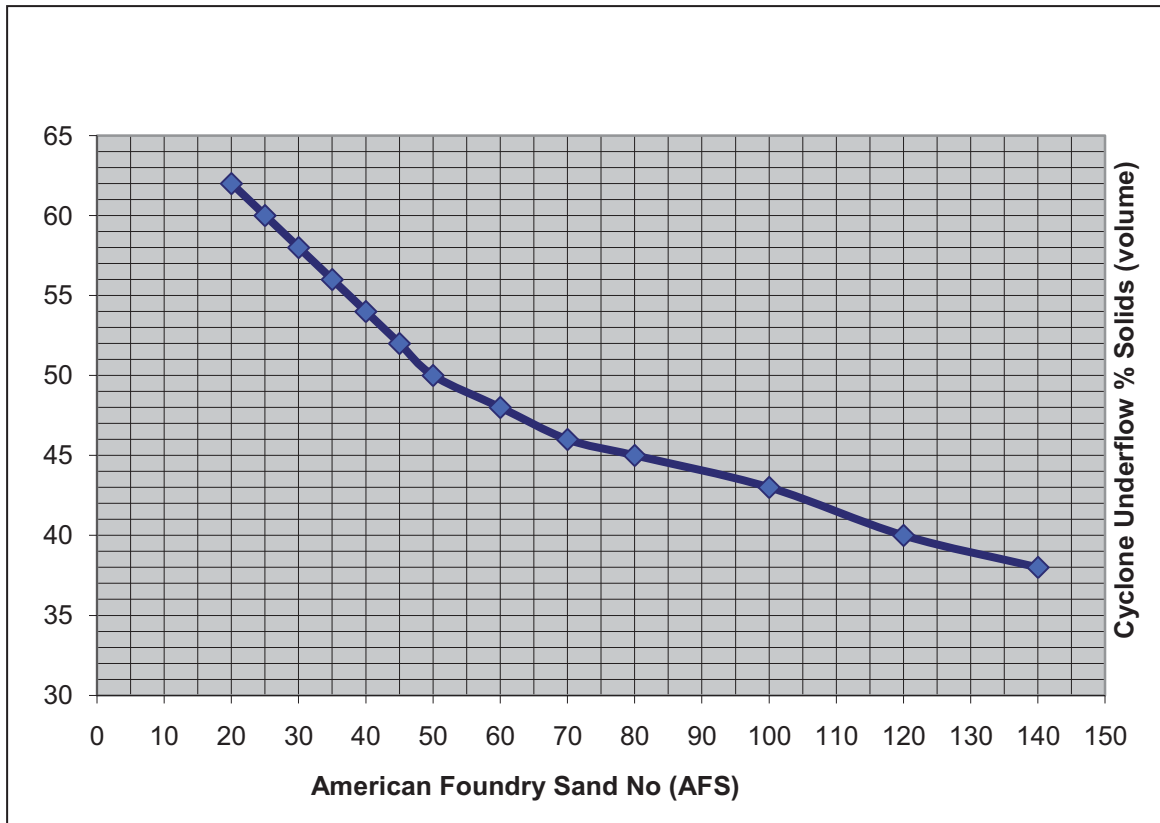


Figure 2: AFS number and achievable cyclone underflow density

2.3.3. Basic reaction of the grinding circuit to cyclone underflow density variation

2.3.3.1. The influence of underflow density to the circulating load of a closed grinding circuit

As shown in figure 3, the circulating load decreases with increasing underflow density. This is a quite important result because the lower circulating load can be used to increase the new feed to the system and increase production.

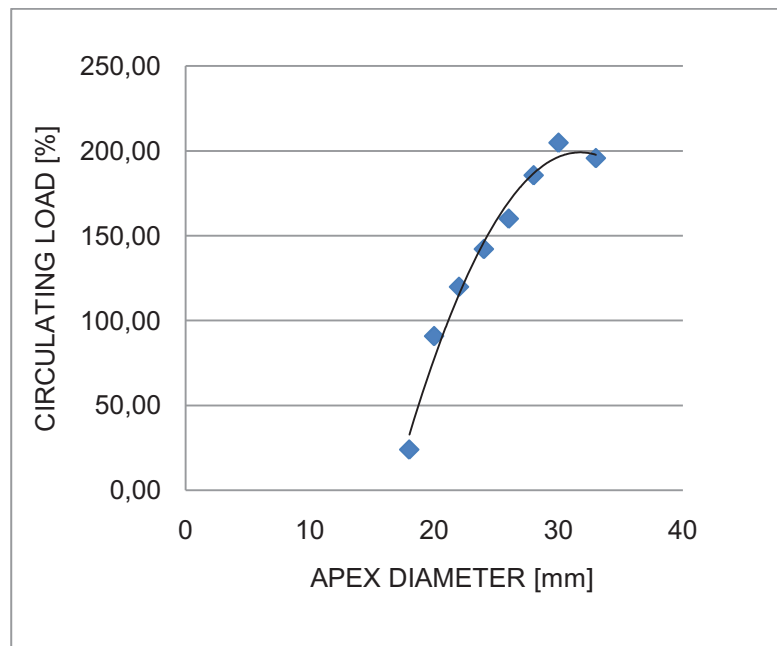


Figure 3: Apex diameter and circulating load

With smaller apex diameter, the water split to the overflow increases and the water split to the underflow decreases. Because of that, the not classified fines content in the slurry gets discharged preferentially to the overflow with decreasing apex diameter and the circulating load drops. With close monitoring of apex diameter the mill throughput in plants can be maximized.

2.3.3.2. The influence of circulating load to slurry viscosity in closed circuit grinding

As shown in figure 4, the viscosity increases with decreasing circulating load. The reason for that is the change in the composition of the particle size distribution to the total mill feed. As commonly known, slurry viscosity rises with increasing fines and slimes content. Hydrocyclone underflow by nature is perfectly deslimed material with low viscosity. The lower the circulating load is in the system, the lower is the proportion of deslimed recycled underflow back to the mill and consequently the viscosity rises because slimes rich new feed (raw material is

slimes rich by nature) gets proportionally higher. Very often this relationship is considered to be the other way round in operations.

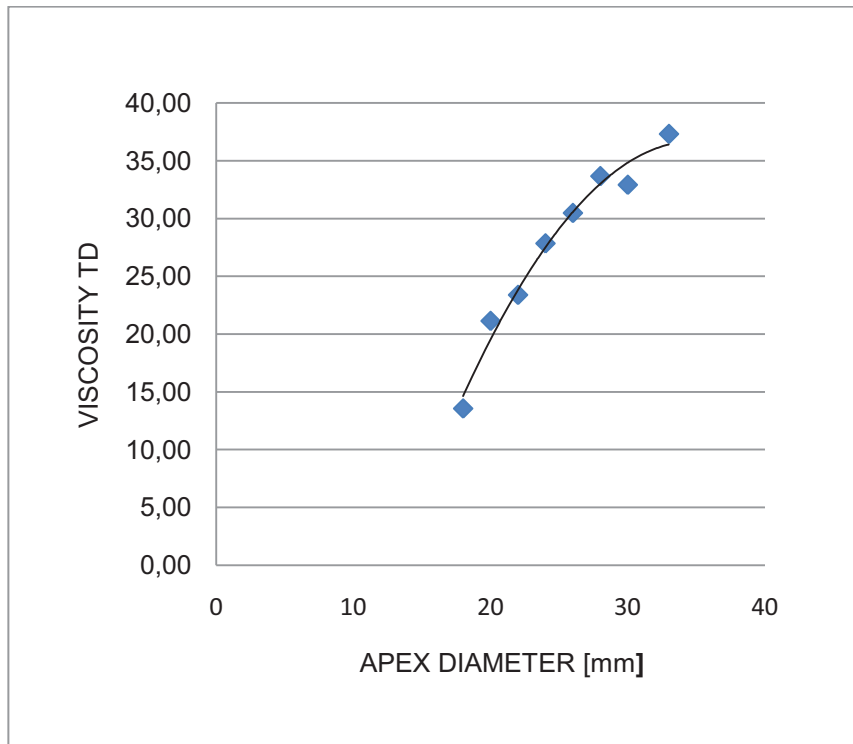


Figure 4: Apex diameter versus slurry viscosity

2.3.3.3. *The influence of underflow density to hydrocyclone D50 in closed circuit grinding*

With rising underflow density, the cut point (D50) of the hydrocyclone gets coarser (Figure 5). The reason for that effect is the reduction of the circulating load with increasing underflow density and the rise in slurry viscosity because of the lower circulating load, resulting in coarser separation of the hydrocyclone.

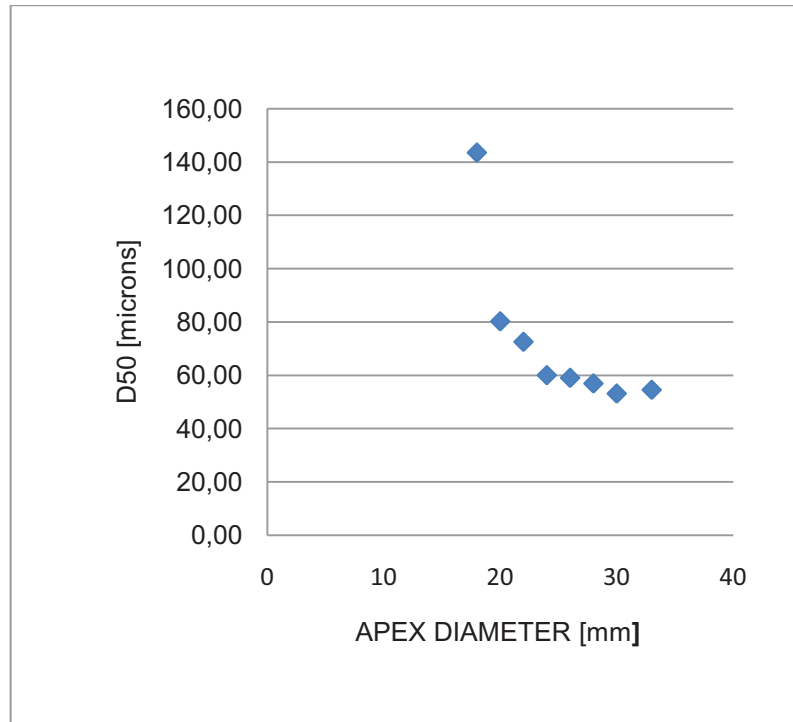


Figure 5: Apex diameter versus D50

2.3.4. The influence of underflow density to the overflow product quality in closed circuit grinding

The product quality of hydrocyclone overflow can be evaluated best by looking at the pitch as well as to the upper and lower ends of the recovery curve. An important value is the Ecart Probable or the alpha value (Lynch-Rao equation), describing the pitch of the recovery curve.

As shown in Figure 6, the relationship between the sharpness of separation and apex diameter (underflow density) describes a curve that trends to sharper separation with increasing underflow slurry density, reaching a maximum and then declining again. It is easy to see that there is a distinctive optimum underflow density (or apex diameter) that results in the sharpest possible recovery.

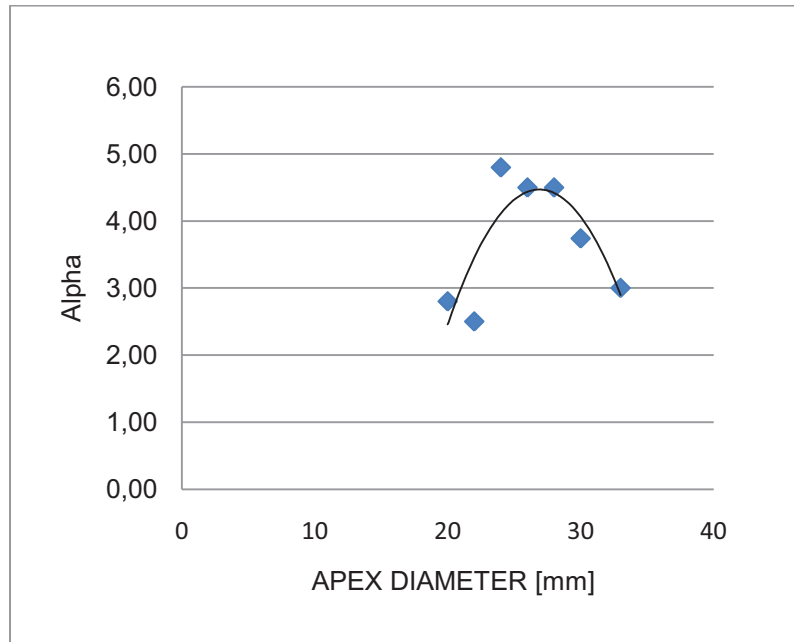


Figure 6: Apex diameter versus alpha value

In addition to the middle part of the curve the upper and lower tails are of great importance for the cyclone performance evaluation. Especially misplaced coarse particles in the overflow and excessive fines in the underflow are of big importance to overall plant recovery and the economical success of an operation.

The first look is to the lower tail of the recovery curve. Figure 7 below shows the content of -10 μm and -20 μm in cyclone underflow with varying apex diameter and Figure 8 the recovery figures to the underflow the -15 μm fraction.

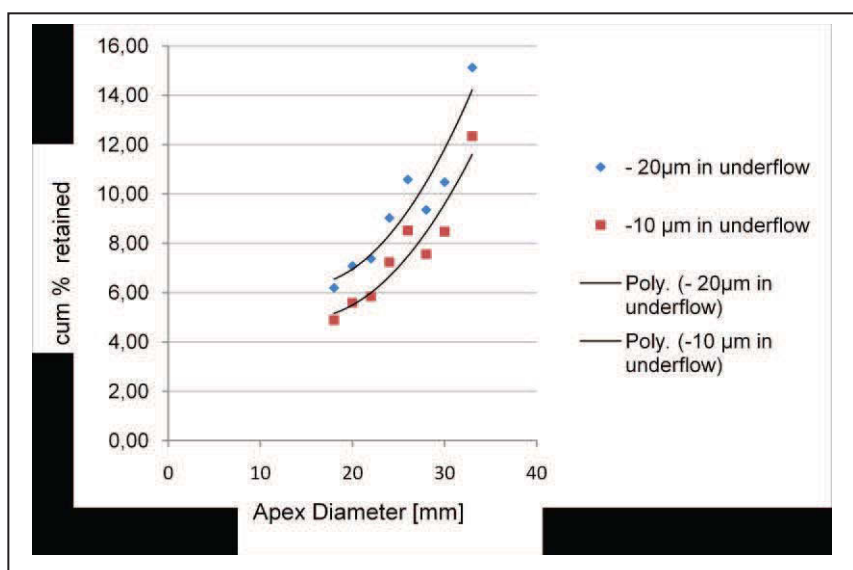


Figure 7: -20 and -10 μm particles in underflow versus apex diameter

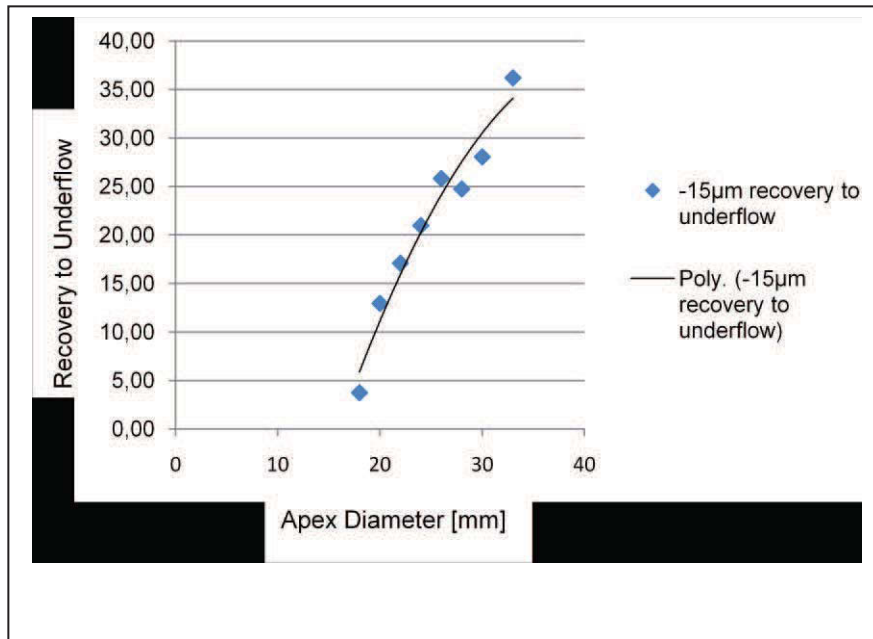


Figure 8: Recoveries to underflow of -15 µm versus apex diameter

The content of fine particles as well as their recovery decreases with decreasing apex diameter.

When looking at the top end of the recovery curve things get interesting again. Below figure 9 shows the content of +140 µm and +180 µm particles in cyclone overflow with varying apex diameter and figure 10 their recoveries.

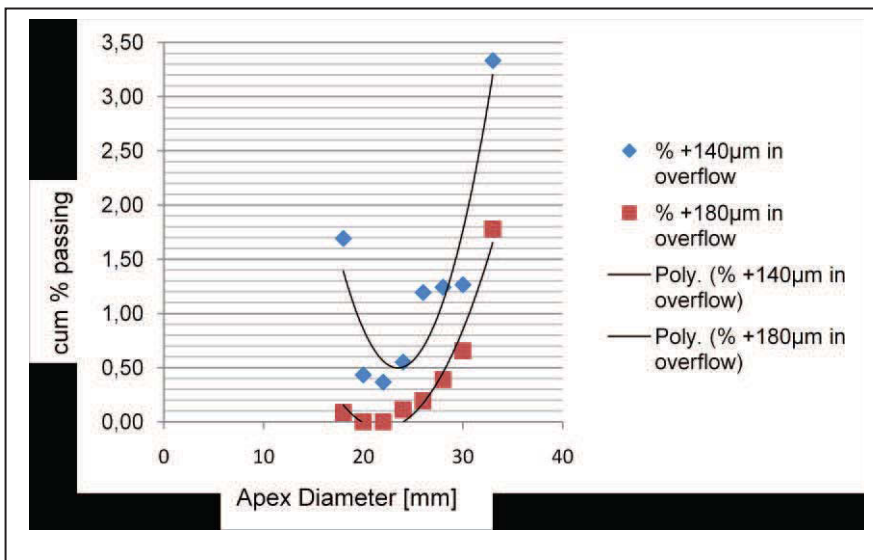


Figure 9: +140 µm and +180 µm particles in cyclone overflow versus apex diameter

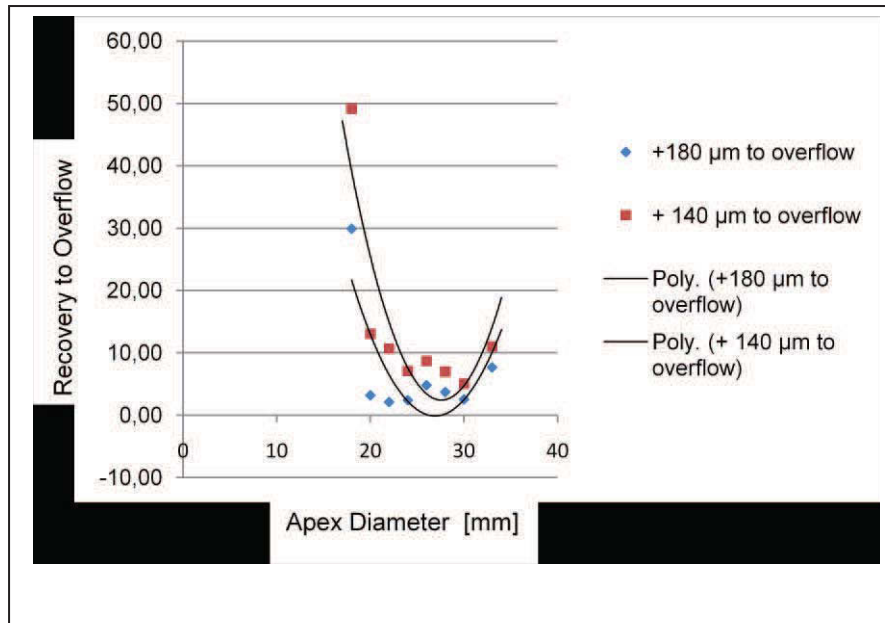


Figure 10: Recovery of +140 µm and +180 µm to overflow versus apex diameter

Figures 9 and 10 show results that had never been experienced before or in other words are against main stream thinking in the cyclone industry. The effect that is supported by this data and that is also commonly known in the industry is that with too high underflow density or too small apex diameter the number of misplaced particles in the overflow gets higher and reaches a point when the cyclone is roping were almost no classification work is done by the cyclone at all.

What can be clearly seen in both figures 9 and 10 is a clear rise of the coarse particles in the overflow when the cyclone operates with a too large apex diameter. Mainstream thinking was that the curve as shown above would remain flat for larger apex diameters, but a distinctive rise can be obtained.

When trying to explain the cause of this phenomenon, it is important to interpret the data by looking at the whole circuit and not to evaluate the cyclone as an isolated device. With the variation of the apex diameter the grind or the P80 of the system changes as well as shown in this chapter above. With a changing P80, also the amount of top size fractions changes as a consequence. Therefore the effect of higher misplaced particles on diluted cyclone underflows in closed circuit grinding systems needs to be evaluated independently from this variation in grind.

A good comparison is the spread and the ratio of the relative top size content to the grind which can be obtained by calculating the ratio of the P80 to the P99 of the overflow particle size distribution. This approach eliminates the usage of definitive particle size fractions and leads to a comparable result which is

independent from the actual P80 and shows the relative proportion of coarse bypass in the cyclone overflow.

	33	30	28	26	24	22	20	18
	RUN 3	RUN 6	RUN 9	RUN 12	RUN 15	RUN 18	RUN 21	RUN 24
P80	29,00	39,00	43,00	46,00	44,00	50,00	49,00	61,00
P99	231,00	158,00	151,00	148,00	131,00	136,00	131,00	134,00
P80/P99	7,97	4,05	3,51	3,22	2,98	2,72	2,67	2,20

Figure 11: P80 and P99 for various test runs and P80/P99 ratio

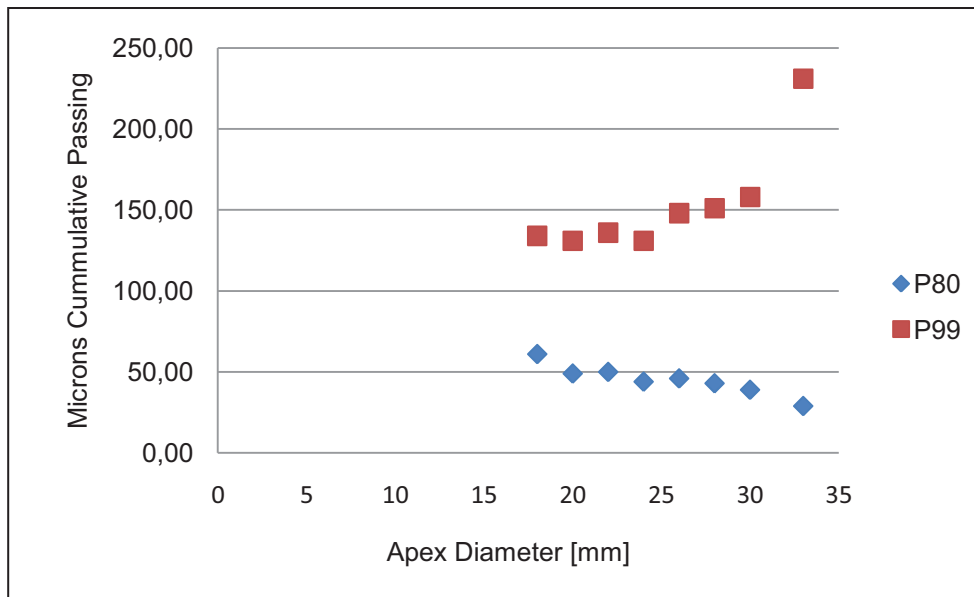


Figure 12: P80 and P99 versus apex diameter

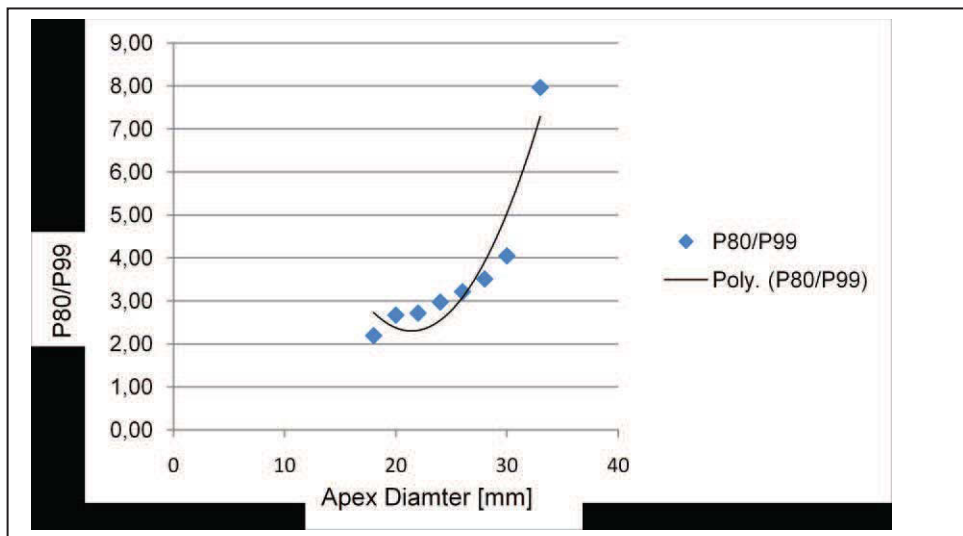


Figure 13: Apex diameter versus P80/P99 ratio

The result of this way looking at the results is quite surprising. With the apex getting bigger the spread, the absolute percentage and also the relative value of P80/P99 goes up.

The suggested explanation of this effect is not trivial. The air core diameter in a hydrocyclone is a function of the ratio of the vortex finder diameter, cyclone pressure, feed density and apex diameter. If all variables remain constant and only the apex diameter is varied, the air core diameter gets bigger with larger apex diameter. If the air core is getting too big in diameter the remaining area between cyclone wall and the air core is getting smaller and smaller until it reaches a point where the volume of slurry reporting to the underflow cannot pass this open flow area anymore as the slurry velocity is a constant and cannot be increased. The result of this flow constraint is that the excessive volume that cannot pass this bottleneck is pushed towards the overflow and by that increasing the coarse fractions.

2.3.7. Recovery curve shapes and cyclone simulation

For the complete evaluation of the recovery curve also the upper and the lower ends have to be looked at as clearly shown above. As shown in figure 14, there is a major difference in quality between too dilute density (right picture) and optimized underflow density using a 25mm Apex insert as per picture

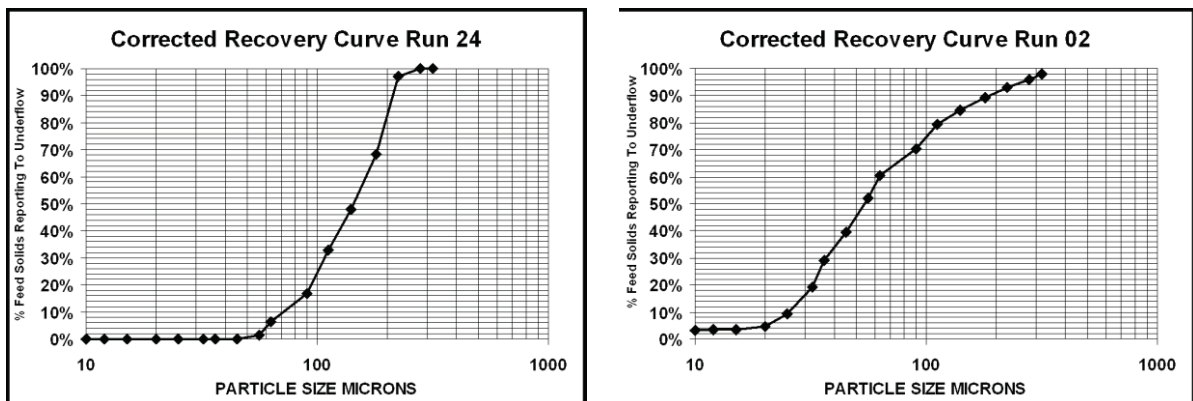


Figure 14: Recovery curve for optimized underflow (Run24) and too dilute underflow (Run02)

It can be clearly seen that the shape of these two curves is very different and that the quality of the overflow product can be influenced significantly by varying the water split¹. Also the discharge patterns vary significantly as per Figure 15.

¹ van Ommen, R., Flachberger H.; "Selected examples of the influence of cyclone underflow density to a closed circuit grinding system, AT Mineral Processing, Heft 11, 2009, pp. 56-61



Figure 15: Picture of underflow discharge. Left run 24 and right run 02

In addition, the shape of the recovery curves at the tops and tails differ quite significantly.

Cyclone performance simulation is split into two different disciplines which is the establishing of the cyclone D50 and the realistic modelling of the shape of the estimated recovery curve.

$$T_{\alpha}(D) = \frac{e^{\alpha \frac{D}{D50}} - 1}{e^{\alpha \frac{D}{D50}} + e^{\alpha} - 2} \quad \text{Equation 1: Lynch Rao Equation}$$

- T(D): Partition Number for a selected particular fraction D
- D: particular size fraction [μm]
- D50: calculated D50 of cyclone [μm]
- α : Alpha value

In this equation, the alpha value is the only free variable that can be modified to change the shape (slope) of the recovery curve. The resulting curve derived from equation 1 is symmetrical around the D50 point. The upper and lower tails of the recovery curve are symmetrical as well and cannot be shaped differently. The systematic test work, as well as plant data, show that the shape of the upper and the lower tail of the recovery curve vary significantly with the variation of the water split in the hydrocyclone (see figure 14 and 16). At this point the clear limitation of that model is obvious to the reader. This variation and the influence of the water split to the overall shape of the recovery curve cannot be described sufficient with the symmetrical model.

To mitigate the shortcomings of the symmetrical approach, an improved equation for the modelling of the recovery curve is needed to provide the possibility to modify the shape of the upper and the lower tail of the recovery curve

independently to adjust for varying water splits, but at the same time the approximated linear shape around the D50 should be maintained.

This new model shall eliminate the shortcomings of the symmetrical approach and allow the separate shaping of the lower section of the curve ($D < D_{50}$) and the upper section of the curve ($D > D_{50}$), and at the same time keep the linearity around the D50.

This equation however has a step at the D_{50} point for $\alpha \neq \beta$ and is therefore not perfectly suited because such a step does not exist in real recovery curves.

To resolve this, the function $U_{\alpha\beta}$ is modified such that the weighted value of $T_{\alpha}(D)$ and $T_{\beta}(D)$ is in a linear relation to D . This leads to equation

$$V_{\alpha\beta}(D) = 1 - \frac{D}{k} \cdot T_{\alpha}(D) + \frac{D}{k} \cdot T_{\beta}(D) \quad \text{Equation 2}$$

When comparing results calculated from equation 2 against the recovery curves from hydrocyclones derived from actual data, it is observed that the shift of the influence of $T_{\alpha}(D)$ and $T_{\beta}(D)$ with the variation of D is not showing the desired shape around the D_{50} value.

To align equation 2 to the separation characteristics of a hydrocyclone, a solution is suggested that achieves results somehow between $U_{\alpha\beta}$ and $V_{\alpha\beta}$. In particular the shift in weight between $T_{\alpha}(D)$ and $T_{\beta}(D)$ must be balanced and set around the critical D_{50} value. After a critical review with actual results from practical experiences it was discovered that the Lynch-Rao equation itself is well suited as a suitable function for balancing the weighing around the D_{50} value correct. This leads to the *weighted two parameter Lynch-Rao function*.

$$W_{\alpha\beta}(D) = 1 - \gamma_{\alpha}(D) \cdot T_{\alpha}(D) + \gamma_{\beta}(D) \cdot T_{\beta}(D) \quad \text{Equation 3}$$

A reality check of equation 3 shows that for small values of D , $W_{\alpha\beta}$ is similar to $T_{\alpha}(D)$ and for large values similar to $T_{\beta}(D)$. This equation now nicely allows defining different shapes/slopes of the recovery curve for the upper portion of the

curve ($D > D_{50}$) and the lower portion of the curve ($D < D_{50}$) without having a step function around D_{50} .

This *weighted two parameter Lynch-Rao function* is now much more suitable to describe the partition curve of a hydrocyclone under varying water splits. It is suitable for both, simulating and analyzing hydrocyclone performance more precisely as when using the symmetrical model.

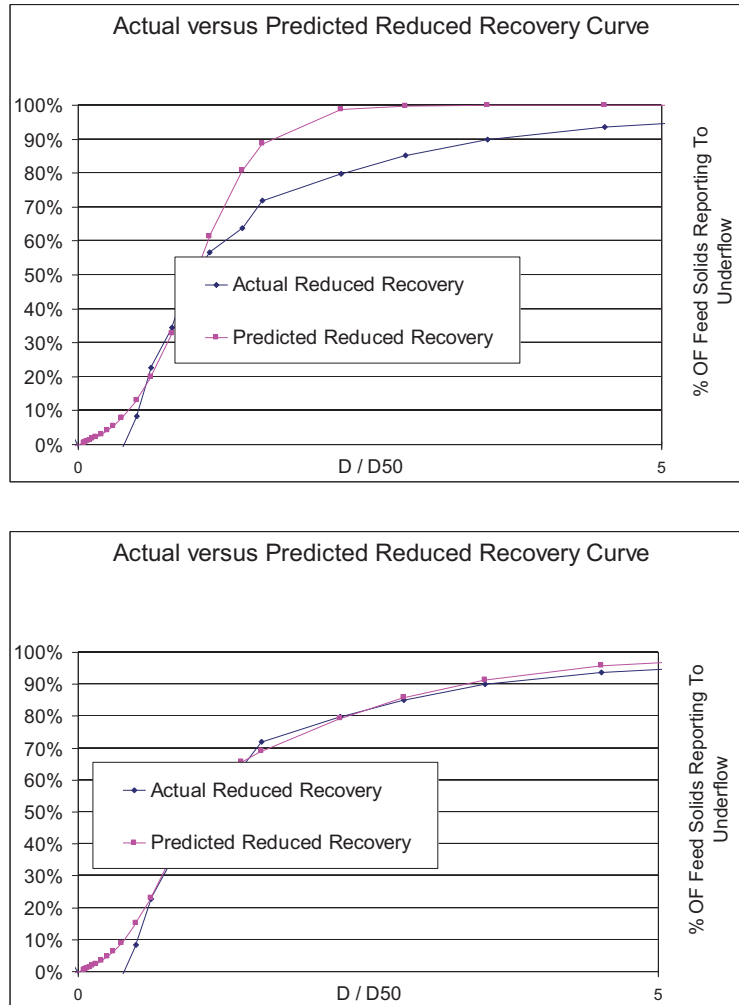


Figure 16: Actual versus reduced recovery curve with traditional and advanced model

Figure 16 shows the predicted curve with a symmetrical model ($\text{Alpha} = 3.5$) with a great discrepancy between the predicted and the actual curve and the lower graph shows the predicted curve matching the actual very well with the use of the introduced new model ($\text{Alpha} = 3.5$, $\text{Beta} = 0.7$).

2.4. Economical results

Continuously operating mineral processing plants generate remarkable cash flows. All operational and strategic efforts must strive towards the achievement of best operating practices as these directly translate to cash flow. The most important step to best practices is proper knowledge management and the understanding, recognizing, and growth of a firm's intellectual capital. A company's environment must be designed such that it supports innovation and the transfer of knowledge. Only with innovative and knowledgeable employees technical and structural changes for improvement can be leveraged. These changes lead to projects that have to be carefully evaluated by capital budgeting tools. The active managing of intellectual capital requires a working intellectual capital management system where all different intangible assets have to be evaluated in their context separately and then managed integrative in the desired direction. Surprisingly this is not a new concept as it had already been laid out 500 BC from the famous General Sun Tzu of the kingdom of Qi, in his strategy book:

"The unlighted ruler lays his plans well ahead; the good general cultivates his resources."

Two main technical approaches can be made on hydrocyclone economics. First the reduction of operating pressure which leads to savings in energy and maintenance cost. Second improved density regimes lead to improved separation and grinding circuit performance. There the economical result is improved recovery in the downstream processes and higher throughput in grinding circuits generating more product.

The benefits of both approaches can be summarized as follows:

- Improved recovery results in more product and enhanced revenues
- Higher recovery leads to better utilization of exhaustible, non-renewable resources and thus increases the amount of recoverable reserves on a company, national and global level
- Lower power requirements result in a reduction of operating costs leading to higher profits at given revenues
- Lower power requirements result in a reduction of power-related environmental effects, notably CO₂-emissions

2.5. Conclusions and evaluation of hypothesis

The conducted work has clearly shown that there is a definitive relationship between overflow quality and cyclone density regime in a closed grinding circuit.

Product quality and circuit throughput can be significantly influenced and controlled in plant operations.

Slurry viscosity, circulating load, D50 and the sharpness of separation are the main process parameters that can be modified successfully.

CHAPTER 3: Scientific background and state of knowledge

3.1 A brief history of hydrocyclones used in grinding circuits

The history of cyclones dates back to 1891 when Bretney obtained the very first patent for a hydrocyclone. The Bretney cyclone was designed with a closed Apex for intermittent discharge and was the forerunner to present day Desanders which are used for separating sand from water in pressurized systems.

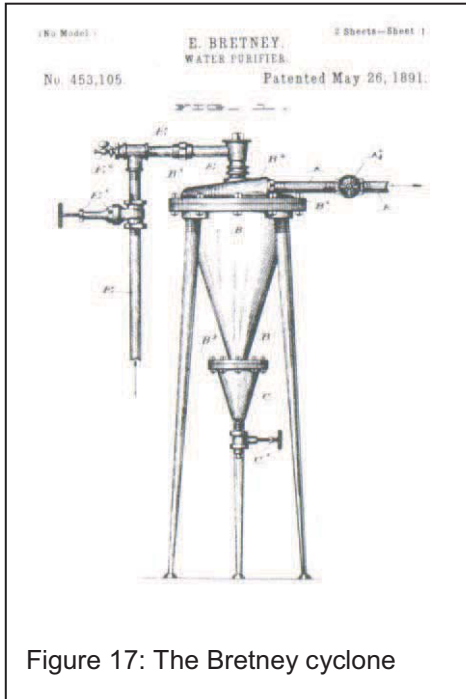


Figure 17: The Bretney cyclone

Between 1891 and 1939 a number of patents were granted but little commercial applications emerged from these.

The most dynamic development took place between 1939 and 1948 when M.G. Driessen of Dutch State Mines led the effort to develop cyclones for coal preparation.

1948 was a year of tremendous activity around cyclones around the world. Also at this time the cyclone was first introduced into the minerals industry and several industrial companies started to explore the commercial use of hydrocyclones in the minerals industry and

other disciplines. The use of cyclones in closed circuit grinding was pioneered in South Africa. In the 1948-1950, Anglo Vaal's Rand Leases Mine had a small mill that used cyclones. Steve De Kok published 2 papers on the application of cyclones at this mill that were used as the early "Bible". Some of the reasons cyclones were preferred in closed circuit grinding applications:

- High capacity and relatively small footprint for the larger tonnage mills.
- The underflow % solids produced from a cyclone was a good match for the preferred grinding mill pulp density.
- Preferential classification.

For copper mills the cyclones provided a higher flotation feed density that helped limiting the flotation cell volume required for the larger concentrators.

For the iron ore installations, cyclones were better able to provide the finer separations required for liberation in pellet plants.

Iron Ore

The first US application was on large (200 MTPH) pilot plants at Reserve Mining (1951) and Erie Mining (1953) on the Iron Range. There was also a small installation at Bethlehem's Pea Ridge operation in Missouri. These installations proved that cyclones had advantages over spiral classifiers.

In 1955-56 Reserve Mining installed 12" Dorr supplied (DSM design) cyclones. Also in 1955-56 Erie Mining installed "Home Made" 15 inch diameter cyclones built by the Gallagher Company. Following the first 2 installations and the acceptance of cyclones in the grinding circuit Krebs Engineers was able to place cyclones in the following iron ore concentrators:

- Reserve Mining (replaced all Dorr Cyclones), 1962
- Hanna Groveland, 1963
- Hanna Butler, 1965
- Hanna National, 1965
- Cleveland Cliffs, Empire, 1964

Copper

Early use of cyclones has been documented at Acoje in the Philippines (1955) and at Madjenpek in Yugoslavia and at Chuquicamata in Chile (1959-60).

The first major installation in copper was in 1956 at American Smelting and Refining Company's Silver Bell Concentrator. Cyclones were tested in the grinding circuit in 1955-56. Russ Salter, Mill Supt and Ed King, Metallurgist were open minded enough to replace relatively new twin 48" spiral classifiers with 4 model D20B Krebs cyclones.

Dorr got the initial order for 24" cyclones but because of very long delivery (1 year) Silver Bell turned to Krebs because they could deliver much faster and took the order from Dorr.

At the time the Silver Bell decision was made, the design of the Pima Mining Company Concentrator was being finalized. Pima was partially owned by Utah Construction (later Utah Mining) and the plant engineering group (now Flour Daniel) was located in Palo Alto. Their metallurgical department shared Krebs laboratory and Krebs Engineers kept them well informed about the work at Silver Bell. A last minute decision was made to retain the building design for classifiers

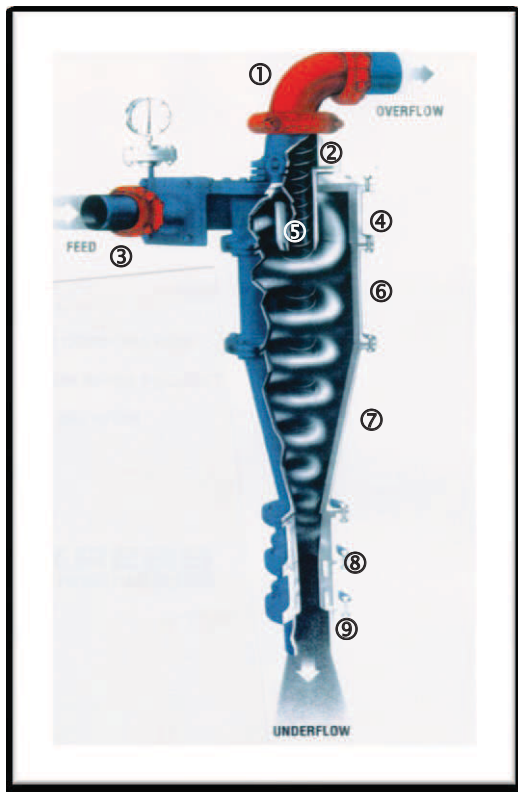
but install cyclones initially. If cyclones didn't work the classifiers could be put in. Krebs got their second major installation in 1956 at Pima Mining in Arizona. Kellogg Krebs, the company's founder, had the most significant impact on the company's early successes and especially the key installations at Silver Bell and Pima. Kelley spent 25 years working for American Cyanamid as a flotation reagent specialist. As a result of his worldwide travels he was personally acquainted with most of the key people in the mining industry.

After the success of the first 2 installations in Tucson, Krebs Engineers was able to install cyclones in the following copper concentrators:

- Kennecott, McGill, 1959
- ASARCO, Mission, 1961
- Inspiration, Christmas, 1962
- Kennecott, Hurley, 1963
- Anaconda, Butte, 1963

Today the hydrocyclone is the standard classifying device for all large grinding circuits around the world.

3.2. The basic function of a hydrocyclone



- ① Overflow Pipe
- ② Overflow Adapter
- ③ Inlet Adapter
- ④ Inlet Head
- ⑤ Vortex finder
- ⑥ Cylindrical section
- ⑦ Cone section
- ⑧ Apex or Spigot
- ⑨ Splash Skirt

Figure 18: Parts of a hydrocyclone

The cyclone is perhaps the most dramatic illustration of the old engineering axiom - the most efficient and dependable machines are those with the smallest number of working parts. With no moving parts at all, the cyclone is not only remarkably clean in design, but is also uniquely efficient in dynamic classification.

In a hydrocyclone, 4 different velocities can be distinguished. Radial velocity, tangential velocity, vertical velocity upwards and vertical velocity downwards, the latter two are separated by the zero vertical velocity locus.

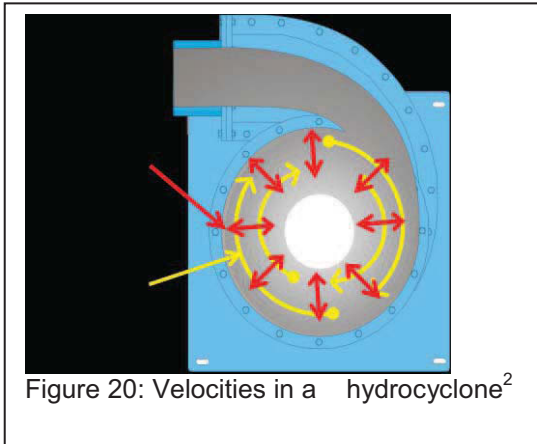


Figure 20: Velocities in a hydrocyclone²

When slurry is introduced to the inlet head, the linear motion of the pipe flow is converted into a circular flow in the inlet head. Once the centrifugal force impacts

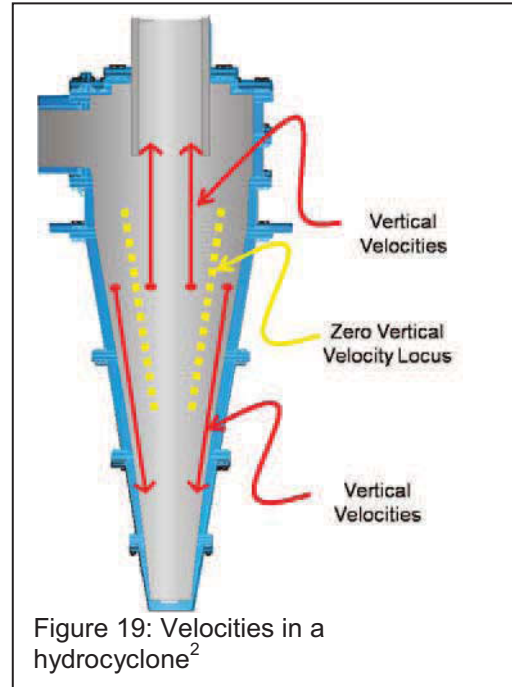


Figure 19: Velocities in a hydrocyclone²

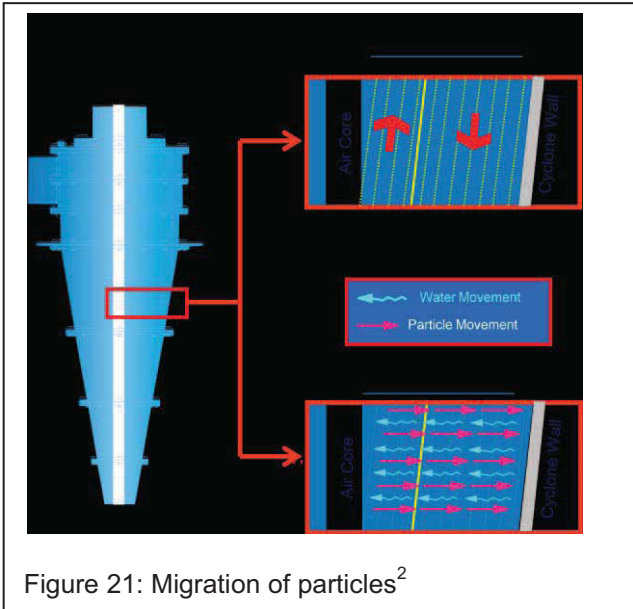


Figure 21: Migration of particles²

the particles, they start moving towards the outer wall of the cyclone. The larger or heavier the particle, the faster the radial velocity of each particle is. In the cyclone an inner ascending flow area exits through the vortex finder and an outer descending flow area exits through the apex, separated by the zero velocity locus. The particles are classified according to their settling velocity,

combined with the residence time

as well as other variables that will be discussed at a later stage. Large particles move very straight to the apex and small particles move very straight to the vortex finder. Fine particles move to the cyclone overflow. Ultrafine particles are split according to the water split. Near size particles orbit within the cyclones mixing/recirculation zone (see Figure 22) before finally being classified towards the overflow or underflow.

² Graphics by Robert Moorehead; FLS Krebs

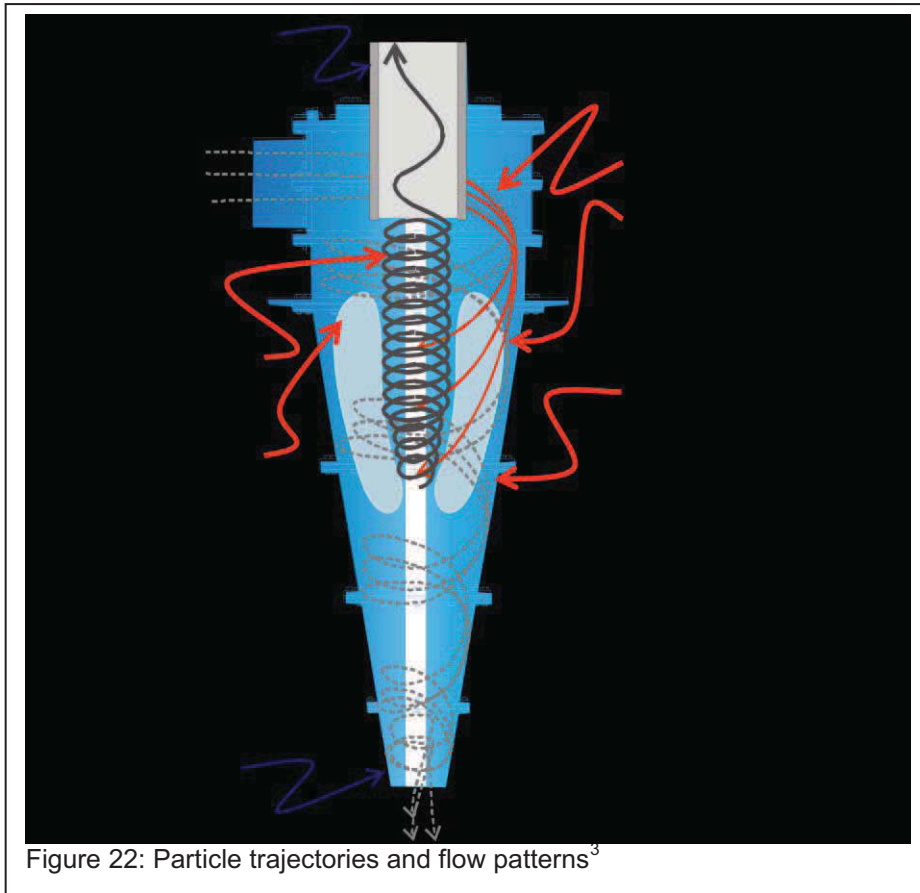


Figure 22: Particle trajectories and flow patterns³

Two types of misplaced particles exist – fines in the underflow which are carried

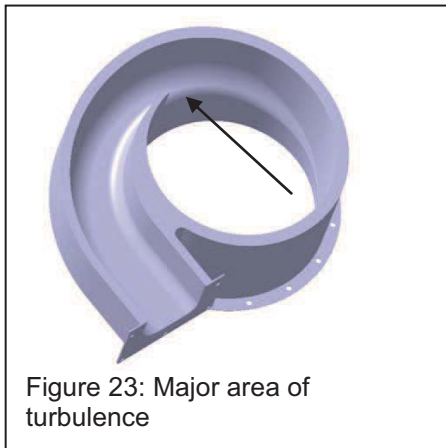


Figure 23: Major area of turbulence

with the water split (see also chapter 3.4.4.1.) or by drag forces from larger particles (aspect ratio) and coarse bypass to the overflow. Coarse bypass to the overflow is caused by turbulences in the inlet head and as a consequence all efforts are made from the industry to seek for designs minimizing this effect. The major area of turbulence (Figure 23) is at the end of the inner section of the feed chamber where the linear new introduced feed collides with the circular motion

of the slurry in rotation. Other causes for coarse bypass are of mechanical nature, like reverse steps, worn or disintegrated liners, misaligned parts or holes in the vortex finder.

³ Graphic by Moorhead R., FLS Krebs

3.3. Models for calculating hydrocyclone performance

3.3.1. Simple, fundamental theories that take little or no account of the effect of flow split, feed density and particle size distribution

The influence of hydrocyclone geometrical parameters is included in these types of models.

3.3.1.1. *The equilibrium orbit theory:*

The basis of the equilibrium orbit theory are particles of a defined size reaching an equilibrium radial orbit where their terminal settling velocity in the liquid is equal to the radial velocity of the liquid. The terminal settling velocity is usually based on Stokes law. All models do not take particle residence time into account. Also these models only produce reasonable predictions when applied to low feed solids concentration and equal or similar hydrocyclone geometry as used in the individual test work. Research work was conducted by Criner (1950), Driessen (1951), Bradley (1965) and Svarovsky (1984).

3.3.1.2. *The residence time theory*

The residence time theory assumes non equilibrium conditions and considers whether a particle will reach the outer wall of the cyclone in the available residence time. Various research work and different approaches were done by Rietema (1961), Holland – Batt (1982), Trawinsky (1969) and Kupetov (1977). All these models have the disadvantages that they only produce comparable and good predictions for low feed concentrations and only for similar geometry cyclones as used in the specific test work.

3.3.2. Two phase flow theory taking the effects of slurry feed density and mean particle size distribution into account

The effect of turbulences is integrated into these models, especially aspects modifying the tangential velocity profile. Early models were introduced by Rietema (1961), Ingham (1975) as well as Duggins and Frith (1987). More recent work was conducted by Schubert and Neesse (1980; 1984), these models are the first ones that also consider the effect of the feed solids concentration.

3.3.3. Crowding theory, considering also the effect of the apex diameter to cyclone performance

This theory suggests that the cut size is primarily a function of the capacity of the apex and the particle size distribution of the feed. Early work was conducted by

Fahlstrom (1960). From 1974-1980, Bloor, Ingham and Laverack, of Leeds University picked up the concept and refined it. Their model uses a correlation for the slurry viscosity as a function of particle concentration and is using concentration averaged across the boundary layer. The model allows plots of particle concentrations, volume fluxes and layer thickness around the boundary layer. Crowding theory is suggested to be valid in principle, however it cannot describe the effect of the underflow concentration quantitatively and the conditions of the cut off point (roping) are erratic.

3.3.4. Empirical models

These models are based on regression analysis of test data. Lynch and Plitt developed such empirical models; however the fit to cyclones different to the test cyclone used is difficult. Also these models are not based on any physical model and are therefore treated as non academic and it is said that their predictability is limited.

The author has to disagree with that opinion as the Krebs model which is based on test data in closed circuit copper grinding has served the industry for many years for cyclone simulation and sizing and shall be presented therefore.

Establishment of the cyclone D50:

Base D50:

Vortex Finder Diameter: _____

Inlet Head: _____

Pressure Drop:

Slurry Density: _____

Density of solids and liquid: _____

Various other factors like cone angle and combinations, cylindrical section, liquid viscosity, mounting angle (horizontal cyclones), SSC, Cyclowash, circulating load.

Establishment of the recovery curve:

In the Krebs model the recovery curve is approximated by the Lynch Rao equation. The combination of both, D50 and recovery curve is the basis of cyclone performance prediction.

$$T_{\alpha}(D) = \frac{e^{-\alpha \frac{D}{D50}}}{e^{-\alpha \frac{D}{D50}} + e^{\alpha}}$$

T(D): partition number for a selected particular fraction D

D: particular size fraction [μm]

D50: calculated D50 of cyclone [μm]

α : Alpha value

d_c : hydrocyclone diameter [inch]

d_v : vortex finder diameter [inch]

A: inlet area [inch^2]

Δp : pressure drop [psi]

TD: density correction factor []

V%: slurry density in volume %

ρ_s : density solids [kg/dm^3]

ρ_L : density liquid [kg/dm^3]

3.3.5. Chemical engineering approach, which is combining the above models

At Bradford University a dimensionless model was developed by experiment and not by correlation leading to a more reliable prediction of cyclones for various sizes and feed concentrations. It concentrates around 3 dimensionless equations which fully describe the function of a hydrocyclone within its operational limits. This model is the basis of many commercially available software packages for cyclone optimization. This theory and the available software is however more useful for plant optimization but is not really useful for green field cyclone sizing.

3.3.6. Analytical mathematical models of the flow patterns inside the hydrocyclone, particle trajectories including the boundary layer flow, the short circuit flow and the internal eddies.

These models describe the performance at low densities only.

The analytical flow models are based on mathematical solution of the basic flow mechanisms. Bloor and Ingham (1987) pioneered this discipline; however the models have been abandoned in favour of numerical simulation methods.

3.3.7. Numerical models using CFD

Instead of solving the equations of flow analytically, the methods of computational fluid mechanics can be used to develop numerical simulations of the flow. Work was done by Boyson, Ayers and Swithenbank (1987), Bloor, Ingham and Ferguson (1989), Rajamani and Milin (1992).

FLS Krebs has investigated the use of Computational Fluid Dynamics (CFD) as a development tool to eliminate the need to fabricate and test each new design concept. This tool would allow the evaluation of an increased scope of hydrocyclone geometries. Krebs currently follows a methodology that incorporates both CFD analysis as well as traditional fabrication testing methods to evaluate hydrocyclone designs.

The model used by Krebs Engineers has been validated to the degree that there is confidence it can be used to evaluate the expected relative difference in hydrocyclone performance between different hydrocyclone geometries. A higher order Reynolds stress turbulence model (RSM) provided the best agreement with velocity profiles. The air core has been successfully modeled using this tool and as a result the throttling effect of this on the underflow and overflow orifices has been defined. The flow-splits from an actual hydrocyclone test are very close to predicted flows from the model at two different vortex finder sizes. A CFD tool also provides the ability to track the path of various size particles along the internal hydrocyclone flow field. The particle recovery curve from the CFD model shows good agreement with the actual hydrocyclone performance measured in a controlled test. The CFD model predictions to different vortex finder sizes and the addition of other hydrocyclone geometry changes have also been in the correct direction and magnitude based on validation test results.

The CFD model has provided a means to evaluate the effect of design changes on component wear. The tool has the demonstrated ability to keep track of the number, angle and magnitude of particle collisions on the hydrocyclone internal surface.

The CFD model does have some notable limitations. The method chosen doesn't consider the effects of the particles on the fluid flow or other particle interaction

3.4. Evaluation of cyclone performance

3.4.1. Cut Point – D50

The D50 is that particle size that reports with a probability of 50 % to the overflow and with a probability of 50 % to the underflow of a classifier. The D50 is the common figure used to describe the cut point worldwide. The D50 of a cyclone does not depend on the feed particle size distribution. Very often other figures like a D95 or even a D99 are used to describe the desired separation for a classifier in an inquiry. These figures are somehow problematic as their location on the tromp curve are such that their positioning is in the top tail of the tromp curve. Below correlations values are used in the industry to covert such figures to a D50 value that can be realistically calculated when sizing a hydrocyclone:

ALPHA	D95	D98	D99
1.00	3.52	4.44	5.14
2.70	2.07	2.42	2.68
3.50	1.83	2.10	2.30
4.00	1.73	1.97	2.14
5.00	1.59	1.78	1.92
6.00	1.49	1.65	1.77

Figure 24: Recovery curve correlation values

Very often the D50 or D95 value is confused with a P80 value. A P80 value is very often a specification for a grinding circuit. Here the P80 value is describing the overflow particle size distribution of the closed circuit grinding product, which is the cyclone overflow. This P80 value depends on the D50 value of the hydrocyclone and the particle size distribution of the mill discharge.

3.4.2. EP and Alpha value

The probable error of separation or the Ecart Probable is commonly used to assess the efficiency of the separation for heavy media cyclones. It is defined as half of the difference between the D75 and the D25. The lower the EP, the closer the separation is to the ideal separation with a vertical line (EP=0).

Many prediction models for hydrocyclones use the Lynch Rao equation as shown below.

$$T_{\alpha}(D) = \frac{e^{\alpha \frac{D}{D50}} - 1}{e^{\alpha \frac{D}{D50}} + e^{\alpha} - 2} \quad \text{Lynch Rao Equation}$$

T(D): partition Number for a selected particular fraction D

D: particular size fraction [μm]

D50: calculated D50 of cyclone [μm]

α : alpha value

The alpha value is the free variable that can be selected to change the shape of the recovery curve. The curve is symmetrical around the D50 point and the pitch of the recovery curve can be changed by changing the Alpha value. The higher the Alpha value is, the better the separation. For normal cyclone operation an Alpha value of 3,5-4,5 applies.

3.4.3. Imperfection

Imperfection is a dimensionless number describing the sharpness of a separation and calculates as $I=EP/D50$. Imperfection is commonly used in the North African Phosphate processing industry.

3.4.4. The Recovery Curve (Tromp Curve)

3.4.4.1. *Introduction and Fines Bypass*

To evaluate the efficiency of a separation, the Tromp- or recovery curve is the best suited instrument to get comparable results to describe differences in the performance of separation devices as well as the difference in performance of a particular separation device run at different operating conditions.

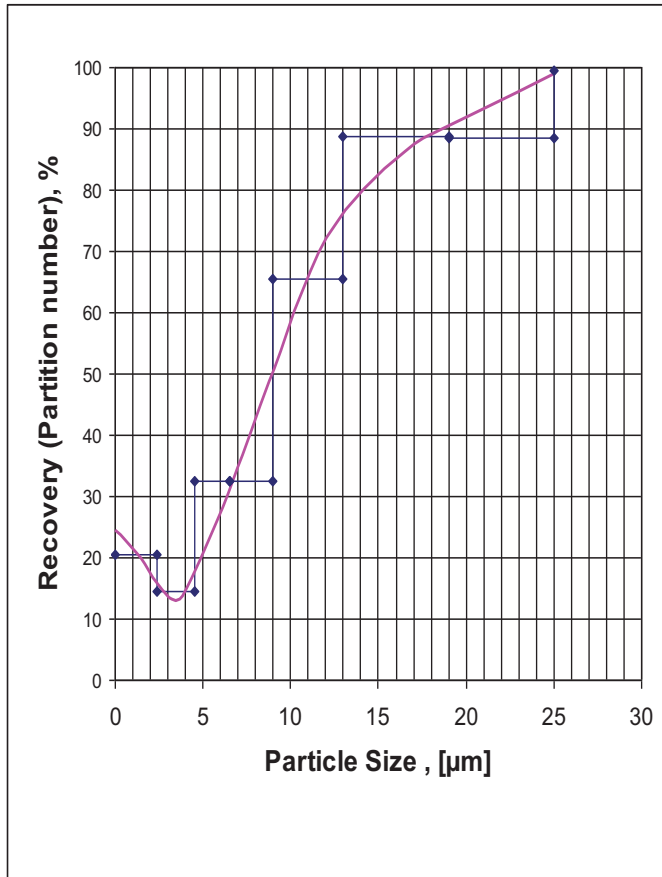


Figure 25: Typical recovery curve of a hydrocyclone⁴

A hydrocyclone has a least one partition curve for the particular matter or solids and a partition number for water (which is commonly used as process fluid). The water split is governed by the ratio between apex and vortex finder diameter as well as the feed pressure and the partition curve for the solids is governed by slurry rheology and the geometry of the cyclone. Also, on hydrocyclones a portion of particles is not classified by separation but is bypassing through the classifier. This bypassing is governed by the process water split. When looking at Figure 25 - a plot of a typical recovery curve of a hydrocyclone

- it can be seen that the fines fractions recovery has the same value as the water split. To get more comparable results, this bypass can be eliminated by calculating a corrected and a reduced recovery curve.

3.4.4.2. The Recovery Curve (Tromp Curve)

Tromp introduced 1937 the partition number $T_{\mu j}$ as a definition of the recovery for a particular category. With the fractional analysis of a particular category of the products of a separation, a partition curve can be calculated. This partition curve describes the quality of the separation with respect to the selected category and is specific to the separation device used. The partition curve can be calculated as follows:

$$T_{\mu j} = \frac{r_{mj} * i_{\mu j}}{m_{\mu}}$$

μ value of a fraction as description for a particular category

$m_{\mu j}$... mass of a particular category μ in product j

⁴ Vorlesungsskriptum Prof. Flachberger, Montanuniversität Leoben, 2010

$m_{\mu 0}$... mass of a particular category μ in feed

r_{mj} ... mass recovery of product j

$T_{\mu i}$... partition number of a particular category μ in relation to product j

If drawn up in a graph (see Figure 25), the partition numbers result in a step function. If the intervals of the fractional analysis are chosen infinitesimal small, this step function can be shown as a curve – the recovery curve.

The guideline for interpreting the shape of a recovery curve is: the steeper the curve, the better or sharper the separation (The perfect separation is a step function). The recovery curve is to a large extent independent from the feed material and the particle size distribution and can be used to describe the separation quality of a particular separation device.

3.4.4.3. The Corrected Recovery curve

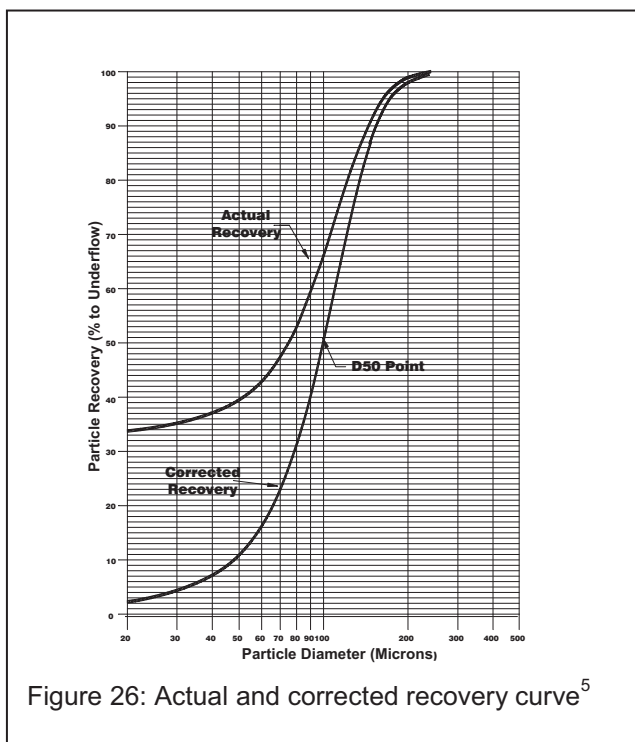


Figure 26: Actual and corrected recovery curve⁵

“Many hydrocyclone simulations or performance analysis use the term “corrected recovery curve”. A closer examination of the actual recovery plot shows that the curve does not reach zero on the recovery axis and furthermore this point changes from one application to another. If the point on the recovery axis for the small micron size material is compared to the percentage of liquid that is recovered in the underflow, it is found that they are approximately the same. Therefore, it can be assumed that if a given percentage of water in the cyclone feed is recovered to the underflow, at least an equal percentage of all solid particle sizes would be collected in the underflow in the same ratio. The curve can then be "corrected" for this percentage of material and shifted down to achieve a value of zero for the very fine particle sizes. This curve is also shown in Figure 26 as the corrected recovery curve. Kelsall (1953) suggested that solids of

⁵ Arterburn “The sizing of Hydrocyclones”, Krebs Engineers internal publication, 1976

all sizes are entrained in the coarse product liquid by short-circuiting in direct proportion to the fraction of feed water reporting to the underflow.”⁶

As a practical example we can assume that a feed contains 30 th⁻¹ of a certain size. If 20 th⁻¹ report to underflow the percentage of the normal partition curve is 66.67 %. If we now assume that 20 % of the feed water reports to the underflow, 20 % of the feed material will short circuit with it. Thus 6 th⁻¹ report to the underflow by short circuiting and only 14 th⁻¹ due to classification. The corrected recovery calculates as (20-6)/(30-6)*100 = 58.33 %.

The corrected partition curve can be described as follows:

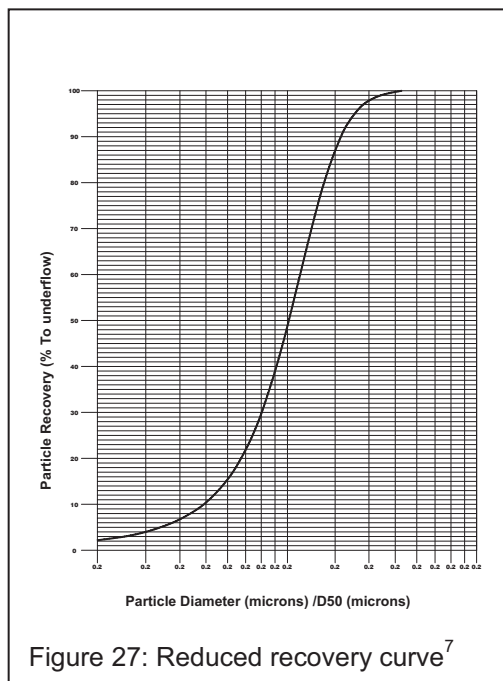
$$T_c = \frac{T - \lambda}{1 - \lambda}$$

T_c... corrected recovery of a particular mass fraction to the underflow

T..... recovery of a particular mass fraction to the underflow

R..... fraction of feed liquid that is recovered in the coarse product

3.4.4.4. The Reduced Recovery curve



“To further utilize this graph and make it applicable to any D50 point, each particle size is divided by the D50 value and a "reduced" recovery curve can be plotted (See Figure 27). Investigations have shown that this curve remains constant over a wide range of cyclone diameters when applied to a homogeneous solid of the normal size distribution. Krebs has completed additional tests which verifies this relationship and extends it to an even greater range of cyclone diameters.”⁸

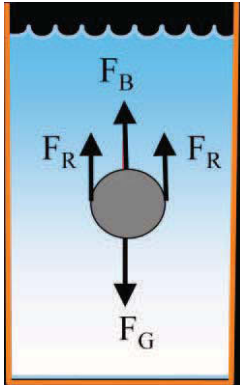
⁶ Wills B.A., Mineral Processing Technology, Elsevier Ltd, 2006, ISBN 978-0-7506-4450-1

⁷ Arterburn, The sizing of Hydrocyclones”, Krebs Engineers internal publication, 1976

⁸ Arterburn, The sizing of Hydrocyclones”, Krebs Engineers internal publication, 1976

3.5. Variables effecting Hydrocyclone performance

The separation principle of a hydrocyclone, the equal settling velocity of a solid in a fluid, is governed by 3 major forces, being gravity, buoyancy and resistance (Figure 28).



Buoyancy: $F_r = V \times \rho_l \times a$

Resistance: $F_r = 3 \times \pi \times d \times v^2$ (Stokes)

$F_r \equiv k^2 \times \rho_l \times v^2$ (Newton)

Gravity: $F_g = V \times \rho_s \times a$

With: $a = v_i^2 / r$

Figure 28: Forces on a particle

The superposition of these 3 forces ($F_G = F_B + F_R$) allows the calculation of the settling velocity of a particle in a liquid.

Equation 1: Stokes

$$v \equiv \frac{d^2 \times v_i^2 \times (\rho_s - \rho_l)}{r \times \rho_l}$$

Equation 2: Newton

$$v \equiv \sqrt{\frac{d \times v_i^2 \times (\rho_s - \rho_l)}{\rho_l}}$$

Equation 3: Reynolds Number

$$Re = \frac{d \times v \times \rho_l}{\eta}$$

(Assumption the particle is a sphere: $V = 1/6 \times \pi \times d^3$)

- a radial acceleration [m/s²]
- v settling velocity of a particle [m/s]
- V volume [m³]
- v_i cyclone inlet velocity [m/s]
- r cyclone radius [m]
- k side length of a cube [m]
- d diameter of particle [m]
- η dynamic viscosity [Ns/m]
- ρ_l density of liquid [kg/m³]
- ρ_s density of solid [kg/m³]

The approach for laminar flow using Stokes equation is valid for Reynolds figures below 10^{-1} , with an acceptable upper limit of $Re = 0.2$. This represents flows with particles smaller than 40 microns. For larger particles and Reynolds figures greater than 10^3 , flows are turbulent and Newton's law applies, however the following evaluations and principles will be described with Stokes approach.

When closely looked at, equation 1 describes most of the variables effecting cyclone performance, which is particle size, inlet velocity (or cyclone feed pressure), density difference between solids and liquid, cyclone diameter and slurry viscosity. The remaining variables that influence cyclone performance are cone angle and cone combinations, other geometrical variables like cylinder length, vortex finder diameter, apex diameter, circulating load in closed circuit grinding systems, and the manifold distribution system.

3.5.1. Particle Size

The larger the particle, the higher is the settling velocity. This means that larger particles do reside closer to the outer wall of a cyclone and get discharged to the underflow, versus finer particles do reside more towards the air core of the cyclone and get discharged to the overflow.

3.5.2. Inlet velocity

The inlet velocity is proportional to the feed pressure at a given inlet head diameter. The higher the inlet pressure, the higher the inlet velocity and the finer the D50 of separation will be. For some cyclones various sizes of inlet heads are offered – the smaller the opening, the higher the inlet velocity and the finer the separation. The finer separation due to a smaller inlet head diameter however is earned at the cost of a lower hydraulic capacity.

3.5.3. Solid/Liquid density

The density difference of solids and liquid is governing the settling velocity – the higher the differential, the finer the separation is. It must be kept in mind that a cyclone cannot distinguish particles with an equal settling velocity. This means that large size low density particles are classified at the same D50 as smaller particles of higher density. Keeping this in mind is important for multi phase cycloning and prediction modelling. See also 3.6.4. preferential classification.

3.5.4. Cyclone diameter and up scaling

The D50 of a cyclone varies with its diameter. The greater the diameter, the coarser separation is. This is very often a phenomenon that is not understood correct in the industry. Usually laboratory test work is done with small diameter cyclones and big mistakes are made when up scaling these results to industrial sizes. Test work can only be successfully conducted with the cyclone that fits the separation. As a consequence most coarse and high flow separations can only be simulated with software as laboratory testing or even pilot plant testing cannot handle the high flows required to operate larger diameter cyclones.

3.5.5. Slurry Viscosity

In practical and well as in theory, the slurry viscosity has the biggest influence to cyclone D50. The viscosity depends on the base viscosity of the process liquid, the slurry density and the particle size distribution. With the fineness of the particles and with elevated slurry density, the viscosity rises. The slurry viscosity is the most unknown variable when sizing a green field application and a vast experience on existing installation is the basis for successful cyclone sizing.

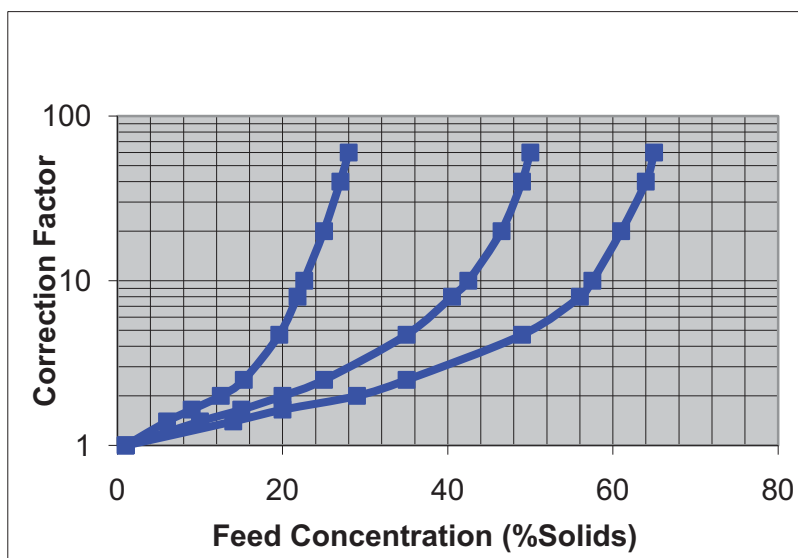


Figure 29: Slurry viscosity versus slurry density

Varying the slurry density is the most powerful tool in a plant. A variation of 5 percent points only, can change a cyclones D50 substantially. No other change can create a bigger effect on cyclone separation. Figure 29 is an excerpt of a FLS

Krebs manual, showing multipliers of for D50 relative to slurry density and viscosity systems. The curves apply to primary grinding circuits (right) for regrind circuits (middle) and tailings (left).

3.5.6. Circulating load

Slurry viscosity plays a big role on closed circuit grinding. The higher the circulating load, the lower the viscosity is. Mill feed consists of perfectly deslimed, low viscosity cyclone underflow and slimes rich, high viscosity new feed. The higher the ration of deslimed cyclone underflow is, the lower the viscosity in the total system will be. Just to give an example, in a grinding circuit with a circulating load of 300 %, 75 % of the total mill feed is deslimed cyclone underflow.

3.5.7. Cylinder Length

The longer the cylindrical section in a conventional cyclone is, the longer the residence time of a particle becomes in the cyclone. This results in a finer separation and a slightly higher hydraulic capacity of the cyclone.

3.5.8. Vortex Finder Diameter

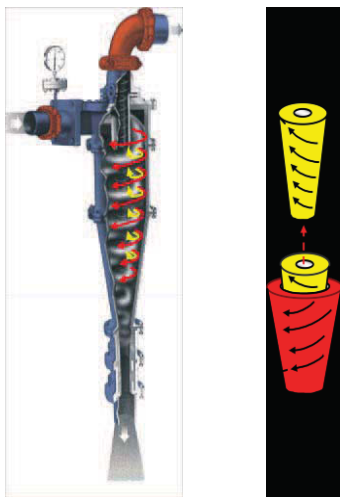


Figure 30: Flow patterns⁹

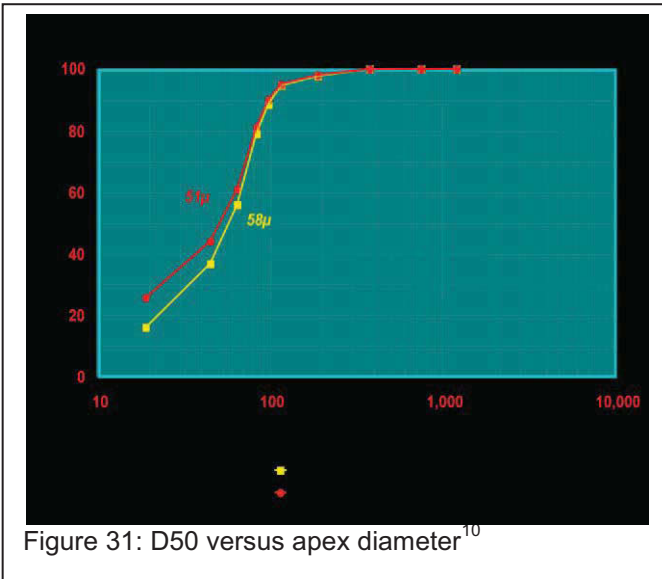
The vortex finder diameter governs in combination with the apex diameter the flow split to the overflow. The larger the vortex finder is, the larger the area within the cyclone (see yellow portion of Figure 30), that reports to the overflow. The larger the diameter of that area is, the closer the boundary of the uprising and the down rising current gets toward the outer side of the cyclone. As elaborated in 3.5.1 coarser particles will report as a consequence to the overflow product.

3.5.9. Apex Diameter

The apex diameter is probably one of the most misunderstood parameters on hydrocyclones. What the apex diameter does is governing the water split in a hydrocyclone (at a given vortex finder diameter). The variation of the apex diameter will not affect the cyclone separation directly, but the water split only and the underflow density. The D50 of the cyclone will be affected when the cyclone starts roping when the apex diameter is too small (see 3.6.3.), however a small impact on cyclone D50 must be noted. The lower tail of the tromp curve is shifted by varying the apex diameter, and as a consequence the water split, and thus the

⁹ Graphic by Moorhead R., FLS Krebs

D50 is slightly shifted because the overall tromp curve is shifted as well as illustrated in Figure 31.



3.5.10. Cone angle and cone combinations

On conventional hydrocyclones cone angles of 4°, 6° and 12° on diameters of 150 mm and smaller are standard, on larger diameter cyclones 20° and 10-11° are common. The longer the cone section, the longer the residence time of the slurry is in the cyclone and the finer resulting the separation is. The concept of multiple cone section will be presented in chapter 3.6. An exception is the so called flat bottom cyclone which is described in chapter 3.7.

¹⁰ Graphic by Moorhead R., FLS Krebs

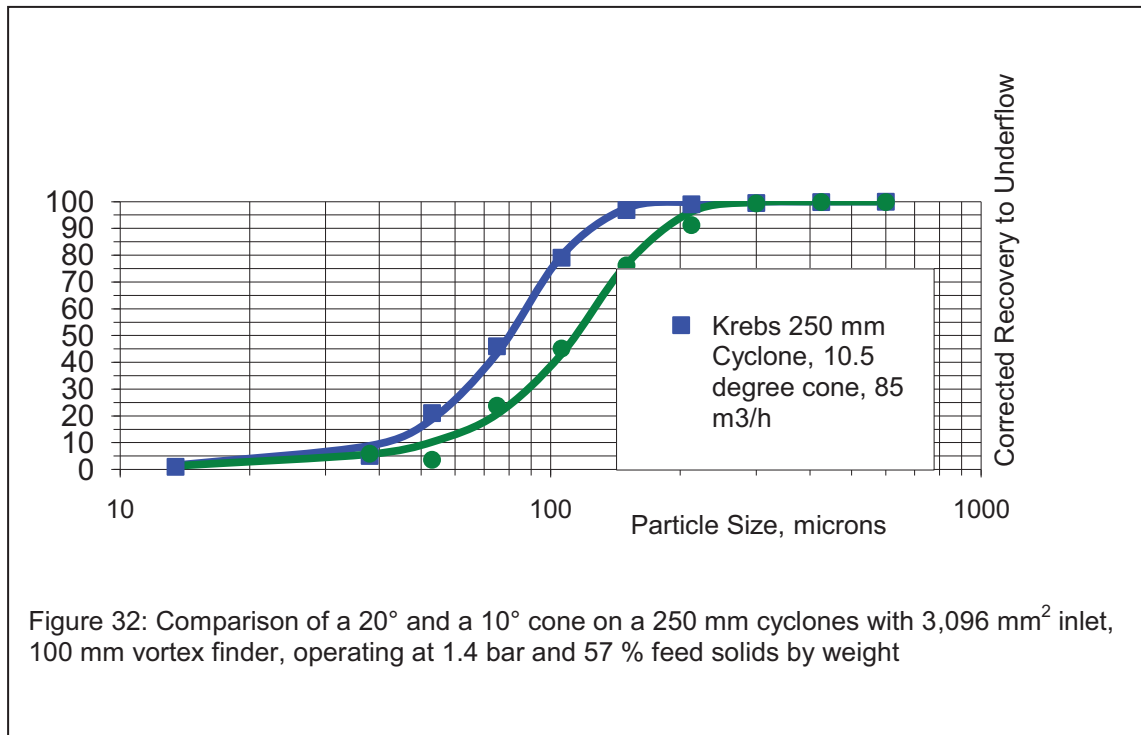


Figure 32: Comparison of a 20° and a 10° cone on a 250 mm cyclones with 3,096 mm² inlet, 100 mm vortex finder, operating at 1.4 bar and 57 % feed solids by weight

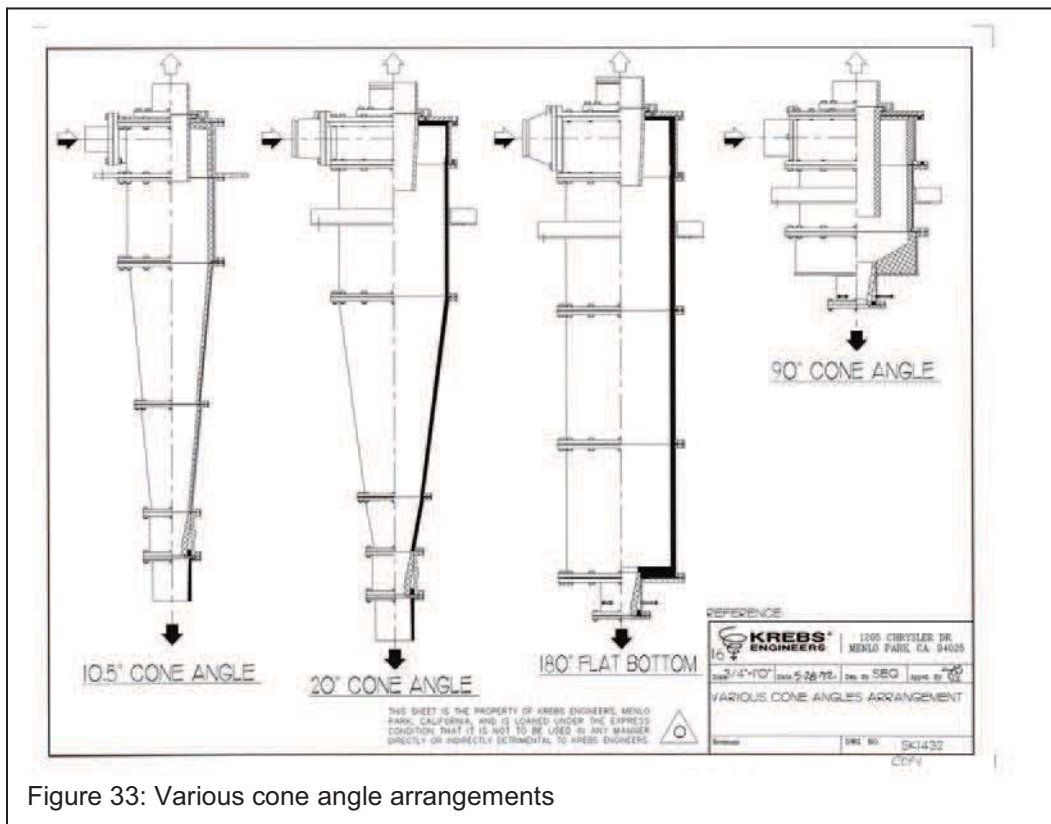


Figure 33: Various cone angle arrangements

3.5.11. Manifold distribution system

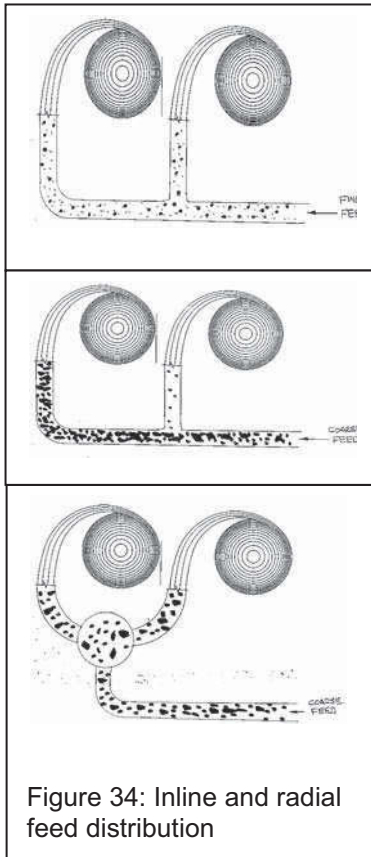


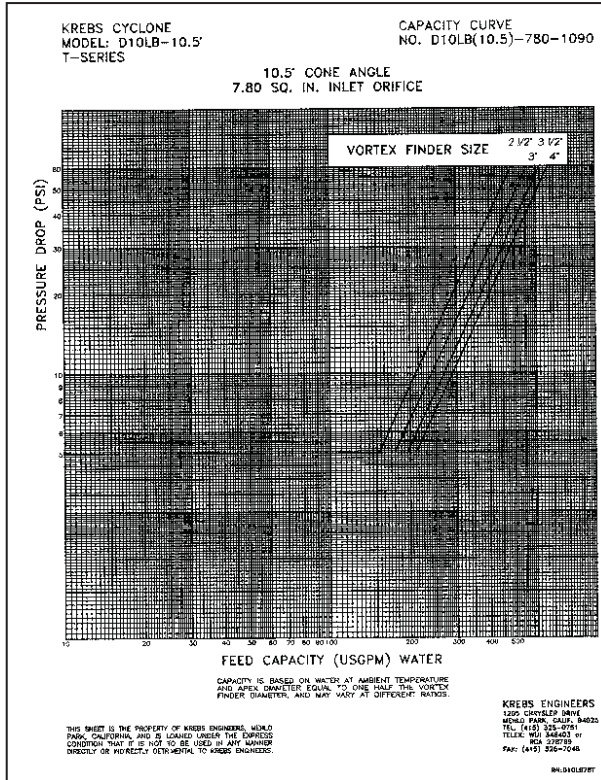
Figure 34: In-line and radial feed distribution

A manifold distribution system is needed if the process requires more than one operating cyclone to handle the total slurry flow. As indicated in 3.5.4., for specific operating conditions and required separations a certain cyclone diameter has to be selected to achieve the required performance. As cyclones are limited in flow (see also 3.6.1.) many systems require a multiple number of cyclones. The role of the manifold system is in first place providing an even slurry flow, pressure, density and particle size distribution to each individual cyclone. For very fine particle sizes, combined with low solids concentrations, in line systems can be used, for a mixture of fine and coarse particles and higher slurry densities only radial systems can realize these requirements.

3.6. Selected Chapters of cyclone Theory

3.6.1. Cyclone Capacity

The capacity of a hydrocyclone depends on the cyclone diameter, inlet area, vortex finder diameter and the pressure drop. The capacity of conventional hydrocyclones (20 and 10° Cones) is calculated with below formula:



$$Q = 8,7 \times P^{0,5} \times A^{0,5} \times D_v^{0,75} \times D_c^{0,14}$$

- Q capacity in USGPM
- P pressure drop in PSI
- A inlet area in sq.inch
- D_v inner diameter of vortex finder
- D_c inner diameter of cyclone

In practical, capacities of cyclones are tested with water throughput and as a result capacity curves are plotted. Instead of plotting capacity curves,

Figure 35: Hydrocyclone capacity curve
the following relationship can be used to calculate cyclone capacities based on test work with water:

$$Q = k \times \Delta p^{0,5}$$

- Q capacity in USGPM
- k factor established for a cyclone with a defined inner diameter, inlet area and vortex finder diameter
- Δp pressure drop in PSI

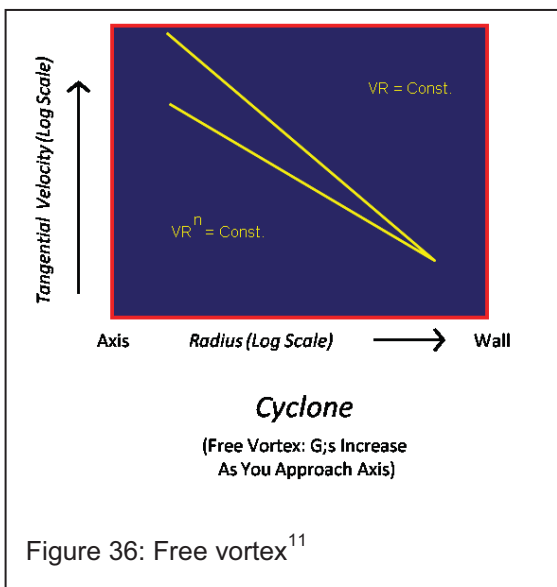
Sufficient empirical data has shown that the hydraulic capacity of hydrocyclones increases with increasing slurry density. Based upon empirical data analyzed from a number of closed circuit grinding circuits, the volume of solids reporting to the cyclone underflow product may be disregarded when defining the feed capacity to pressure drop relationship for a given application. So the underflow solids volume should be deducted from the cyclone slurry feed volume when ascertaining the pressure drop across the cyclone in a water based capacity curve. This results in a

higher capacity on slurry in the range of 5-9 %. This correction for higher slurry densities is of utmost importance for closed grinding circuit calculations as these circuits are always operated at elevated slurry densities.

3.6.2. Horizontal Cyclones

Mounting a large (≥ 380 mm in diameter) cyclone horizontally (15-45 degree from horizontal) reduces the static head that is present compared to a vertical mount at about 2-3 meters. With the vertical head reduced, the apex is no longer critical, and the cyclone can be operated with a larger apex with maintaining a high underflow density but with a greatly reduced risk for roping and plugging the apex. By this the difficulty of cyclone operation with swings in the feed volume is eliminated. With the reduction of the slurry velocity (by eliminating the energy from the static head) the wear on the cyclone liners is greatly reduced. Horizontal cyclones do have a coarser separation compared to vertically mounted cyclones, because there is less energy available for the classification process. This factor is used to coarsen up separations and to optimise wear and operational stability. Compared to a D50 of a vertical cyclone, a cyclone installed at 45° has a D50 that is 1.1-1.5 times coarser, and a cyclone installed at 30° a D50 about 1.2 times coarser.

3.6.3. Air Core, discharge patterns and Roping, Apex sizing



The free vortex condition that is needed for the functionality of a hydrocyclone is established by an air core around the axis of a hydrocyclone starting at the apex orifice and ending at the end of the overflow pipe. This air core is transporting air by sucking it in at the bottom and discharging it in the overflow. Under this condition a hydrocyclone will show a characteristic spray discharge. Other discharge patterns like roping lead to unstable operating conditions and finally to the blockage of the

hydrocyclone. Rope discharge can be initiated by increasing the mass flow of solid to the underflow or be reducing the diameter of the apex orifice. Then the air core

¹¹ Graphic by Moorhead R., FLS Krebs

collapses and this leads to a significant change of the shape of the underflow discharge. The flow is of cylindrical nature and has the physical appearance of a rope. There are numerous models on roping and air core diameters found in the literature from researchers like Yancey and Geer, Fitch and Johnson, Driessen and Fontein, Tarr, Abott, Mular and Jull, Plitt, Jull and Plitt, the SPOC model and Bustamante. The latter one is of more practical importance and shall be mentioned in this work.

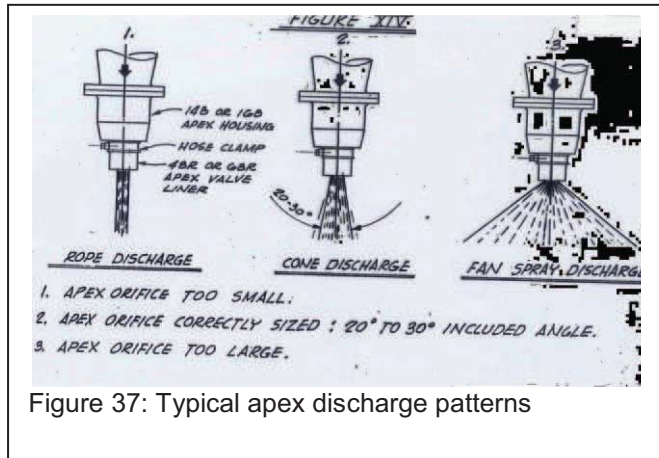


Figure 37: Typical apex discharge patterns

Bustamante investigated the discharge of hydrocyclones by operating them with water only. The experiment was conducted such that he started running a cyclone with water only at very low pressure, then increasing the pressure until normal overflow and underflow was established and finally elevated the pressure so that no water was escaping through the apex. By altering the vortex finder to apex diameter ratio he found out that at ratios of 0.34 and larger always a small portion of water was discharged through the apex. He further showed that if he operates a hydrocyclone with slurry at the same experimental conditions no discharge was obtained with water, roping occurred when running with slurry. The following ratios were developed for spray and rope discharge:

- | | |
|-------------------------|---|
| $d_u/d_o < 0.34$ | always rope discharge |
| $0.34 < d_u/d_o < 0.05$ | rope or spray discharge depending on pressure and other variables |
| $0.5 < d_u/d_o < 0.9$ | always spray discharge |

The relationship that Bustamante found is not universal, but would apply only to the cyclone he was testing with a specific diameter, cylinder length, cone angle, and mounting orientation (vertical versus laid over). For example if a 250 mm cyclone with a 20° cone is set up a vertical with a 4 inch vortex finder and 2 inch apex and operated at 10 psi approximately 8 % of the water will be going to the underflow. If the pressure is increased to 15 psi the water might go to zero. If a 10 degree cone is installed on the same cyclone, then 14 % of the water might report at 10 psi and 5 % at 15 psi. Further on a 26-inch cyclone with a 10-inch vortex finder and 5 inch apex 25 % of the water at 10 psi would report to the underflow, but if the cyclone is laid over to 11.25 degrees only 10 % would discharge through

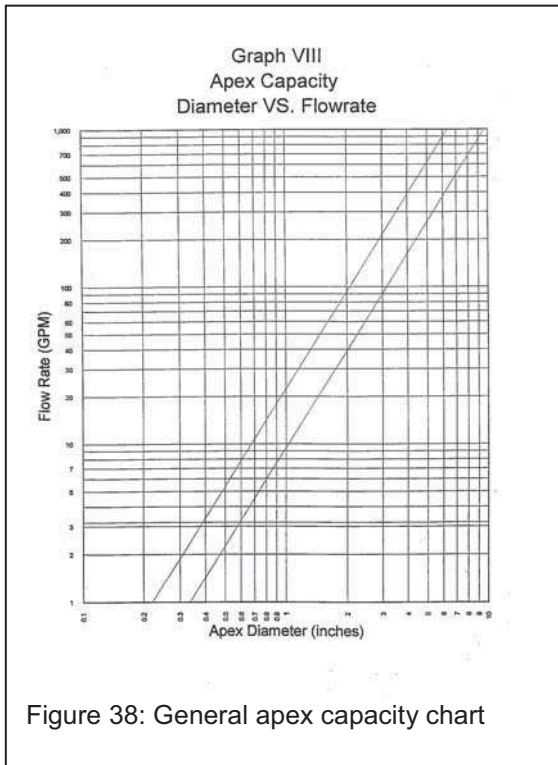


Figure 38: General apex capacity chart

the apex. Wemco and Krebs have conducted extensive research work and testing on that subject and have empirically developed apex capacity charts for each individual cyclone with various vortex finders and pressure drops. For each cyclone type and size of Apex such a capacity curve was established, see figure 39.¹²

Summarizing the above, there is no model that can really fully explain roping. All current models are based on small diameter cyclone laboratory test work which is not relevant for an industrial application as up scaling to larger diameter cyclones is not possible. Within

the industry these ratios are a fluid opinion but in general at a ratio of 0.4 to 0.33 the separation will begin to coarsen. The vortex at the apex strengthens as the ratio goes up. Also it has been experienced that the separation coarsens once the water split is less than 8 % of the feed water reporting to the underflow.

When roping the classification of a cyclone collapses completely and coarse particles are discharged of to the overflow. This leads to catastrophic consequences in downstream processes like flotation or leaching.

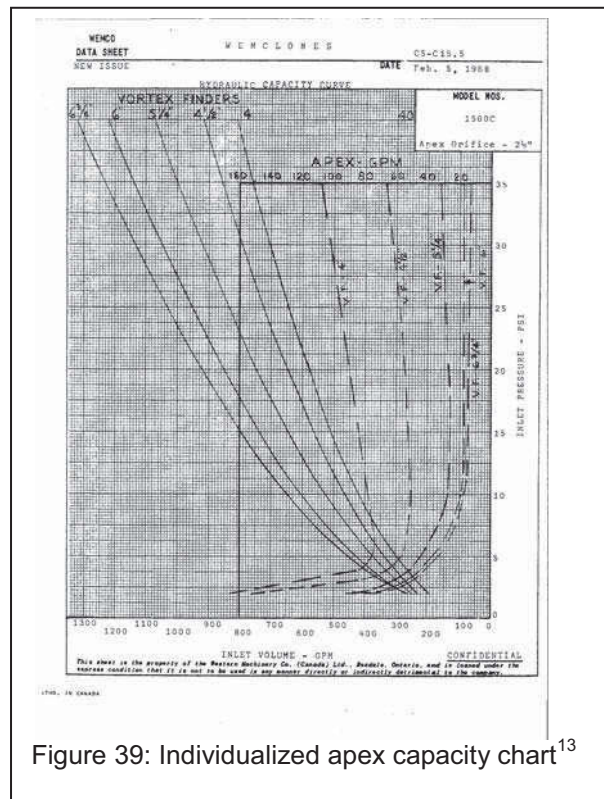


Figure 39: Individualized apex capacity chart¹³

¹² Arterburn., The sizing of Hydrocyclones, Krebs Engineers internal publication, 1976

¹³ Wemco/Sacramento, 26" cyclone – hydraulic test results, internal memo 20, January 1977

At the same time, cyclone separation efficiency is at the highest just ahead of the roping condition as the fines bypass is at its minimum. Therefore the establishment of a save operating condition close to roping, but not too close to enable the cyclone and the operator to handle flow fluctuations in the plant is of utmost importance. As a rule of thumb from Krebs an underflow density of 50-51 % by Volume for cyclone underflow in grinding circuits is such a safe but optimized operating condition.

Usually when cyclones are sized any model would calculate an underflow volume stream at a set slurry density. Correct apex sizing for such volume streams can be obtained in figure 38.

3.6.4. Preferential classification

Because of the nature of the classification of a hydrocyclone (principle of equal settling velocity), the device is able to differentiate particles of the same size, but different density. This is an important advantage in closed circuit grinding with heavier valuable minerals and lighter gangue minerals, like in the grinding of porphyry copper ores. Lighter gangue particles leave grinding circuits directly through the cyclone overflow and frees up capacity in the circuit as gangue minerals are not ground to final grind size. High specific gravity middle sized particles are preferentially classified to the cyclone underflow and returned back to the mill for further comminution and liberation. The benefit of preferential classification to porphyry copper grinding circuits was analyzed by P.A. Turner and D.D. Schlepp in their paper "Influence of Circulating Load and Classification Efficiency on Mill Throughput", in 1990.

3.7. Cyclone design and development

Cyclone design and development can be divided into three major disciplines:

- Sharper separation: reduction of misplaced particles in the overflow.
- Finer Separation: finer separation combines with high hydraulic capacity.
- Cost and ease of ownership: assisting operators and maintenance personnel to optimize cyclone operation and reduce total cost of ownership

3.7.1. Sharper separation

The main cause for misplaced particles in the cyclone overflow is turbulences in the inlet head. Tremendous research work has been undertaken to optimize the geometry of inlet heads. The first hydrocyclones had tangential inlets, followed by scrolled (Multotech) and involuted designs (Krebs), and outer wall ramped designs (Warman). The 3 latest developments of inlet heads in the industry shall be presented.

In the eighties the Krebs involuted feed entrance introduced the feed stream into the cyclone through a long, “swept” inlet as a narrow ribbon of feed. In order to separate solids and concentrate them in the cyclone underflow stream, they must first make their way to the outer wall of the cyclone. Unlike a tangential feed nozzle that introduces some solids near the axis of the cyclone (requiring them to travel a long distance to reach the wall), involuted feed nozzles pre-classify the feed by introducing all of the feed near the cyclone wall. This results in sharper separations.



Figure 40: Warman inlet head

Around 1993 Warman introduced the outer wall ramped design. This design introduced a new feature – the inlet stream was extended in the cyclone by a ramp that allowed the solids to a smooth transition from the horizontal flow to the downward spiralling motion once entered into the cyclone. This design was a tremendous step forward to sharper separation. The downside was a relatively low hydraulic capacity and relatively short life time due to wear caused by the wide angle between the two slurry streams around the inlet horn. In 2000 Krebs countered with the ramped involuted inlet head with the introduction of the second generation of gMAX hydrocyclones.

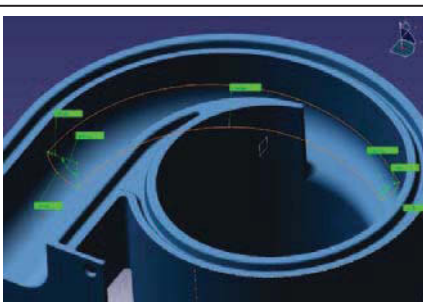


Figure 41: Krebs gMAX inlet head

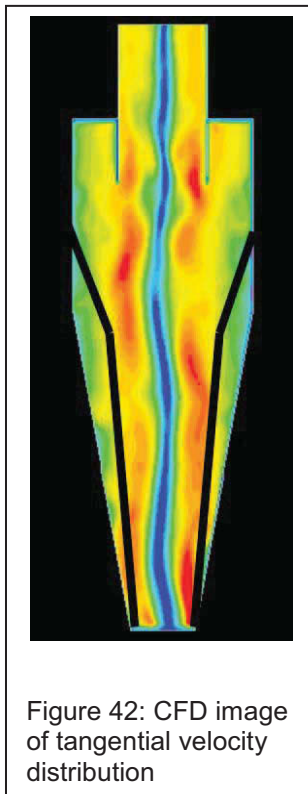
This head was developed first time in the industry with the assistance of computational fluid dynamics (CFD). The slurry was now introduced at such an angle into the cyclone

that the slurry stream continues without any change in pitch into the downward spiralling motion, supported by a ramp. Because of the long swept involute the angle at the inlet horn is very sharp, minimizing the development of eddy currents.

This design combines the traditional high capacity involute design with low turbulences, sharp separation and long wear life, extending the wear life by 100 % compared to standard involute style inlets and by 30-60 % compared to ramped outer wall inlets. Practical testing and comparisons were made with paint test – see chapter 3.6.4.

3.7.2. Finer separation

The main separation work in a hydrocyclone is done in its conical sections. The



first hydrocyclones were equipped with 20 degree cones. This applies for hydrocyclones of diameter 250 mm and larger. Smaller cyclones traditionally were equipped with 12°, 6° and 4° cones. The next generation of cyclones were furnished with 10-11° cones. This was a major step forward in separation as these cones provided a 15 % finer separation (D50) combined with a 40 % (!) higher hydraulic capacity. In the late nineties Krebs started investigating cyclone separation with the help of CFD. Figure 25 shows a CFD image of the tangential velocity distribution in a hydrocyclone. This image shows very clear high and low velocity areas. The idea was to create a cyclone shape that excludes the low velocity areas as shown by the black lines. The gMAX design consists of a steep upper cone that accelerates the slurry to a very high velocity, followed by long conical sections with increasing cone angles to provide a long residence time in a high velocity area. The

gMAX cone combination provides a 35 % finer separation compared to 20 degree cones and a 20 % finer separation with matching capacity compared to 10 degree cones. This benefit can now be utilized in two ways. First a large hydrocyclone can now be used for fine separations resulting in less larger cyclones and a cheaper and maintenance easier installation. The second possibility is financially interesting as hydrocyclones can be operated with extreme low pressures (0.35 – 0.4 kPa) which reduces pumping cost significantly and increased the lifetime of cyclone liners and pump wet end parts.

3.7.3. Modular design

Modern hydrocyclones are built in a modular system that allows the interchangeability of parts. For example, cones with different angles etc. can be

installed on the same cyclone body. Each individual section is furnished with an exchangeable liner that is available in various materials. Today all types of elastomeres and ceramics are available to build a cyclone to be resistant against chemical attack and wear. Monolythic Ceramic liners are preferred above tile lining because of their better wear resistance and less creation turbulence.

The research and development today is focussed on automation around hydrocyclones, such as wear indicators that report liner thickness into plant systems and maintenance planning as well as roping sensors that indicate the proximity of hydrocyclone roping (and the risk of plugging) and, if linked to a plant control system, initiate counter measures to avoid getting into this operational mode.

3.7.4. Product development using CFD at FLS Krebs

Historically cyclone manufacturers have relied on experience to provide the basis for estimating hydrocyclone performance. The effects of different hydrocyclone geometries, most notably cone angles and orifice sizes, have been documented and the effect of the difference in geometries is generally expressed as a function of a change in the expected cut point or D50 that the hydrocyclone will provide. Some geometry changes will have a more pronounced effect on coarse particle flows within a hydrocyclone and the very fine particles will respond much differently. Empirical models therefore are not always adequate to evaluate the effects of the different and varied geometric modifications that are the focus of modern product development programs. Recent changes in hydrocyclone design have shown the effect that geometry changes can offer (Olson, 2000).

Computational Fluid Dynamics (CFD) has revolutionized the way fluid dynamics is practiced and has become a preferred development tool where the flow of a fluid is important. The use of CFD has lagged in mineral processing applications primarily because of limitations of the algorithms to solve problems with a high concentration of solid particles. However, a large amount of information is available from investigating hydrocyclone fluid dynamics at lower solids concentrations.

The task for the Krebs Engineers group was to evaluate the difference in the flow fields from hydrocyclones with different cone angles to explain the different expected performance. What was initially a single-phase problem quickly became a multiphase problem with the air core approximated and was run using a k-epsilon turbulence model in the interest of time and computational speed (Oluwole

et al, 2001). The tangential velocity profile shown for the flow field was a forced-vortex type not the Rankine-type vortex that has been documented by Kelsall (1952) and further by Petty (2001) and others.

Krebs went on to work with CFD specifically to study inlet head design. Further complications appeared since this software was not able to use the higher-level turbulence models with the unstructured mesh required to approximate the fairly complex inlet head geometry. The turbulence model selection was proving to be critical for solving the highly swirling flows within a hydrocyclone. We have a model that has been validated based on several criteria including hydrocyclone performance and have constructed a matrix of mesh geometries that cover the range of Krebs hydrocyclone models and sizes. The initial industrial problem — to study the flow field response with cone angle changes — was successfully completed as a result of the validation process for this model.

Inlet Head Design

The new inlet head liner for the 250 mm Krebs hydrocyclone will be used as an example of the methodology used at Krebs Engineers to test a design concept. After a potential conceptual design was agreed upon the inlet head design was created using a 3D model shown in Figure 44. The intent was to increase the use of the fluid model in this area to refine the conceptual design prior to prototyping. The prototype inlet shown in Figure 43 was tested in the lab both for wear resistance and performance.



Figure 44: 3D model of inlet head



Figure 43: Prototype inlet

Evaluation of Design for Erosion Resistance

The ultimate goal in the design of a component part for a hydrocyclone is to provide a benefit in performance, which is a sharper and/or finer separation and

for the component part to be resistant to wearing out. In closed circuit grinding applications it is not uncommon for parts to wear out and be replaced several times a year. The wear life of the lower cones and apex can easily be increased by using premium grades of wear materials, but the target is normally to get everything to last as long as the inlet head liner so the plant maintenance crew has to disassemble the hydrocyclone once to replace parts. The difficulties in testing for wear have been described earlier but because we have a well defined wear location in the standard inlet, we attempted a methodology that would highlight the same area. A satisfactory technique was developed where the part was painted with multiple coatings of different colour paints. High solids slurry was run through the hydrocyclone with the painted inlet at a predetermined pressure for a defined amount of time, and the part was washed off and inspected. The coatings of paint that were worn away on this test part very clearly mimicked the actual wear location on an operating hydrocyclone (Figure 46). The goal became a design that eliminated or spread out this wear pattern over the entire inlet. The prototype inlet was substituted for the standard inlet and the wear-paint test was repeated with the same slurry at the same pressures and duration. Figure 45 illustrates that this new inlet has eliminated the hot spot and shows a much more spread out and lower level of concentrated wear.



Figure 46: Wear/paint test standard inlet



Figure 45: Wear/paint test new inlet

The ability of the CFD model to predict the wear response was also examined for these two inlets. The erosion rate can be expressed by the following formula:

$$R_{erosion} = \sum_{p=1}^{N_{particles}} \frac{\dot{m}_p C(D_p) f(\alpha) V^b}{A_{face}}$$

- \dot{m}_p : mass flow rate of the particles
- $f(\alpha)$: function of impingement angle α
- V : impact velocity
- b : velocity exponent
- $C(D_p)$: function of particle diameter

The CFD model has the ability to record the number, velocity, mass, and the impact angle of the of various size particles for each of the grids that form the internal geometry of the hydrocyclone. Figure 47 shows the wear response for the coarse particle fraction in the standard design inlet. Note that the wear hot spot for this inlet design was identified in a similar location to that shown both for the paint test and by the inspection of a great deal of worn inlet head liners. Figure 48 shows the erosion rates for the new style inlet. Notice the very low predicted erosion levels for the inlet.

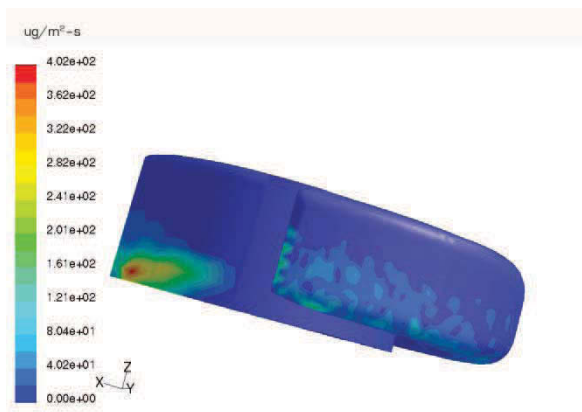


Figure 47: CFD erosion old inlet

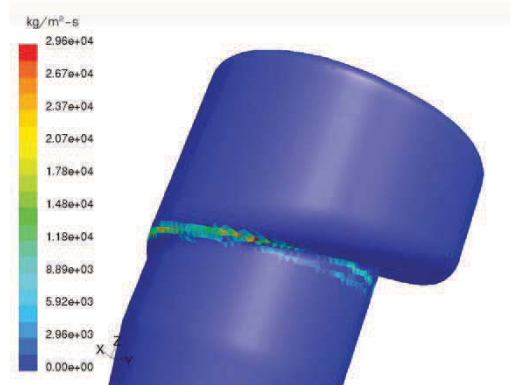


Figure 48: CFD erosion new inlet

A spiral wear pattern is shown in Figure 50 for the standard 250 mm hydrocyclone. This is not an accurate reflection of the known wear pattern for this hydrocyclone and is a result of the limitations of the CFD model. In addition the solids accumulate at the transition between the cylinder and cones, which is typically a low wear area. Because the solids cannot interact with each other they are not allowed to accumulate together in a broad band of solids that migrate downward. The solids that accumulate at the upper cone corner are not pushed down the hydrocyclone by colliding with incoming solids. Figure 49 shows the wear for this hydrocyclone with the new design inlet. The indication of wear on this inlet is relatively low compared to the rest of the hydrocyclone. The increased erosion level is shown in the lower cone and apex regions, which is similar in degree to wear in operating plants.



Figure 50: CFD erosion 250 mm cyclone old head



Figure 49: CFD erosion 250 mm cyclone new head

Evaluation of Design for Performance

The performance of the two inlets was also compared in a pilot test using the same feed slurry and operating conditions for both. The top part of the recovery curve is shown in Figure 51. Notice that the recovery of the coarser particles in the corrected recovery curve is improved with the new design inlet.

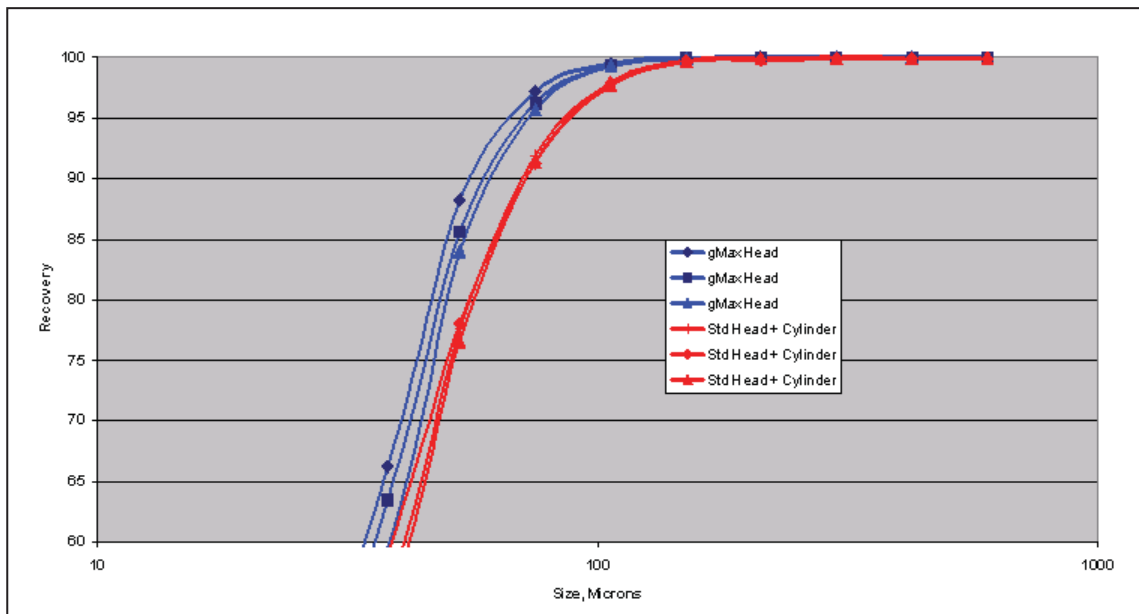


Figure 51: Laboratory test results - standard and gMAX head

KREBS ENGINEERS CFD MODEL

The model currently used by Krebs Engineers has the following features:

- Turbulence Model: Reynolds Stress (RSM). This turbulence model provided the best agreement with known velocity profiles.
- Multiphase Model: algebraic mixture model (ASMM). The air core has been successfully modelled using the ASMM and the liquid phase density has been adjusted to the slurry density to account for any solid material. The slurry density does have an important effect on the flow split and pressure drop.
- Particle Model: Lagrangian. Once the air core and the resultant flow split have been calculated, the solids are introduced as a post processing stage using Lagrangian particle modelling.

Figure 53 below illustrates the surface grid for a standard 250 mm hydrocyclone. This hydrocyclone has the standard involute inlet style and conventional 20-degree cone. Notice the special mesh used to join the inlet to the main body. The air core produced with this model is shown in Figure 52 for the same 250 mm hydrocyclone.



Figure 53: 250 mm cyclone grid

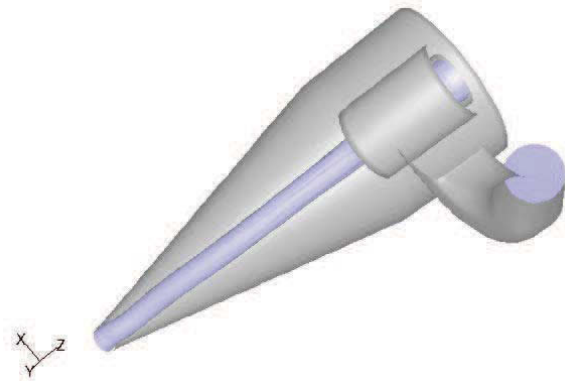


Figure 52: 250 mm cyclone air core

Model Conditions:

Fluid density:	1.118 kg/m ³
Inlet velocity:	1.83 m/s
Solid Density:	2.650 kg/m ³
Volume % solids in slurry:	7.2 %
Vortex Finder ID:	89 mm
Apex (spigot) Opening:	50 mm
Pressure:	70 kPa

In addition to the air core shown in Figure 52, notice the contours shown for both static pressure and tangential velocity (Figures 54 & 55). The tangential velocity is at a maximum at about the diameter of the vortex finder, which is consistent with the literature where these velocities have been measured (Kelsall 1952). The pressure is at a minimum in the central core and a maximum in the inlet nozzle area.

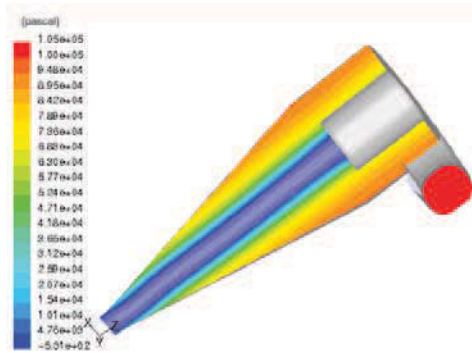


Figure 54: Contours of static pressure

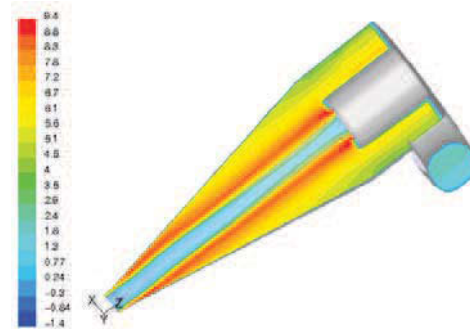


Figure 55: Contours of tangential velocity

The particle tracks show the paths of both a relatively large and a small particle that report to the underflow and overflow respectively (Figure 57). Notice how the coarser particle was spun out towards the outer wall after entering the internal high tangential velocity area. The smaller particle, following the predominant flow path, successfully traversed this area and exited the overflow stream. Both particles showed a residence time in the hydrocyclone of about 1,5 seconds for this validation case. When a 250 mm cylinder section was added, the residence time increased to three seconds. In addition, both particles show a sharp change in direction as they enter the open cylindrical section of the hydrocyclone. This is in contrast to very smooth particle path from the inlet to the main body for the new design inlet shown in Figure 56 below. This particle path is for a very coarse particle at similar conditions (same inlet velocity, % solids etc) as shown above for the standard 250 mm hydrocyclone and inlet.

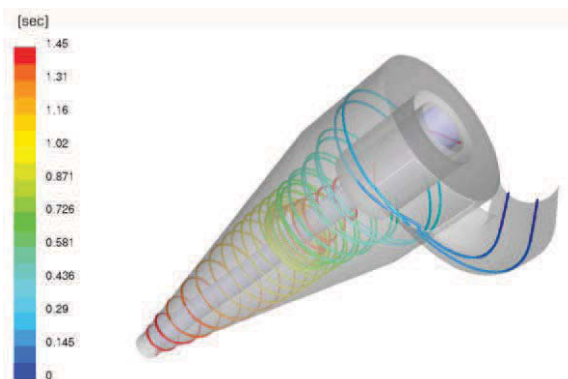


Figure 57: Coarse and fine particle tracking old head

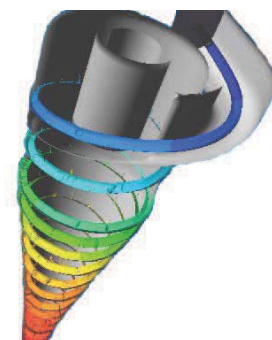


Figure 56: Coarse particle tracking new head

CFD Validation

For the conditions specified above, the results of the CFD model was compared to data obtained from a hydrocyclone with similar geometry run at the same feed density and pressure. The mid point of the particle size data was used for comparison because the model was considering a particle sphere of exactly the specified diameter. This was done for the same flow rate and slurry with two different vortex finder sizes. Figure 58 below is included to show the comparative data from the CFD model and the actual hydrocyclone test results.

The 70 Kpa pressure drop from the model was indistinguishable from the measured value at the gauge and the predicted flowsplit of 16 % is very close to the 14 % recorded. For the smaller vortex finder tests the recorded and actual pressure drops went up to 131 and 105 kPa respectively.

The predicted flowsplit for the model at the smaller vortex finder size with the same feed inlet velocity and 50 mm apex size was 40 % versus the test at 34 %. The model flowsplit was not as close as for the larger vortex finder but increased substantially and in the right direction because the underflow orifice was larger in relation to the overflow orifice. The ability to reliably predict the hydrocyclone flowsplit is a function of the accuracy of the air core simulation because of the throttling effect of this on the actual available opening in both orifices. Because of the initial assumptions and as the solids loading is increased in the apex region, the model will become less accurate because the solids can not effect the flow field or the predicted path of other solids.

	Krebs Lab Test	CFD Model	Krebs Lab Test	CFD Model
Vortex Finder Size	89 mm	89 mm	64 mm	64 mm
Flow Split % to Underflow	14	16	34	40
Inlet Pressure, Kpa	69	70	131	105

Figure 58: CFD validation of hydrocyclone inlet pressure

Figure 59 shows the actual recovery curve from the lab test with the larger 89 mm vortex finder and the particle recovery predictions from the fluid dynamics model. Notice that the model predicts that all the 45 micron and above particles would report to the underflow. The actual recovery at 31 microns was just over 70 % compared to 68 % predicted from the CFD model.

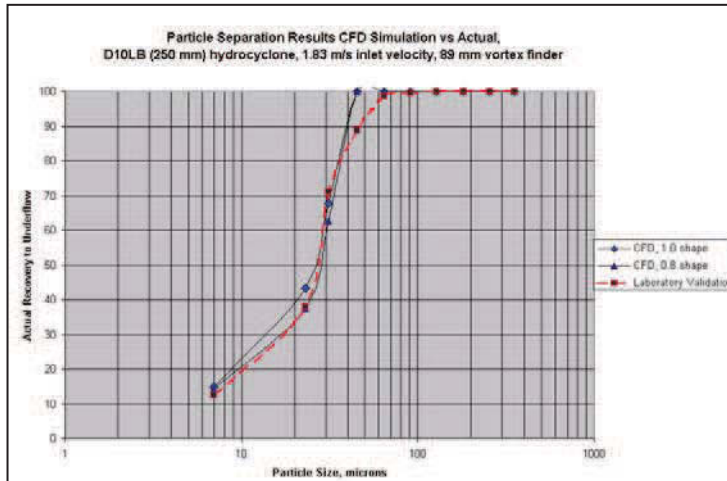


Figure 59: Actual recovery curves

The simulated recoveries at 23 microns were less than 5 % higher than actual, and overall the model predicted a sharper cut than was produced pumping the slurry to the test hydrocyclone. The model allows use of a shape factor to change the drag force on a particle of a given diameter. The initial separation performance

results were run assuming the particle were perfect spheres with shape factor of 1.0.

$$\text{Shape factor } \phi = \frac{\text{surface area of sphere having the same volume as particle}}{\text{surface area of particle}}$$

This factor has been calculated for a variety of solids (Allen 1974) and the sub angular and rounded particles exhibited shape factors from 0.65 to 0.85. Because we know the particles that were used in the hydrocyclone test were not perfect spheres, a shape factor of 0.8 was used to see if the effects of the resultant difference in drag caused by the irregular shaped particles brought a reasonable response in the particle separation. As shown in the figure below the addition of the particle shape factor did lower the predicted recoveries for some sizes, and as a result, closer to the measured performance .

Figure 60 below shows both the lab and CFD model for the separation results for tests with two different size vortex finders. The model prediction of the performance shows a finer cut than for the larger vortex finder and also a steeper curve. The ability of the model to predict the hydrocyclone performance and track with a similar magnitude and direction the effect of changes in hydrocyclone geometry gave us an increased confidence in the potential benefit of this tool.

	Laboratory Data	CFD Simulation	Laboratory Data	CFD Simulation
Particle Size, Microns	89 mm vortex finder	89 mm vortex finder	64 mm vortex finder	64 mm vortex finder
350	100	100	100	100
256	100	100	99.9	100
181	100	100	99.9	100
128	99.9	100	99.8	100
91	99.5	100	99.2	100
64	98.6	100	99.1	100
46	88.7	100	96.1	100
32	71.1	67.2	87.5	98.6
22.5	37.9	43.4	84.4	64.3
7	12.5	14.9	38.7	38

Figure 60: Validation data of 89 mm and 64 mm vortex finder tests

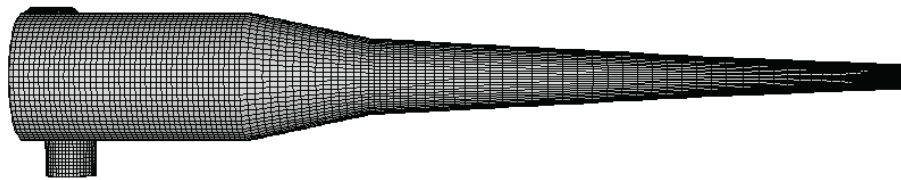


Figure 61: gMAX mesh

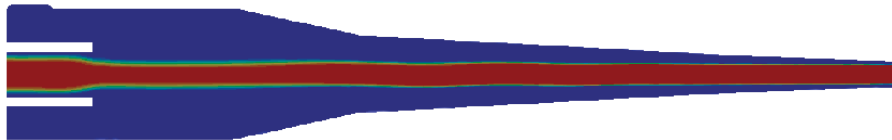


Figure 62: gMAX pressure distribution

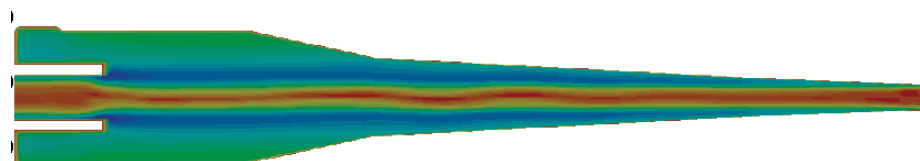


Figure 63: gMAX Tangential velocity distribution

As a final validation step we changed the cone angle from the standard 20-degree cone to the multiple cone angle gMAX lower cones. This geometry is shown in Figure 61. Notice the tangential velocity profile and that the high velocity region is extended much further down the hydrocyclone by the longer cone angle (Figure 63). The expected performance of this geometry change is shown in Figure 64. This simulation was performed with the larger 89 mm vortex finder and 70 Kpa

pressure drop. The modelled performance of this hydrocyclone shows a much finer recovery curve. The expected increase in particle recovery was very close to the expected 35 % difference that has been measured for this hydrocyclone.

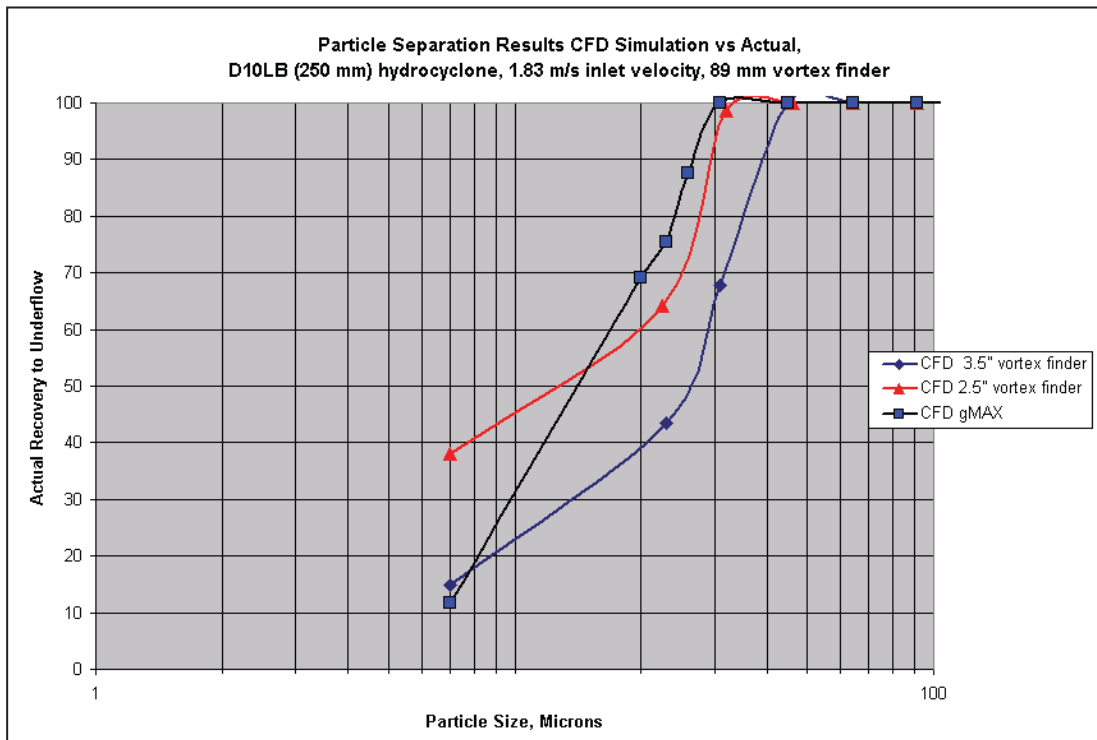


Figure 64: Recover curve validation

3.8. Special Types of Hydrocyclones

3.8.1. Flat Bottom Cyclone

Flat bottom cyclones (see Figure 33) have to be used when low flows combined with coarse separations must be realized with hydrocyclone classification. A flat bottom cyclone has a D50 that is roughly 2.4 times coarser compared to a conventional cyclone with a 20 degree cone. The disadvantage of this type of cyclone is its flat Tromp curve and the high wear at the bottom of the cyclone due to orbiting particles. Good substitutions for such cyclones are high frequency screens, however at a much higher cost of investment.

3.8.2. Water only cyclone

The water only cyclone is used in coal processing to make a density separation without the use of heavy media. The cyclone consists of a short body, and a 90 degree cone and a truncated cone as the apex. The vortex finder is extended far down into the conical section. The principle of this type of cyclone is to develop a rotating bed of particles at the bottom of the cyclone and by doing so, creating an artificial bed that acts like heavy media. Low density particles orbit at the top of this bed and are sucked into the overflow by the extended vortex finder while heavy

particles penetrate through the bed, discharging through the apex. Water only cyclones are always used in two stages – rougher and cleaner – in the coal industry (on easy to wash coal) and in the recycling industry to separate various type of plastics.

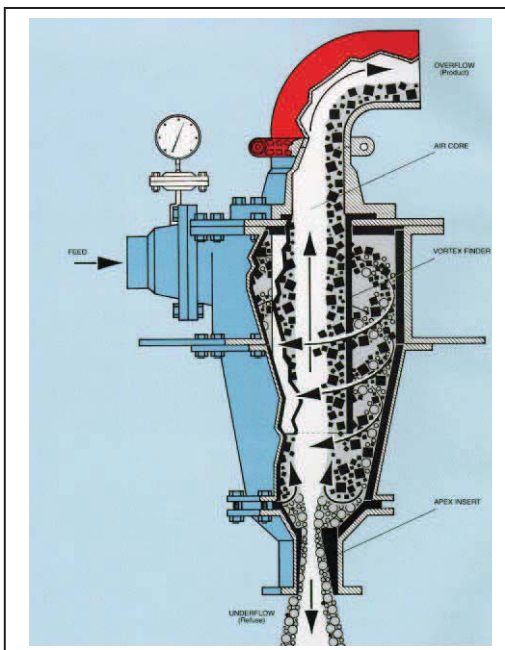


Figure 65: Water only cyclone

3.8.3. Dense media cyclones

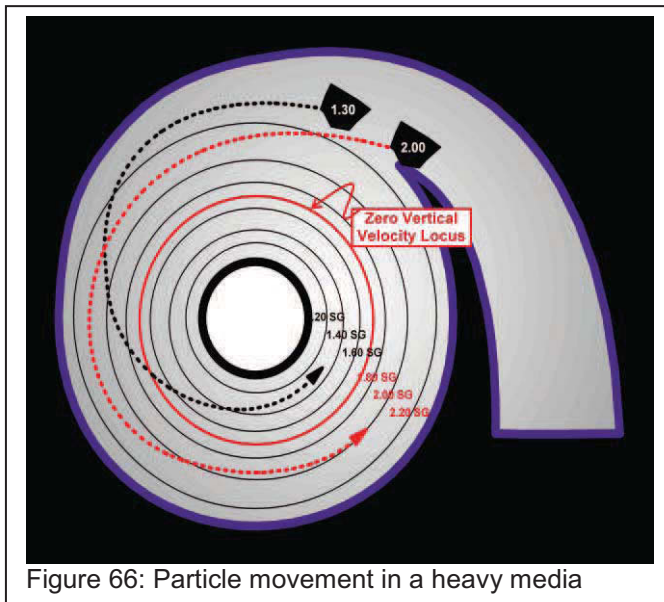


Figure 66: Particle movement in a heavy media

In essence a heavy media cyclone is of no difference to a classifying cyclone. In a heavy media cyclone magnetite is classified and a radial density gradient is established within the cyclone. When particles are introduced their movement towards the outer wall of the cyclone is stopped at the density layer where the particle begins to float because of the density difference. By the ratio of vortex

to apex the separating density is dialled in be enlarging or reducing the zero vertical velocity locus.

3.8.4. SSC cyclones

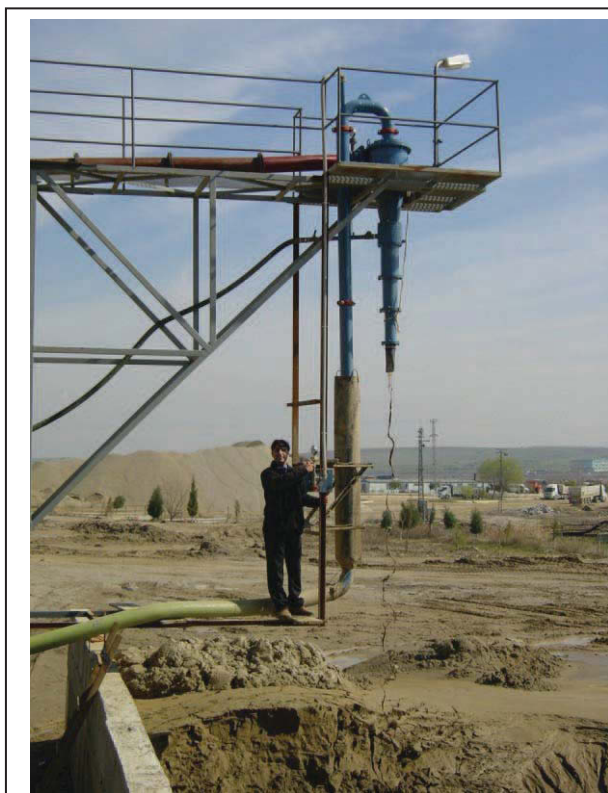


Figure 67: SSC cyclone

Sand Stacking Cyclones are widely used for dewatering applications in the sand and gravel industry. A sand stacking cyclone has an extended overflow pipe to roughly 1m below the apex and a cyclostack underneath the Apex which is a Urethane flap, also known as “fishtail”. The extended overflow pipe creates a siphoning effect that closes the cyclostack. When operated with water only this cyclone does not have any discharge out of the apex. When solids are present they accumulate above the cyclostack and discharge in a pulsating stream trough gravity trough the cyclostack. This allows excellent dewatering with up to 85% solids by weight with solids of a

density of 2.65 kg/dm^3 . Also this cyclone can easily handle fluctuating slurry densities which are common in sand plants.

3.8.5. Cyclowash



Figure 68: CycloWash

A cyclowash is a device that can be installed between the lower cones of a hydrocyclone where wash water is radially injected. This wash water creates an artificial water curtain that can only be penetrated by high energy (large) particles. Small particles get washed out to the overflow. The cyclowash can successfully remove 50% of the minus 25-30 micron fractions and is used for desliming applications like mine backfill. Two stage cycloning can be replaced by single stage cycloning with a cyclowash, however it is more

difficult to operate and so two stage cycloning is the more stable installation with fluctuating feed.

3.8.6. Desanders

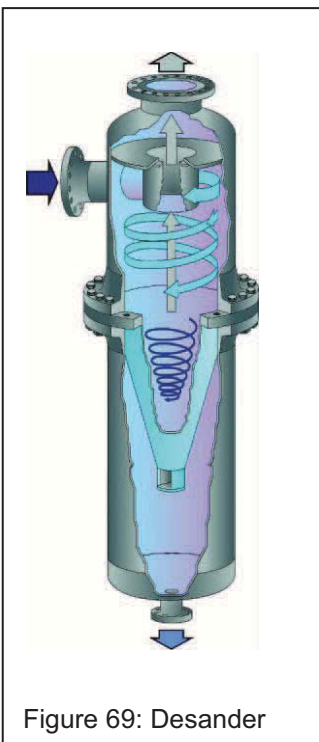


Figure 69: Desander

A desander is a cyclone with a closed chamber underneath the apex for the collection of solids. It is designed to remove small quantities of solids out of process streams (<1% solid by weight). The chamber is discharged by opening a discharge valve which is automated by a timing system or a level sensor in the collection chamber. A desander can be used within a pressurized piping system as the underflow is closed. The system will only suffer the pressure drop from the device. Desanders are commonly used in all industries where small amounts of solids have to be removed from a liquid stream, like water pipelines, removal of particles ahead of filtration systems, mill scale removal, but also well head desanding in the oil and gas industry.

3.8.7. Liquid – Liquid cyclones

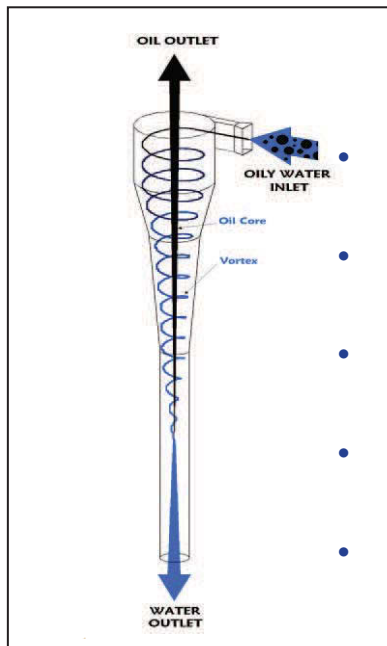


Figure 70: Liquid-liquid cyclone

Liquid liquid cyclones do separate tow liquids with different density. The majority of the applications is the removal of oil from water in the oil and gas industry or in industrial water cleaning systems.

CHAPTER 4: Hypothesis

The quality of milled product in closed circuit grinding can be influenced significantly by controlling the underflow density of a hydrocyclone.

The guideline to operate hydrocyclones at their lowest possible overflow density and their highest possible underflow density in closed circuit grinding is of common knowledge. The underlying principle is minimizing of recycled ultrafines back to the mill.

To describe the recovery curve of a hydrocyclone, two separate curves have to be evaluated. There is a recovery curve for the solids and one for the liquid. The two main figures to evaluate a recovery curve are the D50 and the shape of the curve.

The water recovery curve depends on the ratio of apex and vortex finder diameter. Ultrafine particles in larger cyclones (150 mm and larger) are not separated according to the recovery curve of the solids, but follow the recovery curve of the water. In other words the ultrafines are carried along with the water.

This explains why hydrocyclones shall be operated with the highest possible underflow density. The higher the underflow density the lower is the amount of water that reports to the underflow and consequently the less the content of ultrafines in the underflow. This is important because these ultrafines represent final ground material that shall report to the overflow and not being recycled back to the mill feed.

So the overall performance of a grinding circuit can be altered by just changing the Apex diameter. In practice this effect can be seen when apex inserts wear out on large installation with the consequence of reduced mill circuit capacity.

The influence of underflow density variation to overflow product quality and overall circuit performance, although being of highest economical interest to all production sites, was never investigated in detail. This thesis and the subsequent test work is an attempt to quantify and qualify this influence.

CHAPTER 5: Practical work and results

The practical research work can be divided into 3 segments being pilot plant test work at CEMTEC, laboratory/pilot plant test and research work at Krebs' headquarter in Tucson, AZ, USA, and many years of consultancy work at many operations worldwide with main focus on the gold industry in East and West Africa.

5.1. Test and research work at FLS Krebs in Tucson AZ

Krebs' product development and research work is structured on a global basis. At the headquarter in Tucson AZ., USA, 2 full time employees operate a laboratory and pilot plant with one research engineer designated to do detailed research work on specific projects. One project worked on, before starting this thesis, was the establishment of CFD modelling and subsequent cyclone design research exercises. The CFD computation was performed by T.J. Olson in Tucson, AZ and the author was involved in brainstorming sessions and contributed to validation strategies as well as in the design of new cyclone shapes. The results of this work are summarized in chapter 3.7.4. A paper was published on the Hydrocyclone conference 03 in Cape Town and the author was jointly presenting this paper with T.J. Olson.

2 projects for this thesis were jointly executed by the author and the R&D staff in Tucson:

5.1.1. Apex capacity and cyclone cone angle

After the introduction of the gMAX cyclone practical field data strongly suggested that the capacity of the apex differs significantly with the variation of cyclone cone angles. Krebs cyclones are designed in a modular way, where different cones can be mounted to a cyclone design. Because of that it became obvious that the conventional sized apex orifices were not suitable for the new design. To further investigate this phenomenon, comparative tests were conducted in the pilot plant in Tucson with 380 mm (15") cyclone with a 20 degree cone, an 11 degree cone and a gMAX cone combination (multiple cone angles) with a number of different apex orifices. Figure 55 shows that the 20 degree cone cyclone has less apex capacity compared to the 11 degree cone and the highest capacity is obtained by the gMAX cone combination. The results were summarized in a new apex capacity chart envelope (Figure 72) that now allows selecting the correct apex diameter for various cone angles in hydrocyclones.

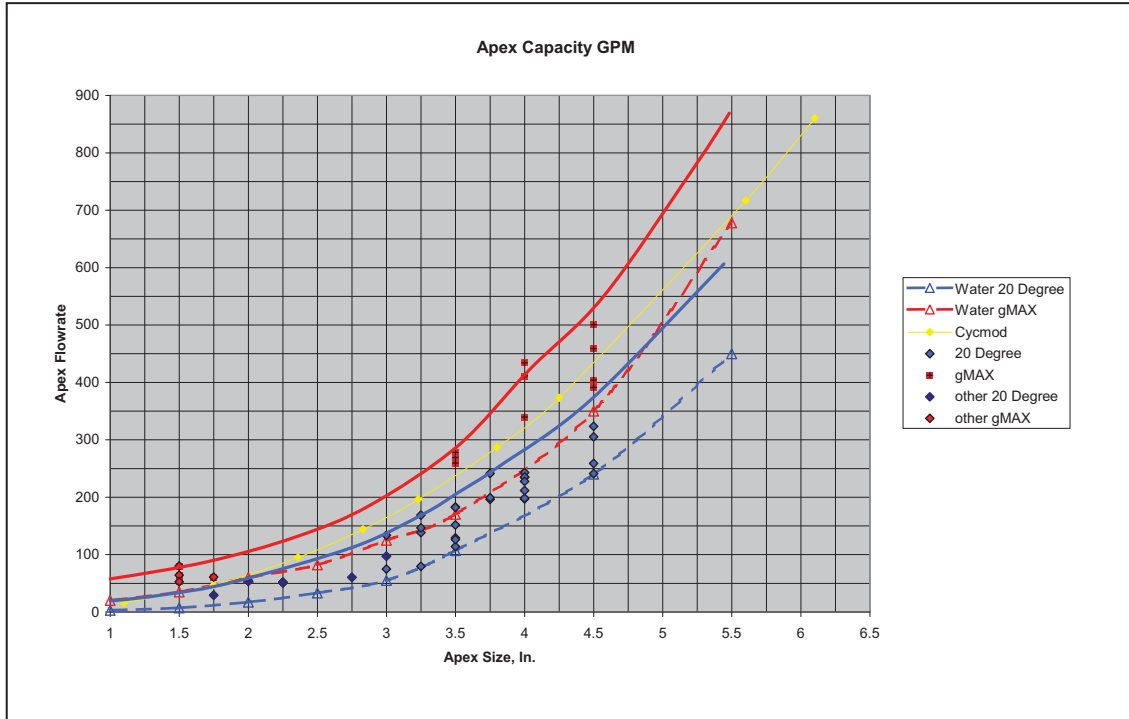


Figure 71: Apex capacity test results

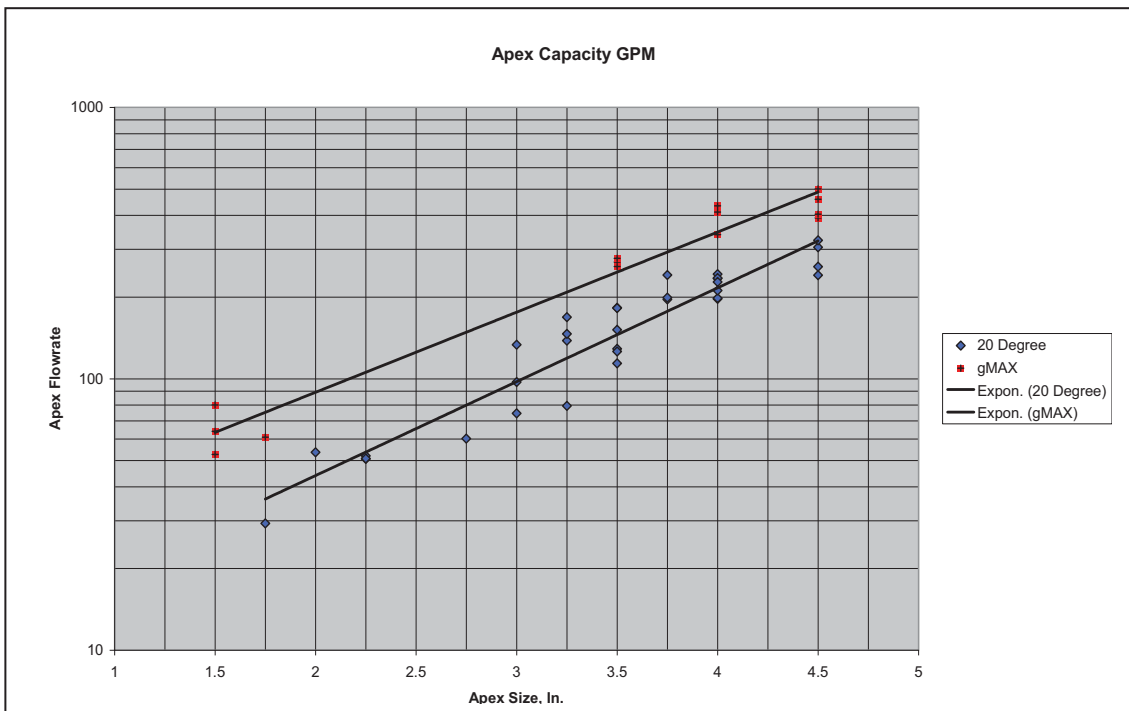


Figure 72: Apex capacity chart envelope

A CFD validation showed that the vertical slurry velocity within the hydrocyclone increases with decreasing cone angle and that because of the higher slurry velocity the capacity of the apex orifice varies. With this work new capacity charts for various cone angles were developed which are in practical use in the industry today.

5.1.2. Achievable underflow density with varying particle size distribution

As shown in this thesis, it is important to operate cyclones at the highest possible underflow density in order to minimize misplaced fine particles in the underflow. Field data and literature strongly suggest that the achievable underflow density in a hydrocyclone does not only depend on the apex diameter but also to a great part on the feed particle size distribution. Unfortunately it is very difficult to compare particle size distributions and link this to underflow density.

In a new approach the AFS (American Foundry Sand) Number was selected as a comparison criterion for particle size distributions and a strong affinity to achievable underflow density was found.

AFS Example Calculation			
U.S.Mesh Size	Wt% Ret.	AFS Factor	Product
6	0	3	0
12	2	5	10
20	4	10	40
30	6	20	120
40	10	30	300
50	15	40	600
70	31	50	1,550
100	20	70	1,400
140	10	100	1,000
200	2	140	280
Pan	0	300	0
Sum	100		5,300
AFS No.			53
Blue = Input			
Red = Calculation			

Figure 73: AFS number calculation example

To calculate the AFS number, first a sieve analysis using the US Mesh sizes shown in the table has to be performed. Next, the individual weight percentages are multiplied by factors. Then the sum of the products is calculated and divided by 100 to obtain the AFS Number.

In 2009 a 3 months testing campaign was conducted in Tucson where approximately 100 different particle size distributions were ran through the same cyclone under the same conditions with an adjustable apex assembly the relationship as shown in Figure 74 was established. This approach now allows to evaluate the achievable cyclone underflow density for a given feed particle size distribution.

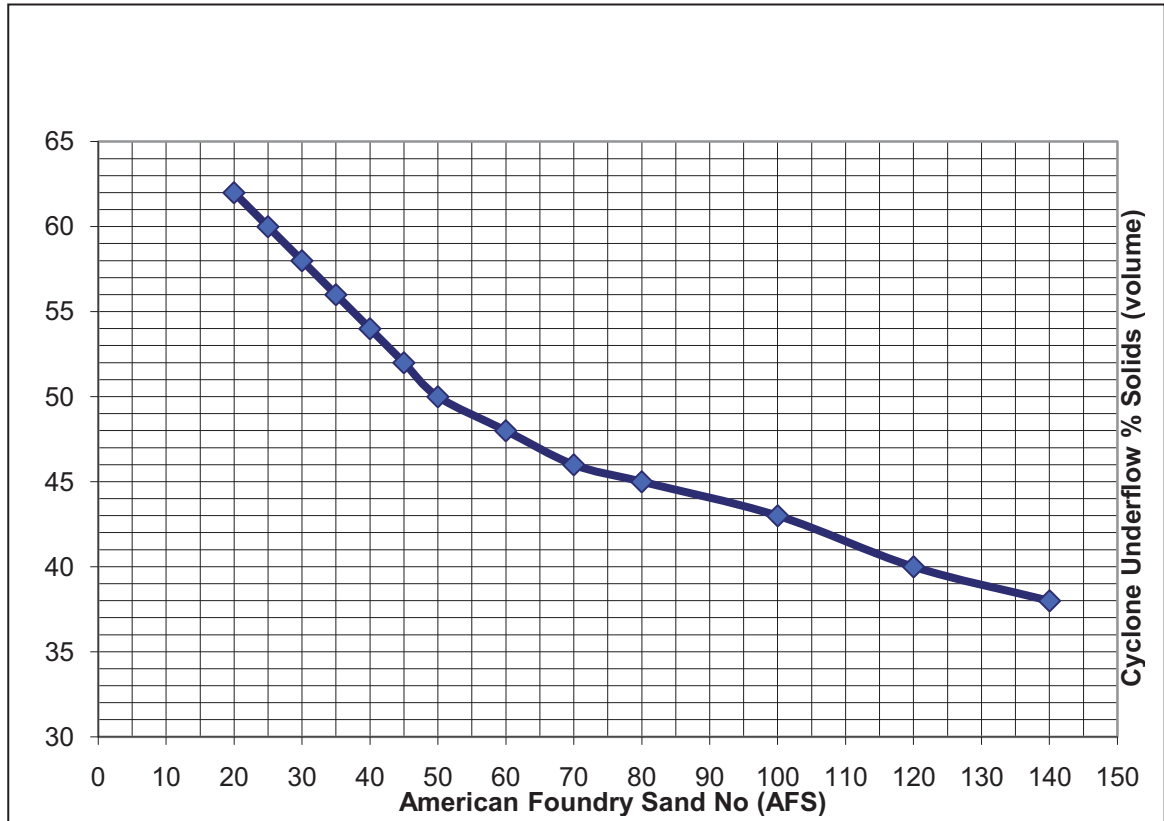


Figure 74: AFS number and achievable cyclone underflow density

5.2. Experiences gained in consultancy selling

During 15 years of consultancy sales in the process industry it became obvious that there is a direct relation between the density regime of a cyclone and the quality of the overflow product. Almost all major gold operations in West and East Africa, like AngolgoldAshanti- Obuasi, Bibiani, Iduapriem, Geita, Morila, Siguiri, Newmont- Ahafo, Red Back Mining- Chirano and Tasiast, Randgold Resources- Loulu and Tongon, Adamus- Nzema, Barrick- North Mara, Buzwagi, Bulyanhuly and many more were assessed and visited. Over the years the concept of density optimization was refined and proved on large scale plant tests. The problem with such large scale tests is the big variation in the processed ore, significant swings in feed tonnage and mostly non functional dilution systems. Also the quality of sampling is very poor and as a consequence it is very difficult to obtain comparable data. Because of these difficulties the decision was made to investigate this relationship more closely on a pilot plant scale in a well organized and controlled environment and use the obtained plant data for the case stories presented in chapter 8.

5.3. Pilot plant test work at CEMTEC, Austria

Cyclone test work is always a challenge. The big advantage of hydrocyclone of accommodating high flow with a small footprint works against testing. On a laboratory scale the maximum cyclone diameter that can be handled is around 50 mm in diameter, for larger cyclones the flows are too high. Also small diameter cyclones do have slightly different operational principles and therefore results gathered from test work cannot easily be up-scaled. At the same time the direction of this thesis is targeted towards industrial scale operations and so the laboratory scale is exceeded by far and the scale to be focussed on was rather pilot plant than laboratory. Pilot plant testing is expensive and needs some exhaustive preparations. A minimum required feed of 3 MTPH and projected 12 hours of testing was envisaged, about ~40 tons of raw material as well as a not insignificant volume of tailings for disposal. This scope is usually beyond most existing testing capacities. Fortunately Cement & Mining Technology GmbH situated in Enns, Austria (CEMTEC) offered to modify his pilot plant and to support and sponsor the envisaged test work. CEMTEC also organized the required raw material and the tailings disposal. Without that corporate sponsoring the test work would not have been possible to be conducted in Austria.

5.3.1. Initial circuit calculations

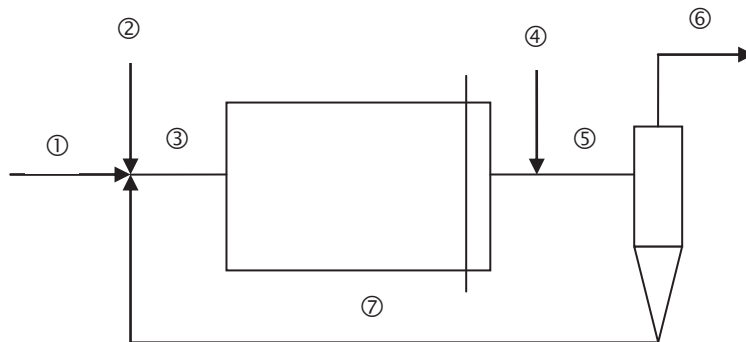
The initial circuit calculation was very critical. The grinding mill in the pilot plant from CEMTEC was initially designed for dry milling and was never run in a wet milling mode before. So in addition to the test work, a complete new wet grinding pilot plant had to be designed up front. The initial calculations were dominated by the selection of the hydrocyclone. The smallest hydrocyclone model that was anticipated to give reasonable results in a pilot plant scale was a 150 mm cyclone and the minimum flow of 15 m³/h had to be achieved in order to operate this cyclone successful. At the same time the grind of the pilot plant mill had to fit the cyclone D50 to produce the right product at an acceptable circulating load. A fine balance between the cyclone from a cut point and the volumetric flow as well as the grinding capabilities of the pilot plant mill was needed.

After some intensive joint calculations, with the need to harmonize cyclone, mill and pump specification and operation, a solution was found that accommodated the specification of all equipment needed for the test work.

New Feed to the Mill: 3 t/h
 Circulating load: 300 %
 P80: 50 µm
 Cyclone operating pressure: 0.53 bar

For the detailed process calculation please see chapter 9, pages 138 and 139.
 Thankfully the calculations turned out to be spot on and the test could be conducted in a minimum period of time.

5.3.2. Pilot Plant Set Up/Flow Sheet



POSITION	DMTPH	m ³ /h Slurry	%WW	m ³ /h H ₂ O
1	3.000	1.237	4.000	0.124
2	0.000	3.1766	0.000	3.176
3	12.000	10,913	65.000	6.462
4	0.000	3.700	0.000	3.700
5	12.000	14.613	54.146	10.162
6	3.000	8.113	30.000	7.000
7	9.000	6.500	70.000	6.162

The raw material is discharged to the grinding mill with a dry feeder, in addition with the cyclone underflow and dilution water. The new feed tonnage is measured on a belt scale and the water addition with a flow meter. The mill discharges to a sump where additional dilution water is added, again measured with a flow meter. The slurry is then pumped with a 4x4 slurryMAX pump to a U6-10 Krebs hydrocyclone. The pressure is recorded with a diaphragm manometer. The underflow discharges to atmosphere into a small sump with a slurry hose discharging into the mill. The overflow is also discharging to open atmosphere into a sump with a slurry hose, gravitating the slurry to a pump sump from where the slurry is pumped to a small tailings pond with a 3x2 millMAX pump.

5.3.2.1. Grinding Mill

The mill used at Cemtec is variable in length and was used in the following configuration:

- Length: 3 m
- Inner Diameter: 1.2 m
- L/D Ratio: 2,5
- Grinding Media Fill: 28 % of total Volume
- Grinding Media: balls, 4.7 t/m³ density, max diameter 44.4 mm; total weight 4,540 kg
- Installed Power: 55 kW

For more details see chapter 9, pages 140-143.



Figure 75: Pilot plant at CEMTEC

5.3.2.2. Hydrocyclone

Two Krebs U6-10° cyclones were used for test work.

- Inner Diameter: 150 mm
- Vortex finder diameter: 1.75 inch
- Inlet head: 2.2 sq.in.
- Cone angle: 10 degree

See cyclone drawing and capacity curve in chapter 9, pages 144 and 145.

5.3.2.3. Slurry Pumps

For cyclone feed a 4x4 rubber lined slurryMAX pump was used, running at 903 rpm on a variable frequency drive.

For tailings a 3x2 metal millMAX pump was used, running at 1,059 rpm on a variable frequency drive. See detailed pump calculation and specification in chapter 9, pages 146-149.

5.3.3. Raw material used

As raw material used for the test work Limestone with 10 % clay content of the below properties was used:



- Max Particle size: 4,000 microns
- F80/P80 of 2,749 microns
- Bond work index 12.6 kWh/t

Particle size distribution and Bond test are outlined in chapter 9, pages 150.154.

5.3.4. Conduct of test work



Figure 77: Hydrocyclones in test set up

The test work was conducted on the 17th of November 2008. On the 16th the team was already doing wet commissioning with water only to check if all the piping was OK, the pumps were running to specifications and that the tailings piping which was done by C type fire hoses worked as well.

5.3.4.1. Practical sequence of test work

The aim of the test work was to investigate a grinding circuit's reaction if only the cyclone underflow is varied. For that a set of different apex openings was prepared with diameters from 33 mm to 10 mm in 2 mm increments. Two cyclones were installed and the feed was varied between the cyclones with ball valves. When one cyclone was in operation, the next size apex for testing was mounted on the other cyclone. When the test sequence for the first cyclone was finished, the cyclones were switched over to the other and vice versa.

Sampling was done every 10 minutes, 3 times for one apex size. Samples were taken from cyclone underflow, cyclone overflow and mill discharge. At sampling time, the density was measured, on the overflow with a Marcy scale and on the underflow with a 500 ml cylinder (measuring the slurry weight on a laboratory scale). All sampling was done simultaneous, as well as the reading of dilution water flow into the mill and into the pump sump, cyclone operating pressure and time. Pictures of the underflow discharge pattern were taken on every test run.

On the control system of the mill the power draw and the new feed from the belt scale was recorded at the same time. Both times, external time and system time were synchronized ahead of the test work, so that each test could be linked directly to the system records.

The testing was started with a 33 mm apex insert until roping occurred with the 18 mm insert. Then a second series was run with starting from 33 mm up to 36 mm. On the last attempt with the 38mm apex the system went completely out of balance and the test was stopped.

Beginning time: 11:40 AM

End of testing: 17:55 PM

A total of 99 samples were taken. See analysis results, chapter 9, pages 155-187.

5.3.4.2. Manpower and responsibilities

A total of 8 persons were needed for the work. Two persons at the cyclone overflow, one taking samples and the other for taking pictures of the underflow discharge pattern, measuring the density and the cyclone feed pressure. Two other persons were at the pump sump, with one taking samples and the other one measuring the mill discharge density and dilution water flow. Two persons were

watching the feeder and lifting the big bags with the crane to fill the feeder hopper. One person was giving the commands for the initiation of the sampling and readings and for general control and command (which was the author) and one person was watching the mill controls and helped out wherever help was needed.

5.3.5. Results and laboratory work

5.3.5.1. *Laboratory Equipment*

5.3.5.1.1. Particle size distribution

- Laboratory sieves for manual sieving 300 x 300 according to DIN 4188
- Sieving machine Ø 200 x 50 according to DIN 4188
- Mastersizer 2000 Malvern

5.3.5.1.2. Weight analysis

- AND laboratory scale GX 6100
- AND analytical scale GR 200

5.3.5.1.3. Density analysis

- Bulk density testing barrel
- Micrometics-Pycnometer

5.3.5.1.4. Moisture content

- Moisture analyzer MX 50
- Drying Cabinet TK/L 4105

See also test report CEMTEC, chapter 9, pages 188-205.

5.3.5.2. Table of Test results and data used for evaluation

Table 1 shows all data that were measured and calculated from the sampling and readings. For closer investigations only samples D3, D6, D9, D12, D15, D18, D21, D24, D29, and D36 were used. On these samples the mill was already running for 30 minutes with one apex size which allowed the system to stabilize the circuit. The other sampling was done to assess the time until the system of mill and cyclone was stabilized again after switching over to a new apex size.

All measured data was evaluated with FLS Krebs software that allows calculating the recovery curve, D50, P80, alpha and viscosity. The analysis of each sample is shown in chapter 9, pages 206-215.

Platz für die Tabelle - A3 Ausdruck zum einschlagen.

5.3.5.3. Cyclone Discharge Patterns

A photo of all cyclone discharge patterns was taken. The change from fan discharge at large apex diameters to umbrella discharge and finally to roping discharge can be seen nicely in chapter 9, pages 226-229..

5.3.5.4. Feed rate

The feed rate was held constant at 3 MTPH, see monitoring diagram form CEMTEC in chapter 9, page 230. The diagram can be related to the samples by the time line.

5.3.5.5. Power consumption

Also the power consumption was monitored by the CEMTEC system, see diagram in chapter 9, page 231. The diagram can be related to the samples by the time line.

CHAPTER 6: Technical Conclusions

6.1. Introduction

The main point of discussion in this chapter are conclusions drawn from the conducted test work at CEMTEC as the results from the Tucson test work were already presented in chapter 5.

6.2. Conclusions and Discussion of data obtained from test work

6.2.1. The influence of underflow density to the circulating load of a closed grinding circuit

As shown in figure 78, the circulating load decreases with increasing underflow density. This is a quite important result because the lower circulating load can be used to increase the new feed to the system and increase production. However it must be noted that this has to be evaluated together with the influence of the circulating load to slurry viscosity and thus cannot be seen as an isolated phenomenon.

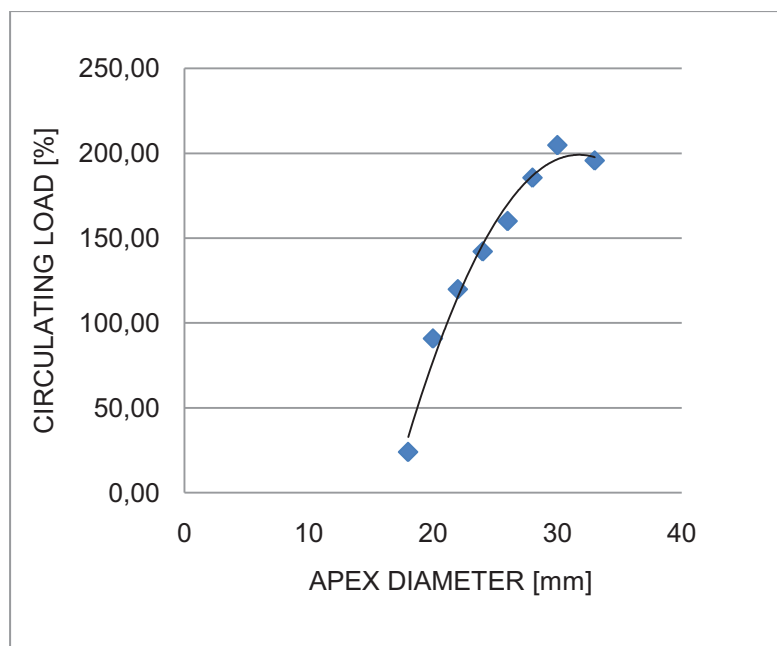


Figure 78: Apex diameter and circulating load

The reason for that relationship is the lower recirculation of fines material with decreasing apex diameter. With smaller apex diameter, the water split to the overflow increases and the water split to the underflow decreases. Because of that, the not classified fines content in the slurry gets discharged preferentially to

the overflow with decreasing apex diameter and the circulating load drops. In practice this happens when the apex insert gets worn out in plant operation. By widening the apex the water split to the underflow increases and as a consequence the fines recirculation. The net result is an unnecessary high circulating load that occupies mill capacity combined with higher power consumption. This higher power consumption however is not utilized properly for the comminution process. With close monitoring of apex diameter the mill throughput in plants can be maximized.

6.2.2. The influence of circulating load to slurry viscosity in closed circuit grinding

To describe viscosity, the TD value (Terminal density) is used. This value is the figure used by Krebs Engineers for viscosity correction. Here the TD shows the relative change in viscosity according to the variation of the hydrocyclone underflow density. With increasing viscosity the TD value gets lower. As shown in figure 79, the viscosity increases with decreasing circulating load. The reason for that is the change in the composition of the particle size distribution to the total mill feed. As commonly known, slurry viscosity rises with increasing fines and slimes content. Hydrocyclone underflow by nature is perfectly deslimed material with low viscosity. The lower the circulating load is in the system, the lower is the proportion of deslimed recycled underflow back to the mill and consequently the viscosity rises because slimes rich new feed (raw material is slimes rich by nature) gets proportionally higher. The result of these tests show that with decreasing circulating load, slurry viscosity rises and not vice versa. Very often this relationship is considered to be the other way round in operations, but these results do match with the practical experience on sites from the author and the above theory.

It is of interest to now look at the system reaction of an apex optimization when combining this result with the result from Para 6.2.1. When optimizing the apex diameter in a plant, the circulating load gets lower and as a consequence slurry viscosity rises because of the relative higher fines content in the mill feed due to less recirculated deslimed underflow combined with a relative higher portion of slimes rich new feed. As a consequence of the higher slurry viscosity the settling velocity of the particles within the cyclone is reduced and the cyclone will separate at a coarser cut and the circulating load further decreases because more particles will discharge to the cyclone overflow. To overcome this effect more dilution water has to be added to the pump sump ahead of the cyclones to reduce viscosity to

such a value that the cyclone separation dials in as per design. This is the most important method of controlling the grind in a large grinding circuit.

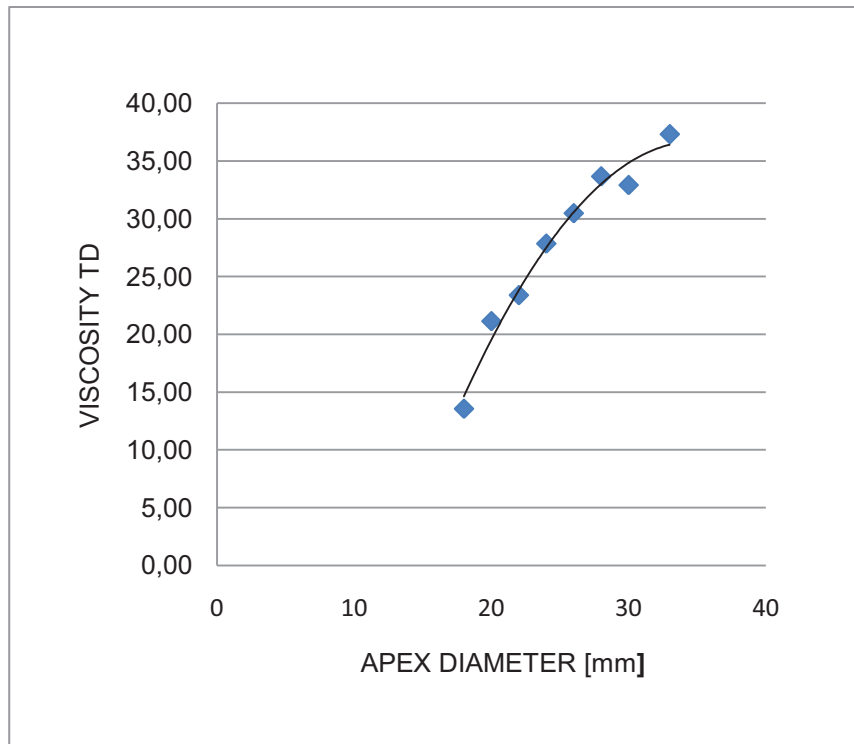


Figure 79: Apex diameter versus slurry viscosity

6.2.3. The influence of underflow density to hydrocyclone D50 in closed circuit grinding

With rising underflow density, the cut point (D50) of the hydrocyclone gets coarser (Figure 80). D50 is that particle size that has an equal chance to either report to the underflow or to the overflow of a hydrocyclone. This relationship however is not a direct one, but a result of the systems reaction as described above.

The reason for that effect is the reduction of the circulating load with increasing underflow density and the rise in slurry viscosity because of the lower circulating load, resulting in coarser separation of the hydrocyclone that separates according to equal settling velocities of solids in a liquid.

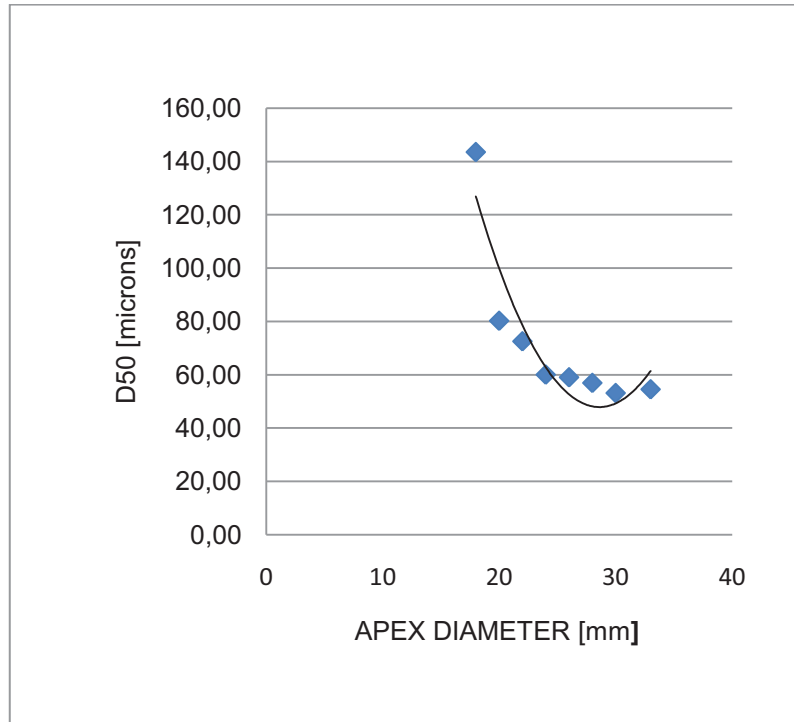


Figure 80: Apex diameter versus D50

6.2.4. The influence of underflow density to the overflow product quality in closed circuit grinding

As described earlier, the product quality of hydrocyclone overflow can be evaluated best by looking at the pitch as well as to the upper and lower ends of the recovery curve. An important value is the Ecart Probable or the alpha value (Lynch-Rao equation), describing the pitch of the recovery curve.

$$T(D) = \frac{e^{\alpha \frac{D}{D50}} - 1}{e^{\alpha \frac{D}{D50}} + e^{\alpha} - 2}$$

Lynch Rao Equation

First a closer look at the alpha value to describe the slope of the recovery curve is necessary. As shown in Figure 81, the relationship between the sharpness of separation and apex diameter (underflow density) describes a curve that trends to sharper separation with increasing underflow slurry density, reaching a maximum and then declining again. It is easy to see that there is a distinctive optimum underflow density (or apex diameter) that results in the sharpest possible recovery. This result is in line with the various theories describing roping described in Para 3.6.2.

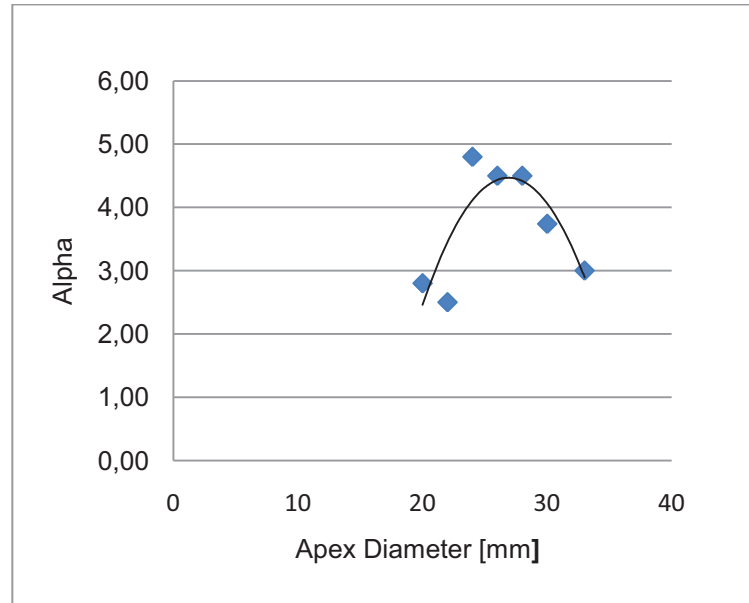


Figure 81: Apex diameter versus alpha value

In addition to the middle part of the curve the upper and lower tails are of great importance for the cyclone performance evaluation. Especially misplaced coarse particles in the overflow and excessive fines in the underflow are of big importance to overall plant recovery and the economical success of an operation.

The first look is to the lower tail of the recovery curve. Figure 82 below shows the content of -10 μm and -20 μm in cyclone underflow with varying apex diameter and Figure 83 the recovery figures to the underflow the -15 μm fraction.

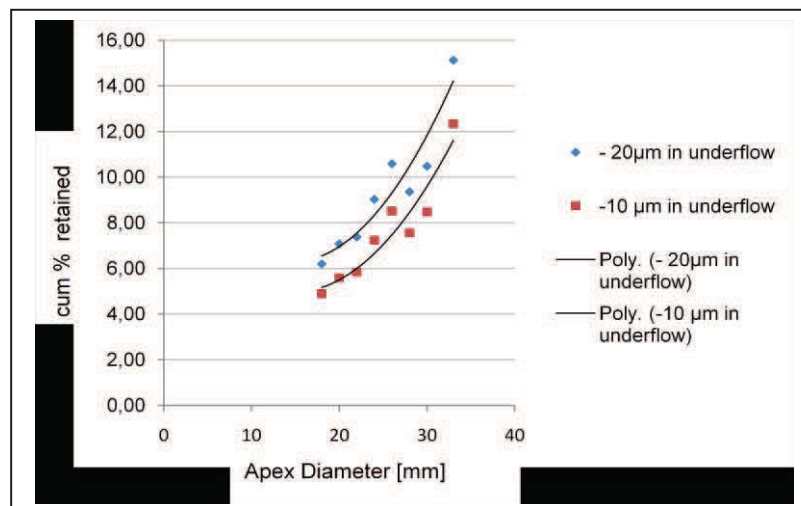


Figure 82: -20 and -10 μm particles in underflow versus apex diameter

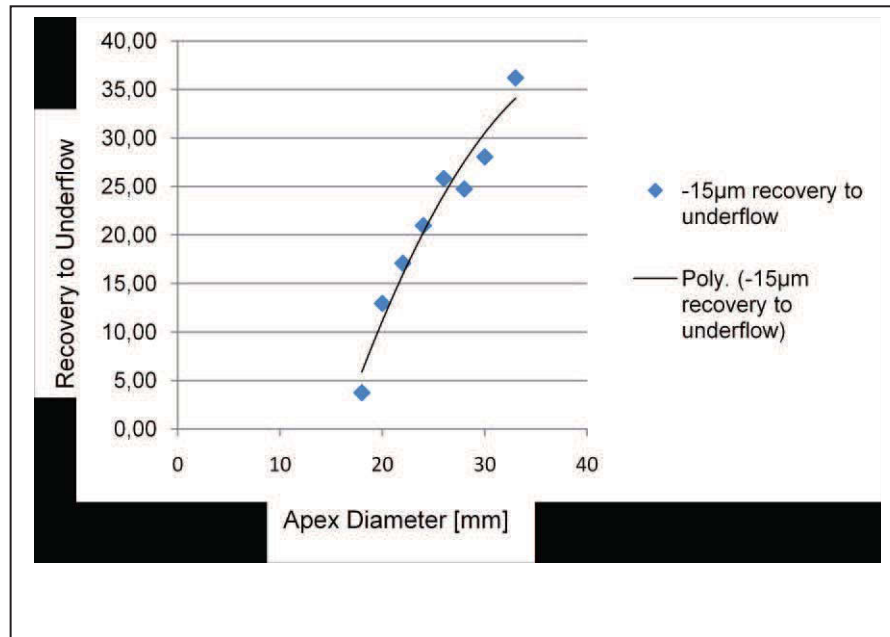


Figure 83: Recoveries to underflow of -15 µm versus apex diameter

The results are as expected. The content of fine particles as well as their recovery decreases with decreasing apex diameter. No real surprise here.

When looking at the top end of the recovery curve things get interesting again. Below figure 84 shows the content of +140 µm and +180 µm particles in cyclone overflow with varying apex diameter and figure 85 their recoveries.

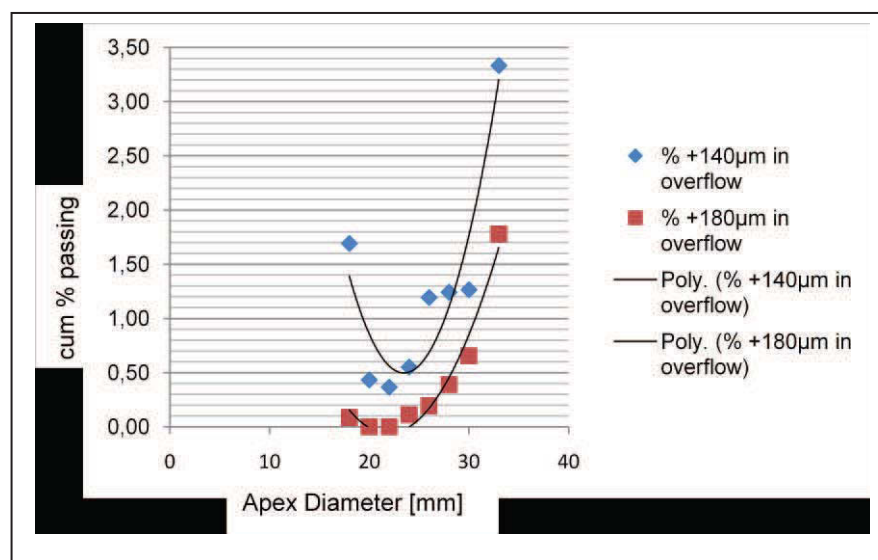


Figure 84: +140 µm and +180 µm particles in cyclone overflow versus apex diameter

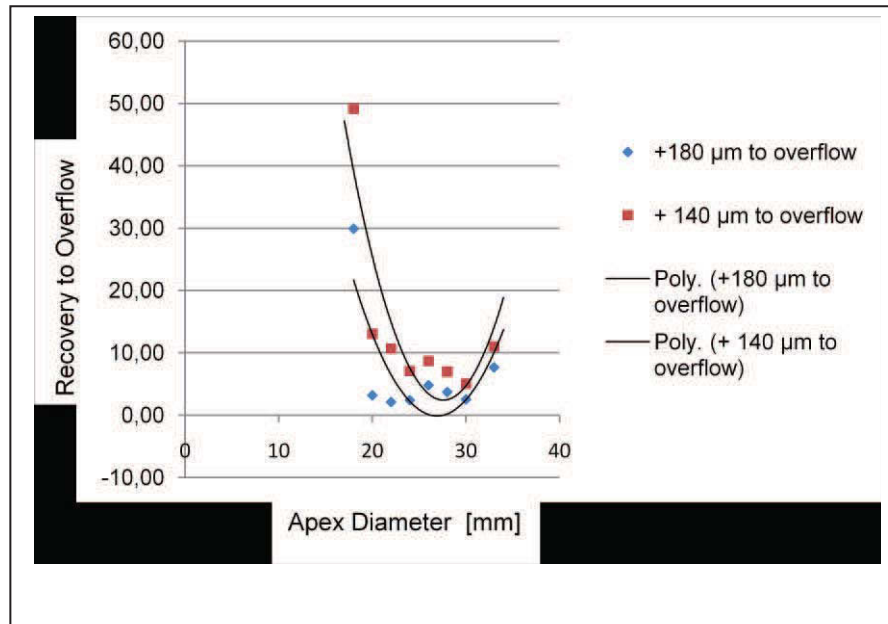


Figure 85: Recovery of +140mm and +180μm to overflow versus apex diameter

Figures 84 and 85 show results that had never been experienced before or in other words are against main stream thinking in the cyclone industry. The effect that is supported by this data and that is also commonly known in the industry is that with too high underflow density or too small apex diameter the number of misplaced particles in the overflow gets higher and reaches a point when the cyclone is roping whereby almost no classification work is done by the cyclone at all.

What can be clearly seen in both figures 84 and 85 is a clear rise of the coarse particles in the overflow when the cyclone operates with a too large apex diameter. Mainstream thinking was that the curve as shown above would remain flat for larger apex diameters, but a distinctive rise can be obtained.

When trying to explain the cause of this phenomenon, it is important to interpret the data by looking at the whole circuit and not to evaluate the cyclone as an isolated device. With the variation of the apex diameter the grind or the P80 of the system changes as well as shown in this chapter above. With a changing P80, also the amount of top size fractions changes as a consequence. Therefore the effect of higher misplaced particles on diluted cyclone underflows in closed circuit grinding systems needs to be evaluated independently from this variation in grind.

A good comparison is the spread and the ratio of the relative top size content to the grind which can be obtained by calculating the ratio of the P80 to the P99 of the overflow particle size distribution. This approach eliminates the usage of

definitive particle size fractions and leads to a comparable result which is independent from the actual P80 and shows the relative proportion of coarse bypass in the cyclone overflow.

	33	30	28	26	24	22	20	18
	RUN 3	RUN 6	RUN 9	RUN 12	RUN 15	RUN 18	RUN 21	RUN 24
P80	29.00	39.00	43.00	46.00	44.00	50.00	49.00	61.00
P99	231.00	158.00	151.00	148.00	131.00	136.00	131.00	134.00
P80/P99	7.97	4.05	3.51	3.22	2.98	2.72	2.67	2.20

Figure 86: P80 and P99 for various test runs and P80/P99 ratio

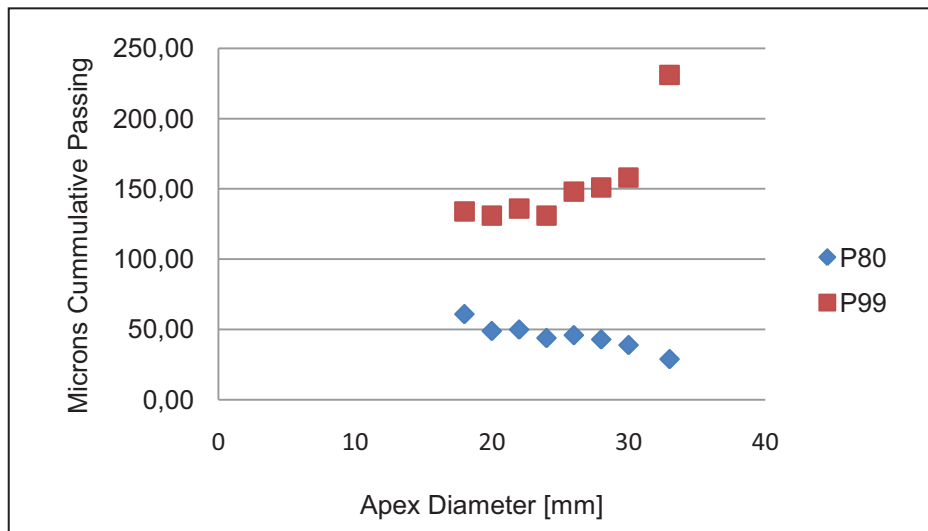


Figure 87: P80 and P99 versus apex diameter

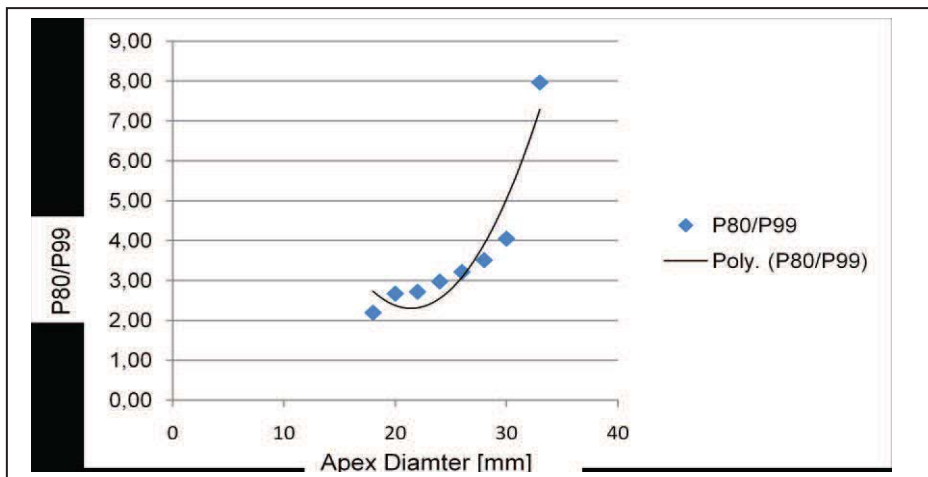


Figure 88: Apex diameter versus P80/P99 ratio

The result of this way looking at the results is quite surprising. With the apex getting bigger the spread, the absolute percentage and also the relative value of P80/P99 goes up.

The suggested explanation of this effect is not trivial. The air core diameter in a hydrocyclone is a function of the ratio of the vortex finder diameter, cyclone pressure, feed density and apex diameter. If all variables remain constant and only the apex diameter is varied, the air core diameter gets bigger with larger apex diameter. If the air core is getting too big in diameter the remaining area between cyclone wall and the air core is getting smaller and smaller until it reaches a point where the volume of slurry reporting to the underflow cannot pass this open flow area anymore as the slurry velocity is a constant and cannot be increased. The result of this flow constraint is that the excessive volume that cannot pass this bottleneck is pushed towards the overflow and by that increasing the coarse fractions.

6.2.5. Recovery curve shapes and cyclone simulation

For the complete evaluation of the recovery curve also the upper and the lower ends have to be looked at as clearly shown above. As shown in figure 89, there is a major difference in quality between too dilute density (right picture) and optimized underflow density using a 25 mm Apex insert as per picture

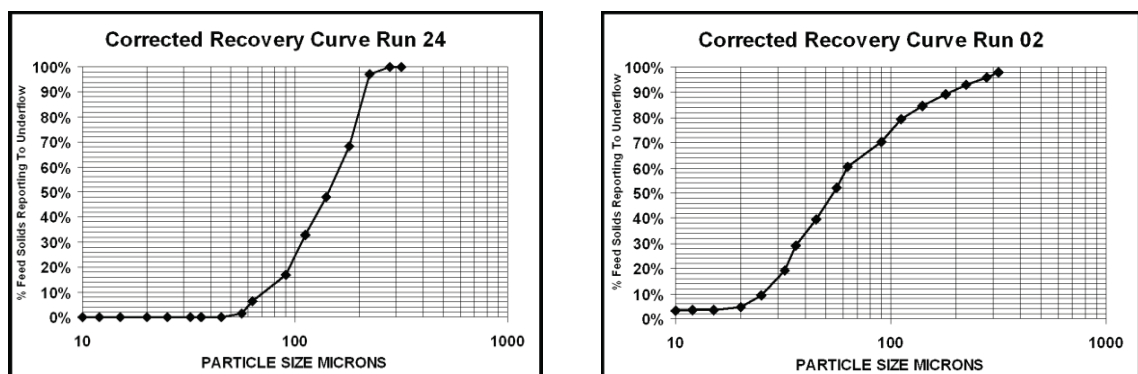


Figure 89: Recovery curve for optimized underflow (Run 24) and too dilute underflow (Run 02)

It can be clearly seen that the shape of these two curves is very different and that the quality of the overflow product can be influenced significantly by varying the water split¹⁴. Also the discharge patterns vary significantly as per Figure 90.

¹⁴ van Ommen R., Flachberger H., Selected examples of the influence of cyclone underflow density to a closed circuit grinding system, AT Mineral Processing, Heft 11, 2009, pp. 56-61



Figure 90: Picture of underflow discharge. Left run24 and right run 02

In addition, the shape of the recovery curves at the tops and tails differ quite significantly. Not only between the two runs shown in Figure 89, but also within a single recovery curve. For cyclone performance simulation and prediction this aspect is important as traditional mathematical models of recovery curves suggest a symmetrical shape. It is realized immediately that for a wide range of operating conditions this assumption does not apply. Therefore, a revised mathematical model was established allowing shaping the tops and tails of a recovery curve separately, but not fully independently, to avoid a step function around the D50 point. This model of the recovery curve allows a much more precise analysis and prediction of hydrocyclone performance under varying flow splits.

6.3. New approach to cyclone recovery curve simulation

6.3.1. Shortcomings of existing models

Cyclone performance simulation is split into two different disciplines which is the establishing of the cyclone D50 and the realistic modelling of the shape of the estimated recovery curve. The first is subject of many publications and is also described in Chapter 3. The latter is done in most models by the earlier presented Lynch Rao equation (Equation 1) as shown below.

$$T_{\alpha}(D) = \frac{e^{\alpha \frac{D}{D50}} - 1}{e^{\alpha \frac{D}{D50}} + e^{\alpha} - 2} \quad \text{Equation 1: Lynch Rao Equation}$$

T(D): Partition Number for a selected particular fraction D

D: particular size fraction [μm]

D50: calculated D50 of cyclone [μm]

α : Alpha value

In this equation, the alpha value is the only free variable that can be modified to change the shape (slope) of the recovery curve. The resulting curve derived from equation 1 is symmetrical around the D50 point. The upper and lower tails of the recovery curve are symmetrical as well and cannot be shaped differently. The systematic test work, as well as plant data, show that the shape of the upper and the lower tail of the recovery curve vary significantly with the variation of the water split in the hydrocyclone (see figure 84). At this point the clear limitation of that model is obvious to the reader. This variation and the influence of the water split to the overall shape of the recovery curve cannot be described sufficient with the symmetrical model.

To mitigate the shortcomings of the symmetrical approach, an improved equation for the modelling of the recovery curve is needed to provide the possibility to modify the shape of the upper and the lower tail of the recovery curve independently to adjust for varying water splits, but at the same time the approximated linear shape around the D50 should be maintained.

6.3.2. Advanced model of cyclone recovery curve simulation and analysis

This new model shall eliminate the shortcomings of the symmetrical approach and allow the separate shaping of the lower section of the curve ($D < D_{50}$) and the upper section of the curve ($D > D_{50}$), and at the same time keep the linearity around the D_{50} .

The improved model is also based on equation 1, $T_{\alpha}(D)$. However a second variable depending on D is introduced.

The first step to the above concept is the below function

This equation however has a step at the D_{50} point for $\alpha \neq \beta$ and is therefore not perfectly suited because such a step does not exist in real recovery curves.

To resolve this, the function $U_{\alpha\beta}$ is modified such that the weighted value of $T_{\alpha}(D)$ and $T_{\beta}(D)$ is in a linear relation to D . This leads to equation

$$V_{\alpha\beta}(D) = 1 - \frac{D}{k} \cdot T_{\alpha}(D) + \frac{D}{k} \cdot T_{\beta}(D) \quad \text{Equation 2}$$

When comparing results calculated from equation 2 against the recovery curves from hydrocyclones derived from actual data, it is observed that the shift of the influence of $T_{\alpha}(D)$ and $T_{\beta}(D)$ with the variation of D is not showing the desired shape around the D_{50} value.

To align equation 2 to the separation characteristics of a hydrocyclone, a solution is suggested that achieves results somehow between $U_{\alpha\beta}$ and $V_{\alpha\beta}$. In particular the shift in weight between $T_{\alpha}(D)$ and $T_{\beta}(D)$ must be balanced and set around the critical D_{50} value. After a critical review with actual results from practical experiences it was discovered that the Lynch-Rao equation itself is well suited as a suitable function for balancing the weighing around the D_{50} value correct. This leads to the *weighted two parameter Lynch-Rao function*.

$$W_{\alpha\beta}(D) = 1 - \frac{D}{D_{50}} \cdot T_{\alpha}(D) + \frac{D}{D_{50}} \cdot T_{\beta}(D) \quad \text{Equation 3}$$

A reality check of equation 3 shows that for small values of D , $W_{\alpha\beta}$ is similar to $T\alpha(D)$ and for large values similar to $T\beta(D)$. This equation now nicely allows defining different shapes/slopes of the recovery curve for the upper portion of the curve ($D > D_{50}$) and the lower portion of the curve ($D < D_{50}$) without having a step function around D_{50} .

This *weighted two parameter Lynch-Rao function* is now much more suitable to describe the partition curve of a hydrocyclone under varying water splits. It is suitable for both, simulating and analyzing hydrocyclone performance more precisely as when using the symmetrical model.

Much practical work was done with this model on industry level. Green field project simulation as well as brown field evaluation was conducted with various flows and cyclone sizes showing excellent results and fit. Figure 75 shows the different results using a symmetrical and the new model for the analysis of actual plant data. This example illustrates the remarkable improvement of the new model.

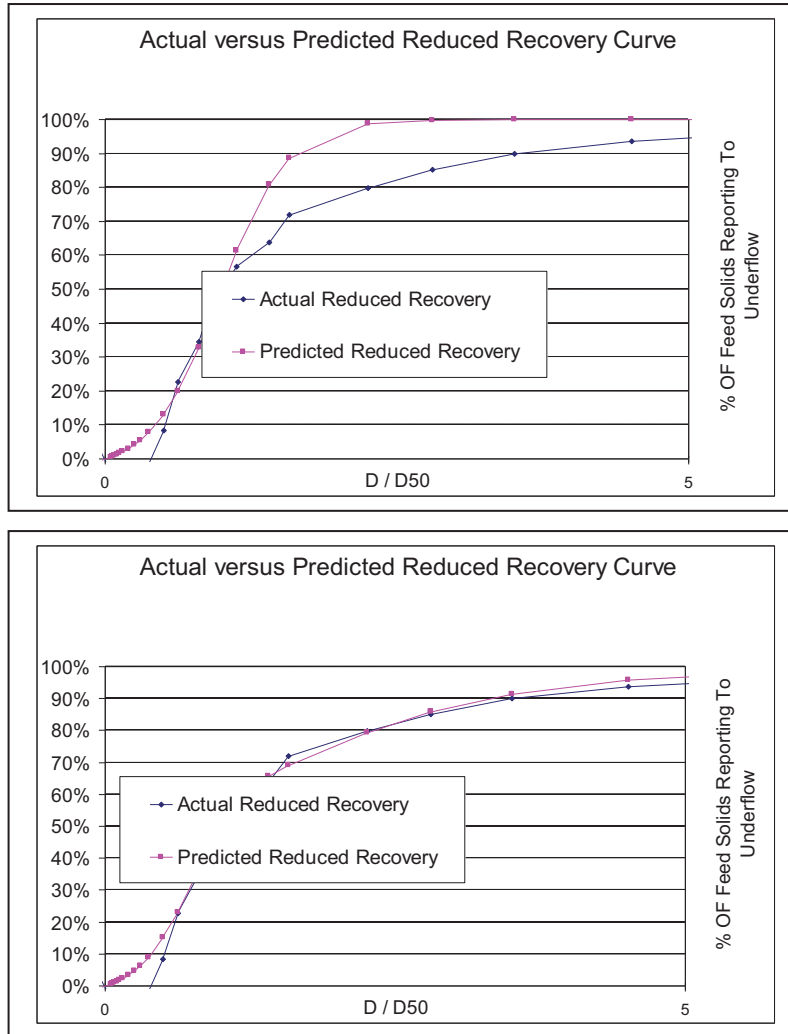


Figure 91: Actual versus reduced recovery curve with traditional and advanced model

Figure 91 shows the predicted curve with a symmetrical model ($\text{Alpha} = 3.5$) with a great discrepancy between the predicted and the actual curve and the lower graph shows the predicted curve matching the actual very well with the use of the introduced new model ($\text{Alpha} = 3.5, \text{Beta} = 0.7$). All tests were re evaluated with the FLS software that was updated with this model, the results and nice fits are shown in the chapter 9, pages 216-225. Cyclone

CHAPTER 7: Economical Considerations

7.1. Objective of the chapter

Chapter 7 presents a brief review of the identified technical opportunities and their related economic consequences. This chapter will only highlight the economic contribution that can be achieved with the correct and optimized use of hydrocyclones in plants with a focus on closed circuit grinding. Other areas of green field plant investment problems like long time line, cost of capital, process and equipment selection and environmental and legal processes will not be highlighted.

The questions addressed are the optimization potentials at the operational level, more specifically the correct operation and maintenance, knowledge management and investment analysis of equipment for modernisation change outs. All these aspects finally lead to increased revenue, savings of operating expenses, lower total cost of ownership and finally to improved cash flow.

7.2. Conclusions and Summary of Chapter 7

Continuously operating mineral processing plants generate remarkable cash flows. All operational and strategic efforts must strive towards the achievement of best operating practices as these directly translate to cash flow. The most important step to best practices is proper knowledge management and the understanding, recognizing, and growth of a firms' intellectual capital. A company's environment must be designed such that it supports innovation and the transfer of knowledge. Only with innovative and knowledgeable employees technical and structural changes for improvement can be leveraged. These changes lead to projects that have to be carefully evaluated by capital budgeting tools.

As elaborated in chapter 7, two main technical approaches can be made on hydrocyclone operation. First the reduction of operating pressure which leads to savings in energy and maintenance cost. Second improved density regimes lead to improved separation and grinding circuit performance. There the economical result is improved recovery in the downstream processes and higher throughput in grinding circuits generating more product. The benefits of both approaches can be summarized as follows:

- Improved recovery results in more product and enhanced revenues
- Higher recovery leads to better utilization of exhaustible, non-renewable resources and thus increases the amount of recoverable reserves on a company, national and global level
- Lower power requirements result in a reduction of operating costs leading to higher profits at given revenues
- Lower power requirements result in a reduction of power-related environmental effects, notably CO₂-emissions.

7.3. Introduction

Whatever sophisticated and smart machines and processes engineers come up with, the decision of plants and equipment being built, replaced or implemented is always based on hard economic facts. The global financial crisis in 2009 has drastically shown how difficult economic survival in the minerals industry is in times of sharply lower commodity prices. Many operations that mushroomed in the vast upturn of the minerals industry during the recent commodity boom were built on high operating and capital cost only able to service in booming raw materials markets, suddenly closed down or went into care and maintenance. So the cost of production is an integral decision making factor in that industry sector. Most of these plant closures however were the result of marginal deposits and low grade ores rather than inadequate process technology.

7.4. Correct operation and maintenance of hydrocyclones

In contrast to most other process equipment a cyclone continues operating even when liners are worn, faulty or the overall set up is incorrect. Because cyclones have no moving parts they are extremely easy to maintain and very often treated on a repair when fail mode. What most operators and process managers do underestimate are the massive downstream consequences of badly operated cyclones. In the primary classification stage the correct particle size distribution for all downstream processes is established and so the overall plant recovery is highly affected by the performance of the classification system. At the same time it must also be highlighted that the comminution process and within that process, mainly primary grinding is the most expensive process in the overall plant and any savings here can be of substantial value.

All the optimization and operating concepts discussed in this work can only be executed successfully when cyclones are always operated in a consistent operational mode and their maintenance is done on a preventive maintenance plan with close cooperation to the plant metallurgists sampling and testing plan. Any negligence of preventive maintenance leads to mechanical deficits (worn or destroyed liners, holes in vortex finders or cyclone housings, too large apex diameter etc.), immediately translating into excessive misplaced particles in the cyclone overflow or underflow and leading to a loss in recovery or higher operating expenses in the most expensive sub system in the plant – the grinding section.

Important aspects of correct cyclone operation:

- Understand the operating principles and factors influencing performance.
- Never run cyclones at a higher overflow or feed density than necessary.
- Run cyclones always on highest possible underflow density.
- Adjust the number of operating cyclones to the current flow.
- Always operate cyclones in a geometric symmetrical way on a manifold.
- Keep records of operating hours and wear rate of each cyclone.
- Set up a material mix of liners so that a cyclone wears out evenly.
- Do maintenance once a set tolerance is exceeded.
- Work in close cooperation with the cyclone manufacturer for gaining expertise or reconfirming changes.

Process-, equipment-, as well as maintenance knowledge is an integral part of successful cyclone and plant operation and shall therefore be highlighted in chapter 7.5.

7.5. Knowledge Management

Knowing the equipment and processes in a plant and knowing how to operate them, is important. Economists used to describe the basic resources necessary to run an enterprise as three major assets, being land, labour and capital –capital in the context of financial and tangible fixed assets.

When asking about the importance of intangible assets like knowledge and intellectual assets, there is full agreement about their importance and someone would realize that these terms are well recognized throughout all industries. But when asked to define what intellectual capital, knowledge or intellectual assets are, answers would be quite different and diverse.

Basically knowledge based companies have three components of intangible assets, being

- Intellectual capital – unique assets
- Structural capital – generic assets
- Complimentary business assets – differentiable assets

As shown in figure 92 below, the basis of each operation is the structural capital which is inventory, cash, the organizational structure and operational methods and procedures. Complementary business assets are business assets that a firm uses to commercialize innovation and ideas (or marketable intellectual assets). These complementary assets are the catalyst to allocate and create commercial value to innovations. These may be manufacturing facilities, logistics, manufacturing techniques, manufacturing processes, suppliers, distribution capabilities and sales as well as service capabilities. “Complementary assets may be thought as the string of assets through which the innovations must be processed in order to reach the customer. No matter how exciting an intellectual asset itself may be, it will have little commercial value unless paired with the appropriate complementary assets.”¹⁵

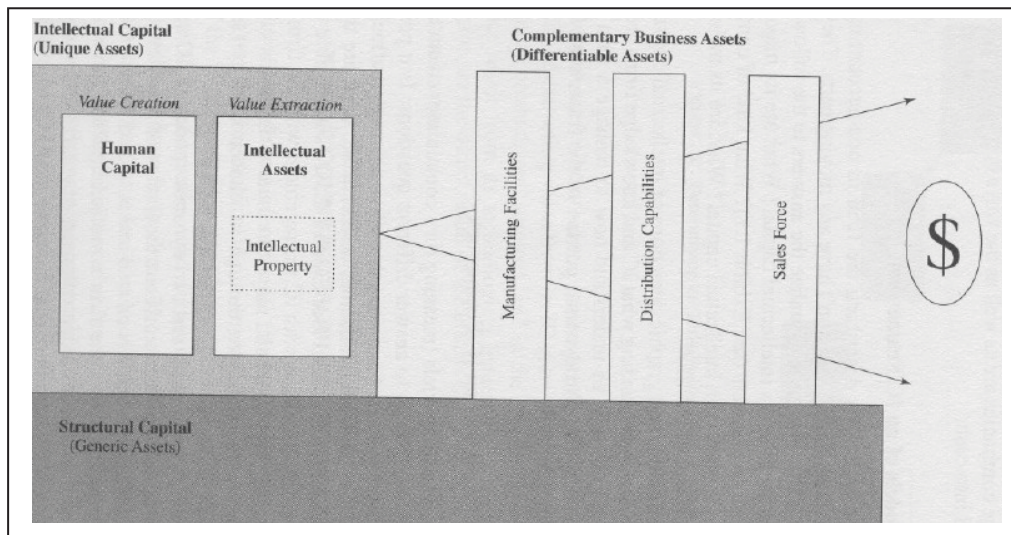


Figure 92: A model of a knowledge company¹⁶

Amongst these three types of knowledge based capital, the concept of Intellectual capital is highlighted because this type is the main driver needed in the mining industry on an operational level running equipment and processes in a process

¹⁵ SULLIVAN, P. H., Value-Driven Intellectual Capital. How to Convert Intangible Corporate Assets into Market Value. New York: John Wiley and Sons, 2000, ISBN 0-471-35104-0, page 232

¹⁶ Sullivan, P.H., Value –Driven Intellectual Capital. How to Convert Intangible Corporate Assets into Market Value. New York: John Wiley and Sons, 2000, p30

plant. Managers do need to understand its structure and principles in order to manage that asset the best possible way.

7.5.1. Intellectual Capital – Unique assets

The intellectual capital of a company is unique in its composition. Firms may have the one or other comparable asset, but the entire asset portfolio is unique and difficult to copy. A specific asset portfolio can only be copied by another firm with the allocation of a large quantity of resources of manpower and time. As these assets are not static, but dynamically moving aligned with the firms' vision and strategy the task is even harder. Unique assets therefore are not duplicable in the short run by another firm.

A firms unique asset portfolio consist of

- Human capital
- Intellectual assets
- Intellectual property.

7.5.1.1. *Human capital*

Human capital is the knowledge, skills and abilities of the employees in an organization. Human capital represents non codified, tacit knowledge. Tacit knowledge resides within an individual. It can be skills, experience, or knowledge that has been passed from teacher to student or from master to apprentice. This is the form of knowledge that leaves the company every day with the individual. It is the brainpower or the knowhow of a firm's employee, but also of the firms suppliers and partners. All elements that together provide a sellable product and the achievement of the firms' vision and strategy.

Human capital is a resource, because it adds value to a company, and its products and processes. This value cannot be delivered without the employee who possesses it. This sort of capital is also commonly understood as knowledge, more precisely, tacit knowledge. Compared to the classic production factors, knowledge has distinct properties:

Knowledge is not exhausted or destroyed by use or consumption, rather its value increases with dissemination. Knowledge is a commodity with increasing returns and an extremely positive impact on its environment.

Data is not knowledge. In the age of Internet there are virtually no limits to its transfer. Data must be converted by people to knowledge, because knowledge is a resource that is essentially and exclusively bound to people. The ability to communicate so called tacit knowledge represents a restriction on the transfer of knowledge, which takes place from one person to another. It also can take place from an institution to an individual.

Within the human capital, knowledge creation plays an important role. Knowledge – tacit knowledge – innovations and new ideas per se are only generated here. This knowledge creation can happen in two ways. First if tacit knowledge is communicated from one person to another- the value of that tacit knowledge increases by its dissemination. Secondly new knowledge can be created by creativity and innovation. Here lies the essential core of the firms' future – its new products and strategies.

Even though in many cases knowledge is readily available, its acquisition by individuals and organizations implies costs and the necessity of learning processes. For the optimum transfer of knowledge from one person to another, suitable structures, conditions and incentives must exist. Knowledge is also expressed in these structures and conditions. Here one element, knowledge and knowledge creation, fosters the other –a suitable structure, each by itself can hardly exist without the other.

7.5.1.2. Intellectual assets

An intellectual asset is codified knowledge extracted from human capital. Codified knowledge is physically possessed by a company in the form of written procedures, manuals, papers and publications or electronically processed knowledge in databases or tables. Codified knowledge is accessible to the company and selected individuals all the time and is independent of an individual's knowledge that leaves the company every day with the employee when going home from work. Intellectual assets can be split into commercializable intellectual assets and supporting intellectual assets. It is tangible, knowledge in databases or writing which the firm possesses and can assert ownership rights.

For a knowledge company the distinction of tacit and explicit knowledge is of utmost importance, since property rights can only be generated on explicit knowledge. But codifying knowledge is not an easy managerial task. First employees must be convinced to be willing to share their knowledge and to finally

put it down on paper. It is still the belief that someone who possesses knowledge others do not have, has a greater value to a firm. Very often people use knowledge as an instrument of power. This indeed may be true, but when sharing knowledge a person might have an even greater value to and within a corporation. In larger entities it also might be a problem to identify knowledge. An ideal situation might be a collective intelligence, like “The Borg” in the series Star Ship Enterprise has. Of course this is science fiction, but databases and smart IT systems are sort of that. The remaining yet unsolved problem is how someone can find something that is new to him, when not yet knowing what to look for? The dialogue seems to be a way of distribution, but then knowledge still remains in human capital, although disseminated within a firm. Although still better for the firm, it does not eliminate the need for codification as the knowledge is still in the possession of individuals and not owned by the company.

7.5.1.3. Intellectual property

Intellectual properties are intellectual assets that receive legal protection. All intellectual assets that are covered by intellectual property law (a patent for example), can be legally protected. That sort of protection must be legalized at the authority, so a firm may decide if an intellectual asset may turn into intellectual property or not.

7.5.2. Value creation and measurement systems

Value is a concept with many interpretations. It is highly subjective and its concept and interpretation depends on a person’s view and attitude. Therefore value is relative. What is of great value to an operation or person might not be of value to another. In the current context, however, the economists point of view shall be used which is expressed usually in dollar terms. This concept, applied to a process plant results in direct value activities. Any intellectual capital (IC) activity that results in additional revenue or cost reduction is considered a direct value activity.

Any knowledge based process seamlessly links intellectual capital and value. Intellectual capital creates best practices that generate best recoveries in the plant, lowest cost of ownership of the equipment, innovation and consequently optimization and such produces the best possible cash flow.

Proper IC management in process plants directly translates to downtime, recovery and operating cost. It does not need sophisticated measurement tools like balanced scorecards or intellectual property reports, although such processes assist managers to drive and communicate their strategies, all it needs is the creation of key data to build a set of benchmarks for future orientation and optimization.

In practice knowledge management in plants related to hydrocyclone optimization is based on two elements, knowledge creation and retention.

For knowledge creation several tools can be used:

- On-the-job training of operators by equipment suppliers
- Workshops for metallurgists by equipment suppliers
- Operating manuals (periodically updated)
- Close monitoring of cyclone performance and feedback to and from cyclone supplier
- Preventive maintenance on cyclones including the registration of operating hours and setting of min/max tolerances on critical cyclone measures like apex diameter and vortex finder diameter.
- Creation of a hydrocyclone by mixing liner materials that wear out evenly
- Regular audits by cyclone suppliers to assess optimization potentials due to changed operating conditions, personnel or infrastructure.

Furthermore key personnel must be retained. The training of people to fully understand cyclone operation is a lengthy process and the created knowledge is usually not codified, but owned by the individual. When this individual leaves the company, all the valuable experience and knowledge is also lost.

Moreover an environment that supports innovation and transfer of tacit knowledge must be created. Finally, if by the structure of the business, a high turnover of personnel is unavoidable, the companies' effort must be codifying tacit knowledge to enable a seamless hand over of the plant to the next set of staff.

7.5.3. Selected regional trends and examples of corporate culture

The presentation of the three examples discussed below shall not point a finger to a region, state or population. But it should make someone think about potentials for improvement. More important this could also serve as a future potential analysis. In areas where bad practices and their consequences are so obvious, at the same time the highest future potential can be identified while in perfectly organized well oiled organizations very often the room for improvement is marginal. In other words by reading between the lines we see our future competition.

7.5.3.1. *Europe*

In Europe usually long time employees on a high educational level operate process plants. These people usually do understand their processes and machinery used very well and as such come very close to the theoretical possible best performance. Best practices are in place, and the retention and creation of intellectual capital are integrated processes in the enterprises strategy. One of the best examples in Europe are Scandinavian companies that employ well paid highly educated long term employees and as such can successfully run large operations in a competitive market although having an extremely high level of personnel cost. It is their productivity and not their cost which is the prevailing factor of success.

7.5.3.2. *Africa*

In Africa plants are run by expatriates, frequently on 2-3 year contracts. Basically African operations are “managed by walking away from it”. The plant operators are mostly poorly educated local people that do only follow guidelines and given orders without understanding the underlying principles and as such only serve the system. Also the contract terms of the expatriates are in general too short to allow the establishment of best practices. After coming new into an operation it takes, depending on experience, several months to understand the local processes and practices. If someone is not really interested, these are never thoroughly understood. Then there is a period of about 1.5 years in which the person can change and influence things until hitting the end of the assignment period that is usually used for seeking new opportunities. Considering the time frame needed to identify improvement, the process of working out a alternative technical solution

and the evaluation of the investment and finally the time needed to get the investment agreed internally and last but not least purchasing, delivery and start up, the assignment of that expatriate is coming to its end or is over already. This is the inherent flaw of such operations and it takes a very strong individual to do changes in a plant as it is so much easier to just carry on with business as usual. More recently operations in Africa have started identifying that issue and employ now well educated locals that stay at the same location for many years and go through a very well designed education process. This concept proved to be quite successful; however it is only in its beginning stages.

7.5.3.3. Russia

Russia is somehow different. The author describes the Russian approach often as management on a need to know basis. All operations are still organized in a very hierarchical way, best compared to military. People are usually well educated and often stay a lifetime in one operation. A major cause for this is also the immobility of Russians within Russia which is still a major problem in that region. Also the options of employment are often limited to one big company in such regions and therefore people are extremely risk adverse in order not to lose their employment in a highly hierarchical structure. As a consequence it is almost impossible to initiate any type of change as someone would have to take a decision to do so and should the project fail would immediately lose his position. The only chance of change is in the case of new projects, expansions, major rehabilitations or the change out of obsolete process islands.

7.6. Cyclone sizing and change out of outdated equipment

The metallurgical performance of the various cyclone generations must be known when sizing cyclones for green field applications. It must be noted, that each generation of cyclones still has its applications and none of them shall be neglected. However with a few exceptions like low volumetric flows combined with very coarse separation, the newest technology is usually the best selection. It is easy to see that the multiple cone angle cyclones at the same operating conditions provide a much finer separation compared to a cyclone with a 20 degree and 10 degree cone angle. This advantage can now be leveraged in three different ways:

- First a lower number of larger cyclones can be utilized for duties where a high number of older design cyclones of smaller diameter would have been needed.

- Second, much higher overflow densities can be realized, especially in grinding circuits, without getting too small in cyclone diameter (with low or almost no risk of roping and plugging).
- Third, multiple cone angle cyclones do not depend so much on feed pressure, because the necessary tangential velocity needed for the separation work is generated by the shape of these cyclones, and so these cyclones can be operated at very low pressures compared to all other cyclone designs.

The examples out of the industry described later in chapter 7.8. do reflect these savings potentials. On green field cyclone sizing the main question is if the customer wants a cheap initial price or the lowest possible total cost of ownership. Very often these two very different approaches to equipment selection are not thoroughly evaluated, compared and distinguished especially when large EPC¹⁷ companies execute a project on behalf of a mining company. The initial plant design and equipment selection is always constrained by limited budgets and the outcome is very often to favour a low cost supply alternative. In the case studies outlined below it can be clearly seen that this approach is absolutely wrong as pay back is extremely short for more expensive equipment that is purposely designed for lowest total cost of ownership. However this situation also creates opportunities for improvement later on and often leads to the ability of selling the same equipment twice to the same operation, once the project has sufficient cash flow, allowing room for improvement.

For existing plants the situation is somehow different. In such cases the owner itself evaluates the benefits very often in cooperation with a consultant or a manufacturer. If a change out of equipment is considered to be beneficial, capital has to be raised within the corporation for purchasing new equipment. Mining corporations are large multinational organisations where capital release for expenditure is subject to strict internal rules and regulations. Any investment has to be turned in as a capital project with a description of soft facts, hard technical facts and finally, most important, a budgetary evaluation if the execution of the project makes sense and is feasible based on company guidelines. Methods generally applied in this process are discussed in more detail in the following section.

¹⁷ EPC: Engineering, Procurement and Construction

7.7. Investment analysis and Capital budgeting

All projects submitted in a corporation need to be evaluated with approved and generally accepted tools for capital project evaluations. Typical projects in the mining industry, with the objective of improvements on processing plant in particular can be,

- Replacement of obsolete equipment in order to maintain operation.
- Replacement of equipment to reduce operating expenditures
- Expansion
- Safety projects
- Environmental project
- Other

Out of these types of projects the replacement of equipment to reduce operating expenditures is the most important one to an equipment supplier. The reduction in cost can be maintenance cost like labour and parts consumption, cost of electricity and better performance like higher recovery or downstream benefits due to improved particle size distribution.

There are several methods used in the industry, some of them more applicable to small and shorter projects, others more suited for larger, long term investments. The decision for a replacement of equipment like a hydrocyclone cluster is usually taken when payback or break even is achieved in a very short period of time, usually shorter than 1 year, but the various methods of capital budgeting evaluation must be understood when evaluating any type of project, presented to executive level.

7.7.1. Methods of investment analysis and capital project evaluation

- Payback period
- Accounting rate of return
- Discounted payback
- Net present value
- Internal rate of return
- Modified internal rate of return
- Profitability index

7.7.1.1. Payback and accounting rate of return

The payback period is the expected number of years required to recover the cost of a capital investment. This method is the easiest and also one of the oldest ones used for project evaluation.

The accounting rate of return is the percentage calculated from average annual profits after taxes divided by average investment.

Both of these methods do not take the cost of the invested capital into account and are only suitable for the evaluation of low value and fast payback type of investments. The shorter the payback time, the better a project is. Most of the major mining companies accept this simplified approach for low value capital expenditures provided the payback time is less than one year. The payback period can be calculated as follows:

$$\text{Payback (years)} = \text{Project Investment} / \text{Annual cash flows}$$

7.7.1.2. Discounted payback

This variation of the payback takes the cost of capital into account. The discounted payback period is the time needed to recover the investment from discounted cash flows. Each cash inflow is divided by $(1+k)^t$, with k being the cost of capital and t the time element. Both, the payback and the discounted payback have an inherent flaw as they do not take future generated cash flows, received after the payback period, into account. The basic information acquired from these methods is how long cash is tied up in investments, or in other words, the projects liquidity.

7.7.1.3. Net Present Value (NPV)

The shortcomings of the methods presented above are taken care of in the Net Present Value (NPV) calculation/method. The NPV is calculated by discounting all cash flows and then subtracting all outflows from the cash inflows.

- _____
- _____
- t time period (i.e., year)
n last period of project

R_t cash flow in period t
 O_t cash outflow in period t
 k discount rate or cost of capital

The discount rate k , also called the cost of capital, is the interest rate chosen for project evaluation and the project time n is the total life time of the project. So future cash flows, beyond the payback time are recognized. If the NPV of a project is zero, the project is just able to repay the capital invested plus providing the required return on capital cost. If a project has a positive NPV then it creates more cash than it needs to repay the investment plus the desired return on capital and such is adding additional value to the corporation. As a matter of fact projects with positive NPV shall be accepted and projects with a negative NPV are rejected.

7.7.1.4. Internal rate of Return (IRR)

The calculation of the IRR is very similar to the calculation of the NPV, however the equation is now solved for the variable IRR. The IRR represents the discount rate at which the discounted projects cash outflow equals the discounted projects inflow. The IRR is that discount rate, where the NPV of a project turns to zero.

The decision on a project depends on the cost of capital k required by the investor. If the IRR is higher than k , the project can be approved, if the IRR is lower than k it should be rejected. Solving above equation for IRR is not a trivial matter anymore and is usually done with a financial calculator or a spreadsheet calculation. The IRR method is widely accepted and preferred by executives in the mining industry and therefore a very common instrument.

7.7.1.5. Modified IRR – MIRR

Although the NPV method is the better method of evaluating projects, the IRR is often preferred by executives as they seem to prefer relative figures in percentages over dollar values. Depending on size and project specific cash flow the IRR and the NPV can generate different evaluations. The situation then has to be further evaluated with net present value profiles and viewing at the terminal value of a project.

To eliminate the inherent problem of the IRR, the modified IRR or MIRR represents a better indicator of relative profitability.

“Here COF refers to cash outflows (negative numbers), or the cost of the project and CIF refers to cash inflows (positive numbers). The left term is simply the PV of the investment outlays when discounted at the cost of capital, and the numerator of the right term is the future value of the inflows, *assuming that the cash inflows are reinvested at the cost of capital*. The future value of the cash inflows is also called the terminal value, or TV. The discount rate that forces the PV of the TV to equal the PV of the costs is defined as the MIRR¹⁸”.

7.7.1.6. Profitability index

The profitability index, also called benefit cost ratio shows the relative profitability of a project.

$$\frac{\text{_____}}{\text{_____}}$$

CIF_t expected cash inflows

COF_t expected cash outflows

If the PI is larger than 1, the project can be accepted, the higher the ratio, the better the project.

¹⁸ Brigham, E.F., Financial management; theory and practice, The Dryden Press, 1999, ISBN 0-03-024399-8

7.8. Selected Examples from the industry

7.8.1. Goldfields Ghana, Tarkwa; operating cost gMAX versus 20 degree cone cyclones

Tarkwa Gold mine in Ghana, owned and operated by Goldfields is one of the biggest single mines in West Africa with a plant throughput of 1,400 – 1,600 MTPH depending on the ore type treated. At the current head grade Tarkwa is producing 70 ounces of gold per hour which results at today's (March 2011) gold price of USD 1,400 / ounce in a daily value of USD 2,352,000 and a yearly turnover of 784,000,000 USD. The total cost of production, including operation, capital and amortization is USD 630 per ounce, resulting in a net profit of USD 420,000,000 per year. So someone would ask what a cyclone can contribute to such a big operation.

Goldfields initially started with a capacity of 600MTPH with a manifold of 12 units gMAX26 with 20 degree cones and 8" vortex finders, at an operating pressure of 1.1 bar. The volume flow was handled by a 20x18 Krebs millMAX pump with a power draw of 1,042 kW. On Goldfields 2008 expansion project shown in Fig. 93 the capacity was more than doubled by mirroring the plant. The new cyclone cluster was furnished with 12 units gMAX26 with 12" vortex finders, making the same separation at 0.5 bar. The new power draw on the pump was 896 kW which is a savings of 146 kW.



Figure 93: Tarkwa Gold, expansion 2008. On the left side the original plant and on the right side extension plant with new mill, pumps and cyclones, picture Roman van Ommen, 2009

In all calculations a power cost of 95 EURO/MWh for electrical power out of the grid and 160 EURO/MWh for diesel generated power is used. These figures are

representative values from actual operations. For an average operating year of 8,000 hours the savings in electrical energy due to reduced cyclone operating pressure is USD 110,960 for grid power and USD 186,880 for diesel generated power per cyclone manifold.

After these results were obtained, the first supplied manifold was rebuilt to gMAX cones, resulting in power savings of USD 221,920 on grid power and USD 373,760 for diesel generated power. On average the plant runs 20 % of the time on diesel power which results in a weighted savings of USD 252,288. The investment for the rebuild was USD 84,000 which generated power savings of USD 126,144 per year. In other words the pay back of the investment was 222 days (without considering cost of capital). The main technical data of the expansion project and the related cost savings are summarized in Figure 94.

Tarkwa Gold Mine	CURRENT	OPTIMIZED	Δ
Cyclone Type:	gMAX26-20	gMAX26	
Diameter [mm]	660	660	
Pressure [bar]	1.1	0.5	
Slurry Density [t/m ³]	1,476	1,49	
Pump	20x18	20x18	
Static Head [m]	37	31	6
power Draw [kW]	1,042.0	896.0	146.0
Operating hours	8,000.0	8,000.0	
Cost of Power Grid [EURO/mWh]	95.0	95.0	
Cost of Power ,Generated [EURO/mWh]	160.0	160.0	
COST of Power mix (80 % grid, 20% generated)[EURO/mWh]	108.0	108.0	
Cost of power per year [EURO] for 1 manifold Grid Power	791,920.0	680,960.0	110,960.0
Cost of power per year [EURO] for 1 manifold Generated Power	1,333,760.0	1,146,880.0	186,880.0
Cost of power per year [EURO] for 1 manifold power mix	900,288.0	774,144.0	126,144.0
Cost of power per year [EURO] for 2 manifolds			252,288.0

Figure 94: Cost comparison for Geita expansion

Aside from the power savings substantial savings in maintenance cost on cyclones, piping and pumps were recognized in the range of 20 %, resulting is additional USD 96,000 which totals the savings per annum to USD 352,442. This

is not an insignificant number considering the cost of a new manifold of that size is roughly USD 320,000.

7.8.2. AngloGold Ashanti, Geita Gold Mine; Change out case story

Geita gold mine, located in Tanzania just south of Lake Victoria is feeding its process plant with 650 MTPH new feed with a head grade of around 2 ppm. Their overall plant recovery varies depending on the pit from which the ore is delivered (as no blending bed is available to even out feed conditions), but average is around 94-95 %. The processing technology used in the plant is CIL (Carbon In Leach) and a major problem was identified with the leaching kinetics of particles larger than 150 microns.



Figure 95: Geita Gold Mine, hydrocyclones, 2x16 units gMAX15, top fed by a central feed distributor, picture Roman van Ommen, 2008

These particles do not have enough residence time to leach and consequently the majority of the gold contained in these particles is lost to tailings. After a sampling campaign on the tailings this amount was identified not to be insignificant.

Geita is running their process without a pre leach thickener. This seemed to be an interesting concept in the 1980s but it was widely abandoned because of operational difficulties. In order to produce a suitable feed to the cyanide leaching process, the cyclone overflow must have a slurry density of around 40 % by weight, which translates to a feed density of around 60 % by weight or higher. These types of plants usually use 380 mm cyclones and the model used at Geita was a DS15LB, a cyclone with an older style inlet head and a 20 degree cone. The recovery curve on this type of cyclone is very flat when operated at such elevated densities. The total installation consisted of 2 manifolds with 16 cyclones each, fed

by a radial distributor that distributes the slurry from the SAG-Ball mill sump to the 2 primary grinding manifolds and to two smaller manifolds, feeding a gravity separation section with Knelson concentrators.

As usual the throughput was pushed, leading to even higher feed densities with the consequence of coarser cyclone separation and circulating loads around 600 %. In order to achieve the required high overflow density, larger apex inserts were installed which works out achieving the high overflow density, but also produces a higher circulating load because of the high flow split towards the underflow and the resulting effect of too many fines being recirculated back to the mill. The portion of +150 μm particles in the overflow was 8 % of the total mass yield to the overflow, with consequential losses in CIL recovery to tailings.

In that situation Krebs was called to make an assessment of what is happening and how the problems can be addressed. The recommendation was switching over to gMAX technology as these cyclones do have a much sharper separation at high density slurries, and can easily achieve a 40 % overflow density while still maintaining a 51-52 % by volume which is needed to minimize fines recirculation. Geita installed 32 units of gMAX cyclones shown in Figure 95 and the results were extremely positive to the overall process.

First the operating pressure dropped from around 0.2 bar to 0.75 bar with consequential power savings as elaborated in 7.8.1. Now by maintaining a high density underflow, the circulating load dropped by 100 % points. The remaining excessive circulating load was a consequence of running a plant designed for 500 MTPH at 650 – 700 MTPH, but this is a different story. The most important effect was reducing the content of the +150 μm fraction in the overflow from 8 % to around 4 % which led to a proved and measured increase of overall plant recovery of 1.5 % points.

The financial benefits of that installation are impressive, even when only looking at the effect of the overall recovery increase and leaving the savings in pumping and maintenance cost aside. With a production of 650 MTPH at a head grade of 2 ppm and a recovery of 95 % the hourly production was 43.56 ounces of gold per hour resulting in a gold production equivalent to USD 487,872,000 assuming a gold price of USD 1,400 per ounce. The increase of recovery by 1.5 % points led to an hourly increase in production of 0.65 ounces which results in an yearly increase of production of USD 7,280,000. The cost of changing over to gMAX cyclones was around USD 300,000.

This drastic example shows the dormant potential of many existing operations. Gold however is always a good example because of the high value of the product. Other industries with lower yield products definitively require longer payback periods.

7.8.3. A sand plant in Europe – a thought experiment

The above examples of big operations with huge flows and high value products are impressive, but it shall be shown that there is also potential for savings on a small scale. For this purpose we take the example of sand & gravel plant Riedmueller, located in Schoenfeld near Lasse, Lower Austria, and examine a duty common in most sand and gravel plants in central Europe.

The pump duty for the dewatering cyclone is a static height of about 10 m with 1,5 m sump level. The calculated TDH (total dynamic head) for the 20 degree cone cyclone would be 21.1 m and for the gMAX 13.6 m resulting in the same metallurgical performance and volumetric throughput.

A pump selection results in a 10x8x27 pump with a power draw of 57 kW for the 20 degree cone and 36.7 kW for the gMAX. If we now calculate 4,000 operating hours for such a cyclone per year, the difference in power cost will be EURO 7,714. The cost of a new cyclone is around EURO 12,307. By selecting a better technology up front operating cost can be saved. Considering a life time of a cyclone in operation of about 15 years on average also a new investment by changing out the cyclone can be justified easily. The simplified investment analysis for this example using the NPV- and IRR criterion is presented in Figure 96 below.¹⁹

Sand Plant			
k=	6 %		
Time	0	1	2
Cash Flow	-12,307.0	7,714.0	7,714.0
NPV=	1,835.79		
IRR=	16.49%		

Figure 96: NPV and IRR calculation of a sand plant

¹⁹ In this analysis only the initial investment and the associated energy savings are taken into account while tax benefits resulting from the depreciation of the asset are neglected.

The analysis confirms that based on the assumed cost of capital of 6% this investment yields a positive NPV and an attractive IRR already within a very short 2 year project time frame.

7.8.4. Siguiri Pump Project (Guinea, Africa)

Siguiri Gold plant is owned by AngloGold Ashanti and is located in North East Guinea, close to the border to Mali. The plant is handling a new feed of 2,200 MTPH. The initial grind of the hydrocyclones was designed with 80 % passing 150 μm at a circulating load of 120 %. After 5 years of operation the ore body changes such that leaching kinetics demanded a finer grind of 80 % passing 75 microns. The original hydrocyclone selection of Krebs gMAX26 was based on the coarser grind and to enable the hydrocyclones to cut finer the apex inserts were widened in diameter and the pressure was raised to 1.2 bar. The new resulting circulating load was 140 % because of excessive slimes recirculation back to the mill.

Krebs was called to do an assessment on the circuit and the benchmark was a measureable improvement in grind and operating cost.

The 660 mm diameter cyclone was not able to handle the fine grind and a new cluster with 20 units gMAX 20 was suggested. The new type of hydrocyclone is able to run at 1.0 bar and reduces the circulating load to 120% and further reduced the slurry flow due to the higher feed density. See cyclone calculations chapter 9, pages 232 and 233. The resulting lower flow, combined with the reduced circulating load and the associated energy savings are summarized in figure 97 below together with other key data.

Siguiri Pump Project	CURRENT	OPTIMIZED	Δ
Cyclone Type:	gMAX26	gMAX20	
Diameter [mm]	660	500	
Pressure [bar]	1,216	1	
Slurry Density [t/m ³]	1,476	1.49	
Pump	28x26x64	28x24x64	
Flow [m ³ /h]	7,275.1	6,224.0	1,051.1
rpm [min ⁻¹]	293	281	12
Static Head [m]	37	34.8	2.2
Slurry Power	1,332.1	1,114.0	218.1
power Draw [kW]	1,332.1	1,114.0	218.1
Operating hours	8,000.0	8,000.0	
Cost of Power Grid [EURO/mWh]	95.0	95,0	
Cost of Power Generated [EURO/mWh]	160.0	160.0	
COST of Power mix (3/4 grid, 1/4 generated)[EURO/mWh]	111.25	111.25	
Cost of power per year [EURO]	1,185,569.0	991,460.0	194,109.0

Figure 97: Cyclone comparison and energy savings Siguiri

The power savings of the new cyclone set up is EURO 194,109 per year. The investment cost of a complete new cyclone cluster including installation cost is EURO 520,000. The investment life time was benchmarked by Anglo management with 5 years with a cost of capital of 10%. A NPV and IRR analysis was done on the investment and the results are summarized in Figure 98 below:

<i>Siguiri Pump</i>						
Cost of Capital	10.00 %					
Time	0	1	2	3	4	5
Cash Flow	-520,000.00	194,109.00	194,109.00	194,109.00	194,109.00	194,109.00
NPV=	215,825.83					
IRR=	25.19 %					

Figure 98: NPV and IRR on Siguiri project

Both NPV and IRR strongly suggest taking on the new investment, especially as the usable lifetime of a complete new hydrocyclone cluster is around 15-20 years. This investment is currently under evaluation by Anglo management.

7.9. Optimization potential for various mineral commodities

The examples given in chapter 7.8. are mainly taken from the gold industry but the optimization potential demonstrated and the associated economic benefits can be transferred to most mineral commodities such as coal, copper, iron ore, phosphates, diamonds etc.

All calculations based on energy savings due to lower operating pressure can be used identically in all other industries. The only variation is the local cost of power, but according to the experience of the author there is not a big deviation in the various mining areas all over the world.

When looking at recovery optimization, the gold industry is an extreme example because of the high value of the product. However the potential experienced there can be easily transferred to all other high value raw materials like platinum or diamonds.

In the coal industry the main driver of recovery is the heavy media separation which also needs a good classification ahead of each separation process; however classification there is usually done with screens because of the much coarser particle sizes of these processes.

There is also big potential in improved classification for all materials recovered with flotation circuits, notably with copper, lead and zinc ores, gold, nickel and phosphates. Top size is very critical for these processes as flotation cells can only pull particles up to a certain top size into the product. Usually a regrind circuit is integrated into every flotation circuit to liberate middlings, but the danger lies in producing too coarse particles which lead to sanding out the flotation cells. This often happens when cyclones get into a roping condition and as a consequence discharge unclassified slurry to the flotation circuit. Unfortunately no reliable data is available to quantify the savings potential in such operations.

CHAPTER 8: Literature

Allen, T., Particle Size Measurement, 2nd ed. Chapman and Hall, London.,1974 p. 77

Antunes M. and Medronho R.A., "Bradley hydrocyclones: design and performance analysis, in Svarovsky L., and Thew M.T. (editors), Hydrocyclones, Analysis and Applications, Kluwer Academic Publishers, Dordrecht, 1992, pp. 3-13

Apling, A.C., Montaldo, D. and Young, P.A., "Hydrocyclone models in an ore-grinding context", 9 in Int. Conf. on Hydrocyclones, Cambridge, 1-3 October 1980, BHRA Fluid Engineering, Cranfield, 1980, pp 113 – 125

Arterburn, R.A., The Sizing of Hydrocyclones, Krebs Engineers internal publication, 1976

Arterburn, R.A., The Sizing and Selection of Hydrocyclones, In: Design and Installation of Comminution Circuits, Society of Mining Engineers of AIME, New York, NY, USA, 1982, Volume 1, Chapter 32, pp. 597-607

Barrientos, A., Sampaio, R., Concha, F., Effect of the Air Core on the Performance of a Hydrocyclone, XVIII International Mining Processing Congress, Sydney, 23-28 May 1993, Publication volume, pp. 267-270.

Besendorfer, C., Exert the force of hydrocyclones, Krebs Engineers Bulletin No. v2-194 (3M 12/96)

Bloor, M.I.G. and Ingham, D.B., "Theoretical analysis of the conical cyclone", Paper E6, First European Conf. on Mixing and Centrifugal Separation, Cambridge, Sept. 9-11, 1974, BHRA Fluid Engineering, Carnfield, 1974

Bloor, M.I.G., On axially symmetric flow models for hydrocyclones, Paper D2, BHRA 3rd Int. Conf. on Hydrocyclones, Oxford, Sept.30 – Oct. 2, 1987, Elsevier Applied Science Publishers, Barking, 1987

Bloor, M.I.G., Ingham, D.B. and Ferguson, J.W.J., A viscous model for flow in the hydrocyclone, Session I, Solid-Liquid Separation Practice III, 397th event of the European Federation of Chemical Engineering, Bradford, March 29-31, 1989

Bloor, M.I.G., Ingham, D.B. and Laverack, S.D., "An analysis of boundary layer effects in a hydrocyclone", Paper 5, Proc. Int. Conf. on Hydrocyclones, Cambridge, 1-3 October, 1980, BHRA Fluid Engineering, Cranfield, 1980, pp. 49 to 62

Bochicchio, M. Field and Laboratory Cyclone Test Database – Mathematical Modelling for TD and Alpha as a Function of cyclone Process Variable, Krebs internal memo October 8, 2008

Boyson F., Ayers W.H. and Swithenbank, J.A., Fundamental mathematical modelling approach to cyclone design, Trans. I. Chem.E. 60, 1982, pp 222-236

Brennan M.,P. Holtham, G. Lyman, Rong R., Computational Fluid Dynamic Simulation of Dense Medium Cyclones, 9th Australian Coal Preparation Conference, 2002

Bradley, D. and Pulling, D.J., "Flow patterns in the hydraulic cyclone and their interpretation in terms of performance", Trans. Inst. Chem. Engrs, Vol. 37, 1959, pp 34-45

Bradley, D., The Hydrocyclone, Pergamon Press, London, 1965

Brigham, E.F., Financial management; theory and practice, The Dryden Press, 1999, ISBN 0-03-024399-8

Bustamante, M.O., Effect on the air core on the performance of a hydrocyclone. M.Sc. thesis, University of Concepcion (in Spanish), 1991

Castro, O., Concha, F., Air core modelling for an industrial hydrocyclone, Hydrocyclones International Conference, Cambridge, UK, 2007

Coelho, M.A.Z. and Medronho, R.A., "An evaluation of the Plitt & Rao models for the hydrocyclones", in L. Svarovsky and M.T. Thew (editors), Hydrocyclones, Analysis and Applications, Kluwer Academic Publishers, Dordrecht, 1992, pp 63 - 72

Concha, F., Air core and roping in hydrocyclones. International Journal Mineral Processing, 44-45, 1996, pp 743-749

Criner, H.E. "The Vortex Thickener", Int. Conf. on Coal Preparation, Paris, 1950

Davidson, J.R., Kittel, S., Curtis, A., The improvement of cyclone performance with a special spigot design, 3rd international conference on Hydrocyclones, Oxford, England, Paper K1, September 30 to October 2, 1987,

Deutsche Norm DIN 66142 Teil 1, Darstellung und Kennzeichnung von Trennungen disperser Güter, Beuth Verlag GmbH, Berlin 30, Juli 1981

Devulapalli, B. and Rajamani R. K., Hydrocyclone Modelling of Swirling Flow and Particle Classification in Large Scale Hydrocyclones, KONA Powder and Particle Journal, No. 12, 1994, pp. 95104

Driessen, M.G. Review of Industrial Mining, Special Issue No. 4, St. Etienne, 1951, pp. 449-61

Duggins R.K. and Frith, P.C.W. Turbulence effects in Hydrocyclones, Paper D1, 3rd International Conference on Hydrocyclones, Oxford, 30 Sept. – 2. Oct. 1987, Elsevier Applied Science Publishers, Barking, 1987

Dyakowski, T., Williams, R.A., Prediction of air-core size and shape in a hydrocyclone, International Journal of Mineral Processing 43, 1995, pp. 1-14

Dyakowski, T., Guitierrez, J.A., Beck, M.S., Williams, R.A., Use of impedance tomography for control of a dewatering hydrocyclone, Camborne School of Mines, University of Exeter, UK, 1996

Fahlstrom P.H., Discussion on pages 632 to 643, Proc. Int. Min. Processing Congress 1960, Inst. Mining and Metallurgy, 1960

Gerrad A.M., and Liddle, C.J., Numerical optimization of multiple hydrocyclone systems, The Chemical Engineer, February 1978, pp. 107-109

Gibson K., "Large scale tests on sedimenting centrifuges and hydrocyclones for mathematical modelling of efficiency", pp 1-10, in Proc. Symp. On Solid-liquid Separation Practice, Yorkshire Branch of the I. Chem. E., Leeds 27-29 March 1979

Svarovsky, L., Hydrocyclones, Holt, Rinehart and Winston Ltd., 1984, ISBN 0-03-910562-8

Hansen, D.R., Cost management: accounting and control, South-Western College Publishing, 2000, ISBN 0-324-00232-7

Holland-Batt, A.B. A bulk model for separation in hydrocyclones, Trans. Instn Min. Metall. (Select C: Mineral Process Extr.Metall.), 91, March 1982

Hothershall, P., van Niekerk, C., Barnard, E., Nutor, G., Single Stage SAG Milling at the Tarkwa Gold Mine, SAG conference 2006, Vancouver, Canada, 2006

Ivey, M., Krebs equation check against capacity curves”, internal memo May 15, 1997

Keith, P.G., Managerial Economics: economic tools for today’s decision makers, Prentice-Hall Inc. 1996, ISBN 0-13 013538-0

Kelsall D.F., A Study of the Motion of Solid Particles in a Hydraulic Cyclone, Trans. Inst. Chem Eng., Volume 30, 1952, pp. 87-104.

Kelsall D.F., A Further Study of the Hydraulic Cyclone, Chem. Eng. Sci., 2, 1953, pp 254-270.

Kutepov A.M., et al, Calculation of separation efficiencies in hydrocyclones, Izv.Vuzov, Chim, I Chim. Technol., XX, 1, 1977, pp 144-145

Kutepov A.M., Study and calculation of the separation efficiency of hydrocyclones, Zh. Prikl. Khim., 51, 3, 1978, pp 614-619

Laverack S.D., Trans. I. Chem. E., Vol. 58, 33, 1980

Lynch A.J., and Rao T.C., Modelling and scale-up of hydrocyclone classifiers, Paper 9, 11th International Mineral Processing Congress, Cagliari 1975, Instituto di Arte Mineraria, 9 - 25, 1975

Lynch A.J., Rao T.C., and Prisbrey K.A., Int. J. of Mineral Processing, 1, 1974, pp 173 – 181

Medronho R., de Andrade Scale-up of hydrocyclones at low concentrations, PhD Thesis, University of Bradford, 1984

Medronho R.A., and Svarovsky, L., Tests to verify hydrocyclone scale-up procedure, 2nd Int. Conf. on Hydrocyclones, Bath, 19-21 September, 1984, Paper A1, pp. 1 – 14

Nageswararao K., Further developments in the modelling and scale-up of industrial hydrocyclones, PhD Thesis, University of Queensland, 1978

Nageswararao K., Flow split and water split in industrial hydrocyclones, NFTDC, Hyderabad 500 058, India, email nftdchyd@hd1.vsnl.net.in

Neesse T., and Schubert H., “Die Trennkorngrösse des Hydrozyklones bei Dünnstrom- und Dichtstromtrennungen”, First European Symposium on Particle Classification in Gases and Liquids, Nuremberg, West Germany, May 9-11, 1984

Neesse T., Donhauser F., Advances in the Theory and Practice of Hydrocyclone Technique, University of Erlangen – Nuernberg, Germany and AKW Apparate + Verfahren GmbH & Co. KG, Hirschau/Oberpfalz, Germany

Narasimha M., Brennan M., Holtham P.N., A review of CFD modelling for performance predictions of hydrocyclone, Engineering Applications of Computational Fluid Mechanics Vol. 1, No. 2, 2007, pp.109-125

Moorhead, R., Classifying Cyclone Operation and Maintenance, CPSA Journal – Spring 2005, Volume 4, No.1

Olson, T. J., Hydrocyclone Design for Fine Separations at High Capacities, Symposium on Recent Advances in Cyclones and Hydrocyclones, AIChE Annual Meeting, 2000

Olson, T.J. and Turner P. A., Hydrocyclone Selection for Plant Design, In: Mineral Processing Plant Design, Operating Practices and Control Proceedings, Volume 1, 2003, pp. 880-893

Olson T.J., van Ommen R., Optimizing hydrocyclone design using advanced CFD model. Minerals engineering0892-6875/\$ Elsevier Ltd. Doi:10.1016/j.mineng.,2003.12.008, 2003

Oluwole L., Wehbe W., Parks S., Influence of Cone Angle and Inlet Reynolds Number on Hydrocyclone Separation, NSF/CRCO MTP Case Study, 2001

Petty C.A., and Parks S.M., Flow Predictions within Hydrocyclones, Filtration + Separation, Vol. 38 (6), 2001, pp 28-34

Petty C.A., Parks S.M., and Olson T.J., Flow Simulations within Hydrocyclone Separators, Symposium on Centrifugal Separation, Minerals Engineering Conference on Solid-Liquid Separation, Falmouth, UK, 2002

Petty C.A., and Parks S.M., The Influence of Hydrocyclone Geometry on Separation Performance, Symposium on Particulates and Multiphase Flows, Annual AIChE Meeting, Reno, NV, 2001

Plitt L.R., Roping in Hydrocyclones, 3rd international Conference on Hydrocyclones, Oxford, England 30.9. – 2.10., 1987

Plitt L.R., A mathematical model of the hydrocyclone classifier, CIM Bulletin, December, 1976, pp 114 – 122

Plitt L.R., Estimating the cut (D50) size of classifiers without product particle size measurement, International Journal of Mineral Processing, 5, 1979, 369-378

Rajamani R.K., Devulapalli B., Vortex flow model of an industrial hydrocyclone, SME Annual Meeting Albuquerque, New Mexico – February 14-17, 1994

Rajamani R.K. and Milin L., “Fluid flow model of the hydrocyclone for concentrated slurry classification”, in L. Svarovsky and M.T. Thew (editors), Hydrocyclones, Analysis and Applications, Kluwer Academic Publishers, Dordrecht 1992, pp 95-108

Rao T.C., Nageswararao K., and Lynch A.J., Int. J. of Mineral Processing, 3, 1976, pp 357 – 363

Renner D., La Rosa D., DeKlerk W., Valery W., Sampson P., Bonney Noi S., Jankovic A., AngloGold Ashanti Iduapriem Mining and Milling process integration and optimization, SAG conference 2006, Vancouver, Canada

Rhodes N., Pericleous K.A. and Drake S.N., The prediction of hydrocyclone performance with a mathematical model, Paper B3 BHRA 3rd Int. Conf. on Hydrocyclones, Oxford, Sept.30 – Oct. 2, 1987, Elsevier Applied Science Publishers, Barking 1987

Rietema K., Chapter 4, The mechanism of the separation of finely dispersed solids in cyclones, in “Cyclones in Industry”, ed. by K. Rietema and C.G. Verver, Elsevier, Amsterdam, 1961

Rietema K., Performance and design of hydrocyclones, Parts I to IV, Chemical Engineering Science, Vol. 15, 1961, pp. 298 to 325

Schlepp D.D., Turner P.A., “Influence of Circulating Load and Classification Efficiency on Mill Throughput”, SME Annual Meeting, February, 1990.

Schmidt M.P., Turner P.A., Flat Bottom or Horizontal Cyclones ...which is the right one for you, World Mining Equipment issue September 1993

Schubert H., On the Origin of “Anomalous” Shapes of the separation Curve in Hydrocyclone Separation of Fine Particles – Above All on the So-Called Fish-Hook Effect, Specific and extended version of a lecture which was held at the conference “Aufbereitung und Recycling” on 13./14.11.2002 in Freiberg, Aufbereitungs Technik 44, (2003) Nr.2

Schubert H., and Neesse T., “A hydrocyclone separation model in consideration of the turbulent multi-phase flow”, Paper 3, Proc. Int. Conf. on Hydrocyclones, Cambridge, 1-3 October, 1980, BHRA Fluid Engineering, Carnfield, 1980, pp 23 – 36

Slack M.D., Prasad R.O., Bakker A., and Boysan F., Advances in Cyclone Modelling using Unstructured Grids, Fluent Europe LTD, 2001

Slack M.D. and Wraith A.E., Modelling the Velocity Distribution in a Hydrocyclone, 4th International Colloquium on Process Simulation, 1997, pp. 65-83.

Sullivan P.H., Value –Driven Intellectual Capital. How to Convert Intangible Corporate Assets into Market Value. New York: John Wiley and Sons, 2000

Svarovsky L., "A critical review of Hydrocyclone models". Department of Chemical Engineering, University of Bradford, UK, 1996

Svarovsky L., SPS report on Hydrocyclones, SLS Vol. V, Sedimentation Processes, Separation Process Service, Warren Spring Laboratory, 1992

Svarovsky L., Hydrocyclones, Holt, Rinehart and Winston, London 1984

Svarovsky L., Selection of hydrocyclone design and operation using dimensionless groups, BHRA 3rd Int. Conf. on Hydrocyclones, Oxford, Sept. 30 – Oct. 2, 1987, Elsevier Applied Science Publishers, Barking, 1987

Trawinski H.F., Filtration and Separation, 6, July/ August and November/ December, 1969

Trawinski H.F., Theory, applications, and practical operation of hydrocyclones, E/MJ Operating Handbook of Mineral Processing, Vol.I-E/MJ Library of Operating Handbooks, September 1976, pp. 146-158

Turner P., The hydrocyclone its influence on the economy of processing plants, Krebs internal publication

Turner P., Best hydrocyclone operating practices for SAG mill circuits, Krebs internal publication

Turner P., Olson T.J., Wedeles, M., Kelton G.P., Hydrocyclone design for large SAG Mill circuits, SAG workshop, Vina del Mar, Chile, May 2001

Turner P., Hoyack M., Arterburn R., The use of hydrocyclones in gold mills without thickeners: Design considerations, Krebs internal publication

van Ommen R., practical and theoretical Aspects of minimizing energy consumption of Hydrocyclone Classification Systems in the Mineral Processing Industry. 6th international Comminution Symposium Falmouth, UK 2008

van Ommen R., Schutte A., Turner P.A., Olson T.J., Improving Milling Circuits through aggressive approach to Cyclone and overall circuit operation. XXII IMPC Cape Town 2003

van Ommen R., Flachberger H., Selected examples of the influence of cyclone underflow density to a closed circuit grinding system, AT Mineral Processing, Heft 11, 2009, pp. 56-61

van Ommen R., Flachberger H., Thuswaldner J., Analyse und Prognoserechnung des Trennverhaltens von Hydrozyklonen mit einem erweiterten Modell der Teilungskurve, AT Mineral Processing, Heft 7-8 2010, pp. 46-53

van Ommen R., Selling Solutions. Master Thesis presented to the faculty of California State University, Hayward and IMDEC University, 2003

van Schalkwyk P., AngloGold Ashanti Geita Gold Mine: upgrade of the 22 foot diameter ball mill, SAG conference, Vancouver, Canada, 2006

Wemco/Sacramento, 26" cyclone – hydraulic test results, internal memo 20, January 1977

Wills B.A., Factors affecting Hydrocyclone performance, Mining Magazine, February 1980, pp. 142-146

Wills B.A., Mineral Processing Technology, Elsevier Ltd, 2006, ISBN 978-0-7506-4450-1

CHAPTER 9: APPENDIX – TABLES, REPORTS AND DATA

TIME	APEX DIA [mm]	SAMPLE NO	DENSITY [t/m ³]	PRESSURE [bar]	CYCLONE FEED [m ³]	H2O SUMP [m ³ /h]	H2O MILL DISCHARGE [m ³ /h]	MILL DISCHARGE SOLIDS [t/h]	H2O MILL DISCHARGE [m ³]	NEW FEED [t/h]	UNDERFLOW SOLIDS [t/h]	CL [%]	CYCLONE FEED DENSITY [WW%]	D50 [µm]	ALPHA	TD	PICTURE NO.	H2O MILL FEED [l/s]	H2O SUMP [l/s]	VOLUME [ml]	WEIGHT [gramms]	MILL DISCHARGE DENSITY [t/m ³]	
11:40	33	D1	62.2	0.35	11.69	4.20	7.49	7.61	4.62	2.60	5.01	192.65	24.55	60.70	3.00		33.87	U1	800	4200	500	816.17	1.63
11:50	33	D2	65.6	0.35	11.69	4.60	7.09	7.86	4.13	2.60	5.26	202.48	25.38	54.00	3.00		34.72	U2	800	4600	500	844.94	1.69
12:00	33	D3	62.23	0.35	11.69	4.20	7.49	7.69	4.59	2.60	5.09	195.75	24.81	54.50	3.00		37.32	U3	800	4200	500	824.40	1.65
12:10	30	D4	74	0.35	11.69	5.80	5.89	8.09	2.84	2.60	5.49	211.22	26.11	59.50	4.00		36.49	U4	1200	5800	500	927.60	1.86
12:20	30	D5	64.6	0.35	11.69	5.20	6.49	7.02	3.85	2.60	4.42	169.87	22.64	54.90	4.00		31.18	U5	2200	5200	500	836.25	1.67
12:30	30	D6	66.5	0.38	12.19	5.20	6.99	7.93	3.99	2.60	5.33	204.82	24.54	53.10	3.74		32.92	U6	2200	5200	500	853.10	1.71
12:40	28	D7	65.6	0.35	11.69	5.20	6.49	7.21	3.78	2.60	4.61	177.13	23.25	57.10	4.20		31.18	U7	2200	5200	500	845.66	1.69
12:50	28	D8	64.9	0.35	11.69	5.20	6.49	7.07	3.83	2.60	4.47	171.93	22.82	55.50	4.50		30.93	U8	2200	5200	500	838.76	1.68
13:00	28	D9	66.8	0.35	11.69	5.20	6.49	7.43	3.69	2.60	4.83	185.62	23.96	56.90	4.50		33.67	U9	2200	5200	500	855.92	1.71
13:10	26	D10	62.1	0.38	12.19	5.20	6.99	7.07	4.32	2.60	4.47	171.86	21.89	57.00	4.80		31.03	U10	2200	5200	500	814.76	1.63
13:20	26	D11	64.2	0.3	10.83	5.20	5.63	5.95	3.38	2.60	3.35	129.01	20.75	67.80	4.50		30.15	U11	2200	5200	500	824.15	1.65
13:30	26	D12	65.9	0.33	11.36	5.20	6.16	6.76	3.60	2.60	4.16	160.04	22.47	59.00	4.50		30.48	U12	2200	5200	500	833.42	1.67
13:40	24	D13	65.9	0.3	10.83	5.60	5.23	5.84	3.02	2.60	3.24	124.71	20.36	73.90	4.50		28.41	U13	1800	5600	500	848.11	1.70
13:50	24	D14	61.5	0.35	11.69	6.20	5.49	5.48	3.43	2.60	2.88	110.65	17.67	62.20	4.50		25.51	U14	2400	6200	500	810.45	1.62
14:00	24	D15	64.6	0.37	12.02	6.20	5.82	6.30	3.45	2.60	3.70	142.13	19.76	60.00	4.80		27.85	U15	2400	6200	500	836.67	1.67
14:10	22	D16	63.3	0.35	11.69	6.20	5.49	5.74	3.33	2.60	3.14	120.79	18.52	66.20	2.50		24.15	U16	2400	6200	500	825.31	1.65
14:20	22	D17	58.9	0.35	11.69	6.00	5.69	5.29	3.70	2.60	2.69	103.65	17.09	75.60	2.50		19.20	U17	3200	6000	500	789.35	1.58
14:30	22	D18	60.7	0.36	11.86	6.00	5.86	5.72	3.70	2.60	3.12	119.84	18.19	72.50	2.50		23.39	U18	3200	6000	500	809.43	1.61
14:40	20	D19	62.7	0.32	11.18	6.00	5.18	5.33	3.17	2.60	2.73	104.96	17.98	78.30	2.80		22.43	U19	3200	6000	500	820.10	1.64
14:50	20	D20	55.8	0.32	11.18	5.80	5.38	4.60	3.65	2.60	2.00	76.95	15.53	90.20	2.70		19.52	U20	3600	5800	500	766.02	1.53
15:00	20	D21	58.6	0.32	11.18	5.80	5.38	4.96	3.51	2.60	2.36	90.79	16.74	80.20	2.80		21.14	U21	3600	5800	500	786.44	1.57
15:10	18	D22	55.7	0.33	11.36	6.00	5.36	4.56	3.63	2.60	1.96	75.48	15.16	93.20	2.80		14.86	U22	3800	6000	500	764.80	1.53
15:20	18	D23	56.7	0.34	11.53	6.00	5.53	4.84	3.70	2.60	2.24	86.25	15.85	85.40	4.00		16.76	U23	3800	6000	500	772.79	1.55
15:30	18	D24	54.7	0.25	9.88	6.00	3.88	3.22	2.67	2.60	0.62	23.88	12.30	143.50	2.00		13.56	U24	3800	6000	500	758.13	1.52
15:40	33	D25	59.3	0.4	12.50	4.20	8.30	7.80	5.36	2.60	5.20	200.12	23.55	45.10	3.00		28.23	U25	800	4200	500	792.55	1.59
15:50	33	D26	68.2	0.35	11.69	4.20	7.49	8.88	4.14	2.60	6.28	241.56	28.66	57.20	2.50		36.18	U26	800	4200	500	868.77	1.74
16:00	33	D27	68.3	0.35	11.69	4.20	7.49	8.91	4.13	2.60	6.31	242.53	28.74	54.30	2.50		38.35	U27	800	4200	500	869.96	1.74
17:10	33	D28	62.5	0.34	11.53	4.20	7.33	7.50	4.50	2.60	4.90	188.34	24.54	53.40	2.50		34.09	U28	800	4200	500	818.65	1.64
17:20	33	D29	68.4	0.37	12.02	4.40	7.62	9.08	4.20	2.60	6.48	249.25	28.50	47.20	2.50		39.75	U29	1000	4400	540	870.69	1.74
17:30	36	D30	65.1	0.37	12.02	4.40	7.62	8.35	4.47	2.60	5.75	221.07	26.20	56.00	2.50		37.20	U30	800	4400	500	840.99	1.68
17:40	36	D31	66.1	0.4	12.50	4.60	7.90	8.88	4.55	2.60	6.28	241.53	26.80	48.20	2.50		40.10	U31	1000	4600	500	850.06	1.70
17:50	36	D32	67.8	0.4	12.50	4.80	7.70	9.03	4.29	2.60	6.43	247.39	27.26	46.20	2.50		41.01	U32	1000	4800	500	864.86	1.73
17:55	38	D33	64.1	0.49	13.84	4.80	9.04	9.64	5.40	2.60	7.04	270.58	26.28	41.20	2.00		39.93	U33	1000	4800	500	831.68	1.66

Client: PHD ROMAN VAN OMMEN
 Problem: Producing 3 MTPH @ 80% passing 50um

Number, Model Krebs Cyclones: 1 operating U6-10

Orifices:	Inlet Area 2.20 sq. in.	Vortex Finder 1.75 in.	Apex	Pressure Drop 7.6 PSI
Specific Gravity:	Solids: 2.700	Liquid: 1.000	Temperature: Amb. °C	Viscosity: 1 Cps

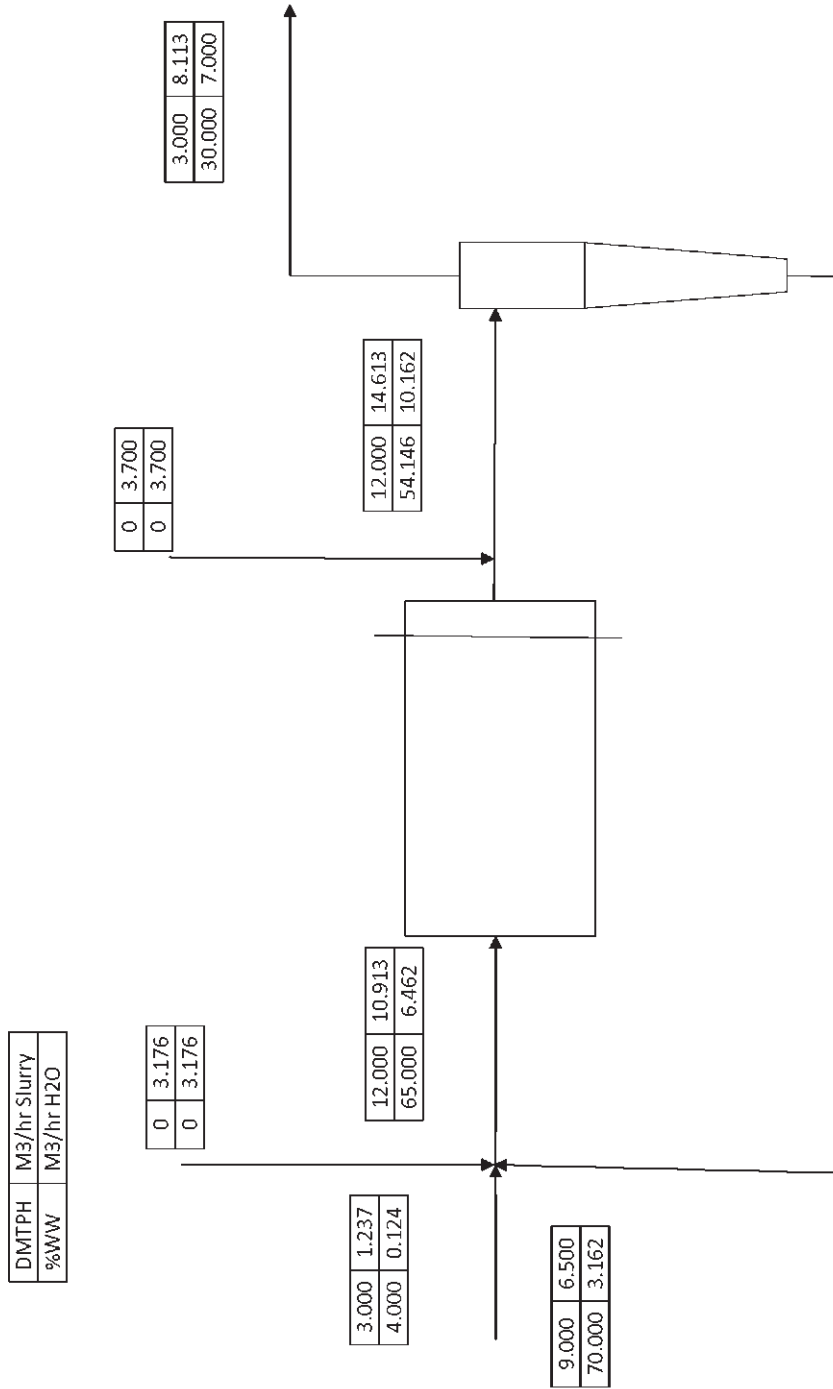
	FEED	OVERFLOW	UNDERFLOW
MTPH Solids	12.000	3.000	9.000
MTPH Liquids	10.162	7.000	3.162
MTPH Slurry	22.162	10.000	12.162
Wt Solids	54.146	30.000	74.000
S.G. Slurry	1.517	1.233	1.872
Vol% Solids	30.428	13.699	51.318
GPM Slurry	64.311	35.712	28.599
M3/Hr. Slurry	14.607	8.111	6.495

Ref: 62.9 4.0 53.0

Circulating Load: 300%

Mesh	Micron	FEED			OVERFLOW			UNDERFLOW			ACT. REC.	CORR. REC.
		Cum. %+	Ind. %+	MTPH	Cum. %+	Ind. %+	MTPH	Cum. %+	Ind. %+	MTPH		
100	149.0	44.17	44.17	5.3	0.00	0.00	0.0	58.89	58.89	5.3	100.0	100.0
150	104.0	56.93	12.76	1.5	2.35	2.35	0.1	75.12	16.24	1.5	95.4	93.3
200	74.0	63.18	6.25	0.7	7.98	5.63	0.2	81.57	6.45	0.6	77.5	67.3
270	53.0	68.71	5.53	0.7	17.97	9.99	0.3	85.62	4.05	0.4	54.9	34.5
400	37.0	74.82	6.11	0.7	32.26	14.29	0.4	89.00	3.38	0.3	41.5	15.1
-400	-37.0	100.00	25.18	3.0	100.00	67.74	2.0	100.00	11.00	1.0	32.7	2.4
TOTAL				12.000			3.000			9.000	75.0	63.7

FLWSHEET PHD ROMAN VAN OMMEN



Kurzbeschreibung

Kugelmühle TECHNIKUM

20090331	First Issue FH	

Index:

1	Allgemeine Daten.....	2
2	Prozessdaten.....	3
2.1	Aufgabematerial.....	3
2.2	Produkt.....	3
2.3	Technische Daten.....	3

1 Allgemeine Daten

Aufstellungsort.....	Cemtec, Ennshafen
Umgebungstemperatur.....	max. 35 °C min. 15 °C
Aufstellungshöhe.....	260m ü NN
Erdbebenzone.....	keine
Luftfeuchtigkeit.....	max. 90%
Ausführung gem. DIN, VDE o. ä. IEC Standards	
Schutzart.....	neutral
Spannung.....	400/230 V ± 5%
Frequenz.....	50 Hz
Steuerspannung.....	24 V DC
Ventilspannung.....	220V ± 5%
Frequenz.....	50 Hz
Druckluft.....	getrocknet, geölt und gekühlt 6-8 bar

2 Prozessdaten

2.1 Aufgabematerial

Material.....	diverse Schüttgüter
Feuchte (bei Trockenmahlung).....	1,0 % (Gew.-%)
Schüttgewicht (ca.).....	0,5 - 2,5 kg/dm ³
Aufgabegröße.....	max. 20 mm
Aufgabetemperatur.....	ca. 5-35 °C

2.2 Produkt

Produktmenge.....	max. 3.000 kg/h
Feuchte (bei Trockenmahlung).....	0,5 % H ₂ O

2.3 Technische Daten

Innendurchmesser der Kugelmühle.....	1.200 mm
Mahlbahnlänge (variabel).....	2.000 / 2.500 / 3.000 mm
L/D Verhältnis (variabel).....	1,7 / 2,1 / 2,5
Füllgrad.....	20 - 32 %
Mahlkörpergewicht.....	4.540 kg @ 28% FG
Installierte Antriebsleistung.....	55 kW
Max aufgenommene Leistung @ 32% FG.....	39 kW
Mühleneinbauten.....	Hubleisten
Anzahl der Hubleisten.....	12
Austragswand mit Schlitz.....	8 mm
Entstaubungsluftmenge.....	ca. 5.000 mP bei max. 120 °C
Mahlkreislauf.....	offen & geschlossen
Mahlart.....	naß & trocken

CEMTEC

PRO-CALC0012

CEMCALC 0.1

Cement and Mining
Technology GmbH

Dokumentname:
Document Name:
Nombre del Document:

Gattierungsauslegung

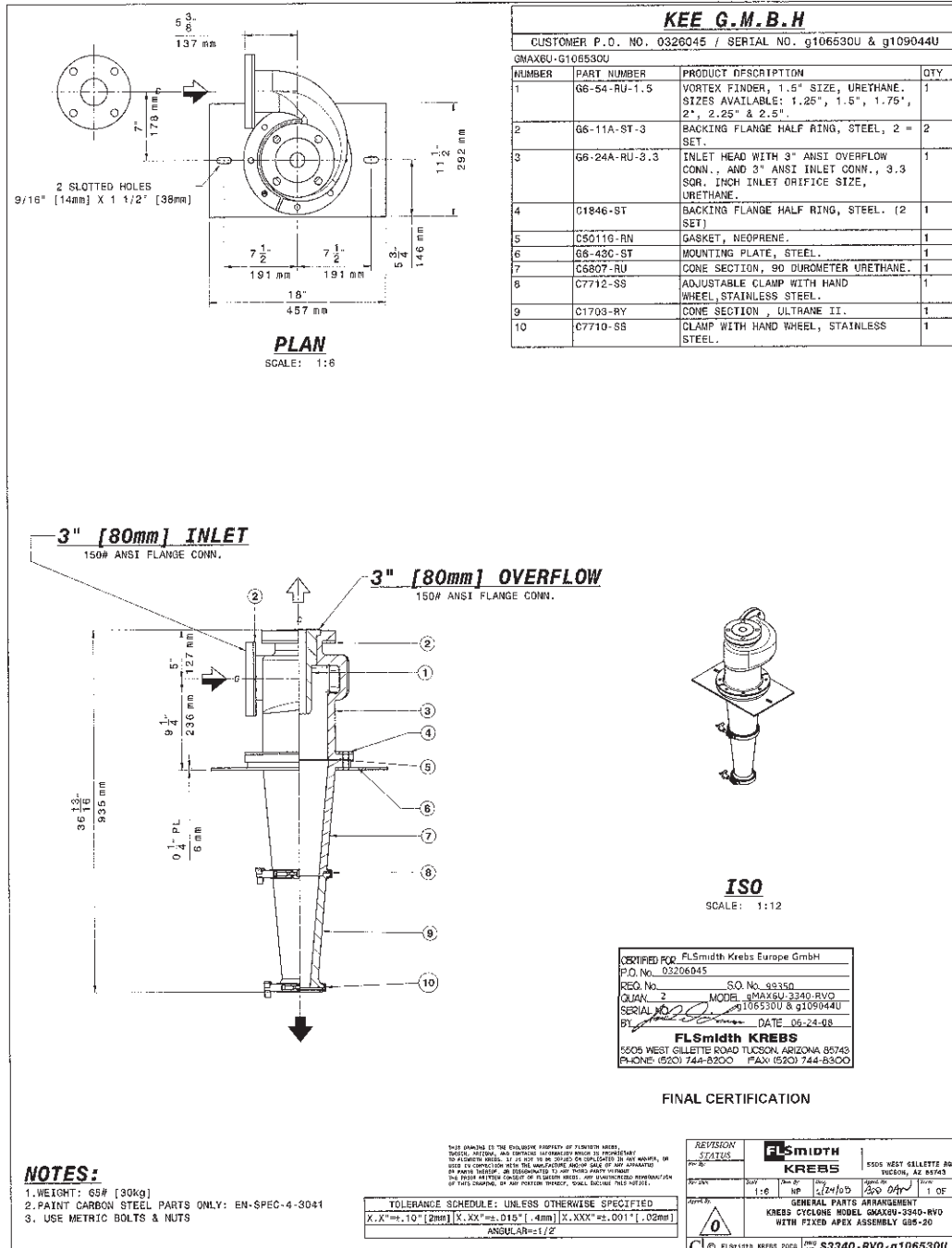
00

Projektname: Nassmahlung RvO
Projektnummer: xxxx
Kunde: Roman van Ommen
Datum: 03.04.2009
Bearbeiter: Gleißenberg

Material **Kalkstein**
Work Index gem. Bond [W_i] kWh/t **12,6**
Dichte Mahlkörper [p_Mk] t/m³ **4,7**
Schüttdichte [p_Mg] t/m³ **1,5**
Rohdichte Mahlgut [p_RMG] t/m³ **2,6**
Aufabe [F_80] um **2800**
Aufgabe [F_max] um **4000**
[n_Mü/n_krit] % **75**
Mahlart **nass**

	Gesamt	1. Kammer	2. Kammer
Mahlraumd. [d_lj] m	1,20	1,2	0
Mahlbahnlänge [l_Mb] m	3,00	3	0
Füllgrad [FG] %	28		
Volumen Mühlenfüllung [V_F] m ³	0,95	0,95	0,00
Masse Mahlgut [m_Mg] t	0,57	0,57	0,00
Masse Mahlkörper [m_Mk] t	4,5	4,5	0,0
Masse Mühlenfüllung [m_ges] t	5,0	5,0	0,0
max. Kugeld. [d_Kmax] mm	42,0		44,4
	bezogen auf F_80		bezogen auf F_max

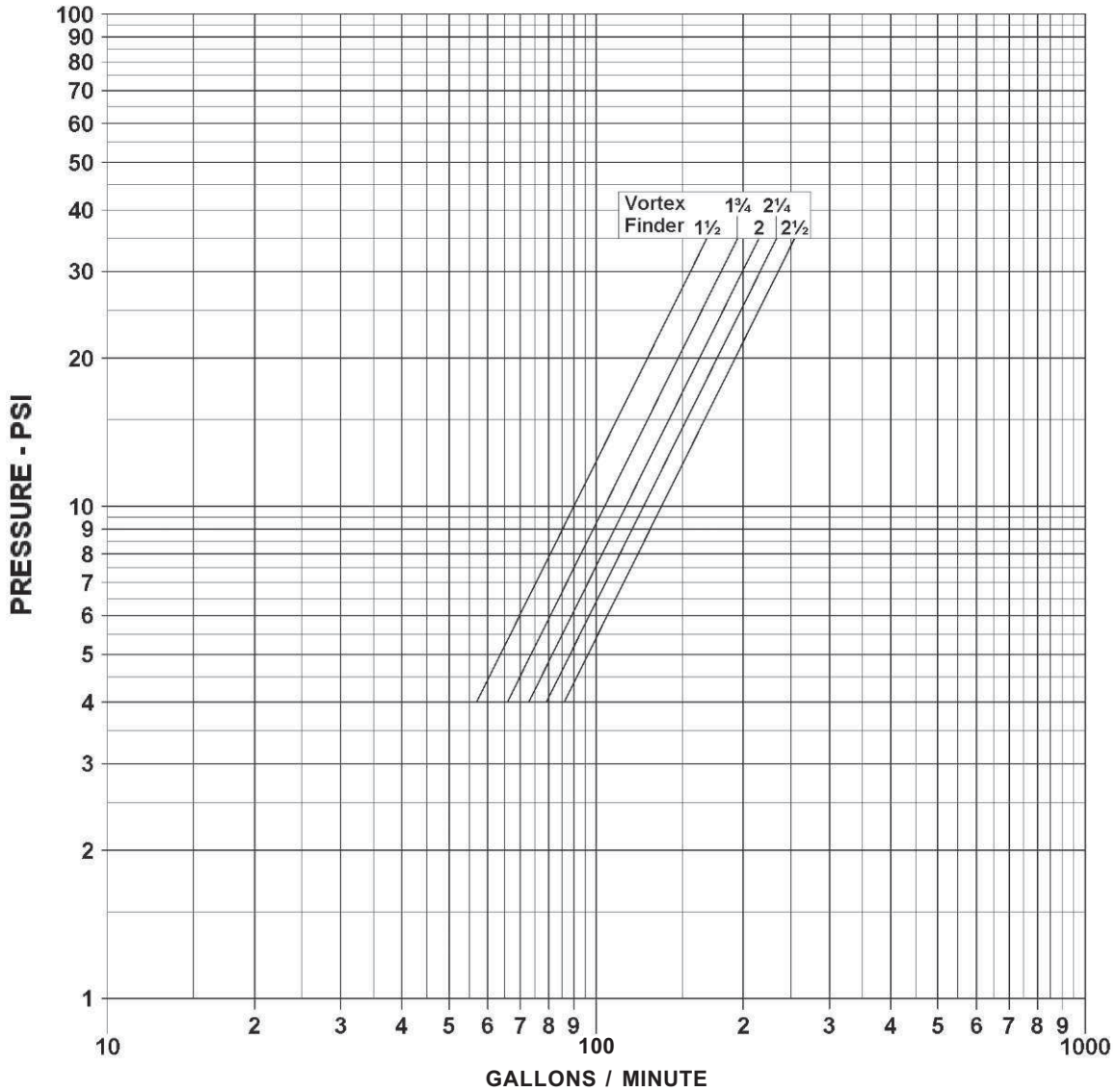
Kugelgröße [d_Ki] mm	1. Kammer			Kugelgröße [d_Ki] mm	2. Kammer			Schüttdichte [p_Ki] t/m ³
	Masse [m_Ki] t	Verteilung 1.Kammer [g_Ki1] %	Verteilung ges [g_Kig] %		Masse [m_Ki2] t	Verteilung 2.Kammer [g_Ki2] %	Verteilung ges [g_Kig] %	
100	0	0,0	0,0	100	0,0	0,0	0,0	4,56
90	0	0,0	0,0	90	0,0	0,0	0,0	4,59
80	0	0,0	0,0	80	0,0	0,0	0,0	4,62
70	0,2	4,4	4,5	70	0,0	0,0	0,0	4,64
60	0,4	8,9	9,0	60	0,0	0,0	0,0	4,66
50	0,5	11,1	11,2	50	0,0	0,0	0,0	4,708
35-40	1	22,2	22,4	40	0,0	0,0	0,0	4,76
30	0,5	11,1	11,2	30	0,0	0,0	0,0	4,78
25	1	22,2	22,4	25	0,0	0,0	0,0	4,85
20	0,9	20,0	20,2	20	0,0	0,0	0,0	4,85
18	0	0,0	0,0	18	0,0	0,0	0,0	4,86
17	0	0,0	0,0	17	0,0	0,0	0,0	4,87
	Gesamt	1. Kammer	2. Kammer					
tats. Schüttdichte [p_Mkj] t/m ³	4,78	4,78	0,00					
Füllgrad [FG_j] %	27,75	27,75	0,00					
Volumen [V_Fj] m ³	0,94	0,94	0,00					
Masse [m_j] t	4,5	4,5	0					
Verteilung [g_j] %	100,8	100,8	0,0					
Erstellt von: Prepared by: Preparado por:	Ch. Huemer			Datum: Date: Fecha:	01.04.2009	zt / substitutes / sustituda:		
Geprüft von: Checked by: Chequead por:				Datum: Date: Fecha:		Seite 1 von 1		
Verteiler / Distribution Distribudor:								



Krebs Cyclone
 Model No.: U6-gMAX

CAPACITY CURVE
 No.: U6-gMAX-330-1203

3.30 SQ. IN. INLET ORIFICE



CAPACITY IS BASED ON WATER AT AMBIENT TEMPERATURE
 AND APEX DIAMETER EQUAL TO ONE HALF THE VORTEX
 FINDER DIAMETER, AND MAY VARY AT DIFFERENT RATIOS

This sheet is the property of Krebs Engineers, Tucson
 Arizona, and is loaned under the express condition
 that it is not to be used in any manner directly or
 indirectly detrimental to Krebs Engineers

KREBS ENGINEERS
 5505 West Gillette Road
 Tucson, AZ 85743
 TEL: (520) 744-8200
 FAX: (520) 744-8300
 e-mail: www.krebs.com



Sheet:
Date: 02-Sep-08
By: _____

Pump Data Sheet

Customer:
Application: MILL DISCHARGE
Equipment / Tag No.: _____

Pump Model: slurryMAX 4X4-12
Reference Curve: RC 100-447-12,0

Application: Flow: 22.2 M3/Hr.	Slurry Head: 12.7 Meters
Slurry S.G.: 1.517	Equivalent Water Head: 13.4 Meters
Solid S.G.: 2.700	Head Ratio: 0.95
Liquid S.G.: 1.000	Slurry Temperature: °C
Wt.% Solids: 54.15	Top Size:
D50: Microns	

Pump Data: Suction Size: 100 mm.	Discharge Size: 100 mm.
Suction Velocity: 0.8 M./Sec.	Discharge Velocity: 0.8 M./Sec.
Impeller Size: 305 mm.	Maximum Sphere Size: 40 mm
Discharge Position:	
Gland Type:	

Motor Data: Kw:	Enclosure:
Nominal Speed:	Frame Size:
Electrical Characteristics:	

Pump Performance Summary

Flow: 22.2 M3/Hr.
Slurry Head: 12.7 Meters
Actual Speed: 903 RPM
Slurry Efficiency: 34.7% *
Slurry Power: 3.4 Kw
NPSH Required:
%BEP: 26.7

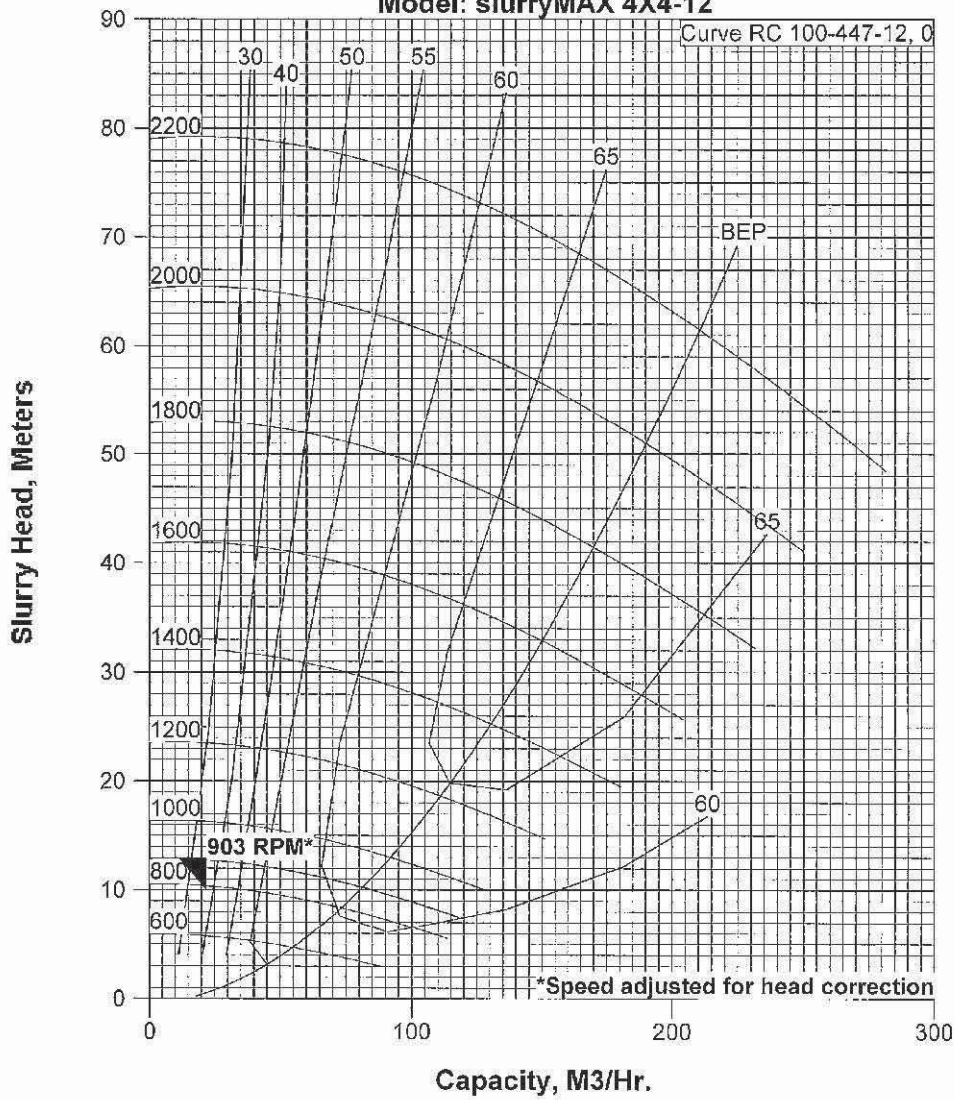
* Slurry efficiency = water efficiency

Krebs Engineers
5505 West Gillette Road Tucson, AZ 85743
Tel: (520) 744-8200 FAX: (520) 744-8300 e-mail: www.krebs.com



Application:

Model: slurryMAX 4X4-12





Sheet: _____
Date: 02-Sep-08
By: _____

Pump Data Sheet

Customer: _____
Application: TAILINGS
Equipment / Tag No.: _____

Pump Model: milIMAX 3X2-9
Reference Curve: PC080-447-9, Rev. 1

Application: Flow: 8.1 M3/Hr.	Slurry Head: 10.0 Meters
Slurry S.G.: 1.517	Equivalent Water Head: 10.6 Meters
Solid S.G.: 2.700	Head Ratio: 0.95
Liquid S.G.: 1.000	Slurry Temperature: °C
Wt.% Solids: 54.15	Top Size:
D50: Microns	

Pump Data: Suction Size: 76 mm.	Discharge Size: 50 mm.
Suction Velocity: 0.5 M./Sec.	Discharge Velocity: 1.1 M./Sec.
Impeller Size: 228 mm.	Maximum Sphere Size: 25.4 mm
Discharge Position:	
Gland Type:	

Motor Data: Kw:	Enclosure:
Nominal Speed:	Frame Size:
Electrical Characteristics:	

Pump Performance Summary

Flow: 8.1 M3/Hr.
Slurry Head: 10.0 Meters
Actual Speed: 1059 RPM
Slurry Efficiency: 21.2% *
Slurry Power: 1.6 Kw
NPSH Required:
%BEP: 24.8

* Slurry efficiency = water efficiency

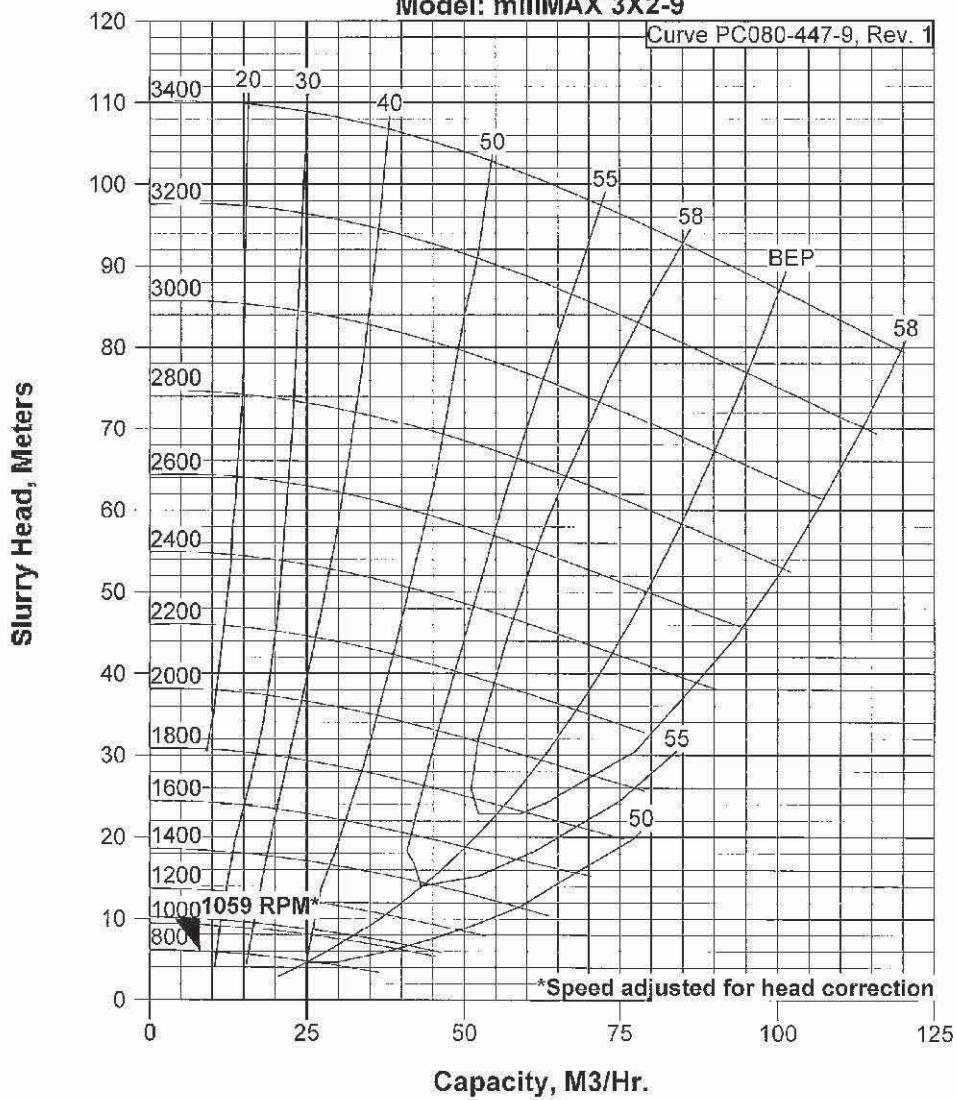
Krebs Engineers
5505 West Gillette Road Tucson, AZ 85743
Tel: (520) 744-8200 FAX: (520) 744-8300 e-mail: www.krebs.com



Application:

Model: millMAX 3X2-9

Curve PC080-447-9, Rev. 1



CEHTEC <small>Cement and Mining Technology GmbH</small>	Labortechnische Untersuchungen, Siebung Technikum Ennshafen	Prüfdatenblatt	
	<small>Dokumentname: Document Name: Nombre del Document:</small>	Siebung von Gesteinskörnungen mit Siebmaschine	<small>Revision</small>

**Prüfdatenblatt für Siebung mit Siebmaschine gemäß EN 933-1/2 und EN 1097
Siebe nach ISO 3310-1**

Laborberichtsnummer: 30-X-08-1
 Material: Kalkstein
 Ort der Probenahme: Aufgabe Bond
 Einwaage [m] g: 1120,62
 Feuchte [w] %: 0,25
 Siebdauer [t] min: 5
 Amplitude a: 2.0
 Intervall l: 5

Siebgröße m	Siebrück-stand g	Siebdurch- gang g	Siebdurch- gang %
4000	0,00	1120,62	100,00
3150	120,60	1000,02	89,24
2000	297,19	702,83	62,72
1000	333,95	368,88	32,92
500	177,90	190,98	17,04
250	69,60	121,38	10,83
150	31,06	90,32	8,06
90	38,49	51,83	4,63
<90	51,83	0,00	0,00
	0,00	0,00	0,00
		0,00	0,00
		0,00	0,00
		0,00	0,00
		0,00	0,00
		0,00	0,00
		0,00	0,00
		0,00	0,00
		0,00	0,00

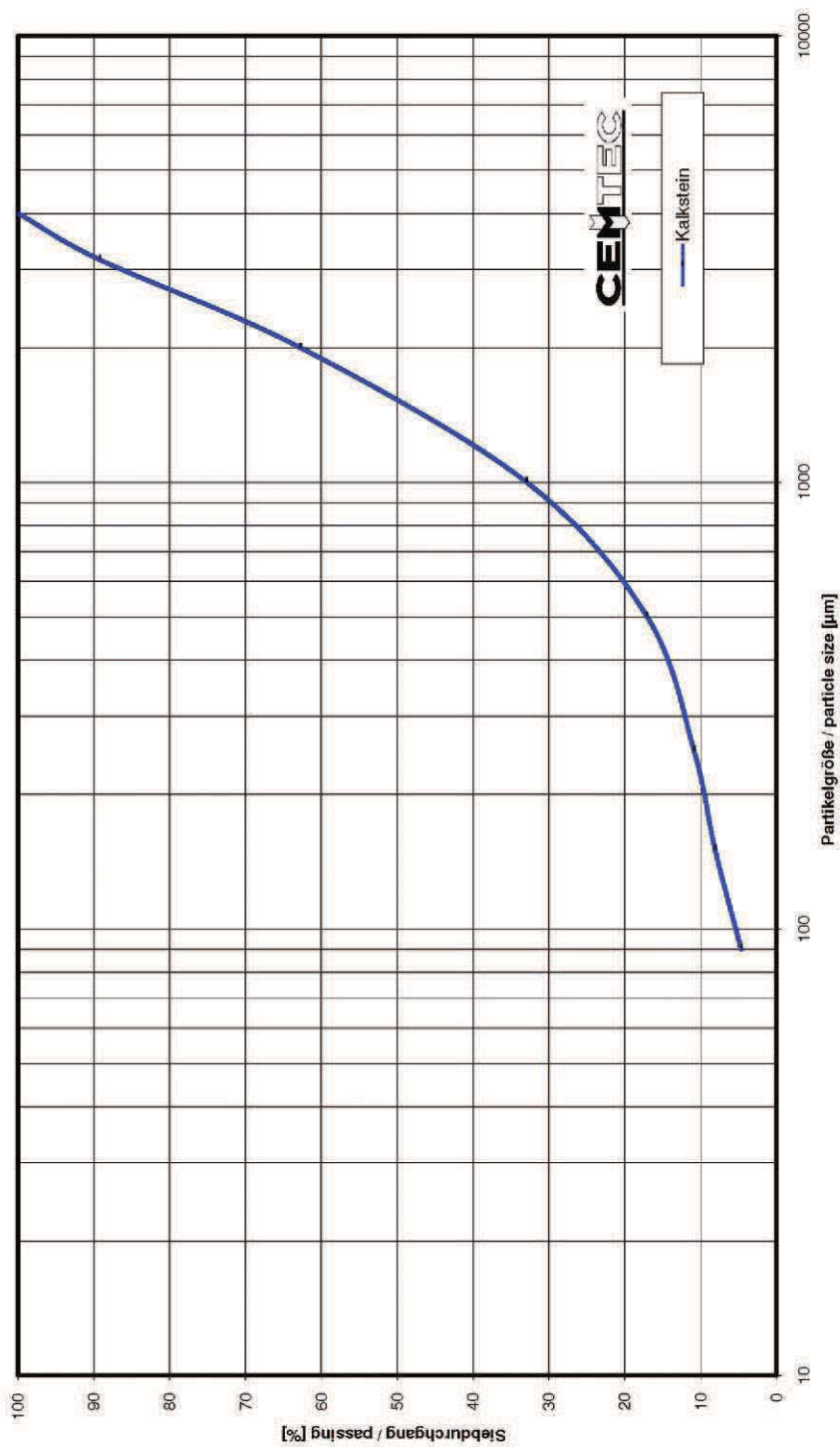
F80/P80 2749

Prüfdatum: 14.11.2008 **Name:** GLB **Prüfnummer:**

<small>Erstellt von: Prepared by: Preparado por:</small>		<small>Datum: Date: Fecha:</small>		<small>ersetzt / substitutes / sustituda:</small>
<small>Gepüft von: Checked by: Chequead por:</small>	J. Gleißenberg	<small>Datum: Date: Fecha:</small>	04.04.2007	<small>Seite 1 von 1</small>
<small>Verteiler / Distribution Distbudor:</small>				<small>gespeichert in: K:\Techcalc\Siebkurve.xls</small>

Kopie von BOND RvO

Aufgabesieblinie BOND



Kunde / Client: **Roman van Ommen**
Laborberichtsnummer: **30-X-08-1**
Projekt / project: **Diss.**
Cemtec GmbH, Einshafenstr. 40, 4470 Erms, Austria
Tel +43-7223-63620-0, Fax +43-7223-6362033

Datum / Date: **14.11.2008**
Name / Name: **Gleifenberg**

Seite/Page 1 von/of 1
Print Date: 01.04.2009, 16:41

CEHTEC Cement and Mining Technology GmbH	Labortechnische Untersuchungen, Siebung Technikum Ennshafen	Prüfdatenblatt	
	Dokumentname: Document Name: Nombre del Document:	Siebung von Gesteinskörnungen mit Siebmaschine	Revision

**Prüfdatenblatt für Siebung mit Siebmaschine gemäß EN 933-1/2 und EN 1097
 Siebe nach ISO 3310-1**

Laborberichtsnummer: 30-X-08-1
 Material: Kalkstein
 Ort der Probenahme: fein nach BOND
 Einwaage [m] g: 136,06
 Feuchte [w] %: 0,25
 Siebdauer [t] min: 5
 Amplitude a: 2.0
 Intervall l: 5

Siebgröße m	Siebrück-stand g	Siebdurch- gang g	Siebdurch- gang %
150	0,27	135,79	99,80
90	57,05	78,74	57,87
63	29,04	49,70	36,53
45	20,30	29,40	21,61
<45	29,40	0,00	0,00
		0,00	0,00
		0,00	0,00
		0,00	0,00
		0,00	0,00
		0,00	0,00
		0,00	0,00
		0,00	0,00
		0,00	0,00
		0,00	0,00
		0,00	0,00

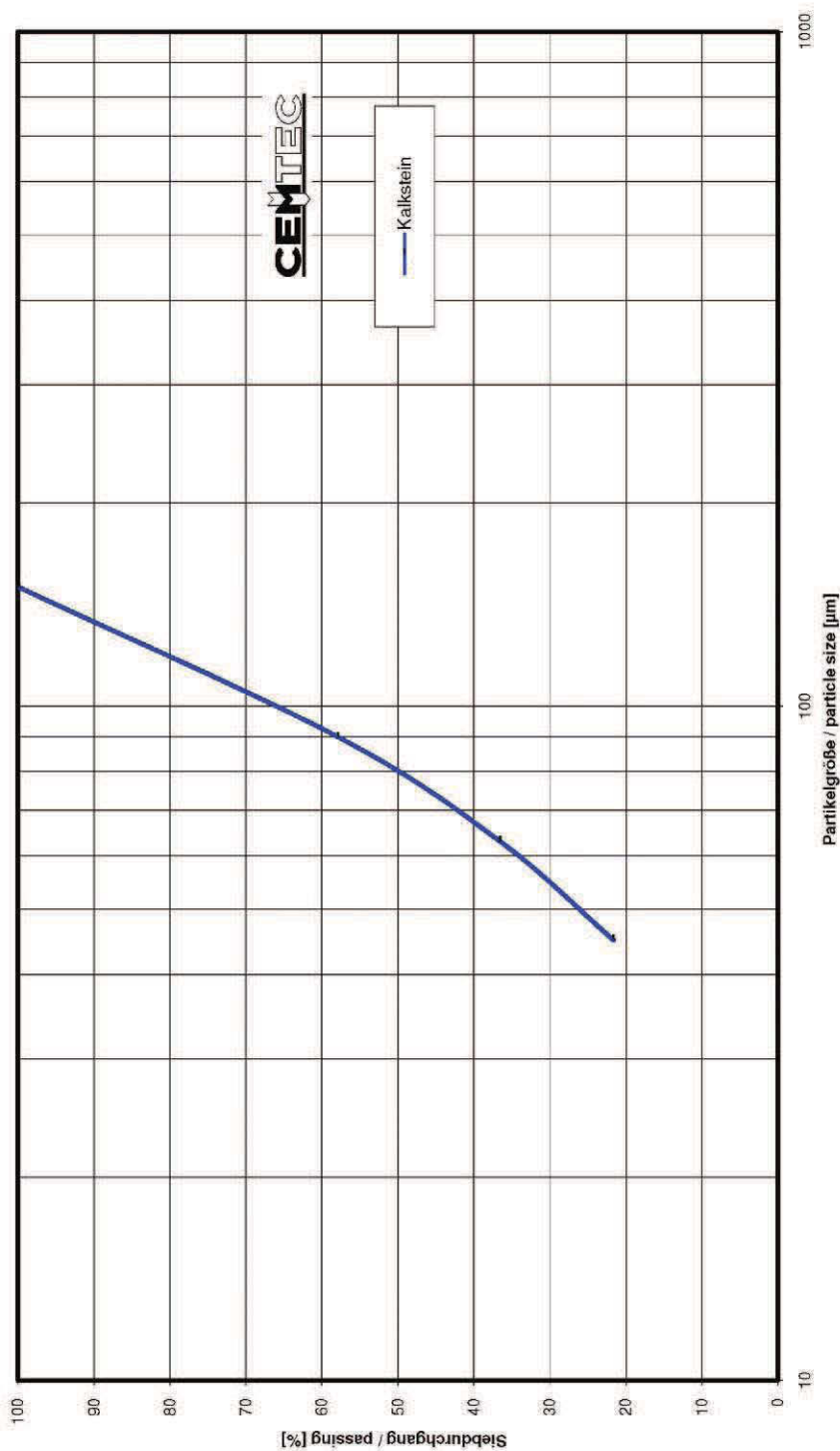
F80/P80 122

Prüfdatum: 04.04.2007 **Name:** GLB **Prüfnummer:**

Erstellt von: Prepared by: Preparado por:		Datum: Date: Fecha:		ersetzt / substitutes / sustituda:
Geprüft von: Checked by: Chequead por:	J. Gleißenberg	Datum: Date: Fecha:	04.04.2007	Seite 1 von 1
Verteiler / Distribution Distbudor:				gespeichert in: K:\Techcalc\Siebkurve.xls

Kopie von BOND RvO


Sieblinie fein nach BOND



Kunde / Client: Roman van Ommen
Laborberichtsnummer: 30-X-08-1
Projekt / project: Diss.
Cemtec GmbH, Ernsdalenstr. 40, 4470 Erms, Austria
Tel +43-7223-83620-0, Fax +43-7223-8362033

Datum / Date: 14.11.2008
Name / Name: Gleißenberg

Seite/Page 1 von/of 1
Print Date: 01.04.2009, 16:44

 Cement and Mining Technology GmbH <small>Dokumentname Document Name Nombre del Document</small>		Labortechnische Untersuchungen, Mahlbarkeitsuntersuchung Technikum Ennshafen Bestimmung des Work-index nach Bond von Gesteinskörnungen										Prüfdatenblatt Revision	
Prüfgröße [P] µm: 150 Masse [m] (700 ml) g: 1009 Aufgabe [d F80] µm: 2293 Produkt [d P80] µm: 122 Feingut unter Prüfgröße %: 7,34		Laborberichtsnummer: 30-X-08-1 Prüfdatum: 14.11.2008 Name: GLB Mühlenotyp: BM 0303		Kalkstein Bernegger		00							
Nummer	Aufgabe	<Prüfgröße	250%	Umdrehung	Rückstand	Durchgang	neues Feingut	g/Umdrehung	Wh	Bemerkung			
1	1009,0	74,1	214,23	100	753,2	255,8	181,78	1,82					
2	255,8	18,8	269,51	148	742,9	266,1	247,32	1,67					
3	266,1	19,5	268,75	161	708,9	300,1	280,57	1,74					
4	300,1	22,0	266,26	153	704,0	305,0	282,97	1,85					
5	305,0	22,4	265,90	144	708,1	300,9	278,51	1,93					
6	300,9	22,1	266,20	138	714,0	295,0	272,91	1,98					
7	295,0	21,7	266,63	135	718,0	291,0	269,35	2,00					
8	291,0	21,4	266,93	134	720,0	289,0	267,64	2,00					
9	289,0	21,2	267,07	134	720,0	289,0	267,79	2,00					
10	289,0	21,2	267,07	134	720,0	289,0	267,79	2,00					
11	289,0	21,2	267,07	134	0,0	0,0	0,00	0,00					
12	0,0	0,0	0,00	0	0,0	0,0	0,00	0,00					
Mahlbarkeitskoeffizient g/U:		2,00		Work-Index kWh/t:		12,6							
Erstellt von: Prepared by: Preparado por:										ersetzt / substitutes / sustituye:			
Geprüft von: Checked by: Chequeado por:		J. Gleißenberg								Seite 1 von 1			

PARTICLE SIZE DISTRIBUTION TEST 1

[µm]	overflow		discharge		underflow	
	D	%R	D	%R	D	%R
		ΣR		ΣR		ΣR
315	99,647	0,353	96,245	3,755	90,479	9,521
280	99,523	0,124	94,613	5,387	87,709	12,291
224	99,097	0,426	90,627	9,373	81,521	18,479
180	98,254	0,843	85,539	14,461	74,361	25,639
140	96,575	3,425	78,309	21,691	65,104	34,896
112	94,295	5,705	70,941	29,059	56,415	43,585
90	91,244	8,756	63,317	36,683	48,002	51,998
63	84,510	15,490	51,377	48,623	35,814	64,186
56	81,860	18,140	47,849	52,151	32,447	67,553
45	76,540	23,460	42,070	57,930	27,206	72,794
36	70,811	29,189	37,254	62,746	23,173	76,827
32	67,762	32,238	35,118	64,882	21,509	78,491
25	61,484	38,516	31,360	68,640	18,810	81,190
20	56,016	43,984	28,530	71,470	16,969	83,031
15	49,180	50,820	25,231	74,769	14,955	85,045
12	43,901	56,099	22,726	77,274	13,456	86,544
10	39,547	60,453	20,661	79,339	12,220	87,780
8	34,209	65,791	18,126	81,874	10,706	89,294
6	27,582	72,418	14,973	85,027	8,830	91,170
5	23,724	76,276	13,121	86,879	7,737	92,263
4	19,492	80,508	11,057	88,943	6,526	93,474
3,2	15,818	84,182	9,212	90,788	5,446	94,554
2,6	12,851	87,149	7,665	92,335	4,539	95,461
2	9,635	90,365	5,908	94,092	3,506	96,494
-2	0,000	100,000	0,000	100,000	0,000	100,000
				100,000		100,000

PARTICLE SIZE DISTRIBUTION TEST 2

[µm]	overflow		%R		discharge		%R		underflow	
	D	ΣR	D	%R	D	ΣR	D	%R	D	ΣR
315	99,771	0,229	95,217	0,000	95,217	4,783	91,477	4,783	91,477	8,523
280	99,688	0,312	93,498	0,083	93,498	6,502	88,764	1,719	88,764	11,236
224	99,327	0,673	89,389	0,361	89,389	10,611	82,569	4,109	82,569	17,431
180	98,588	1,412	84,206	0,739	84,206	15,794	75,228	5,183	75,228	24,772
140	97,059	2,941	76,891	1,529	76,891	23,109	65,561	7,315	65,561	34,439
112	94,924	5,076	69,471	2,135	69,471	30,529	56,394	7,420	56,394	43,606
90	92,025	7,975	61,835	2,899	61,835	38,165	47,504	7,636	47,504	52,496
63	85,575	14,425	50,015	6,450	50,015	49,985	34,749	11,820	34,749	65,251
56	83,031	16,969	46,571	2,544	46,571	53,429	31,286	3,444	31,286	68,714
45	77,914	22,086	40,990	5,117	40,990	59,010	25,990	5,581	25,990	74,010
36	72,382	27,618	36,404	5,532	36,404	63,596	22,030	4,586	22,030	77,970
32	69,421	30,579	34,384	2,961	34,384	65,616	20,435	2,020	20,435	79,565
25	63,284	36,736	30,832	6,157	30,832	69,168	17,901	3,552	17,901	82,099
20	57,816	42,184	28,130	5,448	28,130	71,870	16,189	2,702	16,189	83,811
15	50,872	49,128	24,926	6,944	24,926	75,074	14,289	3,204	14,289	85,711
12	45,425	54,575	22,463	5,447	22,463	77,537	12,848	2,463	12,848	87,152
10	40,894	59,106	20,423	4,531	20,423	79,577	11,652	2,040	11,652	88,348
8	35,312	64,688	17,918	5,582	17,918	82,082	10,187	2,505	10,187	89,813
6	28,365	71,635	14,803	6,947	14,803	85,197	8,383	3,115	8,383	91,617
5	24,323	75,677	12,976	4,042	12,976	87,024	7,338	1,827	7,338	92,662
4	19,896	80,104	10,939	4,427	10,939	89,061	6,183	2,037	6,183	93,817
3,2	16,054	83,946	9,119	3,842	9,119	90,881	5,154	1,820	5,154	94,846
2,6	12,950	87,050	7,593	3,104	7,593	92,407	4,291	1,526	4,291	95,709
2	9,586	90,414	5,860	3,364	5,860	94,140	3,306	1,733	3,306	96,694
-2	0,000	100,000	0,000	9,586	0,000	100,000	0,000	5,860	0,000	100,000
				99,771				100,000		100,000

PARTICLE SIZE DISTRIBUTION TEST 3

[µm]	overflow		discharge		underflow	
	D	%R	D	%R	D	%R
		ΣR		ΣR		ΣR
315	99,485	0,515	95,644	4,356	92,720	7,280
280	99,344	0,656	93,944	6,056	90,188	9,812
224	98,950	1,050	89,812	10,188	84,288	15,712
180	98,221	1,779	84,526	15,474	77,147	22,853
140	96,667	3,333	77,004	22,996	67,574	32,426
112	94,434	5,566	69,352	30,648	58,377	41,623
90	91,389	8,611	61,482	38,518	49,377	50,623
63	84,760	15,240	49,352	50,648	36,349	63,651
56	82,212	17,788	45,837	54,163	32,788	67,212
45	77,179	22,821	40,173	59,827	27,323	72,677
36	71,834	28,166	35,562	64,438	23,216	76,784
32	68,999	31,001	33,549	66,451	21,556	78,444
25	63,132	36,868	30,046	69,954	18,912	81,088
20	57,944	42,056	27,407	72,593	17,118	82,882
15	51,309	48,691	24,290	75,710	15,122	84,878
12	46,074	53,926	21,889	78,111	13,604	86,396
10	41,698	58,302	19,896	80,104	12,343	87,657
8	36,278	63,722	17,445	82,555	10,797	89,203
6	29,496	70,504	14,394	85,606	8,890	91,110
5	25,532	74,468	12,604	87,396	7,783	92,217
4	21,167	78,833	10,610	89,390	6,559	93,441
3,2	17,341	82,659	8,828	91,172	5,469	94,531
2,6	14,206	85,794	7,335	92,665	4,552	95,448
2	10,735	89,265	5,644	94,356	3,507	96,493
-2	0,000	100,000	0,000	100,000	0,000	100,000
		100,000		100,000		100,000

PARTICLE SIZE DISTRIBUTION TEST 4

[µm]	overflow		discharge		underflow	
	D	%R	D	%R	D	%R
315	99,423	0,577	95,582	4,418	91,871	8,129
280	99,346	0,654	93,881	6,119	89,006	10,994
224	99,203	0,797	89,682	10,318	82,200	17,800
180	98,946	1,054	84,229	15,771	73,824	26,176
140	98,224	1,776	76,444	23,556	62,580	37,420
112	96,870	3,130	68,627	31,373	51,986	48,014
90	94,597	5,403	60,792	39,208	42,029	57,971
63	88,518	11,482	49,287	50,713	28,827	71,173
56	85,913	14,087	46,107	53,893	25,585	74,415
45	80,549	19,451	41,126	58,874	21,038	78,962
36	74,743	25,257	37,156	62,844	18,044	81,956
32	71,683	28,317	35,414	64,586	16,946	83,054
25	65,472	34,528	32,274	67,726	15,274	84,726
20	60,125	39,875	29,737	70,263	14,079	85,921
15	53,380	46,620	26,526	73,474	12,561	87,439
12	48,034	51,966	23,982	76,038	11,309	88,691
10	43,517	56,483	21,812	78,188	10,257	89,743
8	37,864	62,136	19,161	80,839	8,980	91,020
6	30,726	69,274	15,856	84,144	7,431	92,569
5	26,534	73,466	13,909	86,091	6,538	93,462
4	21,913	78,087	11,728	88,272	5,545	94,455
3,2	17,889	82,131	9,766	90,234	4,646	95,354
2,6	14,589	85,431	8,114	91,886	3,879	96,121
2	10,943	89,057	6,236	93,764	2,990	97,010
-2	0,000	100,000	0,000	100,000	0,000	100,000
		100,000		100,000		100,000

PARTICLE SIZE DISTRIBUTION TEST 5

[µm]	overflow		discharge		underflow	
	D	%R	D	%R	D	%R
315	100,000	0,000	95,235	4,765	91,998	8,002
280	100,000	0,000	93,512	6,488	89,154	10,846
224	99,988	0,012	89,323	10,677	82,362	17,638
180	99,957	0,043	83,926	16,074	73,940	26,060
140	99,396	0,604	76,181	23,819	62,515	37,485
112	98,024	1,976	68,290	31,710	51,599	48,401
90	95,843	4,157	60,249	39,751	41,185	58,815
63	90,233	9,767	48,226	51,774	27,130	72,870
56	87,845	12,155	44,878	55,122	23,644	76,356
45	82,881	17,119	39,658	60,342	18,770	81,230
36	77,382	22,618	35,578	64,422	15,641	84,359
32	74,413	25,587	33,831	66,169	14,546	85,454
25	68,217	31,783	30,763	69,237	12,997	87,003
20	62,727	37,273	28,340	71,660	11,980	88,020
15	55,717	44,283	25,281	74,719	10,692	89,308
12	50,195	49,805	22,822	77,178	9,596	90,404
10	45,585	54,415	20,754	79,246	8,661	91,339
8	39,874	60,126	18,207	81,793	7,525	92,475
6	32,690	67,310	15,045	84,955	6,167	93,833
5	28,441	71,559	13,193	86,807	5,398	94,602
4	23,702	76,298	11,126	88,874	4,556	95,444
3,2	19,498	80,502	9,274	90,726	3,803	96,197
2,6	16,028	83,972	7,716	92,284	3,165	96,835
2	12,181	87,819	5,943	94,057	2,430	97,570
-2	0,000	100,000	0,000	100,000	0,000	100,000
		100,000		100,000		100,000

PARTICLE SIZE DISTRIBUTION TEST 6

[µm]	overflow		discharge		underflow	
	D	%R	D	%R	D	%R
315	99,659	0,341	96,374	3,626	93,119	6,881
280	99,609	0,391	94,844	5,156	90,529	9,471
224	99,527	0,473	90,990	9,010	84,159	15,841
180	99,344	0,656	85,831	14,169	75,983	24,017
140	98,735	1,265	78,199	21,801	64,538	35,462
112	97,509	2,491	70,243	29,757	53,328	46,672
90	95,384	4,616	61,999	38,001	42,444	57,556
63	89,552	10,448	49,487	50,513	27,541	72,459
56	87,007	12,993	45,977	54,023	23,824	76,176
45	81,690	18,310	40,497	59,503	18,640	81,360
36	75,820	24,180	36,228	63,772	15,357	84,643
32	72,677	27,323	34,409	65,591	14,234	85,766
25	66,204	33,796	31,238	68,762	12,698	87,302
20	60,550	39,450	28,742	71,258	11,723	88,277
15	53,380	46,620	25,583	74,417	10,480	89,520
12	47,724	52,276	23,035	76,965	9,403	90,597
10	42,983	57,017	20,893	79,107	8,477	91,523
8	37,104	62,896	18,263	81,737	7,354	92,646
6	29,761	70,239	15,017	84,983	6,019	93,981
5	25,488	74,512	13,127	86,873	5,268	94,732
4	20,823	79,177	11,029	88,971	4,446	95,554
3,2	16,794	83,206	9,159	90,841	3,712	96,288
2,6	13,562	86,438	7,595	92,405	3,088	96,912
2	10,082	89,918	5,827	94,173	2,367	97,633
-2	0,000	100,000	0,000	100,000	0,000	100,000
		100,000		100,000		100,000

PARTICLE SIZE DISTRIBUTION TEST 7

[µm]	overflow		discharge		underflow	
	D	%R	D	%R	D	%R
315	99,916	0,084	94,331	5,669	92,326	7,674
280	99,903	0,097	92,276	7,724	89,524	10,476
224	99,871	0,129	87,338	12,662	82,699	17,301
180	99,763	0,237	81,109	18,891	74,037	25,963
140	99,047	0,953	72,443	27,557	62,075	37,925
112	97,467	2,533	63,912	36,088	50,553	49,447
90	94,877	5,123	55,501	44,499	39,591	60,409
63	88,267	11,733	43,471	56,529	25,091	74,909
56	85,531	14,469	40,252	59,748	21,612	78,388
45	80,021	19,979	35,367	64,633	16,904	83,096
36	74,196	25,804	31,671	68,329	14,054	85,946
32	71,161	28,839	30,115	69,885	13,109	86,891
25	65,036	34,964	27,398	72,602	11,819	88,181
20	59,756	40,244	25,230	74,770	10,949	89,051
15	53,056	46,944	22,459	77,541	9,766	90,234
12	47,727	52,273	20,224	79,776	8,733	91,267
10	43,231	56,769	18,354	81,646	7,857	92,143
8	37,622	62,378	16,063	83,937	6,809	93,191
6	30,565	69,435	13,237	86,763	5,577	94,423
5	26,425	73,575	11,587	88,413	4,885	95,115
4	21,858	78,142	9,750	90,250	4,125	95,875
3,2	17,854	82,146	8,106	91,894	3,441	96,559
2,6	14,580	85,420	6,726	93,274	2,855	97,145
2	10,971	89,029	5,162	94,838	2,178	97,822
-2	0,000	100,000	0,000	100,000	0,000	100,000
		100,000		100,000		100,000

PARTICLE SIZE DISTRIBUTION TEST 10

[µm]	overflow		discharge		underflow	
	D	%R	D	%R	D	%R
315	99,989	0,011	94,462	5,538	93,099	6,901
280	99,987	0,002	92,485	7,515	90,358	9,642
224	99,986	0,001	87,797	12,203	83,584	16,416
180	99,940	0,060	81,935	18,065	74,852	25,148
140	99,290	0,710	73,762	26,238	62,644	37,356
112	97,773	2,227	65,634	34,366	50,803	49,197
90	95,291	4,709	57,510	42,490	39,530	60,470
63	88,874	11,126	45,659	54,341	24,736	75,264
56	86,183	13,817	42,430	57,570	21,238	78,762
45	80,717	19,283	37,468	62,532	16,582	83,418
36	74,882	25,118	33,642	66,358	13,847	86,153
32	71,829	28,171	32,008	67,992	12,967	87,033
25	65,660	34,340	29,121	70,879	11,785	88,215
20	60,365	39,635	26,801	73,199	10,971	89,029
15	53,699	46,301	23,840	76,160	9,817	90,183
12	48,434	51,566	21,461	78,539	8,796	91,204
10	44,003	55,997	19,472	80,528	7,932	92,068
8	38,468	61,532	17,039	82,961	6,904	93,096
6	31,446	68,554	14,039	85,961	5,699	94,301
5	27,268	72,732	12,289	87,711	5,020	94,980
4	22,592	77,408	10,342	89,658	4,270	95,730
3,2	18,434	81,566	8,601	91,399	3,586	96,414
2,6	15,011	84,989	7,140	92,860	2,993	97,007
2	11,248	88,752	5,485	94,515	2,298	97,702
-2	0,000	100,000	0,000	100,000	0,000	100,000
		100,000		100,000		100,000

PARTICLE SIZE DISTRIBUTION TEST 11

[µm]	overflow		discharge		underflow	
	D	%R	D	%R	D	%R
315	99,878	0,122	93,858	6,142	91,358	8,642
280	99,855	0,145	91,584	8,416	88,280	11,720
224	99,791	0,209	86,179	13,821	80,811	19,189
180	99,546	0,454	79,463	20,537	71,429	28,571
140	98,437	1,563	70,279	29,721	58,708	41,292
112	96,349	3,651	61,425	38,575	46,778	53,222
90	93,136	6,864	52,914	47,086	35,809	64,191
63	85,559	14,441	41,256	58,744	22,135	77,865
56	82,608	17,392	38,273	61,727	19,068	80,932
45	76,902	23,098	33,878	66,122	15,134	84,866
36	71,132	28,868	30,641	69,359	12,924	87,076
32	68,206	31,794	29,280	70,720	12,221	87,779
25	62,398	37,602	26,840	73,160	11,221	88,779
20	57,435	42,565	24,797	75,203	10,436	89,564
15	51,118	48,882	22,094	77,906	9,273	90,727
12	46,068	53,932	19,896	80,104	8,267	91,733
10	41,799	58,201	18,061	81,939	7,436	92,564
8	36,470	63,530	15,820	84,180	6,463	93,537
6	29,756	70,244	13,057	86,943	5,328	94,672
5	25,802	74,198	11,439	88,561	4,684	95,316
4	21,415	78,585	9,631	90,369	3,967	96,033
3,2	17,542	82,458	8,008	91,992	3,312	96,688
2,6	14,355	85,645	6,643	93,357	2,747	97,253
2	10,831	89,169	5,095	94,905	2,092	97,908
-2	0,000	100,000	0,000	100,000	0,000	100,000
		100,000		100,000		100,000

PARTICLE SIZE DISTRIBUTION TEST 13

[µm]	overflow		discharge		underflow	
	D	%R	D	%R	D	%R
315	99,837	0,163	94,904	5,096	91,820	8,180
280	99,818	0,182	92,911	7,089	88,884	11,116
224	99,774	0,226	88,122	11,878	81,677	18,323
180	99,661	0,339	82,067	17,933	72,514	27,486
140	98,467	1,533	73,575	26,425	59,977	40,023
112	95,990	4,010	65,136	34,864	48,161	51,839
90	92,183	7,817	56,772	43,228	37,279	62,721
63	83,425	16,575	44,840	55,160	23,734	76,266
56	80,114	19,886	41,677	58,323	20,704	79,296
45	73,890	26,110	36,916	63,084	16,820	83,180
36	67,851	32,149	33,330	66,670	14,620	85,380
32	64,890	35,110	31,811	68,189	13,901	86,099
25	59,209	40,791	29,104	70,896	12,827	87,173
20	54,515	45,485	26,873	73,127	11,941	88,059
15	48,637	51,363	23,957	76,043	10,627	89,373
12	43,946	56,054	21,592	78,408	9,500	90,500
10	39,971	60,029	19,613	80,387	8,572	91,428
8	35,000	65,000	17,192	82,808	7,480	92,520
6	28,726	71,274	14,202	85,798	6,194	93,806
5	25,023	74,977	12,450	87,550	5,458	94,542
4	20,902	79,098	10,492	89,508	4,633	95,367
3,2	17,247	82,753	8,732	91,268	3,876	96,124
2,6	14,224	85,776	7,250	92,750	3,222	96,778
2	10,852	89,148	5,567	94,433	2,463	97,537
-2	0,000	100,000	0,000	100,000	0,000	100,000
		100,000		100,000		100,000

PARTICLE SIZE DISTRIBUTION TEST 14

[µm]	overflow		discharge		underflow	
	D	%R	D	%R	D	%R
		Σ		Σ		Σ
315	99,965	0,035	94,489	5,511	93,202	6,798
280	99,961	0,004	92,348	7,652	90,496	9,504
224	99,948	0,052	87,226	12,774	83,685	16,315
180	99,859	0,141	80,834	19,166	74,765	25,235
140	99,151	0,849	72,051	27,949	62,180	37,820
112	97,669	2,331	63,521	36,479	49,943	50,057
90	95,176	4,824	55,238	44,762	38,343	61,657
63	88,648	11,352	43,685	56,315	23,393	76,607
56	85,922	14,078	40,670	59,330	19,959	80,041
45	80,425	19,575	36,158	63,842	15,523	84,477
36	74,618	25,382	32,757	67,243	13,054	86,946
32	71,601	28,399	31,304	68,696	12,297	87,703
25	65,537	34,463	28,674	71,326	11,293	88,707
20	60,345	39,655	26,468	73,532	10,547	89,453
15	53,800	46,200	23,563	76,437	9,406	90,594
12	48,616	51,384	21,211	78,789	8,384	91,616
10	44,244	55,756	19,249	80,751	7,530	92,470
8	38,779	61,221	16,853	83,147	6,530	93,470
6	31,857	68,143	13,897	86,103	5,377	94,623
5	27,756	72,244	12,165	87,835	4,731	95,269
4	23,181	76,819	10,227	89,773	4,015	95,985
3,2	19,113	80,887	8,487	91,513	3,362	96,638
2,6	15,739	84,261	7,025	92,975	2,796	97,204
2	11,963	88,037	5,372	94,628	2,135	97,865
-2	0,000	100,000	0,000	100,000	0,000	100,000
		100,000		100,000		100,000

PARTICLE SIZE DISTRIBUTION TEST 15

[µm]	overflow		%R		discharge		%R		underflow	
	D	ΣR	D	%R	D	ΣR	D	%R	D	ΣR
315	99,951	0,049	94,599	0,049	94,599	5,401	92,567	5,401	92,567	7,433
280	99,943	0,057	92,325	0,008	92,325	7,675	89,834	2,274	89,834	10,166
224	99,935	0,065	86,814	0,008	86,814	13,186	82,991	5,511	82,991	17,009
180	99,888	0,112	79,860	0,047	79,860	20,140	74,050	6,954	74,050	25,950
140	99,448	0,552	70,269	0,440	70,269	29,731	61,434	9,591	61,434	38,566
112	98,118	1,882	60,993	1,330	60,993	39,007	49,166	9,276	49,166	50,834
90	95,682	4,318	52,088	2,436	52,088	47,912	37,545	8,905	37,545	62,455
63	89,027	10,973	39,995	6,655	39,995	60,005	22,607	12,093	22,607	77,393
56	86,210	13,790	36,945	2,817	36,945	63,055	19,195	3,050	19,195	80,805
45	80,517	19,483	32,519	5,693	32,519	67,481	14,816	4,426	14,816	85,184
36	74,526	25,474	29,337	5,991	29,337	70,663	12,421	3,182	12,421	87,579
32	71,431	28,569	28,023	3,095	28,023	71,977	11,705	1,314	11,705	88,295
25	65,258	34,742	25,690	6,173	25,690	74,310	10,784	2,333	10,784	89,216
20	60,017	39,983	23,735	5,241	23,735	76,265	10,102	1,955	10,102	89,898
15	53,433	46,567	21,133	6,584	21,133	78,867	9,029	2,602	9,029	90,971
12	48,206	51,794	19,015	5,227	19,015	80,985	8,053	2,118	8,053	91,947
10	43,781	56,219	17,252	4,425	17,252	82,748	7,235	1,763	7,235	92,765
8	38,234	61,766	15,107	5,547	15,107	84,893	6,279	2,145	6,279	93,721
6	31,206	68,794	12,471	7,028	12,471	87,529	5,181	2,636	5,181	94,819
5	27,054	72,946	10,929	4,152	10,929	89,071	4,569	1,542	4,569	95,431
4	22,445	77,555	9,202	4,609	9,202	90,798	3,891	1,727	3,891	96,109
3,2	18,382	81,618	7,647	4,063	7,647	92,353	3,270	1,555	3,270	96,730
2,6	15,045	84,955	6,337	3,337	6,337	93,663	2,728	1,310	2,728	97,272
2	11,358	88,642	4,849	3,687	4,849	95,151	2,091	1,488	2,091	97,909
-2	0,000	100,000	0,000	11,358	0,000	100,000	0,000	4,849	0,000	100,000
				100,000				100,000		100,000

PARTICLE SIZE DISTRIBUTION TEST 16

[µm]	overflow		discharge		underflow	
	D	%R	D	%R	D	%R
315	100,000	0,000	96,861	3,139	91,035	8,965
280	100,000	0,000	95,176	4,824	87,904	12,096
224	100,000	0,000	90,824	9,176	80,155	19,845
180	100,000	0,000	84,971	15,029	70,214	29,786
140	99,756	0,244	76,472	23,288	56,560	43,440
112	98,314	1,686	67,942	32,058	43,758	56,242
90	95,603	4,397	59,540	40,460	32,161	67,839
63	88,388	11,612	47,787	52,213	18,355	81,645
56	85,416	14,584	44,723	55,277	15,476	84,524
45	79,538	20,462	40,119	59,881	12,060	87,940
36	73,502	26,498	36,585	63,415	10,415	89,585
32	70,428	29,572	35,035	64,965	9,967	90,033
25	64,351	35,649	32,143	67,857	9,348	90,652
20	59,203	40,797	29,655	70,345	8,753	91,247
15	52,709	47,291	26,369	73,631	7,734	92,266
12	47,538	52,462	23,730	76,270	6,841	93,159
10	43,165	56,835	21,541	78,459	6,125	93,875
8	37,701	62,299	18,878	81,122	5,316	94,684
6	30,810	69,190	15,593	84,407	4,402	95,598
5	26,751	73,249	13,665	86,335	3,887	96,113
4	22,252	77,748	11,504	88,496	3,307	96,693
3,2	18,281	81,719	9,558	90,442	2,766	97,234
2,6	15,010	84,990	7,919	92,081	2,292	97,708
2	11,377	88,623	6,062	93,938	1,739	98,261
-2	0,000	100,000	0,000	100,000	0,000	100,000
				100,000		100,000

PARTICLE SIZE DISTRIBUTION TEST 18

[µm]	overflow		discharge		underflow	
	D	%R	D	%R	D	%R
315	100,000	0,000	95,540	4,460	91,034	8,966
280	100,000	0,000	93,661	6,339	87,672	12,328
224	100,000	0,000	89,007	10,993	79,355	20,645
180	100,000	0,000	82,962	17,038	68,799	31,201
140	99,633	0,367	74,409	25,591	54,578	45,422
112	97,766	2,234	66,007	33,993	41,557	58,443
90	94,558	5,442	57,882	42,118	30,055	69,945
63	86,507	13,493	46,769	53,231	16,871	83,129
56	83,312	16,688	3,195	56,079	14,239	85,761
45	77,124	22,876	6,188	60,336	4,257	11,225
36	70,910	29,090	36,381	63,619	9,857	90,143
32	67,790	32,210	34,917	65,083	9,497	90,503
25	61,696	38,304	32,121	67,879	8,964	91,036
20	56,599	43,401	29,651	70,349	8,386	91,614
15	50,238	49,762	26,349	73,651	7,381	92,619
12	45,219	54,781	23,692	76,308	6,518	93,482
10	41,003	58,997	21,491	78,509	5,839	94,161
8	35,766	64,234	18,814	81,186	5,081	94,919
6	29,187	70,813	15,511	84,489	4,227	95,773
5	25,317	74,683	13,570	86,430	3,743	96,257
4	21,026	78,974	11,395	88,605	3,192	96,808
3,2	17,246	82,754	9,440	90,560	2,675	97,325
2,6	14,149	85,851	7,803	92,197	2,219	97,781
2	10,736	89,264	5,959	94,041	1,844	98,313
-2	0,000	100,000	0,000	100,000	0,000	100,000
		100,000		100,000		100,000

PARTICLE SIZE DISTRIBUTION TEST 19

[µm]	overflow		discharge		underflow	
	D	%R	D	%R	D	%R
315	100,000	0,000	95,688	4,312	90,409	9,591
280	100,000	0,000	93,813	6,187	86,928	13,072
224	100,000	0,000	89,103	10,897	78,304	21,696
180	100,000	0,000	82,962	17,038	67,382	32,618
140	99,527	0,473	74,302	25,698	52,787	47,213
112	97,490	2,510	65,860	34,140	39,620	60,380
90	94,078	5,922	57,777	42,223	28,224	71,776
63	85,810	14,190	46,847	53,153	15,625	84,375
56	82,614	17,386	44,058	55,942	13,222	86,778
45	76,537	23,463	39,872	60,128	10,575	89,425
36	70,546	29,454	36,597	63,403	9,442	90,558
32	67,567	32,433	35,116	64,884	9,147	90,853
25	61,758	38,242	32,257	67,743	8,655	91,345
20	56,863	43,137	29,731	70,269	8,060	91,940
15	50,661	49,339	26,388	73,612	7,043	92,957
12	45,704	54,296	23,724	76,276	6,200	93,800
10	41,516	58,484	21,526	78,474	5,552	94,448
8	36,298	63,702	18,856	81,144	4,838	95,162
6	29,733	70,267	15,557	84,443	4,032	95,968
5	25,866	74,134	13,616	86,384	3,569	96,431
4	21,570	78,430	11,439	88,561	3,036	96,964
3,2	17,770	82,230	9,481	90,519	2,533	97,467
2,6	14,637	85,363	7,839	92,161	2,090	97,910
2	11,158	88,842	5,990	94,010	1,575	98,425
-2	0,000	100,000	0,000	100,000	0,000	100,000
				100,000		100,000

PARTICLE SIZE DISTRIBUTION TEST 20

[µm]	overflow		discharge		underflow	
	D	%R	D	%R	D	%R
315	100,000	0,000	96,273	3,727	88,019	11,981
280	100,000	0,000	94,167	5,833	84,130	15,870
224	100,000	0,000	88,790	11,210	74,811	25,189
180	100,000	0,000	81,699	18,301	63,423	36,577
140	99,505	0,495	71,752	28,248	48,672	51,328
112	97,600	2,400	62,233	37,767	35,710	64,290
90	94,410	5,590	53,373	46,627	24,746	75,254
63	86,565	13,435	42,034	57,966	12,997	87,003
56	83,489	16,511	39,330	60,670	10,840	89,160
45	77,577	22,423	35,492	64,508	8,552	91,448
36	71,685	28,315	32,696	67,304	7,656	92,344
32	68,735	31,265	31,474	68,526	7,445	92,555
25	62,954	37,046	29,112	70,888	7,081	92,919
20	58,064	41,936	26,963	73,037	6,586	93,414
15	51,846	48,154	24,031	75,969	5,714	94,286
12	46,852	53,148	21,658	78,342	5,000	95,000
10	42,611	57,389	19,694	80,306	4,461	95,539
8	37,301	62,699	17,308	82,692	3,879	96,121
6	30,596	69,404	14,360	85,640	3,232	96,768
5	26,640	73,360	12,621	87,379	2,860	97,140
4	22,243	77,757	10,663	89,337	2,429	97,571
3,2	18,346	81,654	8,887	91,113	2,018	97,982
2,6	15,120	84,880	7,384	92,616	1,656	98,344
2	11,515	88,485	5,669	94,331	1,234	98,766
-2	0,000	100,000	0,000	100,000	0,000	100,000
				100,000		100,000

PARTICLE SIZE DISTRIBUTION TEST 21

[µm]	overflow		discharge		underflow	
	D	%R	D	%R	D	%R
315	100,000	0,000	95,327	4,673	90,503	9,497
280	100,000	0,000	93,230	6,770	87,056	12,944
224	100,000	0,000	87,993	12,007	78,532	21,468
180	100,000	0,000	81,202	18,798	67,715	32,285
140	99,566	0,434	71,729	28,271	53,182	46,818
112	97,765	2,235	62,631	37,369	39,980	60,020
90	94,670	5,330	54,078	45,922	28,480	71,520
63	86,955	13,045	42,893	57,107	15,682	84,318
56	83,922	16,078	40,153	59,847	13,232	86,768
45	78,085	21,915	36,177	63,823	10,538	89,462
36	72,229	27,771	33,196	66,804	9,405	90,595
32	69,269	30,731	31,877	68,123	9,121	90,879
25	63,396	36,604	29,332	70,668	8,659	91,341
20	58,354	41,646	27,052	72,948	8,086	91,914
15	51,909	48,091	23,992	76,008	7,080	92,920
12	46,759	53,241	21,544	78,456	6,237	93,763
10	42,419	57,581	19,530	80,470	5,586	94,414
8	37,024	62,976	17,092	82,908	4,869	95,131
6	30,252	69,748	14,091	85,909	4,063	95,937
5	26,273	73,727	12,327	87,673	3,602	96,398
4	21,863	78,137	10,349	89,651	3,071	96,929
3,2	17,971	82,029	8,569	91,431	2,569	97,431
2,6	14,763	85,237	7,076	92,924	2,126	97,874
2	11,200	88,800	5,397	94,603	1,608	98,392
-2	0,000	100,000	0,000	100,000	0,000	100,000

PARTICLE SIZE DISTRIBUTION TEST 22

[µm]	overflow		discharge		underflow	
	D	%R	D	%R	D	%R
		ΣR		ΣR		ΣR
315	100,000	0,000	96,380	3,620	90,931	9,069
280	100,000	0,000	94,373	5,627	87,226	12,774
224	100,000	0,000	89,321	10,679	77,927	22,073
180	100,000	0,000	82,793	17,207	66,150	33,850
140	99,046	0,954	73,788	26,212	50,646	49,354
112	96,511	3,489	65,242	34,758	37,012	62,988
90	92,488	7,512	57,284	42,736	25,585	74,415
63	83,299	16,701	46,784	53,236	13,603	86,397
56	79,891	20,109	44,124	55,876	11,463	88,537
45	73,576	26,424	40,159	59,841	9,234	90,766
36	67,541	32,459	37,007	62,993	8,368	91,632
32	64,600	35,400	35,552	64,448	8,147	91,853
25	58,956	41,044	32,692	67,308	7,716	92,284
20	54,258	45,742	30,137	69,863	7,138	92,862
15	48,321	51,679	26,758	73,242	6,172	93,828
12	43,569	56,431	24,072	75,928	5,406	94,594
10	39,554	60,446	21,856	78,144	4,834	95,166
8	34,559	65,441	19,157	80,843	4,216	95,784
6	28,297	71,703	15,810	84,190	3,347	96,482
5	24,620	75,380	13,835	86,165	3,112	96,888
4	20,547	79,453	11,616	88,384	2,639	97,361
3,2	16,953	83,047	9,620	90,380	1,996	97,810
2,6	13,994	86,006	7,947	92,053	1,673	98,204
2	10,707	89,293	6,065	93,935	1,342	98,658
-2	0,000	100,000	0,000	100,000	0,000	100,000
		100,000		100,000		100,000

PARTICLE SIZE DISTRIBUTION TEST 23

[µm]	overflow		discharge		underflow	
	D	%R	D	%R	D	%R
		ΣR		ΣR		ΣR
315	100,000	0,000	96,337	3,663	91,719	8,281
280	100,000	0,000	94,431	5,569	88,163	11,837
224	100,000	0,000	89,595	10,405	79,106	20,894
180	100,000	0,000	83,283	16,717	67,457	32,543
140	99,294	0,706	74,474	25,526	51,907	48,093
112	97,140	2,860	66,033	33,967	38,072	61,928
90	93,563	6,437	58,095	41,905	26,371	73,629
63	85,111	14,889	47,563	52,437	13,989	86,011
56	81,916	18,084	44,895	55,105	11,763	88,237
45	75,927	24,073	40,864	59,136	9,443	90,557
36	70,107	29,893	37,629	62,371	8,552	91,448
32	67,228	32,772	36,126	63,874	8,335	91,665
25	61,610	38,390	33,155	66,845	7,917	92,083
20	56,845	43,155	30,491	69,509	7,343	92,657
15	50,749	49,251	26,971	73,029	6,362	93,638
12	45,837	54,163	24,187	75,813	5,578	94,422
10	41,668	58,332	21,903	78,097	4,991	95,009
8	36,460	63,540	19,138	80,862	4,357	95,643
6	29,904	70,096	15,729	84,271	3,645	96,355
5	26,051	73,949	13,724	86,276	3,232	96,768
4	21,778	78,222	11,479	88,521	2,749	97,251
3,2	17,994	82,006	9,469	90,531	2,289	97,711
2,6	14,856	85,144	7,796	92,204	1,882	98,118
2	11,332	88,668	5,930	94,070	1,410	98,590
-2	0,000	100,000	0,000	100,000	0,000	100,000
				100,000		100,000

PARTICLE SIZE DISTRIBUTION TEST 24

[µm]	overflow		discharge		underflow	
	D	%R	D	%R	D	%R
		ΣR		ΣR		ΣR
315	100,000	0,000	95,172	4,828	90,137	9,863
280	100,000	0,000	92,904	7,096	86,109	13,891
224	100,000	0,000	87,295	12,705	76,163	23,837
180	99,913	0,087	80,175	19,825	63,858	36,142
140	98,308	1,692	70,543	29,457	48,102	51,898
112	95,206	4,794	61,595	38,405	34,665	65,335
90	90,658	9,342	53,423	46,577	23,756	76,244
63	81,063	18,937	43,010	56,990	12,835	87,165
56	77,683	22,317	40,473	59,527	10,987	89,013
45	71,591	28,409	36,737	63,263	9,139	90,861
36	65,907	34,093	33,823	66,177	8,445	91,555
32	63,156	36,844	32,485	67,515	8,250	91,750
25	57,847	42,153	29,845	70,155	7,797	92,203
20	53,355	46,645	27,472	72,528	7,180	92,820
15	47,591	52,409	24,335	75,665	6,197	93,803
12	42,955	57,045	21,856	78,144	5,445	94,555
10	39,041	60,959	19,823	80,177	4,890	95,110
8	34,181	65,819	17,358	82,642	4,288	95,712
6	28,088	71,912	14,309	85,691	3,594	96,406
5	24,501	75,499	12,511	87,489	3,184	96,816
4	20,508	79,492	10,492	89,508	2,704	97,296
3,2	16,959	83,041	8,676	91,324	2,246	97,754
2,6	14,014	85,986	7,156	92,844	1,846	98,154
2	10,718	89,282	5,450	94,550	1,385	98,615
-2	0,000	100,000	0,000	100,000	0,000	100,000
				100,000		100,000

PARTICLE SIZE DISTRIBUTION TEST 26

[µm]	overflow		discharge		underflow	
	D	%R	D	%R	D	%R
		ΣR		ΣR		ΣR
315	99,708	0,292	92,711	7,289	89,778	10,222
280	99,556	0,444	90,465	9,535	86,932	13,068
224	99,009	0,991	85,377	14,623	80,605	19,395
180	98,039	1,961	79,367	20,633	73,304	26,696
140	96,247	3,753	71,430	28,570	63,896	36,104
112	93,962	6,038	63,853	36,147	55,146	44,854
90	91,056	8,944	56,436	43,564	46,802	53,198
63	84,903	15,097	45,534	54,466	35,007	64,993
56	82,505	17,495	42,451	57,549	31,809	68,191
45	77,647	22,353	37,490	62,510	26,862	73,138
36	72,293	27,707	33,378	66,622	23,036	76,964
32	69,381	30,619	31,533	68,467	21,433	78,567
25	63,250	36,750	28,208	71,792	18,763	81,237
20	57,797	42,203	25,626	74,374	16,876	83,124
15	50,904	49,096	22,581	77,419	14,787	85,213
12	45,559	54,441	20,291	79,709	13,256	86,744
10	41,139	58,861	18,426	81,574	12,016	87,984
8	35,690	64,310	16,157	83,843	10,517	89,483
6	28,869	71,131	13,344	86,656	8,676	91,324
5	24,867	75,133	11,690	88,310	7,603	92,397
4	20,452	79,548	9,841	90,159	6,412	93,588
3,2	16,591	83,409	8,163	91,817	5,347	94,653
2,6	13,453	86,547	6,793	93,207	4,452	95,548
2	10,032	89,968	5,222	94,778	3,433	96,567
-2	0,000	100,000	0,000	100,000	0,000	100,000
		100,000		100,000		100,000

PARTICLE SIZE DISTRIBUTION TEST 27

[µm]	overflow		discharge		underflow	
	D	%R	D	%R	D	%R
		Σ		Σ		Σ
315	99,665	0,335	94,432	5,568	91,809	8,191
280	99,520	0,480	92,352	7,648	89,249	10,751
224	98,978	1,022	87,514	12,486	83,431	16,569
180	97,999	2,001	81,691	18,309	76,557	23,443
140	96,162	3,838	73,896	26,104	67,479	32,521
112	93,775	6,225	66,350	33,650	58,829	41,171
90	90,687	9,313	58,857	41,143	50,404	49,596
63	84,118	15,882	47,671	52,329	38,228	61,772
56	81,593	18,407	44,485	55,515	34,888	65,112
45	76,590	23,410	39,369	60,631	29,713	70,287
36	71,267	28,733	35,171	64,829	25,728	74,272
32	68,448	31,552	33,308	66,692	24,068	75,932
25	62,638	37,362	29,978	70,022	21,310	78,690
20	57,533	42,467	27,385	72,615	19,338	80,662
15	51,024	48,976	24,284	75,736	17,081	82,919
12	45,872	54,128	21,861	78,139	15,368	84,632
10	41,541	58,459	19,876	80,124	13,955	86,045
8	36,141	63,859	17,446	82,554	12,230	87,770
6	29,332	70,668	14,425	85,575	10,100	89,900
5	25,327	74,673	12,648	87,352	8,857	91,143
4	20,902	79,098	10,660	89,340	7,475	92,525
3,2	17,020	82,980	8,877	91,123	6,236	93,764
2,6	13,848	86,152	7,378	92,622	5,193	94,807
2	10,363	89,637	5,679	94,321	4,003	95,997
-2	0,000	100,000	0,000	100,000	0,000	100,000
		100,000		100,000		100,000

PARTICLE SIZE DISTRIBUTION TEST 28

[µm]	overflow		discharge		underflow	
	D	%R	D	%R	D	%R
315	99,648	0,352	92,915	7,085	90,896	9,104
280	99,518	0,482	90,902	9,098	88,453	11,547
224	99,191	0,809	86,405	13,595	83,073	16,927
180	98,629	1,371	81,122	18,878	76,841	23,159
140	97,416	2,584	74,028	25,972	68,585	31,415
112	95,602	4,398	67,003	32,997	60,505	39,495
90	93,034	6,966	59,788	40,212	52,295	47,705
63	87,185	12,815	48,436	51,564	39,577	60,423
56	84,856	15,144	45,054	54,946	35,862	64,138
45	80,131	19,869	39,481	60,519	29,882	70,118
36	74,931	25,069	34,815	65,185	25,116	74,884
32	72,095	27,905	32,744	67,256	23,119	76,881
25	66,076	33,924	29,121	70,879	19,897	80,103
20	60,627	39,373	26,426	73,574	17,776	82,224
15	53,582	46,418	23,333	76,667	15,587	84,413
12	48,024	51,976	21,007	78,993	14,020	85,980
10	43,395	56,605	19,093	80,907	12,740	87,260
8	37,675	62,325	16,743	83,257	11,171	88,829
6	30,519	69,481	13,815	86,185	9,225	90,775
5	26,326	73,674	12,095	87,905	8,091	91,909
4	21,699	78,301	10,179	89,821	6,838	93,162
3,2	17,644	82,356	8,469	91,531	5,724	94,276
2,6	14,333	85,667	7,039	92,961	4,788	95,212
2	10,701	89,299	5,422	94,578	3,716	96,284
-2	0,000	100,000	0,000	100,000	0,000	100,000
				100,000		100,000

PARTICLE SIZE DISTRIBUTION TEST 29

[µm]	overflow		discharge		underflow	
	D	%R	D	%R	D	%R
		ΣR		ΣR		ΣR
315	99,674	0,326	92,941	7,059	92,767	7,233
280	99,568	0,432	90,778	9,222	90,452	9,548
224	99,282	0,718	85,886	14,114	85,146	14,854
180	98,760	1,240	80,107	19,893	78,778	21,222
140	97,609	2,391	72,421	27,579	70,169	29,831
112	95,873	4,127	64,962	35,038	61,704	38,296
90	93,377	6,623	57,491	42,509	53,148	46,852
63	87,566	12,434	46,137	53,863	40,079	59,921
56	85,228	14,772	42,851	57,149	36,318	63,682
45	80,488	19,512	37,532	62,468	30,330	69,670
36	75,317	24,683	33,167	66,833	25,623	74,377
32	72,530	27,470	31,251	68,749	23,670	76,330
25	66,681	33,319	27,909	72,091	20,525	79,475
20	61,432	38,568	25,403	74,597	18,434	81,566
15	54,625	45,375	22,477	77,523	16,216	83,784
12	49,184	50,816	20,245	79,755	14,587	85,413
10	44,595	55,405	18,400	81,600	13,244	86,756
8	38,870	61,130	16,135	83,865	11,593	88,407
6	31,648	68,352	13,316	86,684	9,551	90,449
5	27,399	72,601	11,661	88,339	8,364	91,636
4	22,698	77,302	9,816	90,184	7,053	92,947
3,2	18,563	81,437	8,167	91,833	5,887	94,113
2,6	15,168	84,832	6,785	93,215	4,911	95,089
2	11,410	88,590	5,220	94,780	3,796	96,204
-2	0,000	100,000	0,000	100,000	0,000	100,000
		100,000		100,000		100,000

PARTICLE SIZE DISTRIBUTION TEST 30

[µm]	overflow		discharge		underflow	
	D	%R	D	%R	D	%R
		Σ		Σ		Σ
315	99,678	0,322	94,247	5,753	92,533	7,467
280	99,510	0,168	92,361	7,639	90,133	9,867
224	98,945	1,055	87,981	12,019	84,605	15,395
180	97,952	2,048	82,618	17,382	77,938	22,062
140	96,064	3,936	75,228	24,772	68,936	31,064
112	93,541	6,459	67,848	32,152	60,160	39,840
90	90,192	9,808	60,312	39,688	51,422	48,578
63	82,925	17,075	48,680	51,320	38,478	61,522
56	80,125	19,875	45,288	54,712	34,875	65,125
45	74,625	25,375	39,784	60,216	29,286	70,714
36	68,889	31,111	35,260	64,740	25,044	74,956
32	65,912	34,088	33,271	66,729	23,324	76,676
25	59,927	40,073	29,791	70,209	20,587	79,413
20	54,822	45,178	27,163	72,837	18,744	81,256
15	48,461	51,539	24,064	75,936	16,702	83,298
12	43,487	56,513	21,685	78,315	15,140	84,860
10	39,320	60,680	19,711	80,289	13,831	86,169
8	34,132	65,868	17,282	82,718	12,211	87,789
6	27,597	72,403	14,252	85,748	10,197	89,803
5	23,759	76,241	12,470	87,530	9,020	90,980
4	19,530	80,470	10,481	89,519	7,706	92,294
3,2	15,839	84,161	8,703	91,297	6,514	93,486
2,6	12,841	87,159	7,216	92,784	5,487	94,513
2	9,570	90,430	5,535	94,465	4,279	95,721
-2	0,000	100,000	0,000	100,000	0,000	100,000
		100,000		100,000		100,000

PARTICLE SIZE DISTRIBUTION TEST 32

[µm]	overflow		%R		discharge		%R		underflow	
	D	R	D	R	D	R	D	R	D	R
315	99,904	0,096	91,890	8,110	91,890	8,110	93,401	6,599	93,401	6,599
280	99,889	0,131	89,527	10,473	89,527	10,473	91,112	8,888	91,112	8,888
224	99,642	0,358	84,197	15,803	84,197	15,803	85,727	14,273	85,727	14,273
180	99,109	0,891	77,925	22,075	77,925	22,075	79,072	20,928	79,072	20,928
140	97,936	2,064	69,653	30,347	69,653	30,347	69,883	30,117	69,883	30,117
112	96,229	3,771	61,750	38,250	61,750	38,250	60,772	39,228	60,772	39,228
90	93,807	6,193	54,007	45,993	54,007	45,993	51,605	48,395	51,605	48,395
63	88,132	11,868	42,687	57,313	42,687	57,313	37,959	62,041	37,959	62,041
56	85,831	14,169	39,539	60,461	39,539	60,461	34,171	65,829	34,171	65,829
45	81,143	18,857	34,593	65,407	34,593	65,407	28,336	71,664	28,336	71,664
36	76,004	23,996	30,677	69,323	30,677	69,323	23,971	76,029	23,971	76,029
32	73,224	26,776	28,993	71,007	28,993	71,007	22,227	77,773	22,227	77,773
25	67,366	32,634	26,069	73,931	26,069	73,931	19,491	80,509	19,491	80,509
20	62,078	37,922	23,842	76,158	23,842	76,158	17,670	82,330	17,670	82,330
15	55,180	44,820	21,159	78,841	21,159	78,841	15,646	84,354	15,646	84,354
12	49,656	50,344	19,068	80,932	19,068	80,932	14,087	85,913	14,087	85,913
10	45,003	54,997	17,328	82,672	17,328	82,672	12,781	87,219	12,781	87,219
8	39,211	60,789	15,189	84,811	15,189	84,811	11,170	88,830	11,170	88,830
6	31,919	68,081	12,529	87,471	12,529	87,471	9,184	90,816	9,184	90,816
5	27,627	72,373	10,967	89,033	10,967	89,033	8,034	91,966	8,034	91,966
4	22,873	77,127	9,223	90,777	9,223	90,777	6,765	93,235	6,765	93,235
3,2	18,685	81,315	7,663	92,337	7,663	92,337	5,639	94,361	5,639	94,361
2,6	15,249	84,751	6,355	93,645	6,355	93,645	4,695	95,305	4,695	95,305
2	11,459	88,541	4,876	95,124	4,876	95,124	3,620	96,380	3,620	96,380
-2	0,000	100,000	0,000	100,000	0,000	100,000	0,000	100,000	0,000	100,000
				100,000		100,000		100,000		100,000

PARTICLE SIZE DISTRIBUTION TEST 33

[µm]	overflow		discharge		underflow	
	D	%R	D	%R	D	%R
315	100	0	91,841	8,159	92,59	7,41
280	99,988	0,012	89,469	10,531	90,186	9,814
224	99,709	0,279	84,131	15,869	84,657	15,343
180	98,915	1,085	77,867	22,133	78,016	21,984
140	97,323	2,677	69,621	30,379	69,094	30,906
112	95,24	4,76	61,754	38,246	60,441	39,559
90	92,589	7,411	54,054	45,946	51,861	48,139
63	87,205	12,795	42,812	57,188	39,147	60,853
56	85,216	14,784	39,686	60,314	35,584	64,416
45	81,328	18,672	34,771	65,229	30,001	69,999
36	77,125	22,875	30,872	69,128	25,674	74,326
32	74,804	25,196	29,192	70,808	23,88	76,12
25	69,672	30,328	26,27	73,73	20,956	79,044
20	64,675	35,325	24,041	75,959	18,942	81,058
15	57,69	42,31	21,354	78,646	16,716	83,284
12	51,864	48,136	19,255	80,745	15,046	84,954
10	46,898	53,102	17,507	82,493	13,668	86,332
8	40,704	59,296	15,358	84,642	11,979	88,021
6	32,932	67,068	12,686	87,314	9,891	90,109
5	28,375	71,625	11,117	88,883	8,674	91,326
4	23,342	76,658	9,365	90,635	7,324	92,676
3,2	18,93	81,07	7,793	92,207	6,118	93,882
2,6	15,332	84,668	6,472	93,528	5,104	94,896
2	11,403	88,597	4,972	95,028	3,944	96,056
-2	0	100	0	100	0	100

Cement and Mining Technology GmbH Dokumentname: Document Name: Nombre del Documento:	Nassmahlung von Kalkstein mit 10 % Ton	Roman van Ommen Austria	
	PRÜF 001	Revision	01

Kurzbericht über Mahlung von Kalkstein mit Tonanteil

**Auftraggeber : Roman van Ommen
Austria**

**Auftragnehmer : CEMTEC GmbH
Austria**

Laborberichts Nr.: „30-X-08-1“

Cemtec Projekt Nr.: „XXX“

Cemtec GmbH
Ennshafenstr. 40
A-4470 Enns
Austria

Tel: (43) 7223 / 83620-656
Fax: (43) 7223 / 83620-333
e-mail info@cemtec.at

Erstellt von: Prepared by: Preparado por:	Jürgen Gleißenberg	Datum: Date: Fecha:	01/04/2009	ersetzt / substitutes / sustituda:
Gepfört von: Checked by: Chequeado por:		Datum: Date: Fecha:		Seite Page 1 of 18 Pagina 1 de 18
Verteiler / Distribution Distribuidor:		gespeichert in: Y:\KEE\X\PERSONLICHE ORDNER\ROMAN\PHD\CEMTEC REPORTS UND DATEN\Bericht Roman van Ommen.doc		

CEftüm <small>Cement and Mining Technology GmbH</small>	Nassmahlung von Kalkstein mit 10 % Ton	Roman van Ommen Austria	
		PRÜF 001	Revision 01

Index:

1	Aufgabenstellung	3
2	Probematerial	3
3	Untersuchungsgeräte bzw. Hilfsmittel	4
3.1	Korngrößenbestimmung	4
3.2	Massenbestimmung	4
3.3	Feststoffdichte	4
3.4	Feuchtigkeit	4
3.5	Mahlung	4
4	Untersuchungsergebnisse	5
4.1	Probeneingangsparameter	5
4.2	Korngrößenbestimmung	Fehler! Textmarke nicht definiert.
4.3	Mahlbarkeitsuntersuchung nach Bond	5
4.4	Bilder	5

Erstellt von: Prepared by: Preparado por:	Jürgen Gleißenberg	Datum: Date: Fecha:	01/04/2009	ersetzt / substitutes / sustituda:
Gepüft von: Checked by: Chequeado por:		Datum: Date: Fecha:		Seite Page Pagina
Verteiler / Distribution Distribudor:		gespeichert in: Y:\KEE\PERSONUCHE ORDNER\ROMAN\PHD\CEMTEC REPORTS UND DATEN\Bericht Roman van Ommen.doc		2 von 18 2 of 18 2 de 18

CEfteS <small>Cement and Mining Technology GmbH</small>	Nassmahlung von Kalkstein mit 10 % Ton	Roman van Ommen Austria	
	PRÜF 001	<small>Revision</small>	01

1 Aufgabenstellung

Der Ziel der Untersuchungen war es einen Nassmahlkreislaufes mittels Zyklone ins Gleichgewicht zu bringen und das Verhalten der Gesamtanlage, durch Veränderungen der Apex-Größen, zu beurteilen.

2 Probematerial

Bei dem Versuchsmaterial handelt es sich um einen Kalkstein mit 10 % Tonanteilen



Erstellt von: Prepared by: Preparado por:	Jürgen Gleißenberg	Datum; Date:	01/04/2009	ersetzt / substitutes / sustituda:
Geprüft von: Checked by: Chequeado por:		Datum; Date: Fecha:		Seite Page Pagina
Verteiler / Distribution Distribuidor:		gespeichert in: Y:\KEE\X\PERSONLICHE ORDNER\ROMAN\PHD\CEMTEC REPORTS UND DATEN\Bericht Roman van Ommen.doc		q of 18 de 18

CEftüm <small>Cement and Mining Technology GmbH</small>	Nassmahlung von Kalkstein mit 10 % Ton	Roman van Ommen Austria	
		<small>Dokumentname: Document Name: Nombre del Documento:</small>	PRÜF 001

3 Untersuchungsgeräte bzw. Hilfsmittel

3.1 Korngößenbestimmung

- Handsiebsatz 300 x 300 nach DIN 4188
- Maschinensiebsatz 0 200 x 50 nach DIN 4188
- Mastersizer 2000 Malvern

3.2 Massenbestimmung

- AND Laborwaage GX 6100
- AND Analysenwaage GR 200

3.3 Feststoffdichte

- Schüttdichte-Prüfgefäß
- Micromeritics-Pycnometer

3.4 Feuchtigkeit

- Feuchtebestimmer MX 50
- Trockenschrank TK/L 4105

3.5 Mahlung

- Kugelmühle 1,20m x 3,00m

<small>Erstellt von: Prepared by: Preparado por:</small>	Jürgen Gleißberg	<small>Datum: Date: Fecha:</small>	01/04/2009	<small>ersetzt / substitutes / sustituda:</small>	
<small>Geprüft von: Checked by: Chequeado por:</small>		<small>Datum: Date: Fecha:</small>		<small>Seite Page Página</small>	<small>von of de</small>
<small>Verteiler / Distribution Distribudor:</small>		<small>gespeichert in: Y:\KEE\XPERSONLICHE ORDNER\ROMAN\PHD\CEMTEC REPORTS UND DATEN\Bericht Roman van Ommen.doc</small>		<small>4</small>	<small>18</small>

CEftüm <small>Cement and Mining Technology GmbH</small>	Nassmahlung von Kalkstein mit 10 % Ton	Roman van Ommen Austria	
		<small>Dokumentname: Document Name: Nombre del Documento:</small>	PRÜF 001

4 Untersuchungsergebnisse

4.1 Probeneingangsparameter

Aufgabeparameter

Schüttdichte : 1.442 Mg/m³
 Trockenrohddichte : 2.622 Mg/m³
 Materialfeuchte : 5.10 %
 Abschlämbbare Bestandteile: nicht bestimmt

4.2 Korngrößenbestimmung

siehe Datei Aufgabesieblinie Bond RvO

4.3 Mahlbarkeitsuntersuchung nach Bond

Die Durchführung der Mahlbarkeitsuntersuchung nach Bond ergab einen Workindex von 12,6 kWh/t bei einem F80=2749 μ m und einem Prüfsieb von 150 μ m.

<small>Erstellt von: Prepared by: Preparado por:</small>	Jürgen Gleißenberg	<small>Datum: Date: Fecha:</small>	01/04/2009	<small>ersetzt / substitutes / sustituda:</small>
<small>Gepprüft von: Checked by: Chequeado por:</small>		<small>Datum: Date: Fecha:</small>		<small>Seite Page</small>
<small>Verteiler / Distribution Distribudor:</small>		<small>gespeichert in: Y:\KEE\XPERSONLICHE ORDNER\ROMAN\PHD\CEMTEC REPORTS UND DATEN\Bericht Roman van Ommen.doc</small>		<small>von of</small>
				<small>18</small>
				<small>de</small>

CEfteS Cement and Mining Technology GmbH	Nassmahlung von Kalkstein mit 10 % Ton	Roman van Ommen Austria	
	Dokumentname: Document Name: Nombre del Documento:	PRÜF 001	Revision 01

4.4 Bilder

Rohdichte



Erstellt von: Prepared by: Preparado por:	Jürgen Gleißenberg	Datum: DeTha:	01/04/2009	ersetzt / substitutes / sustituda:
Geprüft von: Checked by: Chequeado por:		Datum: Date: Fecha:		Seite Page ^A of 18 Pagina ^e de 18
Verteiler / Distribution Distribuidor:		gespeichert in: Y:\KEE\PERSONLICHE ORDNER\ROMAN\PHD\CEMTEC REPORTS UND DATEN\Bericht Roman van Ommen.doc		

CEfteg Cement and Mining Technology GmbH	Nassmahlung von Kalkstein mit 10 % Ton	Roman van Ommen Austria	
	Dokumentname: Document Name: Nombre del Documento:	PRÜF 001	Revision 01


Schüttdichte



Malvern



Erstellt von: Prepared by: Preparado por:	Jürgen Gleißenberg	Datum; Date:	01/04/2009	ersetzt / substitutes / sustituda:
Gepüft von: Checked by: Chequeado por:		Datum; Date:		Seite Page Panina
Verteiler / Distribution Distribudor:		gespeichert in: Y:\KEE\XPERSONLICHE ORDNER\ROMAN\PHD\CEMTEC REPORTS UND DATEN\Bericht Roman van		

 Cement and Mining Technology GmbH	Nassmahlung von Kalkstein mit 10 % Ton	Roman van Ommen Austria	
	PRÜF 001	Revision	01

Mühle



Erstellt von: Prepared by: Preparado por:	Jürgen Gleißenberg	Datum: SS* 01/04/2009	ersetzt / substitutes / sustituda:
Geprüft von: Checked by: Chequeado por:		Datum: Date: Fecha:	Seite Page Pagina
Verteiler / Distribution Distribudor:		gespeichert in: Y:\KEE\X\PERSONLICHE ORDNER\ROMAN\PHD\CEMTEC REPORTS UND DATEN\Bericht Roman van Ommen.doc	

C E f t a g	Nassmahlung von Kalkstein mit 10 % Ton	Roman van Ommen Austria	
	PRÜF 001	Revision	01
<small>Cement and Mining Technology GmbH</small>	<small>Dokumentname: Document Name: Nombre del Documento:</small>		



<small>Erstellt von: Prepared by: Preparado por:</small>	Jürgen Gleißenberg	<small>Datum: f*@*</small>	01/04/2009	<small>ersetzt / substitutes / sustituda:</small>	
<small>Geprüft von: Checked by: Chequeado por:</small>		<small>Datum: Date: Fecha:</small>		<small>Seite Pag*</small>	<small>von of 18</small>
<small>Verteiler / Distribution Distribuidor:</small>		<small>gespeichert in: Y:\KEE\XPERSONLICHE ORDNER\ROMANPHD\CEMTEC REPORTS UND DATEN\Bericht Roman van Ommen.doc</small>		<small>Página de</small>	<small>18</small>

<h1>CEfteg</h1>	<h2>Nassmahlung von Kalkstein mit 10 % Ton</h2>	Roman van Ommen Austria	
	Cement and Mining Technology GmbH Dokumentname: Document Name: Nombre del Documento:	PRÜF 001	Revision



Erstellt von: Prepared by: Preparado por:	Jürgen Gleißenberg	Datum: De:Da:	01/04/2009	ersetzt / substitutes / sustituda:
Geprüft von: Checked by: Chequeado por:		Datum: Date: Fecha:		Seite Page Pagina
Verteiler / Distribution Distribudor:		gespeichert in: Y:\KEE\PERSONLICHE ORDNER\ROMANPHD\CEMTEC REPORTS UND DATEN\Bericht Roman van Ommen.doc		

CEfteS	Nassmahlung von Kalkstein mit 10 % Ton	Roman van Ommen Austria	
		Cement and Mining Technology GmbH	
Dokumentname: Document Name: Nombre del Documento:	PRÜF 001	Revision	01



Erstellt von: Prepared by: Preparado por:	Jürgen Gleißenberg	Datum: Date: Fecha:	01/04/2009	ersetzt / substitutes / sustituda:
Geprüft von: Checked by: Chequeado por:		Datum: Date: Fecha:		Seite Page Pagina
Verteiler / Distribution Distribuidor:		gespeichert in: Y:\KEE\X\PERSONLICHE ORDNER\ROMAN\PHD\CEMTEC REPORTS UND DATEN\Bericht Roman van Ommen.doc		von of de

CEfteS Cement and Mining Technology GmbH	Nassmahlung von Kalkstein mit 10 % Ton	Roman van Ommen Austria	
	Dokumentname: Document Name: Nombre del Documento:	PRÜF 001	Revision 01



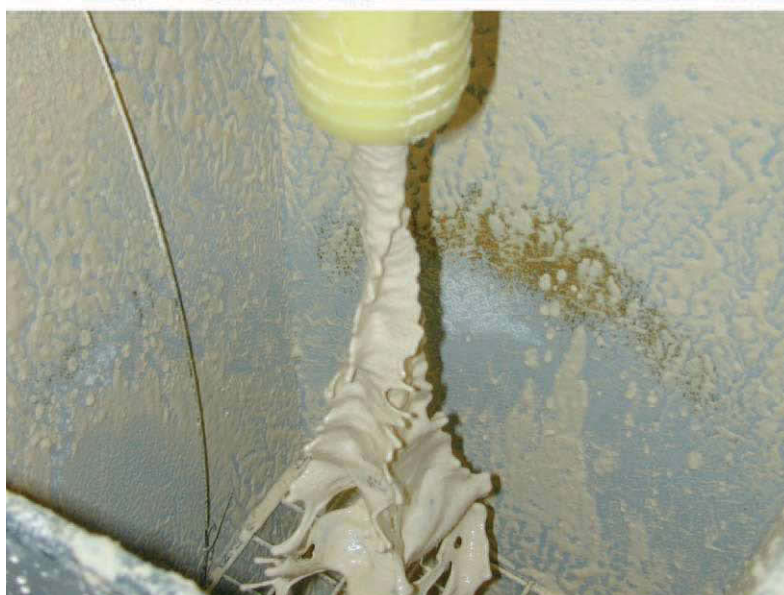
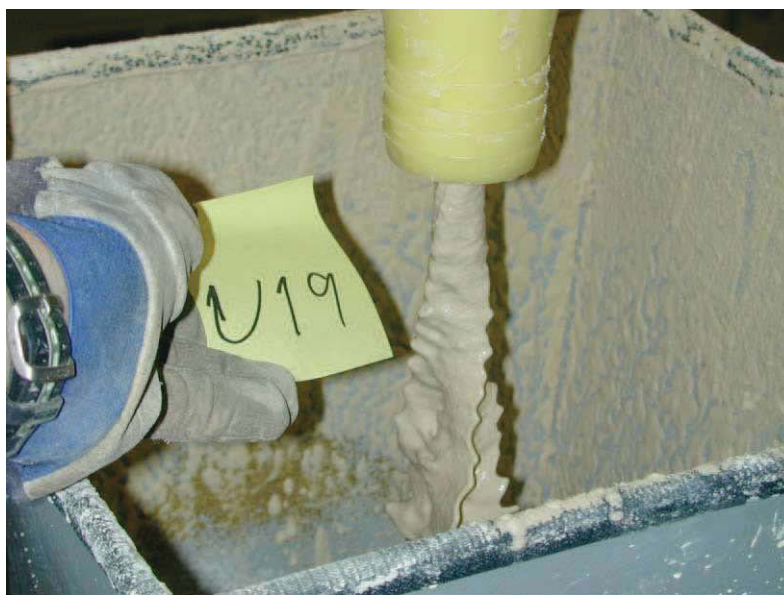
Erstellt von: Prepared by: Preparado por:	Jürgen Gleißenberg	Datum: Date: Fecha:	01/04/2009	ersetzt / substitutes / sustituda:
Geprüft von: Checked by: Chequeado por:		Datum: Date: Fecha:		Seite Page Pagina
Verteiler / Distribution Distribuidor:		gespeichert in: Y:\KEE\X\PERSONLICHE ORDNER\ROMAN\PHD\CEMTEC REPORTS UND DATEN\Bericht Roman van Ommen.doc		12 von 18 12 of 18 12 de 18

C E f t e g <small>Cement and Mining Technology GmbH</small>	Nassmahlung von Kalkstein mit 10 % Ton	Roman van Ommen Austria	
	PRÜF 001	<small>Revision</small>	01



<small>Erstellt von: Prepared by: Preparado por:</small>	Jürgen Gleißberg	<small>Datum; Date:</small>	01/04/2009	<small>ersetzt / substitutes / sustituda:</small>
<small>Gepprüft von: Checked by: Chequeado por:</small>		<small>Datum; Date: Fecha:</small>		<small>Seite Page Pagina</small>
<small>Verteiler / Distribution Distribudor:</small>		<small>gespeichert in: Y:\KEE\PERSONLICHE ORDNER\ROMANPHD\CEMTEC REPORTS UND DATEN\Bericht Roman van Ommen.doc</small>		<small>von of de</small>

C E f t e g Cement and Mining Technology GmbH	Nassmahlung von Kalkstein mit 10 % Ton	Roman van Ommen Austria
	Dokumentname: Document Name: Nombre del Documento:	PRÜF 001



Erstellt von: Prepared by: Preparado por:	Jürgen Gleißberg	Datum; Date: Fecha:	01/04/2009	ersetzt / substitutes / sustituda:
Geprüft von: Checked by: Chequeado por:		Datum; Date: Fecha:		Seite Page Página
Verteiler / Distribution Distribuidor:		gespeichert in: Y:\KEE\PERSONLICHE ORDNER\ROMAN\PHD\CEMTEC REPORTS UND DATEN\Bericht Roman van Ommen.doc		von of 18

CEfteg <small>Cement and Mining Technology GmbH</small>	Nassmahlung von Kalkstein mit 10 % Ton	Roman van Ommen Austria	
	<small>Dokumentname: Document Name: Nombre del Documento:</small>	PRÜF 001	<small>Revision</small> 01



<small>Erstellt von: Prepared by: Preparado por:</small>	Jürgen Gleißenberg	<small>Datum: De'ose:</small>	01/04/2009	<small>ersetzt / substitutes / sustituda:</small>	
<small>Geprüft von: Checked by: Chequeado por:</small>		<small>Datum: Date: Fecha:</small>		<small>Seite Page</small>	<small>von of 18 18</small>
<small>Verteiler / Distribution Distribudor:</small>		<small>gespeichert in: Y:\KEEX\PERSONLICHE ORDNER\ROMAN\PHD\CEMTEC REPORTS UND DATEN</small>	<small>Bericht Roman van Ommen.doc</small>		

C E f t a g Cement and Mining Technology GmbH	Nassmahlung von Kalkstein mit 10 % Ton	Roman van Ommen Austria	
	Dokumentname: Document Name: Nombre del Documento:	PRÜF 001	Revision 01



Diese Bilder sind als Erinnerung und zeigt den Leitstand



Erstellt von: Prepared by: Preparado por:	Jürgen Gleißenberg	Datum; Date: Fecha:	01/04/2009	ersetzt / substitutes / sustituda:	
Geprüft von: Checked by: Chequeado por:		Datum; Date: Fecha:		Seite Página	von o@
Verteiler / Distribution Distribuidor:		gespeichert in: Y:\KEE\PERSONLICHE ORDNER\ROMAN\PHD\CEMTEC REPORTS UND DATEN\Bericht Roman van Ommen.doc			

CEfteS Cement and Mining Technology GmbH	Nassmahlung von Kalkstein mit 10 % Ton	Roman van Ommen Austria	
	Dokumentname: Document Name: Nombre del Documento:	PRÜF 001	Revision 01



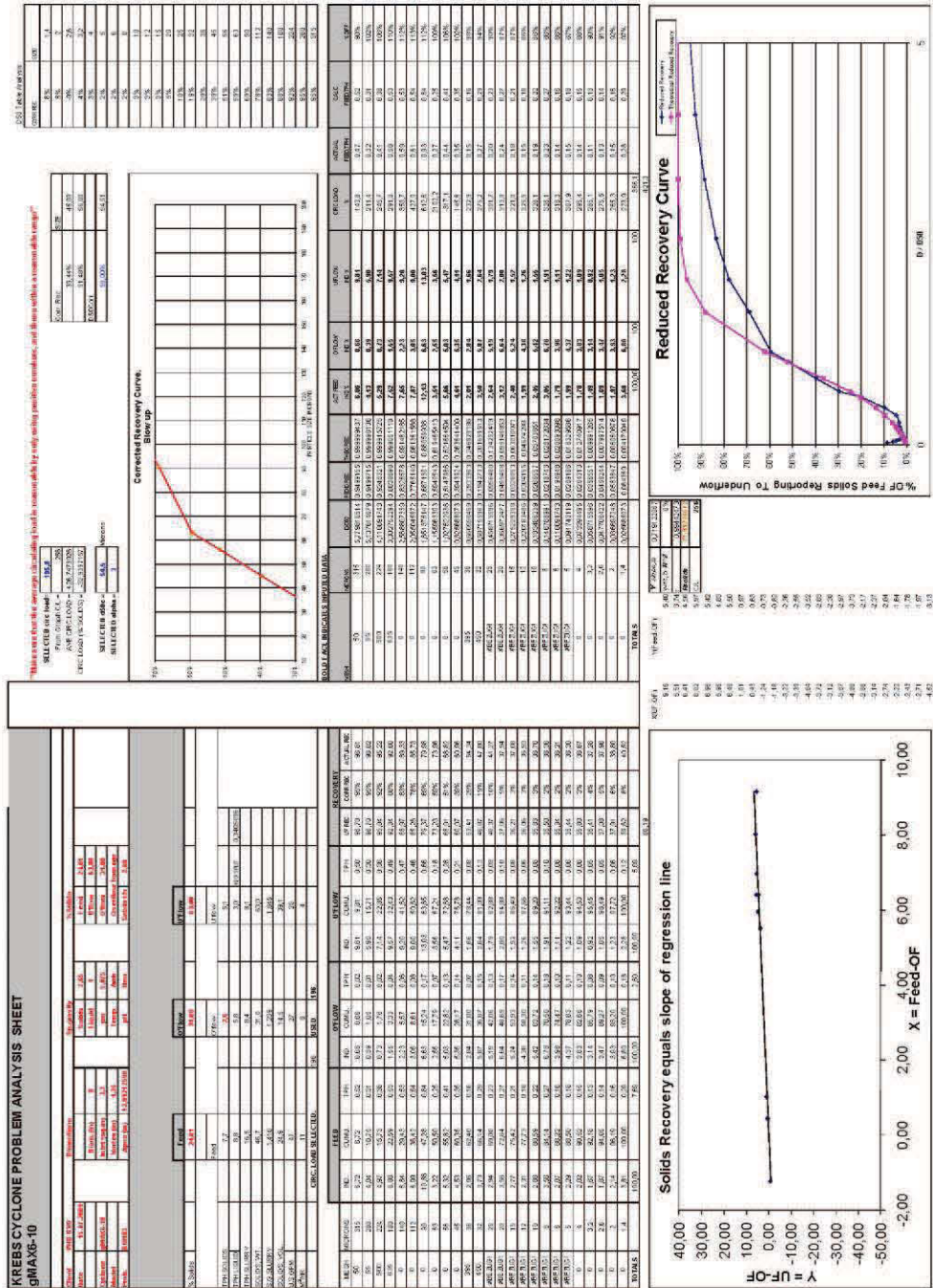
/

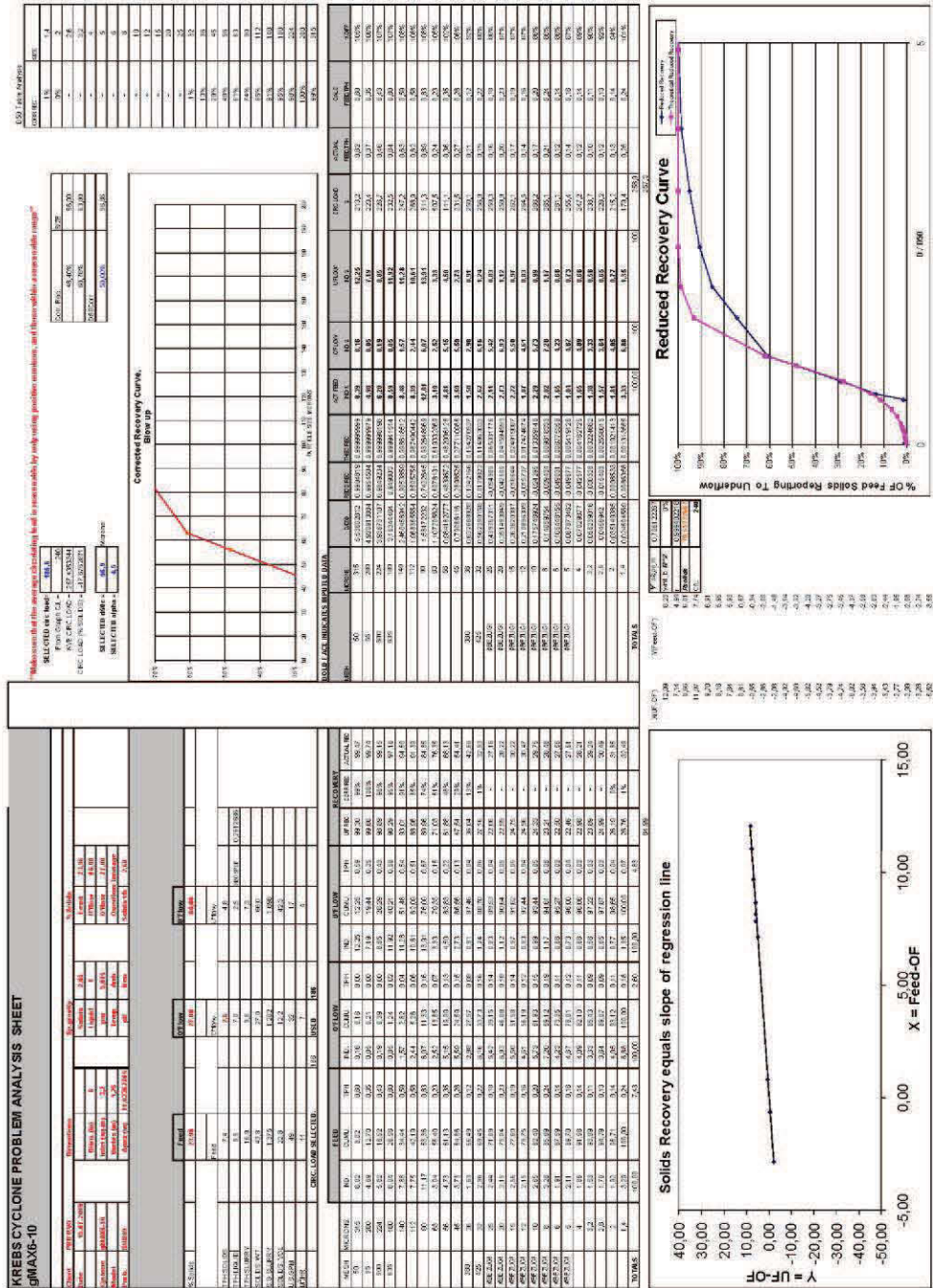
Erstellt von: Prepared by: Preparado por:	Jürgen Gleißenberg	Datum: Date: Fecha:	01/04/2009	ersetzt / substitutes / sustituda:
Geprüft von: Checked by: Chequeado por:		Seite Page Pagina	* -7 of 17	von of de
Verteiler / Distribution Distribuidor:		gespeichert in: Y:\KEE\X\PERSONLICHE ORDNER\ROMANPHD\CEMTEC REPORTS UND DATEN\Bericht Roman van Ommen.doc		

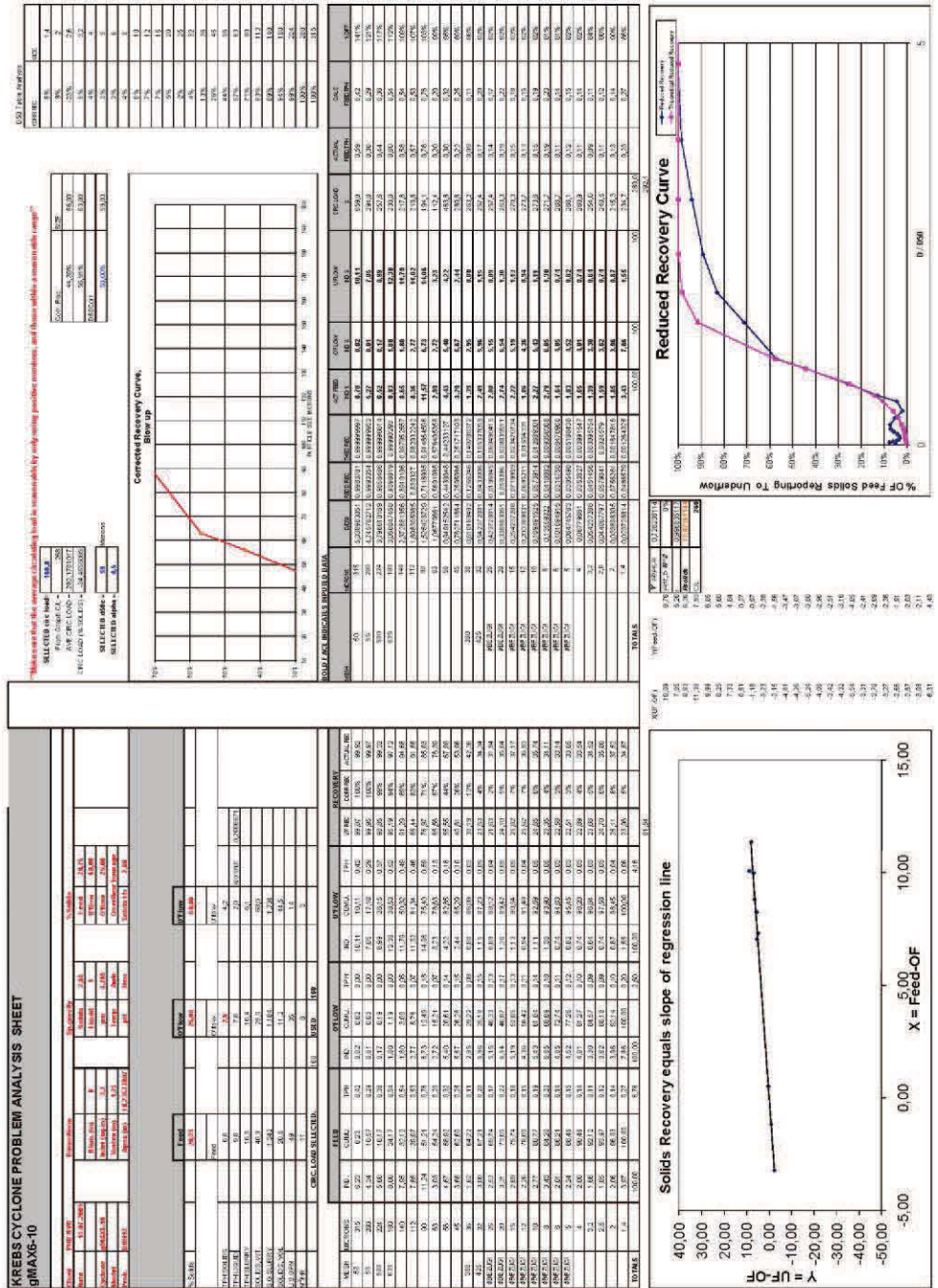
<h1 style="margin: 0;">CEfteg</h1> <p style="font-size: small; margin: 0;">Cement and Mining Technology GmbH</p>	<h2 style="margin: 0;">Nassmahlung von Kalkstein mit 10 % Ton</h2>	Roman van Ommen Austria	
	Dokumentname: Document Name: Nombre del Documento:	<h3 style="margin: 0;">PRÜF 001</h3>	Revision

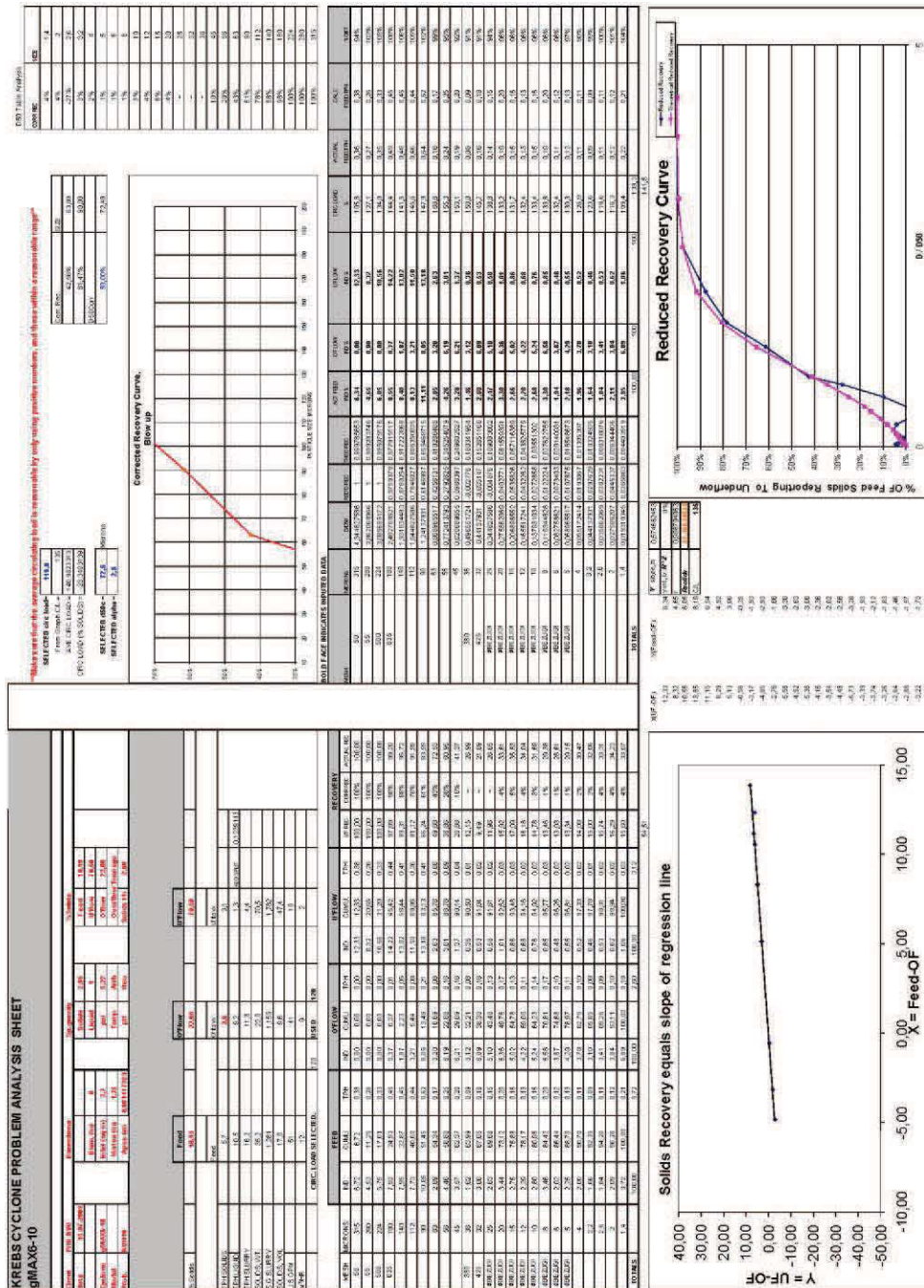


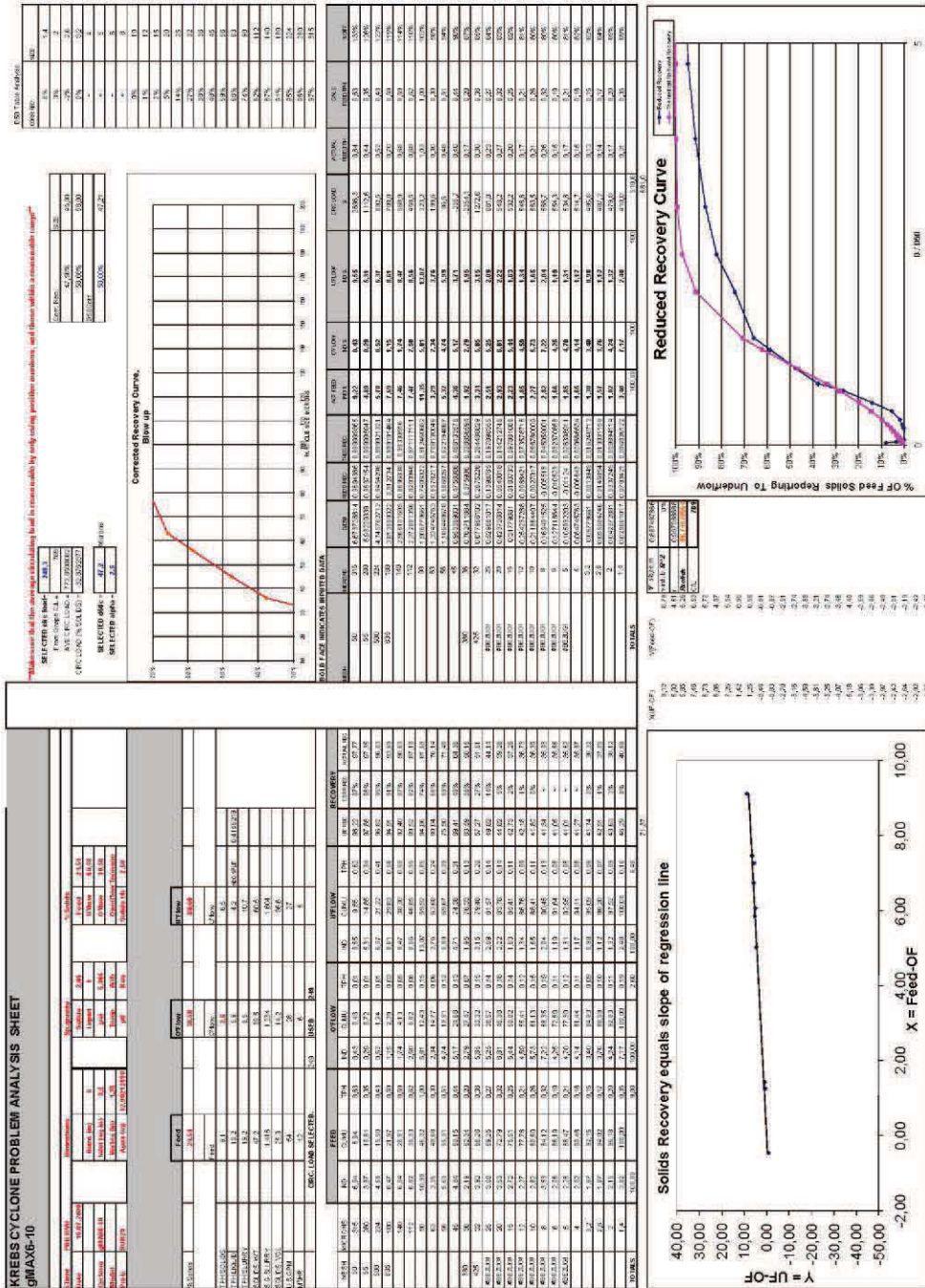
Erstellt von: Prepared by: Preparado por:	Jürgen Gleißenberg	Datum: De'ata:	01/04/2009	ersetzt / substitutes / sustituda:	
Geprüft von: Checked by: Chequeado por:		Datum: Date: Fecha:		Seite Page Pagina	von of d.e.
Verteiler / Distribution Distribudor:		gespeichert in: Y:\KEEW\PERSONLICHE ORDNER\ROMANPHD\CEMTEC REPORTS UND DATEN\Bericht Roman van Ommen.doc			











KREBS CYCLONE PROBLEM ANALYSIS SHEET
gMAX16-10

ITEM	DESCRIPTION	UNIT	VALUE	REMARKS
1	Flow rate	kg/h	1000	
2	Feed size	mm	100	
3	Flow rate	kg/h	1000	
4	Feed size	mm	100	
5	Flow rate	kg/h	1000	
6	Feed size	mm	100	
7	Flow rate	kg/h	1000	
8	Feed size	mm	100	
9	Flow rate	kg/h	1000	
10	Feed size	mm	100	
11	Flow rate	kg/h	1000	
12	Feed size	mm	100	
13	Flow rate	kg/h	1000	
14	Feed size	mm	100	
15	Flow rate	kg/h	1000	
16	Feed size	mm	100	
17	Flow rate	kg/h	1000	
18	Feed size	mm	100	
19	Flow rate	kg/h	1000	
20	Feed size	mm	100	
21	Flow rate	kg/h	1000	
22	Feed size	mm	100	
23	Flow rate	kg/h	1000	
24	Feed size	mm	100	
25	Flow rate	kg/h	1000	
26	Feed size	mm	100	
27	Flow rate	kg/h	1000	
28	Feed size	mm	100	
29	Flow rate	kg/h	1000	
30	Feed size	mm	100	

SOILS RECOVERY CHARACTERISTICS

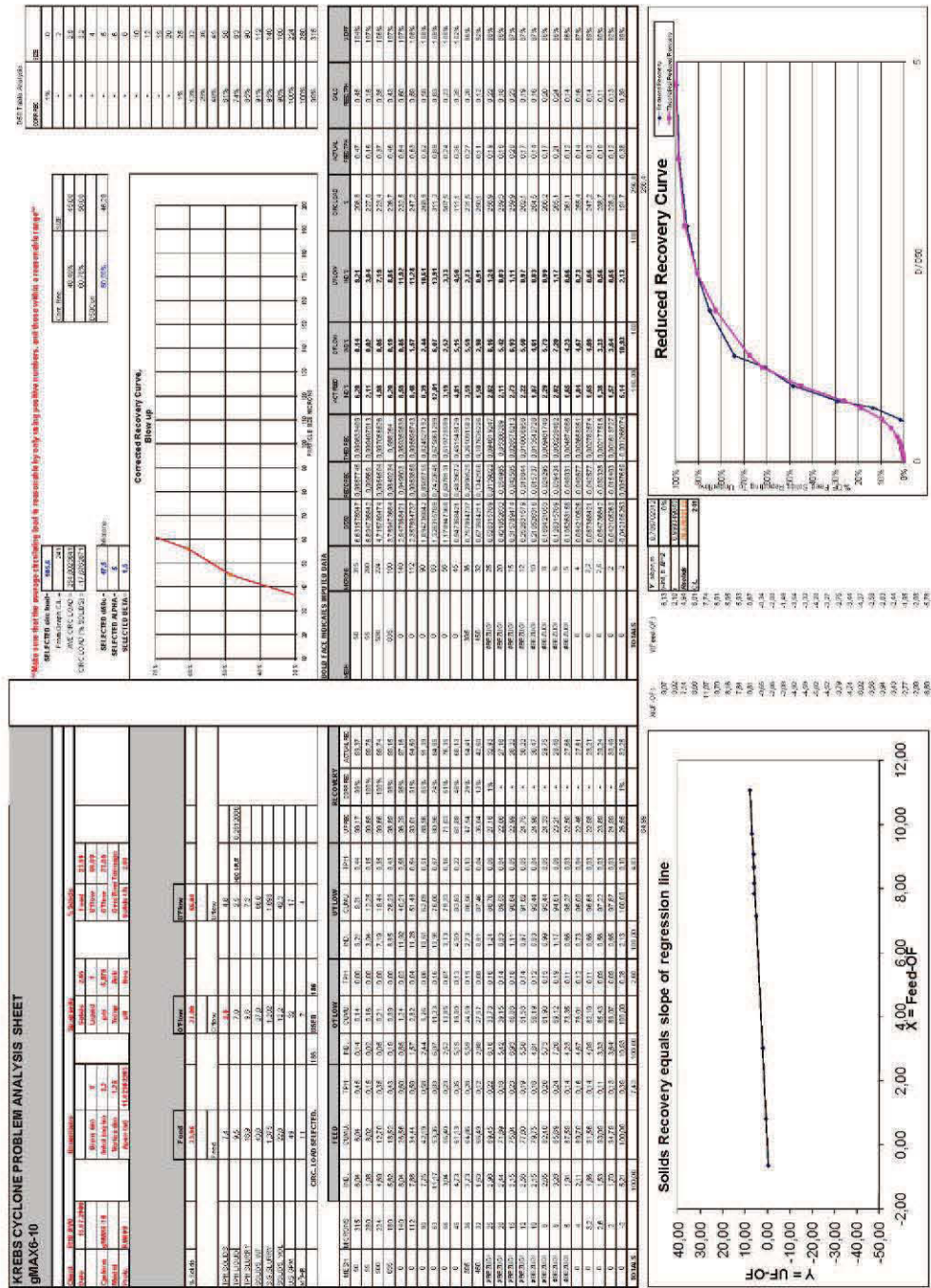
ITEM	DESCRIPTION	UNIT	VALUE	REMARKS
1	Flow rate	kg/h	1000	
2	Feed size	mm	100	
3	Flow rate	kg/h	1000	
4	Feed size	mm	100	
5	Flow rate	kg/h	1000	
6	Feed size	mm	100	
7	Flow rate	kg/h	1000	
8	Feed size	mm	100	
9	Flow rate	kg/h	1000	
10	Feed size	mm	100	
11	Flow rate	kg/h	1000	
12	Feed size	mm	100	
13	Flow rate	kg/h	1000	
14	Feed size	mm	100	
15	Flow rate	kg/h	1000	
16	Feed size	mm	100	
17	Flow rate	kg/h	1000	
18	Feed size	mm	100	
19	Flow rate	kg/h	1000	
20	Feed size	mm	100	
21	Flow rate	kg/h	1000	
22	Feed size	mm	100	
23	Flow rate	kg/h	1000	
24	Feed size	mm	100	
25	Flow rate	kg/h	1000	
26	Feed size	mm	100	
27	Flow rate	kg/h	1000	
28	Feed size	mm	100	
29	Flow rate	kg/h	1000	
30	Feed size	mm	100	

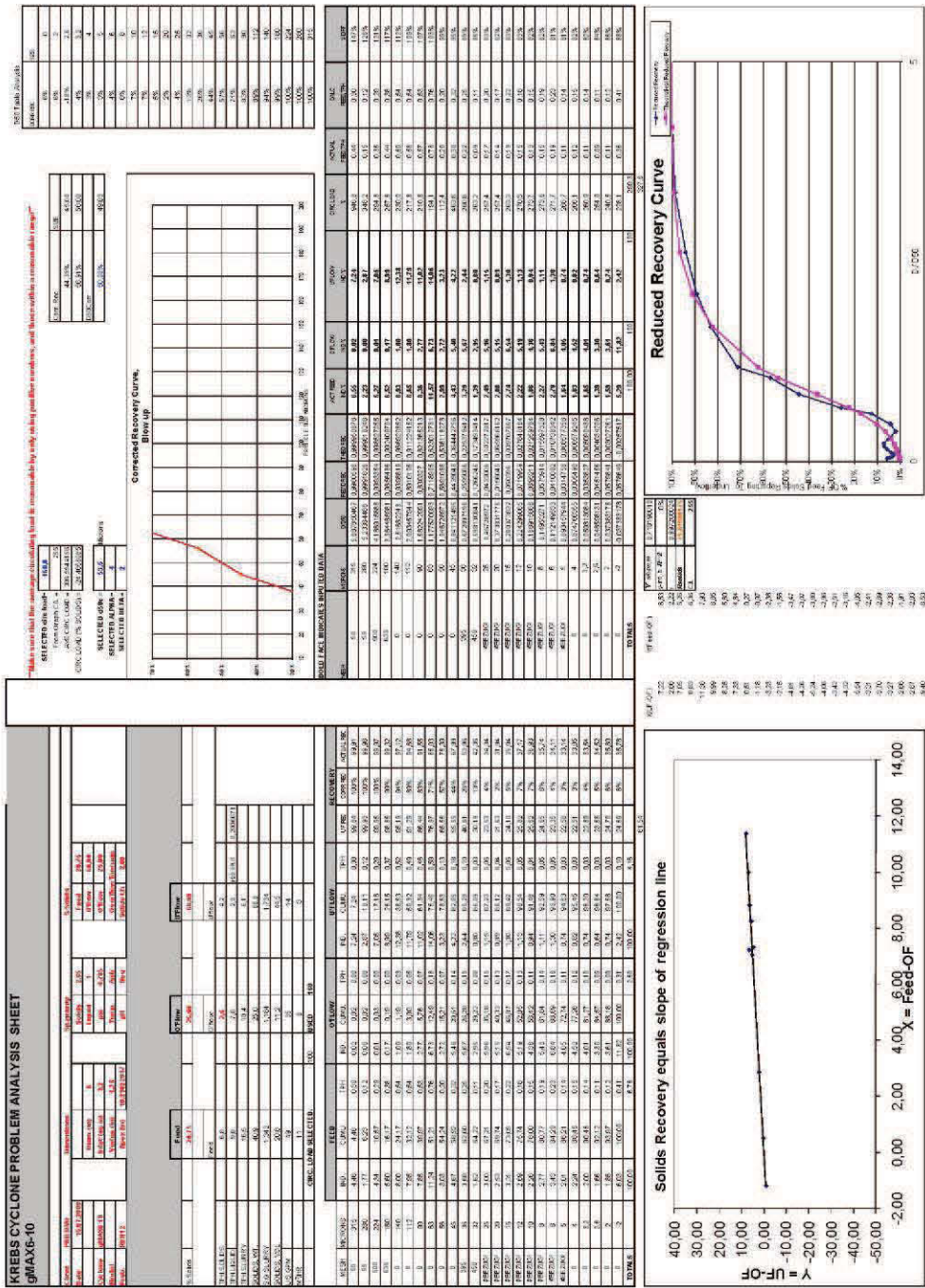
Reduced Recovery Curve

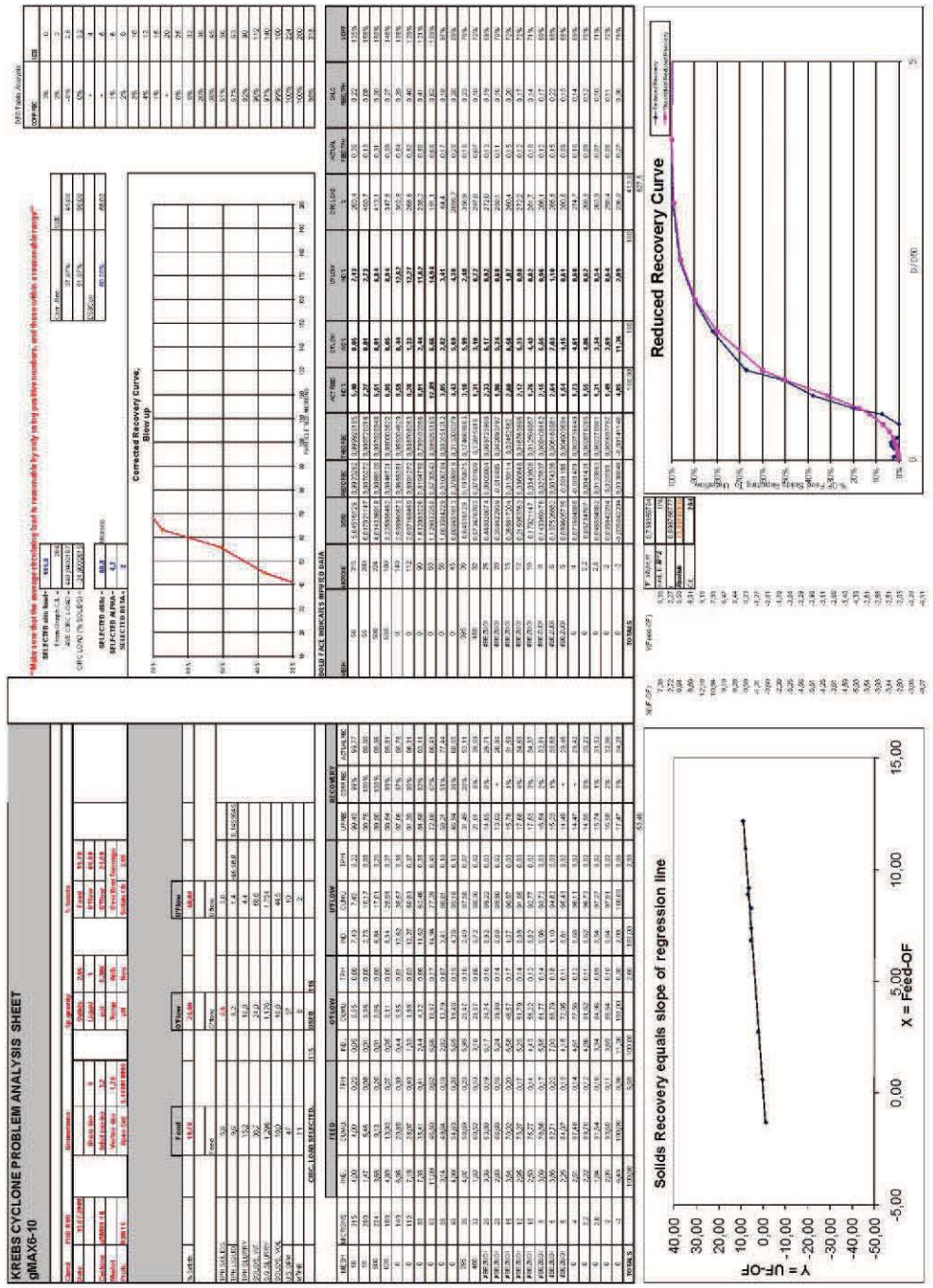
Y = UF-OF
X = Feed-OF

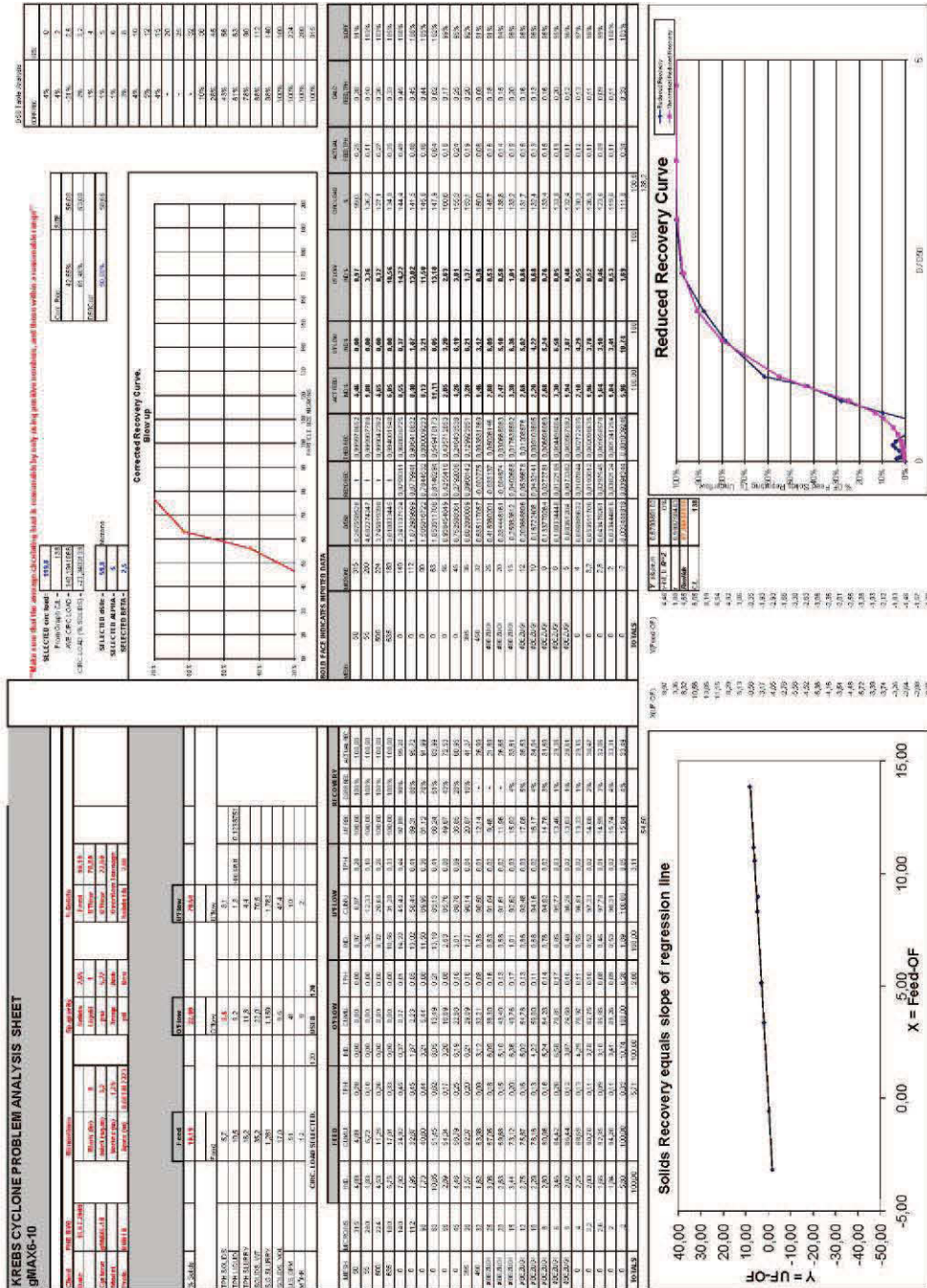
CONVERTED RECOVERY CURVE

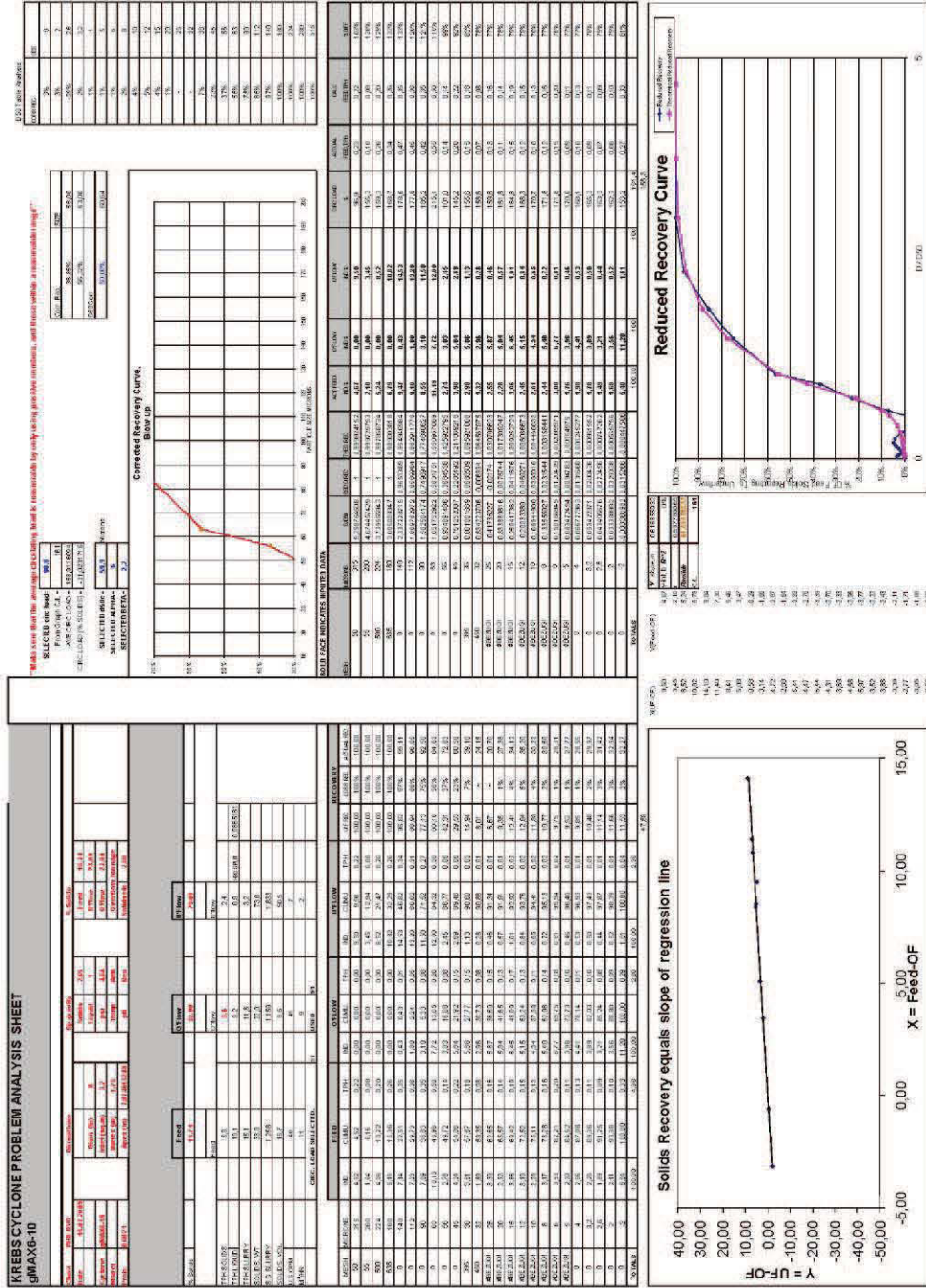
Reduced Recovery Curve







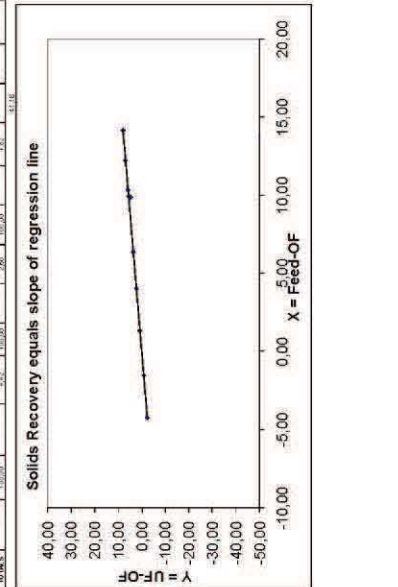




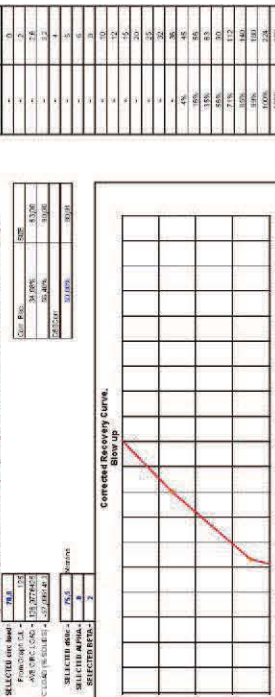
KREBS CYCLONE PROBLEM ANALYSIS SHEET
GMAX16-10

Design		Specifications		% Solids	
Model	GMAX16-10	Model	GMAX16-10	Feed	Underflow
Capacity	100 t/h	Throughput	100 t/h	11.8	3.4
Efficiency	99.8%	Throughput	100 t/h	11.8	3.4
Pressure	1.5 bar	Throughput	100 t/h	11.8	3.4
Temperature	150 °C	Throughput	100 t/h	11.8	3.4
Feed	100 t/h	Throughput	100 t/h	11.8	3.4
Underflow	3.4 t/h	Throughput	100 t/h	11.8	3.4
Overflow	96.6 t/h	Throughput	100 t/h	11.8	3.4

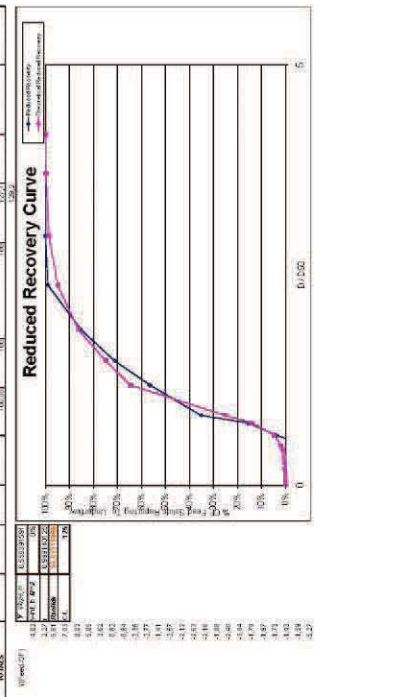
Feed	Inflow		Overflow		Underflow		Recovery	
	Rate	Mass	Rate	Mass	Rate	Mass	Rate	Mass
50	4.00	400	0.10	10	0.01	1	0.00	0.00
60	4.80	480	0.12	12	0.01	1	0.00	0.00
70	5.60	560	0.14	14	0.01	1	0.00	0.00
80	6.40	640	0.16	16	0.01	1	0.00	0.00
90	7.20	720	0.18	18	0.01	1	0.00	0.00
100	8.00	800	0.20	20	0.01	1	0.00	0.00



Concrete Recovery Curve

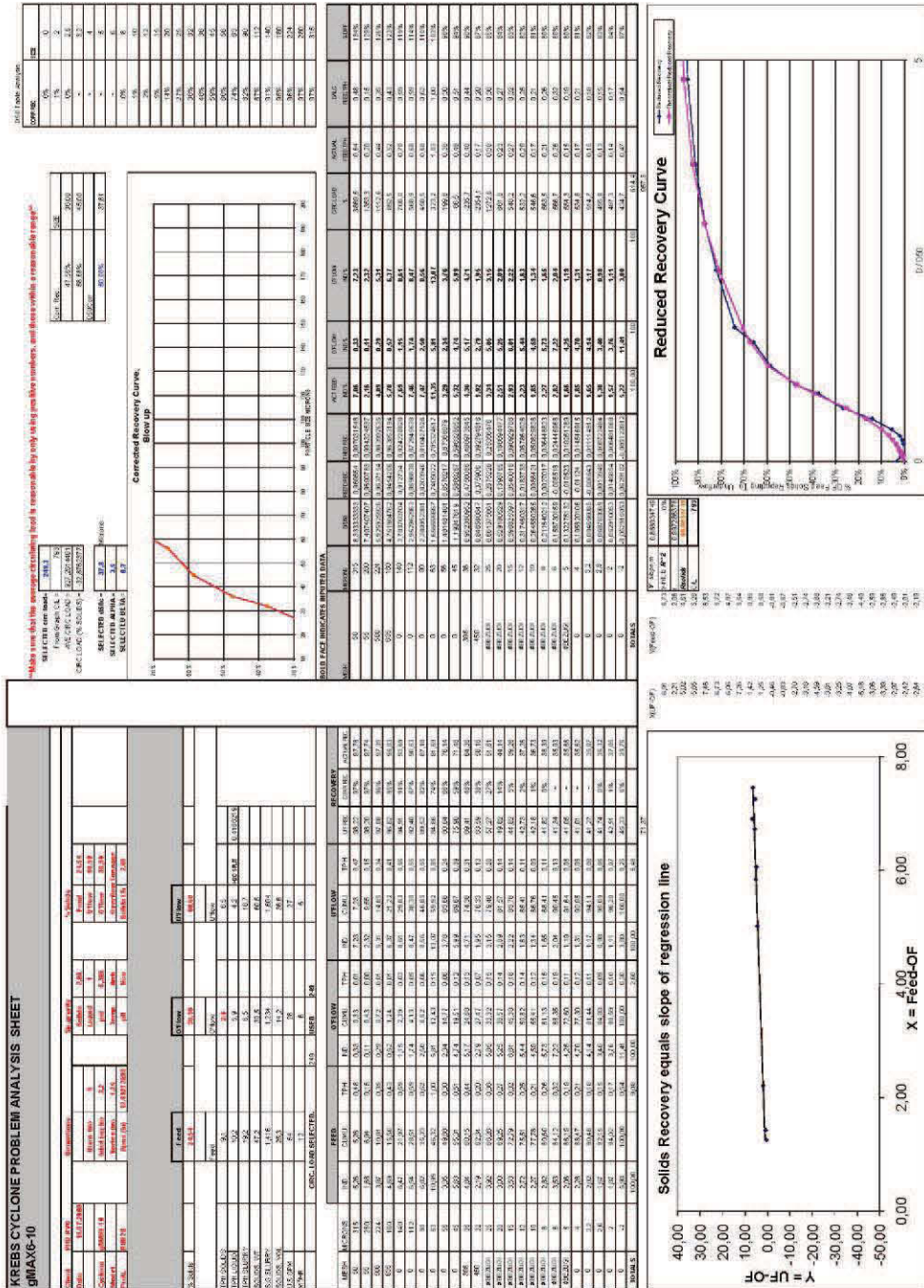


Feed-Of	Underflow	Feed-Of	Underflow	Feed-Of	Underflow	Feed-Of	Underflow
0	0	25	15	50	30	75	45
10	5	30	18	55	33	80	48
20	10	35	21	60	36	85	51
30	15	40	24	65	39	90	54
40	20	45	27	70	42	95	57
50	25	50	30	75	45	100	60



Operating Parameters

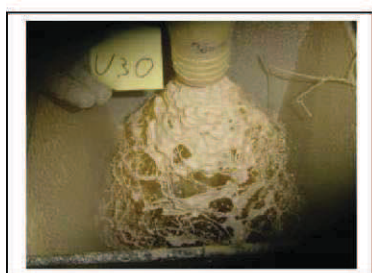
Parameter	Value
Feed-Of	100
Underflow	3.4
Overflow	96.6
Efficiency	99.8%
Throughput	100 t/h
Pressure	1.5 bar
Temperature	150 °C







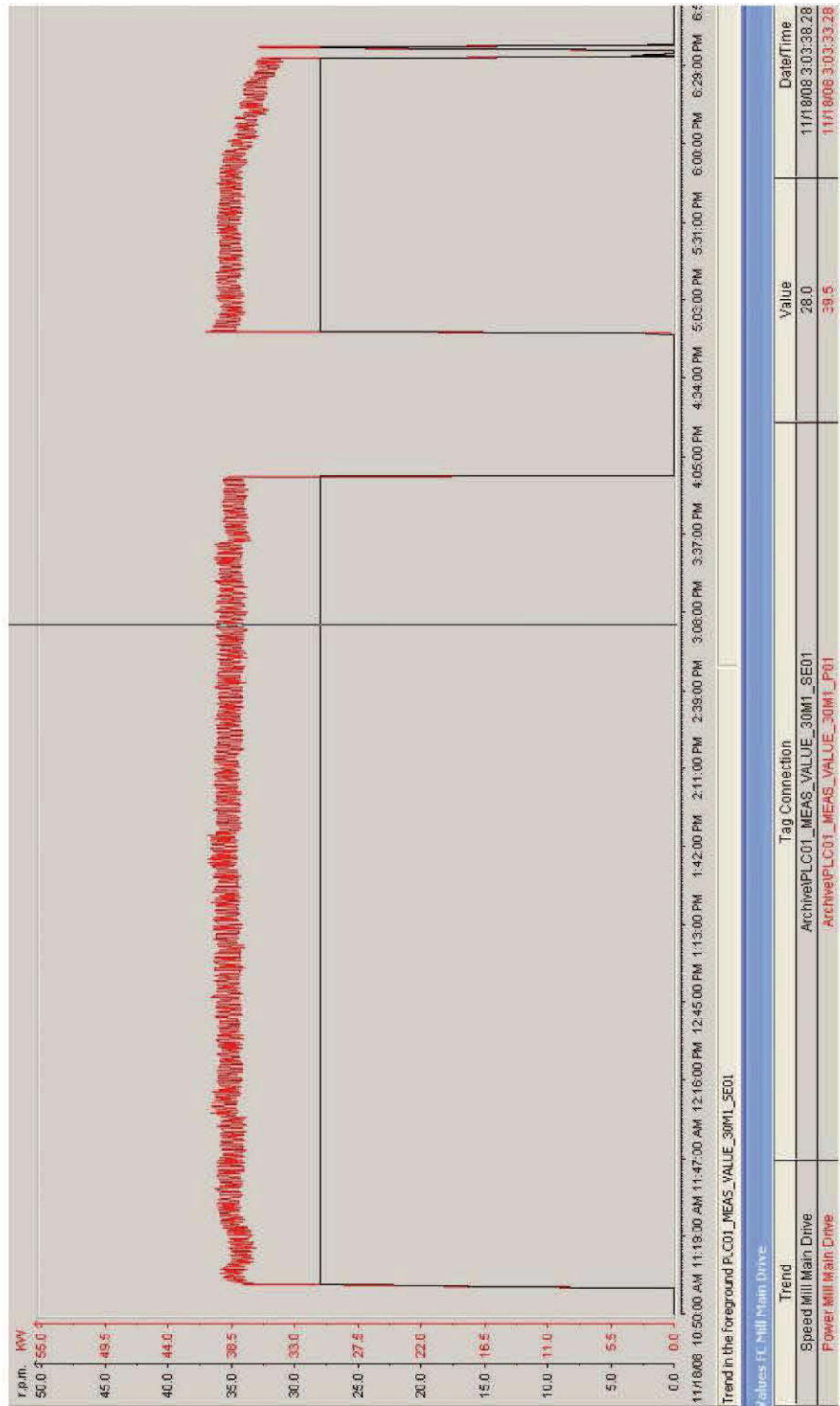




11/18/08 10:52:00 AM 11:17:00 AM 11:42:00 AM 12:07:00 PM 12:32:00 PM 12:57:00 PM 1:22:00 PM 1:47:00 PM 2:12:00 PM 2:37:00 PM 3:02:00 PM 3:27:00 PM 3:52:00 PM 4:17:00 PM 4:42:00 PM 5:07:00 PM 5:32:00 PM 5:57:00

Trend in the foreground PLC01_MEAS_VALUE_10A1_WT1

#Eightfeeder Clinker	
Trend	Tag Connection
weightfeeder Clinker	ArchivePLC01_MEAS_VALUE_10A1_WT1
	Value
	2.6
	Date/Time
	11/18/08 2:26:59.281 F





SHEET 2
DATE 30-Mär-11
BY RVO

Client: Siguri Gold
Problem: Producing 2200 MTPH of solids @ 80% passing 75 microns
Current Situation

Number, Model Krebs Cyclones: 12 operating gMAX26

Orifices: Inlet Area 60,00 sq. in. Vortex Finder 10,00 in. Apex Pressure Drop 121,6 kPa

Specific Gravity: Solids: 2,700 Liquid: 1,000 Temperature: Amb.°C Viscosity: 1 Cps

	FEED	OVERFLOW	UNDERFLOW
MTPH Solids	5500,00	2200,00	3300,00
MTPH Liquids	5238,10	3300,00	1938,10
MTPH Slurry	10738,10	5500,00	5238,10
Wt Solids	51,22	40,00	63,00
S.G. Slurry	1,476	1,337	1,657
Vol% Solids	28,00	19,80	38,67
GPM Slurry	32031,68	18117,12	13914,56
M3/Hr. Slurry	7275,13	4114,82	3160,32

Ref: 97,6 4,2 51,0*

Circulating Load: 150%

Mesh	Micron	FEED			OVERFLOW			UNDERFLOW			ACT. REC.	CORR. REC.
		Cum. % +	Ind. % +	MTPH	Cum. % +	Ind. % +	MTPH	Cum. % +	Ind. % +	MTPH		
65	208,0	3,88	3,88	213,5	0,00	0,00	0,0	6,47	6,47	213,5	100,0	100,0
100	149,0	26,75	22,86	1257,6	2,85	2,85	62,7	42,68	36,21	1194,8	95,0	92,1
150	104,0	37,67	10,92	600,8	9,59	6,74	148,3	56,39	13,71	452,6	75,3	60,8
200	74,0	47,44	9,77	537,1	20,60	11,01	242,3	65,32	8,93	294,8	54,9	28,4
270	53,0	57,34	9,91	544,8	34,21	13,61	299,4	72,76	7,44	245,4	45,0	12,8
400	37,0	65,26	7,92	435,6	45,94	11,72	257,9	78,14	5,38	177,7	40,8	6,0
-400	-37,0	100,00	34,74	1910,7	100,00	54,06	1189,4	100,00	21,86	721,3	37,8	1,2
TOTAL				5500,00			2200,00			3300,00	60,0	36,5

FLSMIDTH KREBS
Obere Hauptstrasse 27/3/4/TOP21
TEL: +43 2167 3345 FAX: +43 2167 3337
www.krebs.com



SHEET
DATE 30-Mär-11
BY RVO

Client: Sigüiri Gold
Problem: Producing 2200 MTPH of solids @ 80% passing 75 microns Optimized

Number, Model Krebs Cyclones: 18 operating gMAX20

Orifices: Inlet Area 35,50 sq. in. Vortex Finder 8,25 in. Apex Pressure Drop 1,0 Bar
Specific Gravity: Solids: 2,700 Liquid: 1,000 Temperature: Amb.°C Viscosity: 1 Cps

	FEED	OVERFLOW	UNDERFLOW
MTPH Solids	4840,00	2200,00	2640,00
MTPH Liquids	4431,43	3300,00	1131,43
MTPH Slurry	9271,43	5500,00	3771,43
Wt Solids	52,20	40,00	70,00
S.G. Slurry	1,490	1,337	1,788
Vol% Solids	28,80	19,80	46,36
GPM Slurry	27403,75	18117,12	9286,63
M3/Hr. Slurry	6224,02	4114,82	2109,21

Ref: 98,2 4,2 50,0*

Circulating Load: 120%

Mesh	Micron	FEED			OVERFLOW			UNDERFLOW			ACT. REC.	CORR. REC.
		Cum. % +	Ind. % +	MTPH	Cum. % +	Ind. % +	MTPH	Cum. % +	Ind. % +	MTPH		
65	208,0	9,57	9,57	463,2	0,00	0,00	0,0	17,55	17,55	463,2	100,0	100,0
100	149,0	29,38	19,81	959,0	2,85	2,85	62,7	51,49	33,95	896,2	93,5	91,2
150	104,0	39,76	10,38	502,3	9,59	6,74	148,3	64,90	13,41	354,0	70,5	60,4
200	74,0	49,26	9,50	459,6	20,60	11,01	242,3	73,14	8,23	217,3	47,3	29,2
270	53,0	58,88	9,62	465,7	34,21	13,61	299,4	79,43	6,30	166,3	35,7	13,7
400	37,0	66,54	7,66	371,0	45,94	11,72	257,9	83,72	4,28	113,0	30,5	6,6
-400	-37,0	100,00	33,46	1619,3	100,00	54,06	1189,4	100,00	16,28	429,9	26,5	1,4
TOTAL				4840,00			2200,00			2640,00	54,5	39,0

FLSMIDTH KREBS
Obere Hauptstrasse 27/3/4/TOP21
TEL: +43 2167 3345 FAX: +43 2167 3337
www.krebs.com